EPRI | ELECTRIC POWER RESEARCH INSTITUTE

Speciation and Attenuation of Arsenic and Selenium at Coal Combustion By-Product Management Facilities

Final Report
October 1, 2002 - September 30, 2005

Mr. Robert Patton

U.S. Department of Energy
National Energy Technology Laboratory
626 Cochrans Mill Road
PO Box 10940, MS 922-273C
Pittsburgh, PA 15236-0940

DOE Award Number: DE-FC26-02NT41590

Submitted By:

K. Ladwig
Electric Power Research Institute
3412 Hillview Avenue
Palo Alto, CA 94304

EPRI DISCLAIMER OF WARRANTIES AND LIMITATION OF LIABILITIES

THIS DOCUMENT WAS PREPARED BY THE ORGANIZATION(S) NAMED BELOW AS AN ACCOUNT OF WORK SPONSORED OR COSPONSORED BY THE ELECTRIC POWER RESEARCH INSTITUTE, INC. (EPRI). NEITHER EPRI, ANY MEMBER OF EPRI, ANY COSPONSOR, THE ORGANIZATION(S) BELOW, NOR ANY PERSON ACTING ON BEHALF OF ANY OF THEM:

(A) MAKES ANY WARRANTY OR REPRESENTATION WHATSOEVER, EXPRESS OR IMPLIED, (I) WITH RESPECT TO THE USE OF ANY INFORMATION, APPARATUS, METHOD, PROCESS, OR SIMILAR ITEM DISCLOSED IN THIS DOCUMENT, INCLUDING MERCHANTABILITY AND FITNESS FOR A PARTICULAR PURPOSE, OR (II) THAT SUCH USE DOES NOT INFRINGE ON OR INTERFERE WITH PRIVATELY OWNED RIGHTS, INCLUDING ANY PARTY'S INTELLECTUAL PROPERTY, OR (III) THAT THIS DOCUMENT IS SUITABLE TO ANY PARTICULAR USER'S CIRCUMSTANCE; OR

(B) ASSUMES RESPONSIBILITY FOR ANY DAMAGES OR OTHER LIABILITY WHATSOEVER (INCLUDING ANY CONSEQUENTIAL DAMAGES, EVEN IF EPRI OR ANY EPRI REPRESENTATIVE HAS BEEN ADVISED OF THE POSSIBILITY OF SUCH DAMAGES) RESULTING FROM YOUR SELECTION OR USE OF THIS DOCUMENT OR ANY INFORMATION, APPARATUS, METHOD, PROCESS, OR SIMILAR ITEM DISCLOSED IN THIS DOCUMENT.

DOE DISCLAIMER

THIS REPORT WAS PREPARED AS AN ACCOUNT OF WORK SPONSORED BY AN AGENCY OF THE UNITED STATES GOVERNMENT. NEITHER THE UNITED STATES GOVERNMENT, NOR ANY AGENCY THEREOF, NOR ANY OF THEIR EMPLOYEES, MAKES ANY WARRANTY, EXPRESS OR IMPLIED, OR ASSUMES ANY LEGAL LIABILITY OR RESPONSIBILITY FOR THE ACCURACY, COMPLETENESS, OR USEFULNESS OF ANY INFORMATION, APPARATUS, PRODUCT, OR PROCESS DISCLOSED OR REPRESENTS THAT ITS USE WOULD NOT INFRINGE PRIVATELY OWNED RIGHTS. REFERENCE HEREIN TO ANY SPECIFIC COMMERCIAL PRODUCT, PROCESS, OR SERVICE BY TRADE NAME, TRADEMARK, MANUFACTURER, OR OTHERWISE DOES NOT NECESSARILY CONSTITUTE OR IMPLY ITS ENDORSEMENT, RECOMMENDATION, OR FAVORING BY THE UNITED STATES GOVERNMENT OR ANY AGENCY THEREOF. THE VIEWS AND OPINIONS OF AUTHORS EXPRESSED HERIN DO NOT NECESSARILY STATE OR REFLECT THOSE OF THE UNITED STATES GOVERNMENT OR ANY AGENCY THEREOF.

EXECUTIVE SUMMARY

The overall objective of this project was to evaluate the impact of key constituents captured from power plant air streams (principally arsenic and selenium) on the disposal and utilization of coal combustion products (CCPs). Specific objectives of the project were: 1) to develop a comprehensive database of field leachate concentrations at a wide range of CCP management sites, including speciation of arsenic and selenium, and low-detection limit analyses for mercury; 2) to perform detailed evaluations of the release and attenuation of arsenic species at three CCP sites; and 3) to perform detailed evaluations of the release and attenuation of selenium species at three CCP sites.

Each of these objectives was accomplished using a combination of field sampling and laboratory analysis and experimentation. All of the methods used and results obtained are contained in this report. For ease of use, the report is subdivided into three parts. Volume 1 contains methods and results for the field leachate characterization. Volume 2 contains methods and results for arsenic adsorption. Volume 3 contains methods and results for selenium adsorption.

Field Leachate Characterization

There has been a large amount of laboratory-generated leachate data produced over the last two decades to estimate CCP leachate concentrations. A wide variety of leaching methodologies have been used, and it is difficult to compare results across test methods. There has been little work done to systematically evaluate field-generated leachates representative of a range of coal types, combustion systems, and management methods.

The specific objective of this part of the research was to characterize CCP leachate samples collected in the field from a wide variety of CCP management settings. Characterization included speciation of arsenic, selenium, chromium, and mercury. This research provides field-scale data that can be compared to laboratory-generated data, and that can be used to develop source terms for models that predict the effects of CCP management methods on leachate quality and the long-term fate of inorganic constituents at CCP management sites.

Field leachate samples were collected from 29 CCP management sites from several geographic locations in the United States to provide a broad characterization of major and trace constituents in the leachate. A total of 81 samples were collected representing a variety of CCP types, management approaches, and source coals. Samples were collected from leachate wells, leachate collection systems, drive-point piezometers, lysimeters, the ash/water interface at impoundments, impoundment outfalls and inlets, and seeps.

At ash management sites, highest median concentrations among major constituents were: sulfate (339 mg/L), calcium (55 mg/L), bicarbonate (53 mg/L), and sodium (52 mg/L). Highest median concentrations among trace constituents were: boron (2,160 µg/L), strontium (829 µg/L), molybdenum (405 µg/L), and lithium(129 µg/L). At flue gas desulfurization (FGD) product management sites, highest median concentrations among major constituents were: sulfate (1,615 mg/L), chloride (921 mg/L), calcium (589 mg/L), and potassium (425 mg/L). Highest median concentrations among trace constituents were: boron (9,605 µg/L), strontium (5,230 µg/L), lithium(3,055 µg/L), and molybdenum (341 µg/L).

Results suggest distinct differences in the chemical composition of leachate from coal ash and FGD products, landfills and impoundments, and from bituminous and subbituminous/lignite coals. Concentrations of many constituents were higher in landfill leachate than in impoundment leachate. Furthermore, aluminum, carbonates, chloride, chromium, copper, mercury, sodium, and sulfate concentrations were higher in leachates for ash from subbituminous/lignite coal; while antimony, calcium, cobalt, lithium, magnesium, manganese, nickel, thallium, and zinc concentrations were higher in leachate from bituminous coal ash.

FGD leachate had a different chemical signature than ash leachate. Concentrations of most major constituents in FGD leachate were higher than in ash leachate; this is particularly true for chloride and potassium. In addition, median concentrations of boron, strontium, and lithium were higher in FGD leachate than in ash leachate, while concentrations of selenium, vanadium, uranium, and thallium were lower.

Analysis of speciation samples indicated that ash leachate is usually dominated by As(V) and Cr(VI). Selenium was mostly in the form of Se(IV), although there were a significant number of samples dominated by Se(VI). Se(IV) dominated in impoundment settings when the source coal was bituminous or a mixture of bituminous and subbituminous, while Se(VI) was predominant in landfill settings and when the source coal was subbituminous/lignite. Mercury concentrations were very low in all samples, with a median of 3.8 ng/L in ash leachate and 8.3 ng/L in FGD leachate. The organic species of mercury always had low concentration, usually less than 5 percent of the total mercury concentration.

Arsenic Adsorption

Chemical attenuation of arsenic in subsurface soils is highly dependent on the arsenic species present in solution (leachate) and the characteristics of the soil. This portion of the project was designed to evaluate chemical attenuation of As(III) and As(V) at three coal-fired power plant sites. One site is located in the northeastern United States (NE), one site is located in the Southeast (SE), and one site is located in the Midwest (MW). These data can be used to model arsenic migration in groundwater at the sites for comparison to monitoring well data.

The specific objectives of this part of the research were to determine arsenic species-specific adsorption rates, using whole soils collected at CCP management facilities and both simulated and CCP-derived leachate, and to evaluate the factors that affect adsorption.

Several soil samples were collected from three power plant sites to conduct the laboratory chemical attenuation studies. Adsorption isotherms and coefficients were developed for both

arsenic(III) and arsenic(V) species. Physical and chemical characterization data for the soils were obtained so that correlations between soil properties and adsorption of arsenic species could be established to the extent possible. Linear, Freundlich, and Langmuir adsorption isotherms were fitted to the data as appropriate.

The effects of calcium and sulfate, the dominant ionic constituents in coal ash leachates, on the adsorption of the As(III) and As(V) by soils were measured. The effects of pH on arsenic species adsorption by soils were also measured. Sequential leaching studies were performed on coal ash samples collected from each of the three landfill sites. Kinetic leaching tests on ash samples were also performed.

Adsorption of arsenic species was generally non-linear with respect to concentration. For all three sites, adsorption of As(V) was significantly greater than As(III). Linear distribution coefficients calculated from adsorption isotherms at a concentration of 1 mg/L ranged from about 30 to 350 L/kg for As(V), and from about 5 to 50 L/kg for As(III). The impact of sulfate concentrations on adsorption were soil dependent and most pronounced for As(III). In general sulfate tends to decrease adsorption of arsenic species onto the soils. Adsorption of As(V) was generally enhanced by calcium in solution but As(III) adsorption was not significantly influenced by calcium.

Linear regression analysis of the adsorption coefficients and soil chemical and physical properties indicates that the best correlation was found with 15-second DC extractable iron. However, reasonably good correlations were also found for percent clay content and for DC-extractable iron and aluminum in soils.

Selenium Adsorption

Attenuation of selenium in the subsurface is highly dependent on the selenium species present and the characteristics of the soil. This portion of the project was designed to evaluate attenuation of selenite [Se(IV)] and selenate [Se(VI)] for soils at three coal-fired power plant sites from different geographical regions within the United States. One site is located in the northeastern United States (NE), one site is located in the Southeast (SE), and one site is located in the Midwest (MW). These data can be used to model selenium migration in groundwater at the sites and to compare to monitoring well data.

The specific objectives of this part of the research were to determine selenium species-specific adsorption rates, using whole soils collected at the CCP management facilities and both simulated and CCP-derived leachate, and to evaluate the factors that affect adsorption.

Several soil samples were collected from three power plant sites to conduct the laboratory chemical attenuation studies. Adsorption isotherms and coefficients were developed for both Se(IV) and Se(VI). Physical and chemical characterization data for the soils were obtained so that correlations between soil properties and adsorption of selenium species could be established to the extent possible. Linear and Freundlich adsorption isotherm models were fitted to the data as appropriate.

Adsorption of selenium species was generally non-linear with respect to concentration. For all three sites, adsorption of Se(IV) was significantly greater than Se(VI). Linearized concentration-

specific distribution coefficients calculated from adsorption isotherms at an initial solution concentration of 1 mg/L ranged from 5 to about 500 L/kg for Se(IV), and from 2 to 18 L/kg for Se(VI) for the soils tested. The presence of sulfate decreases adsorption of selenium with effects being soil dependent but always greatest for Se(VI). The presence of calcium had a small effect on Se(IV) adsorption, and a negligible effect on Se(VI) adsorption.

Linear and a step-wise multiple linear regression analyses of the adsorption coefficients and soil chemical and physical properties indicate that 15-second DC extractable iron was the best single parameter correlation; however, reasonably good correlations for Se(VI) adsorption were also found with clay percentage. For both species, selenium adsorption was negatively correlated with soil isotherm pH. Combining pH with 15 sec-DCB-Fe content of the soils resulted in the best correlation for adsorption of both Se(IV) and Se(VI).

EPRI | ELECTRIC POWER RESEARCH INSTITUTE

Speciation and Attenuation of Arsenic and Selenium at Coal Combustion By-Product Management Facilities

Volume 1: Field Leachate

Final Report
October 1, 2002 - September 30, 2005

DOE Award Number: DE-FC26-02NT41590

Principal Investigators:

K. Ladwig, Electric Power Research Institute
B. Hensel, Natural Resource Technology, Inc.
D. Wallschlager, Trent University

FIELD LEACHATE ABSTRACT

Field leachate samples were collected from 29 coal combustion product (CCP) management sites from several geographic locations in the United States to provide a broad characterization of major and trace constituents in the leachate. In addition, speciation of arsenic, selenium, chromium, and mercury in the leachates was determined. A total of 81 samples were collected representing a variety of CCP types, management approaches, and source coals. Samples were collected from leachate wells, leachate collection systems, drive-point piezometers, lysimeters, the ash/water interface at impoundments, impoundment outfalls and inlets, and seeps.

Results suggest distinct differences in the chemical composition of leachate from coal ash and flue gas desulfurization (FGD) sludge, landfills and impoundments, and from bituminous and subbituminous/lignite coals. Concentrations of many constituents were higher in landfill leachate than in impoundment leachate. Furthermore, aluminum, carbonates, chloride, chromium, copper, mercury, sodium, and sulfate concentrations were higher in leachates for ash from subbituminous/lignite coal; while antimony, calcium, cobalt, lithium, magnesium, manganese, nickel, thallium, and zinc concentrations were higher in leachate from bituminous coal ash.

FGD leachate had a different chemical signature than ash leachate. Concentrations of most major constituents in FGD leachate were higher than in ash leachate; this is particularly true for chloride and potassium. In addition, median concentrations of boron, strontium, and lithium were higher in FGD leachate than in ash leachate, while concentrations of selenium, vanadium, uranium, and thallium were lower.

Analysis of speciation samples indicated that ash leachate is usually dominated by As(V) and Cr(VI). Selenium was mostly in the form of Se(IV), although there were a significant number of samples dominated by Se(VI). Se(IV) dominated in impoundment settings when the source coal was bituminous or a mixture of bituminous and subbituminous, while Se(VI) was predominant in landfill settings and when the source coal was subbituminous/lignite. Mercury concentrations were very low in all samples, with a median of 3.8 ng/L in ash leachate and 8.3 ng/L in FGD leachate. The organic species of mercury always had low concentration, usually less than 5 percent of the total mercury concentration.

CONTENTS

LIST OF FIGURES

LIST OF TABLES

1
INTRODUCTION

Background

Coal combustion products (CCPs)—fly ash, bottom ash, boiler slag, and flue gas desulfurization (FGD) solids—are derived primarily from incombustible mineral matter in coal and sorbents used to capture gaseous components from the flue gas, and as such contain a wide range of inorganic constituents. Concentrations of these constituents in CCPs and their leachability can vary widely by coal type and combustion/collection processes. Since CCP leachates commonly have neutral to alkaline pH, mobility of heavy metal cations such as lead and cadmium is limited. Other constituents, such as arsenic and selenium, typically occur as oxyanions, which are more mobile than metal cations under alkaline pH conditions. Knowledge of factors controlling the leachability and mobility in groundwater of the different constituents is critical to development of appropriate CCP management practices, including treatment of ash ponds and groundwater management at dry disposal sites and large scale land application uses.

There has been a large amount of laboratory-generated leachate data produced over the last two decades to estimate CCP leachate concentrations. A wide variety of leaching methodologies have been used, and it is difficult to compare results across test methods. There has been little work done to systematically evaluate field-generated leachates representative of a range of coal types, combustion systems, and management methods.

Arsenic, selenium, chromium, and mercury are of particular interest due to the multiple species that may be present in CCP leachate. The speciation affects both mobility and toxicity. Previous research has indicated that arsenic and selenium concentrations in laboratory-generated ash leachates generally range from less than 1 µg/L to about 800 µg/L (EPRI, 2003a). Arsenic concentrations higher than 1,000 µg/L in ash porewater have been associated with pyrite oxidation in areas where coal mill rejects are concentrated (EPRI, 2003b). Only limited work has been performed to determine the species of arsenic and selenium present in field leachates. The species of arsenic and selenium present in the leachate will have a significant effect on their release from the ash and mobility in groundwater (EPRI, 1994; EPRI, 2000a; EPRI, 2004).

Speciation of chromium and mercury are also important considerations with respect to mobility and toxicity. Hexavalent chromium (Cr(VI)) is more mobile and more toxic then trivalent chromium (Cr(III)), which has relatively low solubility. Mercury may be present in CCP leachates in very low concentrations, on the order of parts per trillion; there are few measurements of mercury species present in field leachates using ultra clean sampling methods.

Objectives

The objective of this research was to characterize CCP leachate samples collected in the field from a wide variety of CCP management settings. Characterization included speciation of arsenic, selenium, chromium, and, in some cases, mercury. This research provides field-scale data that can be compared to laboratory-generated data, and that can be used to model and predict the effects of CCP management methods on leachate quality and the long-term fate of inorganic constituents at CCP management sites.

2
METHODS

Site Selection

Preliminary information on power plant configurations, emission controls, and CCP management methods was assembled for 274 power plants operated by 32 utilities. A subset of management sites was selected from this list, based on individual site considerations as well as development of a range of site types representative of the industry.

A distribution of sites was selected to encompass:

- a broad geographic distribution;
- a range of CCP types (fly ash, bottom ash, flue gas desulfurization solids);
- a representative distribution of CCP management methods (landfills and impoundments, active and inactive);
- coal types from various coal source regions;
- varying plant characteristics
  - boiler types;
  - particulate controls;
  - NOx controls;
  - SO_2 controls;
  - units with and without flue gas conditioning.

Individual sites were evaluated based on:

- availability of leachate sampling points;
- whether or not the site was believed to have leachate in sufficient quantities for sampling (i.e., wet CCP).
- utility interest in participation;

Based on these criteria, 33 CP sites in 15 states were selected for sampling.

Sample Collection

Leachate samples were collected from several access points, including leachate wells, lysimeters, leachate collection systems, sluice lines, direct push drive-points, core samples, and ponds. The goal was to obtain undiluted samples representative of CCP leachate. Samples were collected by a variety of methods, depending on sample type and accessibility. In all cases, the samples were filtered in-line and collected directly into bottles containing appropriate preservatives.

Direct Push Samples

Shallow porewater samples were collected from within the CCP using two direct-push methods: drive-point piezometers and t-handle probes. The drive-point sampler consisted of a ¾-inch stainless steel drive-point piezometer driven into the CCP to the desired sampling depth using a slide hammer (Figure 2-1). A ½-inch plastic tube was attached to the drive-point and threaded through ¾-inch steel riser pipe. The sample was extracted by sliding chemically-inert ¼-inch FEP tubing through the ½ -inch tubing down the riser pipe and into the screened portion of the stainless steel drive-point. The FEP tubing was then attached to a peristaltic pump via a short length of clean flexible silicone pump tubing.

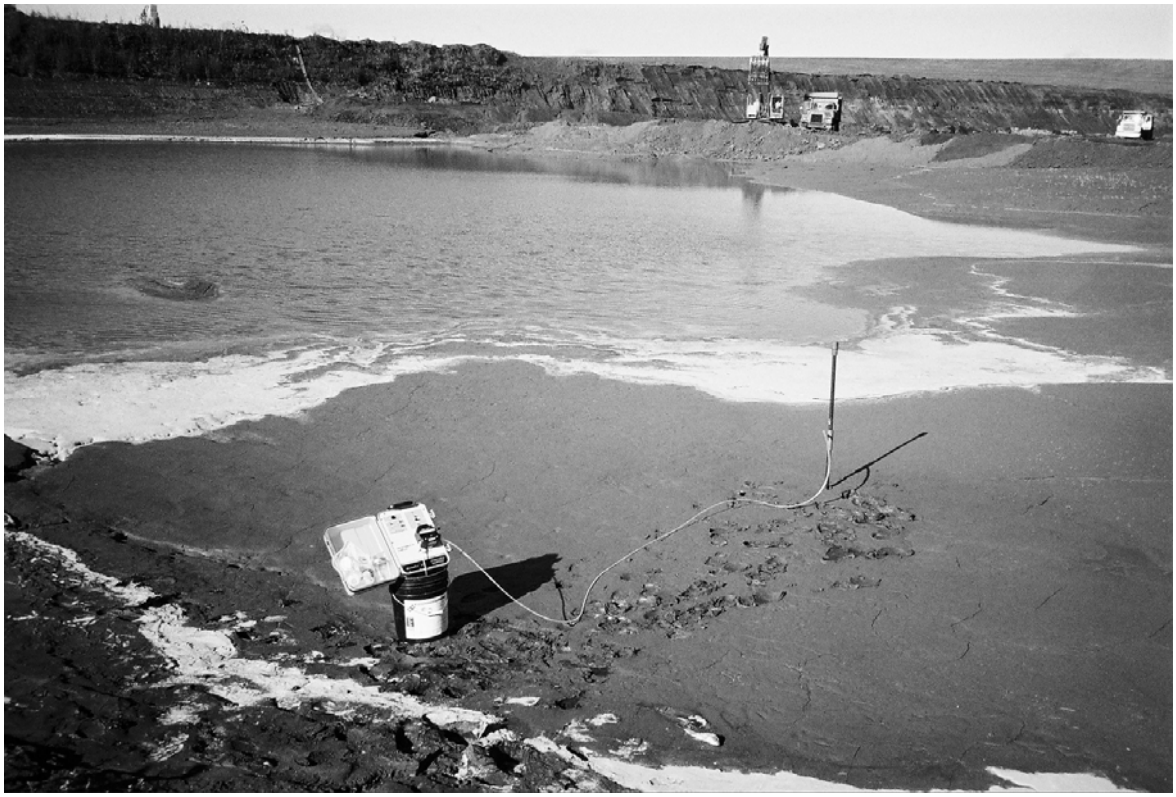

Figure 2-1
Direct push sample collection using a drive point piezometer

The t-handle probe is composed of a single, thin-diameter stainless steel tube that has small manufactured slots cut into the tip for sample collection (Figure 2-2). A short plastic netting was

placed over the tip of the probe just prior to installation to reduce intake of fine-grained sediments. Each t-handle probe was hand-driven into the CCP to a depth of as much as six feet. The top of the t-handle was then connected to a plastic syringe to initiate water flow. Once water flow was established, a short piece of silicone tubing was used to connect ¼-inch FEP tubing to the top of the probe. The ¼-inch FEP tubing was then connected to a peristaltic pump via a short length of clean flexible silicone pump tubing.

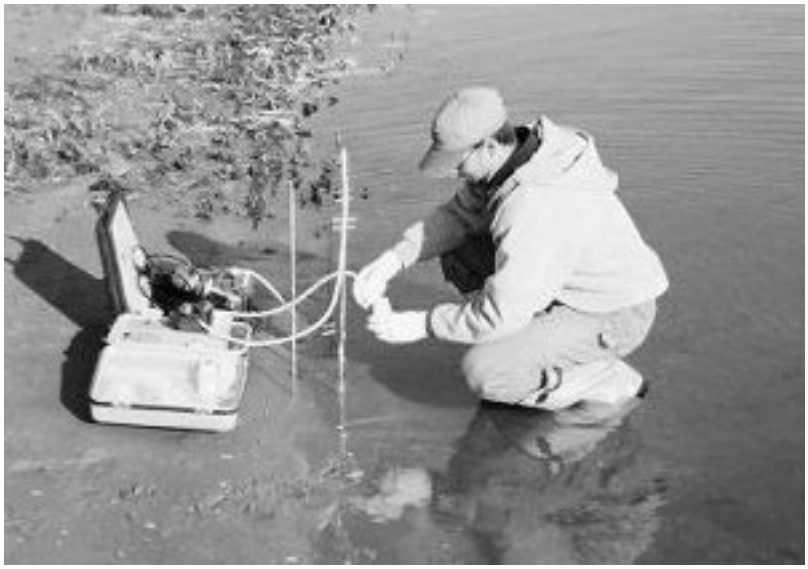

Figure 2-2
Direct-push sample collection using a t-handled probe

Leachate Wells, Lysimeters, and Leachate Collection Systems

Leachate wells, lysimeters, and leachate collection systems collect deep porewater within or immediately beneath the CCP. The leachate wells sampled for this study were installed by the utilities for the purpose of monitoring leachate quality. These wells, which consist of small-diameter (2- to 4-inch) polyvinylchloride (PVC) or stainless steel pipe with slotted screens at the bottom, are installed vertically in the CCP. Lysimeters[1] were also installed to monitor leachate quality, and differ from leachate wells in that they collect porewater beneath the CCP. Lysimeters are large collection devices, usually lined with plastic and filled with sand or gravel. Leachate percolates through the CCP and into the lysimeter, where it is removed from the sand or gravel through piping that extends to land surface. Leachate collection systems are installed to drain leachate from a CCP management unit, thus preventing head build-up on the liner. These systems typically consist of large-diameter (at least 4 inch) slotted plastic pipe embedded in a sand or gravel layer above the liner. Samples may be collected at clean-out ports where the pipes emerge from beneath the fill deposit, or at the tanks where the collected leachate is stored prior to processing.

[1] In a typical installation, lysimeters are installed beneath liners to monitor liner performance. However, the lysimeters monitored for this study were installed immediately beneath the CCP.

Whenever possible, low-flow methods were employed while sampling leachate wells to minimize disturbances within the sampling zone. Low-flow sampling is accomplished by pumping water at a rate that is compatible with the rate of recovery for the well (or similar sample point) and the matrix being sampled, using methods that do not cause water surging within the well (Puls and Barcelona, 1995). Purging and sampling were performed with a peristaltic pump or, for deeper wells, a bladder pump. In a few cases with restricted access, a hand-operated Waterra™ pump or bailer was used to retrieve samples.

When low-flow sampling methods could not be performed, either "minimum purge" sampling or "maximum purge" sampling was used. Minimum purge sampling was used in a few instances where CCP surrounding the well had relatively low permeability and would not achieve a stable drawdown during low-flow pumping. This method was only used on wells that were constructed of PVC. Maximum purge sampling was used in the few instances where an existing well was constructed of stainless steel or any other metal, which may have influenced the water sample, if the well could not support low-flow sampling flow rates. In these instances, the well was completely purged the day before sampling.

Lysimeters and leachate collection systems were sampled by lowering the peristaltic pump FEP tubing to the water surface. However, in some cases, the depth to water was too great for sampling with a peristaltic pump, in which case the Waterra pump or a bladder pump connected to Teflon™ tubing was used to withdraw the sample.

Surface Water and Sluice Samples

Surface water samples were collected from ash or FGD ponds. Typically, the pond samples were accessed from structures that extended above the water, or by boat. In either case, ¼-inch FEP tubing was lowered into the water and connected to a peristaltic pump via a short length of clean flexible silicone tubing. Samples were collected from different depths by attaching the FEP tubing to a clean water level indicator and lowering the tubing to the desired depth. In most cases, samples were collected from as near the ash/water interface as possible. Seep, sluice, and outfall samples were collected directly from the sluice pipe or outfall structure in a clean plastic container or plastic dip cup sampler (Figure 2-3). FEP tubing connected to a peristaltic pump via a short length of clean flexible silicone tubing was lowered into the container and the sample was collected.

Figure 2-3
Seep sampling

Core Samples

Core samples were collected at selected sites where porewater samples could not otherwise be obtained. A hollow-stem auger drill rig was used to advance a lined split-spoon sampler or core barrel sampler into the CCP deposit. Typically, a preliminary borehole was drilled in advance of the sample borehole in order to log the intervals where the wettest CCP was encountered, and the sampler was then advanced in a second, adjacent borehole to the selected depth. Porewater was then extracted from the core in the laboratory.

Sample Preservation

Core Samples

Core samples for leachate analyses were collected in clear, large-diameter, plastic or Teflon liners. After the liner tubes were recovered, the ends were cut so that no air volume or disturbed sample was included in the tube, and the ends of the tubes were sealed with Parafilm™, plastic end caps, and tape. Tubes were stored in coolers with dry ice for shipment to the laboratory via

overnight delivery. Leachate was extracted from wet ash samples in the laboratory by centrifuge, then filtered and preserved as described below for liquid samples.

Liquid Samples

Liquid leachate samples were filtered in the field and then split for the individual analyses. A 0.45 μm filter was used for all liquid samples, and turbid samples were prefiltered using either a 1.0 or 5.0 μm filter.

There are two general approaches for preservation of speciation samples: acid preservation and cryofreezing, each with drawbacks. Acid preservation approaches have limited holding times, and require prior knowledge of redox conditions at the sample point for selection of the appropriate preservation fluid—reducing conditions are particularly problematic. Cryofreezing is not commonly used and there may be nuances to this method that have not been explored. Since prior data on redox conditions were typically not available for this sampling, the freezing approach was employed. Samples for arsenic, selenium, and chromium speciation were immediately cryofrozen in the field using liquid nitrogen (Figure 2-4), and then kept frozen on dry ice with minimal air contact until analysis to prevent changes in speciation by oxidation.

Figure 2-4
Cryofreezing a leachate sample in liquid nitrogen

Separate water samples were collected for the determination of dissolved mercury (Hg_{diss}), dissolved methyl mercury ($MeHg_{diss}$), and dimethyl mercury (DMM). New tubing, filter materials, and sampling containers were used to prevent sample contamination. Samples for Hg_{diss} and $MeHg_{diss}$ were collected using in-line filtration of a defined sample volume (40 mL for Hg_{diss} and 250 mL for $MeHg_{diss}$) and preserved immediately with HCl. The fresh filters used for each of these filtration steps were collected and stored in Petri dishes for the determination of particulate mercury (Hg_{part}) and particulate methyl mercury ($MeHg_{part}$). DMM was purged from the collected water samples with an argon stream (30 min at 1 L/min) in the field, and collected on Carbotrap™ adsorbent tubes (Figure 2-5). These tubes were dried with an argon stream opposite to the adsorption direction (10 min at 1 L/min), sealed, and kept cold and dark until analysis. All collected samples were double-bagged to prevent contamination, and clean sampling protocols (consistent with USEPA method 1631) were followed.

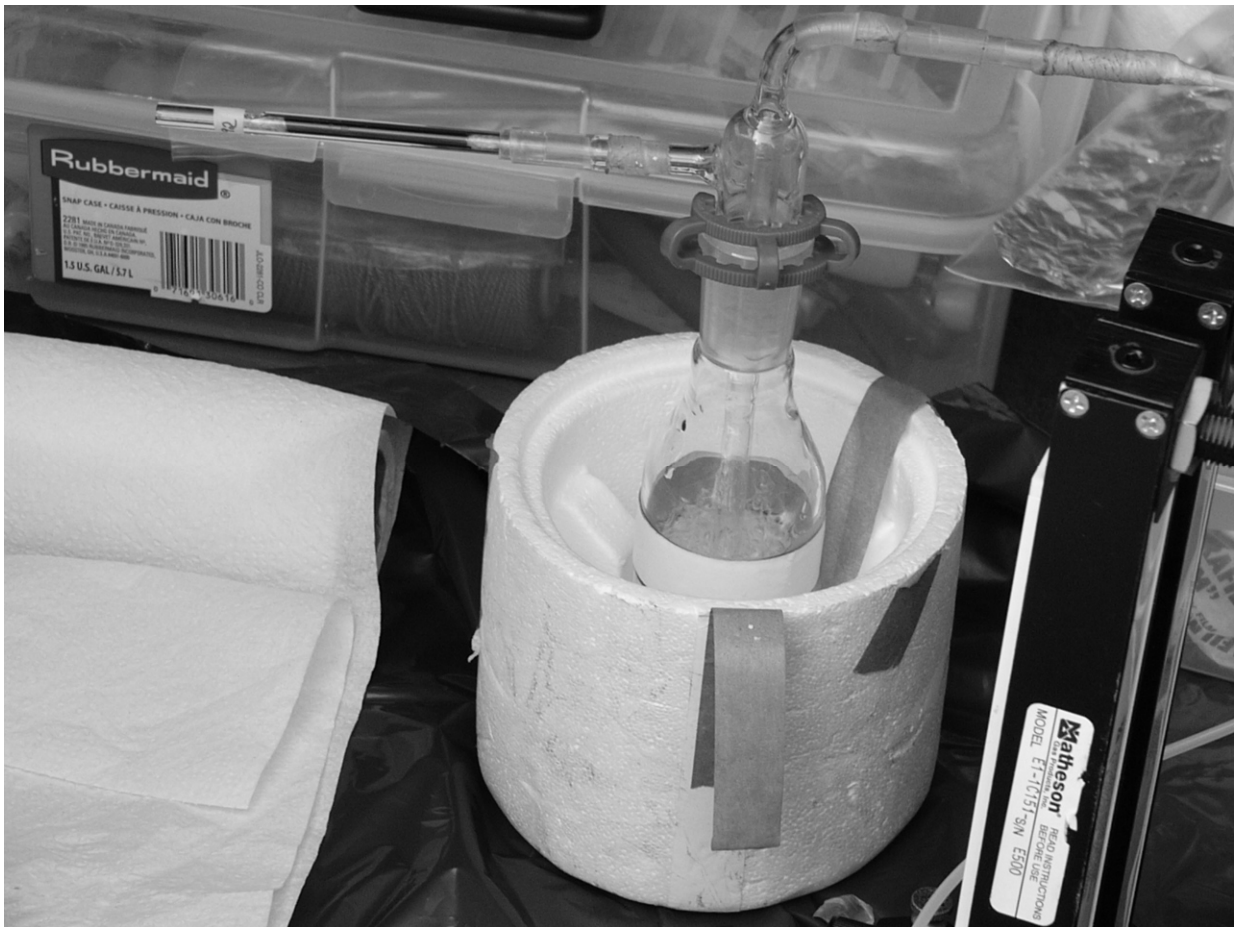

Figure 2-5
Argon bubbling through a leachate sample to vaporize DMM

Field parameters including pH, conductivity, redox potential, and temperature were measured using an in-line flow cell and/or multi-probe sample collected during sampling.

Quality Control

A suite of quality control (QC) samples were analyzed for most sample trips, which consisted of sample and matrix spike duplicates, blanks, and reference materials as appropriate and available. Final data reported may be corrected to reflect the results of the QC samples to yield the most accurate and precise result possible.

Laboratory Preparation and Analysis

Determination of Dissolved Arsenic and Selenium by Dynamic Reaction Cell-ICP-MS (DRC-ICP-MS)

Dissolved arsenic and selenium were determined by a Perkin-Elmer DRC II ICP-MS in dynamic reaction cell (DRC) mode using ammonia as the reaction gas for the determination of arsenic, and a methane/ammonia mixture for selenium. Chromium was also determined together with selenium (under the same conditions), and the obtained results were in good agreement with the DF-ICP-MS results, which were reported in the final data set. Instrument settings and monitored isotopes are reported in Table 2-1, which also contains typical instrumental detection limits (IDLs) for each element. These IDLs represent the overall average of all analytical runs throughout the project, and are comprised of individual IDLs for each data set, which were calculated as three times the standard deviation of four instrument blanks (1 percent HNO_3) in each instrument run.

Table 2-1
Method Parameters for Total Arsenic, Selenium, and Chromium Determinations by DRC-ICP-MS

	As	**Se + Cr**
Measured masses	^{75}As	^{80}Se, ^{52}Cr
Monitor masses	^{77}Se, ^{78}Se, ^{82}Se	^{78}Se, ^{82}Se, ^{53}Cr
Dwell time	200 ms/isotope	200 ms/isotope
Reaction gas	NH_3 = 0.35 mL/min	NH_3 = 0.3 mL/min CH_4 = 0.45 mL/min
Bandpass	RPq = 0.6	RPq = 0.6
Typical IDL [ppb]	0.01	0.01(^{80}Se), 0.01 (^{52}Cr)

Arsenic is monoisotopic and therefore has no confirmation isotope; however, ^{77}Se was measured to compensate for the potential interference of $^{40}Ar^{35}Cl$ on ^{75}As. The major isotope ^{80}Se was used for quantification of selenium. In the absence of interferences, all isotopes of an element should yield the same result, and for most of the samples this was achieved with the selected instrument settings. However in the case of low selenium and high salt concentrations, the three measured selenium isotopes showed different results. In these cases, the result was flagged in the results table (Appendix A). ^{53}Cr was measured as a control isotope for ^{52}Cr, and the two chromium isotopes generally agreed very well. Rhodium and indium were used as internal standards. A certified reference material was analyzed with each analytical run to confirm accurate calibration, and a matrix duplicate, a matrix spike, and a matrix spike duplicate were analyzed with each batch.

Arsenic and Selenium Speciation by Ion-Chromatography Anion Self-Regenerating Suppressor ICP-MS (IC-ASRS-ICP-MS)

As(III), As(V), Se(IV), and Se(VI) were determined simultaneously by IC-ASRS-ICP-MS (Wallschläger and Roehl, 2001; Wallschläger et al., 2005) using a Dionex ion-chromatography system with anion self-regenerating suppressor (ASRS) coupled to a Perkin-Elmer DRC II (Figures 2-6 and 2-7). Method parameters are listed in Table 2-2. The ICP-MS was used in standard mode as the interfering anions are chromatographically separated in time from the analytes. Typical achieved MDLs were 0.1 ppb per species. In addition to the species mentioned above, any other unidentified anionic species such as soluble As-S compounds can be determined by this method.

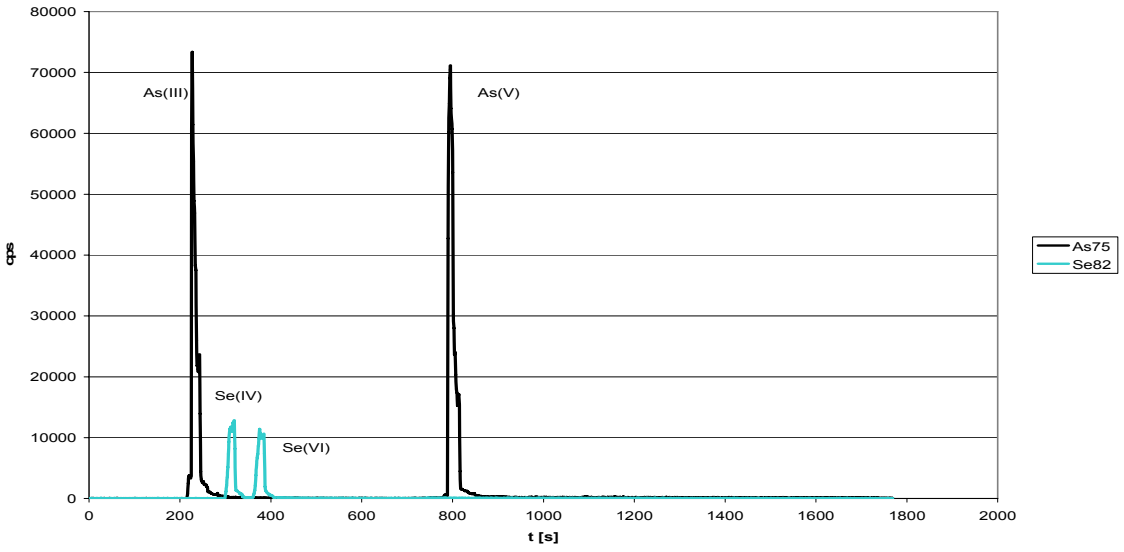

Figure 2-6
Chromatogram showing 5 ppb each for As(III), As(V), Se(IV), and Se(VI)

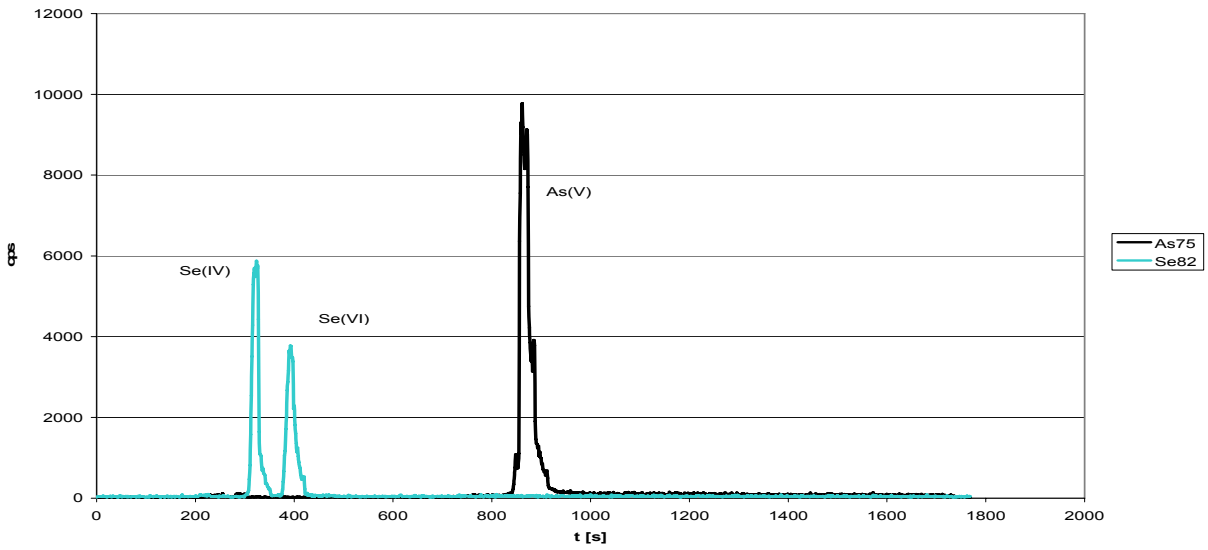

Figure 2-7
Chromatogram showing selenium and arsenic species for a real sample (10x dilution)

Table 2-2
Method Parameters for Arsenic, Selenium, and Chromium Speciation by IC-ASRS-DRC-ICP-MS

	Arsenic and Selenium Species	**Chromium Species**
Column	Dionex AS-16 4-mm + AG-16 4-mm	Dionex AS-16 4-mm + AG-16 4-mm
Eluent	sulfate in 3 mmol/L NaOH with 2 mmol/L oxalate 0→3 min: 1 mM SO_4^{2-} 3→4 min: 1→10 mM SO_4^{2-} 4→14 min: 10 mM SO_4^{2-} 14→16 min: 10→30 mM SO_4^{2-} 16→30 min: 30 mM SO_4^{2-} 30→35 min: 1 mM SO_4^{2-}	20 mM NaOH
Injection volume	1 mL	1 mL
Flow rate	1.2 mL/min	1.5 mL/min
Reaction gas	none	NH_3 = 0.3 mL/min
Bandpass	none	RPq = 0.3
Typical IDL [ppb]	0.1 As(III), 0.4 As(V), 0.05 Se(IV), 0.05 Se(VI)	0.01 Cr(III), 0.01 Cr(VI)

Determination of Dissolved Arsenic, Selenium, and Speciation in Sample Splits

A subset of the CCP leachate samples were split and forwarded to a separate laboratory for arsenic and selenium speciation analysis. These samples were field preserved using hydrochloric acid, rather than cryofreezing, and speciation analysis was performed within 48 hours of collection.

Total arsenic and selenium results were determined by Inductively Coupled Plasma Mass Spectrometry (ICP-MS) using scandium and niobium as internal standards. Due to the relatively high concentration of chloride present in the samples, an interference correction was employed for total arsenic during analysis.

Speciation for As(III), As(V), Se(IV), and Se(VI) was achieved by coupling a Hamilton PRP-X100 anion exchange column to the front end (sample introduction) of the ICP-MS instrument operated in a time domain mode. Lab Alliance pumps were used in conjunction with a gradient phosphate buffer mobile phase to elute and separate the compounds. Peak areas were used to quantitate species. Quality control measures performed during these analysis included reanalysis with greater elution times for samples where the sum of species was considerably different from the total concentration, review of chromatograms for unidentified species spikes, analytical sample duplicates, and analytical spike samples.

Chromium Speciation by Ion-Chromatography Anion Self-Regenerating Suppressor DRC-ICP-MS (IC-ASRS-DRC-ICP-MS)

Cr(III) and Cr(VI) were determined by IC-ASRS-DRC-ICP-MS using a Dionex ion-chromatography system with ASRS coupled to a Perkin-Elmer DRC II in DRC mode. This analysis was performed separately from the arsenic and selenium species determination, because Cr(III) must first be derivatized off-line to $(EDTA\text{-}Cr)^-$ before it can be determined together with Cr(VI) by anion-exchange chromatography prior to ICP-MS detection (Gürleyük and Wallschläger, 2001) (Figures 2-8 and 2-9). Modifications from the originally published method are listed in Table 2-2.

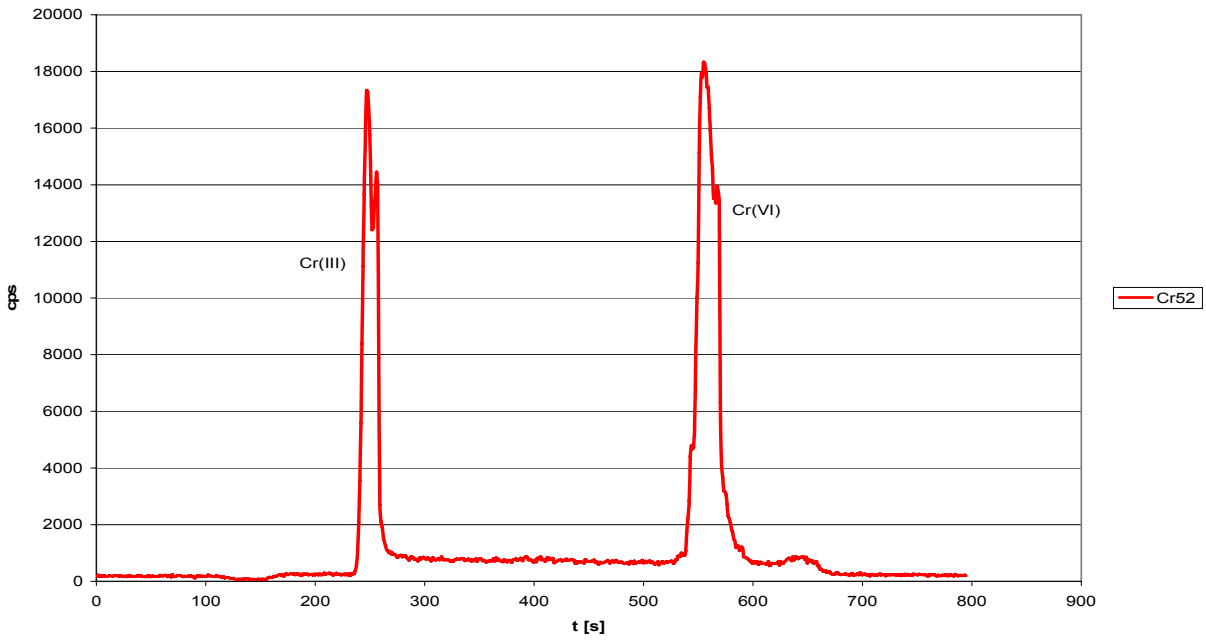

Figure 2-8
Chromatogram showing 0.5 ppb each for Cr(III) and Cr(VI)

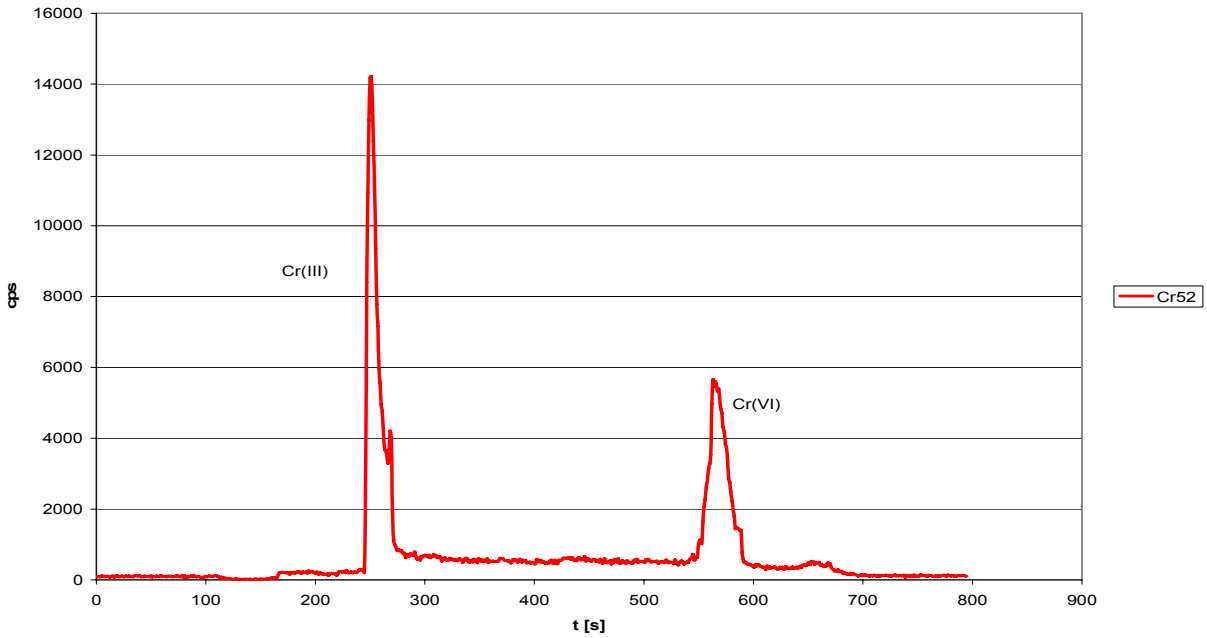

Figure 2-9
Chromatogram for sample 034 analyzed at a 2x dilution

Mercury Speciation Methods

Dimethyl Mercury (DMM): DMM was purged from the collected water samples with an argon stream in the field, and collected on Carbotrap™ adsorbent tubes. These tubes were dried with an argon stream opposite to the adsorption direction, sealed, and kept cold and dark until analysis. DMM was desorbed thermally from the adsorbent trap onto an analytical trap, from which DMM was thermo-desorbed and analyzed by gas chromatography–ICP-MS (GC-ICP-MS) (similar to Lindberg et al., 2004). Figure 2-10 shows a typical chromatogram obtained by this technique: the first peak (around 70 s) is caused by elemental mercury (not quantified in this project), while the second peak (around 120 s) is DMM. The retention time of DMM is determined by analysis of DMM standards, and quantification is achieved by injecting gaseous Hg^0 standards (which is permissible, because the response of ICP-MS to mercury is species-independent).

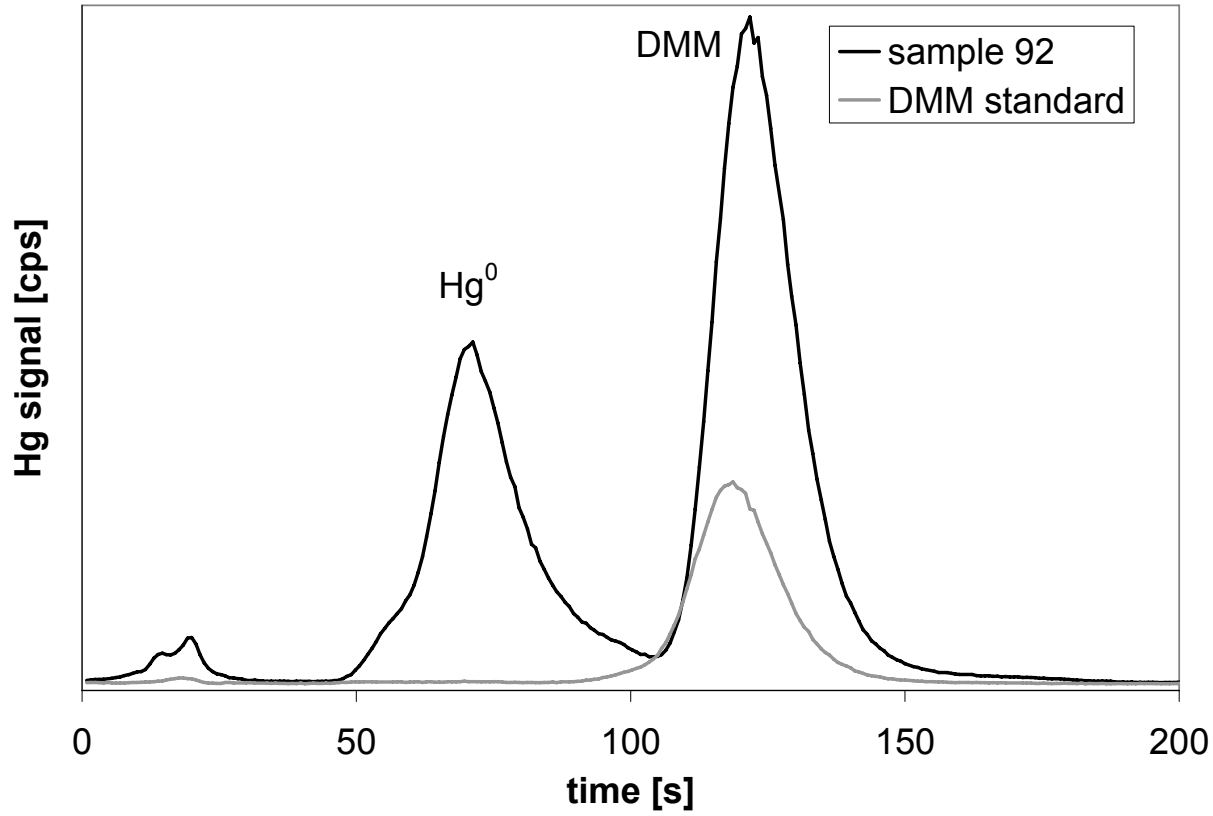

Figure 2-10
GC-ICP-MS chromatogram for the determination of DMM

Monomethyl Mercury (MeHg): MeHg was determined by GC-ICP-MS after derivatization to methylethyl mercury with sodium tetraethylborate. MeHg was isolated from filtered waters and

particulate matter (yielding dissolved and particulate MeHg) by steam distillation as methyl mercury chloride (MeHgCl), and determined using isotope dilution with isotopically-enriched MeHg. For this purpose, each sample is spiked with a known amount of MeHg labeled with the isotope ^{201}Hg prior to the steam distillation process. The result is a GC-ICP-MS chromatogram (Figure 2-11) in which the MeHg signal (around 110 s) shows an altered isotope ratio (compared to the natural isotope abundance) reflecting the added spike. From the change in isotope ratio (in this case: $^{201}Hg/^{202}Hg$), the concentration of MeHg in the native sample is calculated. This isotope dilution technique is used routinely at Trent University for $MeHg_{diss}$ and Hg_{diss} determinations (see below), because it effectively corrects for variable procedural recoveries encountered when normal external calibration methods are used (Hintelmann & Ogrinc, 2003). Figure 2-11 shows a second peak (around 50 s), which represents some unspecific source of mercury in the instrumental setup; this signal has the "normal" mercury isotope ratio, proving that it's not MeHg.

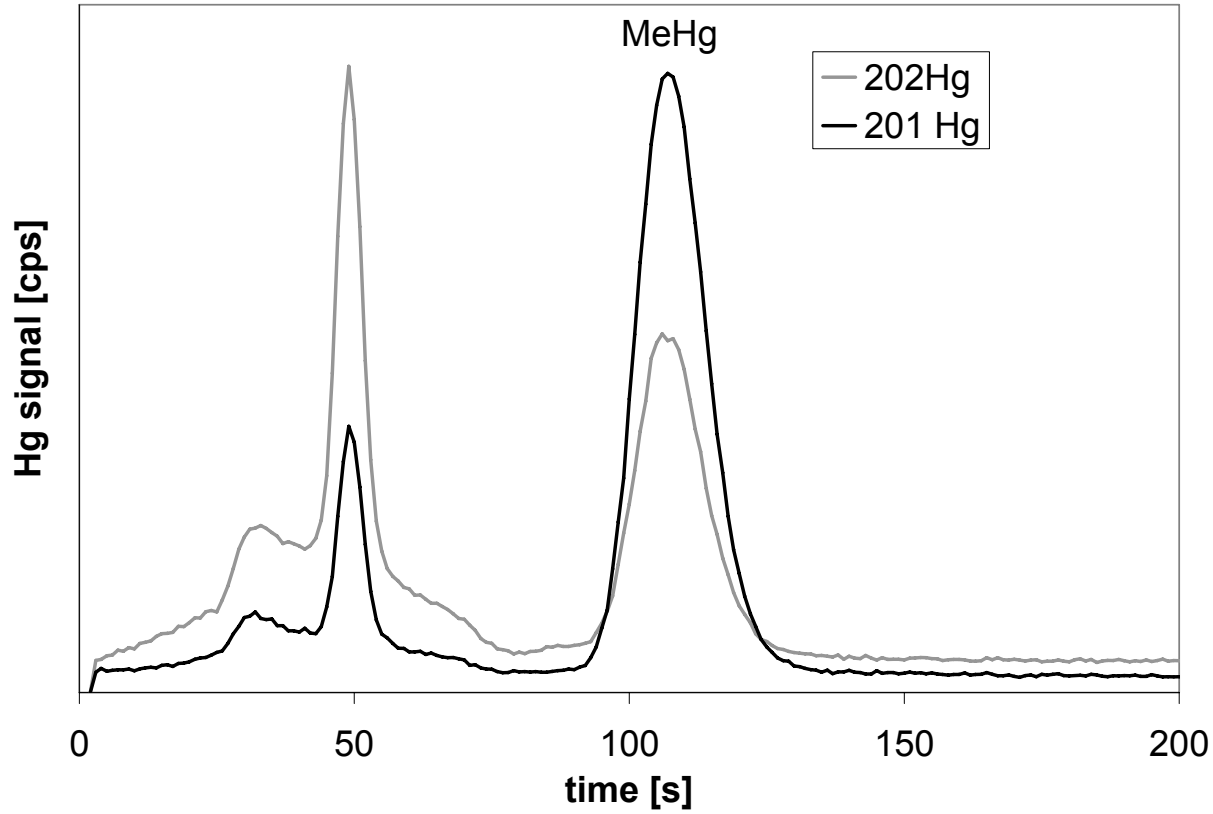

Figure 2-11
GC-ICP-MS chromatogram for the determination of MeHg by isotope dilution

Mercury (Hg): Total mercury in filtered waters and on filters with particulate matter (yielding dissolved and particulate mercury, Hg_{diss} and Hg_{part}) was determined by cold vapor-ICP-MS

(CV-ICP-MS), also using an analog isotope dilution approach with ^{201}Hg for quantification. Samples for Hg_{diss} analysis were digested with BrCl and pre-reduced with NH_2OH•HCl prior to the CV-ICP-MS measurement (Hintelmann and Ogrinc, 2003). Table 2-3 summarizes the different analytical methods used to measure mercury speciation in the collected water samples and their typical performance characteristics. It is noteworthy that the blanks for Hg_{diss} and Hg_{part} are typically larger than many of the analyzed samples; however, since blanks are fairly constant, they can be subtracted.

Table 2-3
Mercury Speciation Methods

Parameter	Analyzed sample volume (mL)	Typical detection limit (ng/L)	Typical analytical blank (ng/L)
DMM	105	0.005	none
$MeHg_{diss}$	50	0.02	0.02
$MeHg_{part}$	250	0.01	0.01
Hg_{diss}	n/a	0.2	1
Hg_{part}	40	1	5

Trace Element Determinations by Double-Focusing ICP-MS (DF-ICP-MS)

A Thermo Finnigan ELEMENT2 double-focusing inductively coupled plasma-mass spectrometer (DF-ICP-MS) was used in medium resolution mode to determine 22 elements of interest (Table 2-4). Each sample was analyzed at three different dilutions (500x, 100x, and 20x) to cover the different concentration ranges of the elements. Due to the high salt load of the samples, a dilution factor of less than 20x might lead to instrument damage and was therefore avoided; however, all field blanks and equipment blanks were analyzed undiluted because they did not contain salts. According to the typical concentrations encountered for different elements, the 500x diluted samples were analyzed for Li, B, Al, Si, Fe, Sr, and Mo; the 100x diluted samples for Li, Be, B, Al, V, Cr, Mn, Fe, Co, Ni, Cu, Zn, Sr, Mo, Ag, Cd, Sb, Ba, Tl, Pb, and U; and the 20x diluted samples for Li, Be, Al, V, Cr, Mn, Fe, Co, Ni, Cu, Zn, Mo, Ag, Cd, Sb, Ba, Tl, Pb, and U. If one element was analyzed at more than one dilution, the result obtained with the lowest dilution factor under consideration of the calibrated range was reported.

Table 2-4
Trace Metals by DF-ICP-MS

Element	Measured Isotope	Control Isotope	Isotopes Agree?	Typical IDL [ppb]
Aluminum	^{27}Al	monoisotopic		0.1
Antimony	^{121}Sb	^{123}Sb	Y	0.004
Barium	^{136}Ba	^{137}Ba	Y	0.06
Beryllium	^{9}Be	monoisotopic		0.01
Boron	^{10}B	^{11}B	Y	0.2
Cadmium	^{110}Cd	^{111}Cd, ^{114}Cd	N	0.004
Chromium	^{53}Cr	^{52}Cr	Y	0.01
Cobalt	^{59}Co	monoisotopic		0.002
Copper	^{65}Cu	^{63}Cu	Y	0.01
Iron	^{56}Fe	^{57}Fe	Y	0.1
Lead	^{208}Pb	^{206}Pb, ^{207}Pb	Y	0.003
Lithium	^{7}Li	not measurable		0.04
Manganese	^{55}Mn	monoisotopic		0.009
Molybdenum	^{98}Mo	^{95}Mo	Y	0.04
Nickel	^{60}Ni	^{58}Ni	Y (except in samples with high Fe concentrations)	0.03
Silica	^{28}Si	^{30}Si	Y	0.3
Silver	^{107}Ag	^{109}Ag	Y? (concentrations close to MDL)	0.005
Strontium	^{88}Sr	^{87}Sr	Y (after Rb correction of ^{87}Sr)	0.05
Thallium	^{205}Tl	^{203}Tl	Y? (concentrations close to MDL)	0.002
Uranium	^{238}U	not available	no interferences	0.001
Vanadium	^{51}V	^{50}V	N	0.004
Zinc	^{66}Zn	^{68}Zn	Y? (concentrations close to MDL)	0.09

At least two isotopes for each element were measured (if possible) to verify the absence of spectrometric interferences. Scandium, indium, rhodium, and germanium were used as internal standards to monitor and correct instrument drift and sample uptake effects. All measured and control isotopes are listed in Table 2-4. Typically, the results obtained for the measured and the control isotope were identical (within the analytical uncertainty); however, some exceptions are explained below. Average IDLs are also listed in Table 2-4. The method detection limit (MDL) was estimated as the IDL times the applicable dilution factor of the analyzed sample. The IDL/MDL was determined with each analytical run and varied slightly depending on the instrument performance on that day. All data reported were instrument-blank corrected. For quality control purposes, a certified reference material (CRM) was analyzed at two different dilutions per analytical run to confirm an accurate calibration. For each sample batch (usually one per sampling trip) one randomly selected sample was analyzed in duplicate and spiked and analyzed in duplicate to assess accuracy and reproducibility.

For some of the elements listed in Table 2-4, the results obtained for the measured and the control isotope did not match. Several elements (e.g., Ag, Zn, Tl) are present in most samples at concentrations of only 5-10 times the detection limit, so that analytical uncertainty and/or insufficient number of samples with detectable concentrations prevented a meaningful isotope comparison. In other cases, the control isotope had a very low abundance and although the sample concentration was very well detectable for the main isotope, the quantification by the minor isotope was impaired by low signal intensities (e.g., ^{50}V; natural abundance 0.25 percent). Also, in the used concentration range, ^{6}Li was not detected in medium resolution mode by the instrument; therefore, it was not used for confirming ^{7}Li.

In medium (or even high) resolution mode, some isobaric and polyatomic interferences could not be resolved: ^{58}Ni was not separated from ^{58}Fe in medium resolution mode (required resolution ~30,000; available resolution ~ 10,000). As the ^{58}Fe abundance is only 0.28 percent, the associated error is normally negligible; however, if the iron concentrations are extremely high, as in some of the analyzed samples, ^{58}Ni will be affected. Also, ^{87}Sr was also not separated from ^{87}Rb in medium resolution mode (required resolution ~300,000); however, the error in this case is not negligible as ^{87}Rb has an abundance of 27.8 percent. If ^{87}Sr is corrected for ^{87}Rb, both ^{87}Sr and ^{88}Sr yield identical results. For cadmium, both ^{111}Cd and ^{114}Cd were interfered with by MoO (required resolution ~100K and ~80K, respectively); in addition, ^{114}Cd was also affected by an isobaric interference of ^{114}Sn. Based on those considerations, ^{110}Cd was used for quantification. Generally, as spectroscopic interferences are normally positive, in the event that two isotopes yield a different result, the lower concentration will most likely be the uninterfered and therefore deliver the correct result.

Ancillary Parameters

Redox potential, pH, conductivity, dissolved oxygen, and temperature were determined in the field on the filtered samples with a YSI multiprobe (for wells, this measurement was made immediately after the low-flow conditions had stabilized; for all other types of water samples, this was done prior to collecting all other aliquots). Separate aliquots were used for these analyses and discarded afterwards.

Sodium, potassium, magnesium, and calcium were determined by cation-exchange chromatography with suppressed conductivity detection, and chloride and sulfate were determined by anion-exchange chromatography using the same detection principle, following standard methods. Total carbon (TC) and total inorganic carbon (TIC) were determined by flow injection-infrared spectrometry (Shimadzu Total Organic Carbon Analyzer) following standard methods, where TIC is liberated from the sample by addition of HCl, while TC is liberated by oxygen combustion; total organic carbon (TOC) is then determined by difference TC-TIC, which may lead to imprecise results in samples with low TOC content.

3
SAMPLE SUMMARY

Site and Sample Attributes

Location

The 33 sample sites are concentrated in the eastern United States where coal-fired power plants predominate (Figure 3-1). Attributes of sampled sites are listed in Table 3-1, and leachate sample attributes are listed in Table 3-2.

Symbols indicate number of sites within a state, but do not correspond to location of sampled sites.

	FA		FGD/SDA	
	LF	IMP	LF	IMP
Sites Completed Thru 2005	★	▼	✦	▼

Figure 3-1
Sample site locations by state

Facility Type

Samples were collected at 15 impoundments and 17 landfills (Table 3-1). One of the sites counted as an impoundment is the 14093 site. This site is a landfill that receives ash originally sluiced to an impoundment. Washing of ash during sluicing is believed to have an effect on ash leachate concentration; therefore, this site was counted as an impoundment.

The 27413 site is not classified as a landfill or impoundment. Ash was originally sluiced to this site, and later it was managed dry. There were no data to indicate whether the samples were collected in areas where ash was sluiced or managed dry; therefore, this site was not used in comparisons of landfill and impoundment ash.

Sample Methods

Landfill Samples

All of the 29 landfill leachate samples represent interstitial water. Three samples were collected from wells screened in the CCP, two samples were collected from lysimeters screened immediately beneath the CCP, one was collected from a surface seep, and 19 were collected from leachate collection systems (Table 3-3). The remaining four samples were core samples from soil borings; however, these samples did not yield sufficient water for analysis when centrifuged in the laboratory. As a result, 25 landfill leachate samples were analyzed.

The four dry cores were each collected from different sites, and, in each case, the dry core was the only sample collected at that site. These samples and sites are not included in the discussions that follow. As a result, for the remainder of this report, only 29 of the 33 sites will be referenced.

Impoundment Samples

Twenty-seven of the 53 impoundment samples represent interstitial water. These include eight samples collected from wells screened in the CCP, 13 samples collected from drive-point piezometers or push point samplers, three seep samples, and three core extracts (Table 3-3). The remaining 26 leachate samples include 12 collected from impoundments near the ash-water interface, and 14 samples collected from sluice lines or at impoundment outfalls.

Other Samples

The three leachate samples from site 27413 are interstitial water collected from temporary leachate wells.

Source Power Plant Attributes

Boiler Type

The majority of sites (24 of 29) sampled received CCP from pulverized coal (PC) plants with dry-bottom boilers (Table 3-1), representing 71 of the 81 leachate samples (Table 3-2). One site (one sample) received CCP from a wet-bottom PC boiler, and three sites (four samples) received CCP from cyclone boilers. The remaining site (five samples) received CCP from a plant that has both dry-bottom PC boilers and cyclones.

A variety of firing configurations are represented in the PC boilers including:

- Tangential: 10 sites, 34 samples
- Wall-fired (mostly opposed): 7 sites, 18 samples
- Multiple configurations: 9 sites, 25 samples

Source Coal

Most sites (11 sites, 48 samples) received CCP from power plants that burned bituminous coal (Tables 3-1 and 3-2). The power plant feeding one of these 11 sites (23214) also burns 5 percent petroleum coke.

Seven sites (13 samples) received CCP from plants that burn subbituminous coal, and four sites (five samples) received CCP from lignite-burning plants. The subbituminous and lignite samples will be grouped together in discussions that follow.

Four sites (seven samples) received CCP from plants that burn a blend of fuels:

- 22346: formerly bituminous, coal units burned a blend of 80 percent subbituminous and 20 percent bituminous coal at the time of sampling. This site also received oil ash.
- 22347: formerly bituminous, coal units burned a blend of 80 percent subbituminous and 20 percent bituminous coal at the time of sampling.
- 25410A and 25410B: an undetermined blend of subbituminous and bituminous coals, plus used tires and petroleum coke.

Three sites (eight samples) have CCP derived from a mixture of sources:

- 50183 received CCP from three different power plants burning bituminous and subbituminous coal.
- 27413 and 50210 received CCP from power plants that switched from bituminous to subbituminous coal.

Emission Controls

Six of the 29 sites received CCP from flue gas desulfurization (FGD) systems, the remaining sites received coal ash, either from plants without FGD systems or that was collected prior to the FGD system (Tables 3-1 and 3-2).

Fly Ash

Most fly ash samples came from plants (17 plants, 48 samples) with cold-side electrostatic precipitators (ESPs). Two sites (7 samples) received CCP from plants with hot-side ESPs and one site (1 sample) received CCP from a plant with a fabric filter. Three sites (11 samples) received CCP from multiple sources:

- 50183 received CCP from three plants, two have cold-side precipitators, and one has a hot-side ESP.
- 33104 received CCP from one plant with cold-side and hot-side ESPs on different units.
- 50213 received CCP from a plant with a cold-side ESP on two units, and a hot-side ESP and fabric filter on another unit.

Thirteen of the ash sample sites (41 samples) received CCP from units with flue gas conditioning to improve precipitator performance. NOx controls included low-NOx burners (12 samples), overfired air (5 samples), selective catalytic reduction (5 samples), and multiple types.

FGD

Five of the six FGD sites, representing 13 samples, received CCP from wet FGD systems. Four of these systems were coupled with cold-side ESPs; three of the four systems with ESPs systems used natural oxidation while the other used inhibited oxidation. The other wet FGD system was not coupled with an ESP or fabric filter, and used forced air oxidation. The FGD systems feeding three of these sites used magnesium-lime sorbent, one used lime, and one used limestone.

One site (1 sample) received CCP from a spray dryer system coupled with a fabric filter. The FGD sorbent used in this system was lime.

At one of the six FGD units, flue gas conditioning was used to improve precipitator performance. That unit also had a low-NOx burner.

Table 3-1
Attributes of Sample Sites and Source Power Plants

Site	Source Fuel Type	Source Plant Boiler Type	PC Boiler Firing	Source Plant Particulate Collection	Source Plant SO2 Control	Source Plant SO2 Sorbent	Source Plant Flue Gas Cond.	Source Plant NOx Control	Byproducts Managed	DUP	IMP	LF	QC
23214	Subbit	Cyclone		ESP cold-side	None	None	None	Combustion-OFA	FA Class C			1	
50183	Mix	Dry Bottom PC Boiler	multiple types	Multiple types	None	None	Yes	Multiple types	FA, BA			4	1
33106	Bit	Dry Bottom PC Boiler	tangential	ESP cold-side	None	None	Yes	Multiple types	FA, BA	1	7		3
20094A	Bit	Dry Bottom PC Boiler	wall-fired opposed	ESP multiple	None	None	None	Multiple types	FA, BA			1*	
20094B	Bit	Dry Bottom PC Boiler	wall-fired opposed	ESP multiple	None	None	None	Multiple types	FA, BA			1*	
34186A	Lig	Dry Bottom PC Boiler	tangential	ESP cold-side	Wet-natural	Mg-Lime	None	Multiple types	FA			1	
34186B	Lig	Dry Bottom PC Boiler	tangential	ESP cold-side	Wet-natural	Mg-Lime	None	Multiple types	FGD, BA		2		2
34186C	Lig	Dry Bottom PC Boiler	tangential	ESP cold-side	Wet-natural	Mg-Lime	None	Multiple types	FGD, FA, BA	1		1	
33104	Bit	Dry Bottom PC Boiler	tangential	Multiple types	None	None	None	Postcombustion SCR	FA, BA	1	5		1
50408	Bit	Dry Bottom PC Boiler	wall-fired	ESP cold-side	None	None	None	Combustion-none	FA, BA			1	
35015A	Bit	Dry Bottom PC Boiler	tangential	ESP cold-side	Wet-natural	Mg-Lime	Yes	Combustion-LNB	FGD, FA			6	
35015B	Bit	Multiple types	multiple types	ESP cold-side	None	None	None	Combustion-LNB	FA	1	5		1
31192	Subbit	Dry Bottom PC Boiler	tangential	Fabric filter	Wet-natural	Limestone	None	Other	FA, FGD, BA			1*	
13115A	Subbit	Dry Bottom PC Boiler	tangential	ESP cold-side	None	None	Yes	Multiple types	BA, FA		3		
13115B	Bit	Dry Bottom PC Boiler	tangential	ESP cold-side	None	None	Yes	Other	FA, BA		3		

Table 3-1 (Continued)
Attributes of Sample Sites and Source Power Plants

Site	Source Fuel Type	Source Plant Boiler Type	PC Boiler Firing	Source Plant Particulate Collection	Source Plant SO2 Control	Source Plant SO2 Sorbent	Source Plant Flue Gas Cond.	Source Plant NOx Control	Byproducts Managed	DUP	IMP	LF	QC
49003A	Bit	Dry Bottom PC Boiler	wall-fired opposed	ESP cold-side	None	None	Yes	Multiple types	FA		8		
49003B	Bit	Dry Bottom PC Boiler	wall-fired opposed	ESP cold-side	None	None	None	Combustion-LNB	FA			4	2
22346	Blend	Dry Bottom PC Boiler	multiple types	ESP cold-side	None	None	Yes	Multiple types	FA, OA	1	3		3
22347	Blend	Dry Bottom PC Boiler	tangential	ESP cold-side	None	None	Yes	Other	FA		1		
40109	Bit	Dry Bottom PC Boiler	tangential	ESP hot-side	None	None	None	Multiple types	FA, BA	1	5		1
27412	Subbit	Dry Bottom PC Boiler	wall-fired opposed	ESP cold-side	None	None	None	Combustion-OFA	FA, BA			1*	
27413	Mix	Dry Bottom PC Boiler	multiple types	ESP cold-side	None	None	Yes	Multiple types	FA				3
50210	Mix	Dry Bottom PC Boiler	multiple types	ESP cold-side	None	None	None	Multiple types	FA, BA			1	
43034	Lig	Wet Bottom PC Boiler	wall-fired	ESP cold-side	Wet-inhib	Limestone	None	Multiple types	FGD,FA			1	
50212	Subbit	Dry Bottom PC Boiler	wall-fired	ESP cold-side	None	None	Yes	Multiple types	FA	1		2	2^{+}
23223A	Subbit	Dry Bottom PC Boiler	multiple types	Fabric filter	Spray Dryer	Lime	no data	Multiple types	SDA			1	
23223B	Subbit	Dry Bottom PC Boiler	multiple types		Wet-FO	Lime	no data	Multiple types	FGD		3		
25410A	Blend	Cyclone		ESP cold-side	None	None	Yes	Combustion-OFA	FA, BA		2		
25410B	Blend	Cyclone		ESP cold-side	None	None	Yes	Combustion-OFA	FA		1		
50211	Bit	Dry Bottom PC Boiler	wall-fired front	Fabric filter	None	None	no data	Combustion-LNB	FA			1	
14093	Bit	Dry Bottom PC Boiler	multiple types	ESP cold-side	None	None	Multiple	Multiple types	FA (sluiced)	1	3		2

Table 3-1 (Continued)
Attributes of Sample Sites and Source Power Plants

Site	Source Fuel Type	Source Plant Boiler Type	PC Boiler Firing	Source Plant Particulate Collection	Source Plant SO2 Control	Source Plant SO2 Sorbent	Source Plant Flue Gas Cond.	Source Plant NOx Control	Byproducts Managed	DUP	IMP	LF	QC
43035	Subbit	Dry Bottom PC Boiler	wall-fired opposed	ESP hot-side	None	None	None	Combustion-LNB	FA,BA,EA (sluiced)	1	2		1
50213	Subbit	Dry Bottom PC Boiler	multiple types	Multiple types	None	None	Multiple	Multiple types	FA			2	

Notes:
Ash at site 27413 was first sluiced, then managed dry.
* indicates that core sample collected at this site did not yield sufficient water for analysis.
+ one of the two leachate samples collected at site 50212 was treated with CO_2

Abbreviations:
Bit = bituminous; Subbit = Subbituminous; Mix = CCP from different units burning different coals; Blend = CCP from a single unit burning two different fuels
PC = pulverized coal; ESP = electrostatic precipitator; OFA = overfired air; LNB = low-NOx burner
FA = fly ash; BA = bottom ash; EA = economizer ash; FGD = flue gas desulfurization sludge; OA = oil ash
LF = landfill; IMP = impoundment; DUP = duplicate sample; QC = quality control sample

Table 3-2
Leachate Sample Attributes

Sample ID	Source	Byproduct	Source Fuel Type	Site	Source Plant PC Boiler Type	PC Boiler Firing	Source Plant Particulate Collection	Source Plant SO2 Control	Source Plant SO2 Sorbent	Source Plant Flue Gas Cond.	Source Plant NOx Control
001	Landfill	FA,BA	Mix	50210	Dry Bottom PC Boiler	multiple types	ESP cold-side	None	None	None	Multiple types
002	Landfill	FA	Subbit	50213	Dry Bottom PC Boiler	multiple types	Multiple types	None	None	Multiple	Multiple types
003	Landfill	FA	Subbit	50213	Dry Bottom PC Boiler	multiple types	Multiple types	None	None	Multiple	Multiple types
004	Landfill	FA,BA	Mix	50183	Dry Bottom PC Boiler	multiple types	Multiple types	None	None	Yes	Multiple types
005	Landfill	FA,BA	Mix	50183	Dry Bottom PC Boiler	multiple types	Multiple types	None	None	Yes	Multiple types
006	Landfill	SDA	Subbit	23223A	Dry Bottom PC Boiler	multiple types	Fabric filter	Spray Dryer	Lime	no data	Multiple types
007	Impoundment	FGD	Subbit	23223B	Dry Bottom PC Boiler	multiple types		Wet-FO	Lime	no data	Multiple types
008	Impoundment	FGD	Subbit	23223B	Dry Bottom PC Boiler	multiple types		Wet-FO	Lime	no data	Multiple types
009	Impoundment	FGD	Subbit	23223B	Dry Bottom PC Boiler	multiple types		Wet-FO	Lime	no data	Multiple types
010	Landfill	FA	Subbit	23214	Cyclone		ESP cold-side	None	None	None	Combustion-OFA
012	Impoundment	FA	Bit	14093	Dry Bottom PC Boiler	multiple types	ESP cold-side	None	None	Multiple	Multiple types
013	Impoundment	FA	Bit	14093	Dry Bottom PC Boiler	multiple types	ESP cold-side	None	None	Multiple	Multiple types
014	Impoundment	FA	Bit	14093	Dry Bottom PC Boiler	multiple types	ESP cold-side	None	None	Multiple	Multiple types
015	Impoundment	FA,BA	Blend	25410A	Cyclone		ESP cold-side	None	None	Yes	Combustion-OFA
016	Impoundment	FA,BA	Blend	25410A	Cyclone		ESP cold-side	None	None	Yes	Combustion-OFA
017	Impoundment	FA,BA	Subbit	13115A	Dry Bottom PC Boiler	tangential	ESP cold-side	None	None	Yes	Multiple types
018	Impoundment	FA,BA	Bit	13115B	Dry Bottom PC Boiler	tangential	ESP cold-side	None	None	Yes	Other
019	Impoundment	FA	Subbit	13115A	Dry Bottom PC Boiler	tangential	ESP cold-side	None	None	Yes	Multiple types
020	Impoundment	FA,BA	Subbit	13115A	Dry Bottom PC Boiler	tangential	ESP cold-side	None	None	Yes	Multiple types
021	Impoundment	FA	Bit	49003A	Dry Bottom PC Boiler	wall-fired opposed	ESP cold-side	None	None	Yes	Multiple types
022	Impoundment	FA	Bit	49003A	Dry Bottom PC Boiler	wall-fired opposed	ESP cold-side	None	None	Yes	Multiple types
023	Impoundment	FA	Bit	49003A	Dry Bottom PC Boiler	wall-fired opposed	ESP cold-side	None	None	Yes	Multiple types
024	Landfill	FA	Bit	49003B	Dry Bottom PC Boiler	wall-fired opposed	ESP cold-side	None	None	None	Combustion-LNB
025	Landfill	FA	Bit	49003B	Dry Bottom PC Boiler	wall-fired opposed	ESP cold-side	None	None	None	Combustion-LNB
026	Impoundment	FA	Bit	49003A	Dry Bottom PC Boiler	wall-fired opposed	ESP cold-side	None	None	Yes	Multiple types
027	Landfill	FGD, FA	Bit	35015A	Dry Bottom PC Boiler	tangential	ESP cold-side	Wet-natural	Mg-Lime	Yes	Combustion-LNB
028	Landfill	FGD, FA	Bit	35015A	Dry Bottom PC Boiler	tangential	ESP cold-side	Wet-natural	Mg-Lime	Yes	Combustion-LNB
029	Landfill	FGD, FA	Bit	35015A	Dry Bottom PC Boiler	tangential	ESP cold-side	Wet-natural	Mg-Lime	Yes	Combustion-LNB

Table 3-2 (Continued)
Leachate Sample Attributes

Sample ID	Source	Byproduct	Source Fuel Type	Site	Source Plant PC Boiler Type	PC Boiler Firing	Source Plant Particulate Collection	Source Plant SO2 Control	Source Plant SO2 Sorbent	Source Plant Flue Gas Cond.	Source Plant NOx Control
030	Impoundment	FA	Bit	35015B	Multiple types	multiple types	ESP cold-side	None	None	None	Combustion-LNB
031	Impoundment	FA	Bit	35015B	Multiple types	multiple types	ESP cold-side	None	None	None	Combustion-LNB
032	Impoundment	FA,BA	Bit	35015B	Multiple types	multiple types	ESP cold-side	None	None	None	Combustion-LNB
037	Impoundment	FA	Bit	33106	Dry Bottom PC Boiler	tangential	ESP cold-side	None	None	Yes	Multiple types
038	Impoundment	FA	Bit	33106	Dry Bottom PC Boiler	tangential	ESP cold-side	None	None	Yes	Multiple types
039	Impoundment	FA	Bit	33106	Dry Bottom PC Boiler	tangential	ESP cold-side	None	None	Yes	Multiple types
042	Impoundment	FA	Bit	33106	Dry Bottom PC Boiler	tangential	ESP cold-side	None	None	Yes	Multiple types
043	Impoundment	FA	Bit	33106	Dry Bottom PC Boiler	tangential	ESP cold-side	None	None	Yes	Multiple types
044	Impoundment	FA	Bit	33106	Dry Bottom PC Boiler	tangential	ESP cold-side	None	None	Yes	Multiple types
049	Impoundment	FA,BA	Bit	33106	Dry Bottom PC Boiler	tangential	ESP cold-side	None	None	Yes	Multiple types
051	Impoundment	FA	Bit	40109	Dry Bottom PC Boiler	tangential	ESP hot-side	None	None	None	Multiple types
052	Impoundment	FA	Bit	40109	Dry Bottom PC Boiler	tangential	ESP hot-side	None	None	None	Multiple types
053	Impoundment	FA	Bit	40109	Dry Bottom PC Boiler	tangential	ESP hot-side	None	None	None	Multiple types
057	Impoundment	FA,BA	Bit	40109	Dry Bottom PC Boiler	tangential	ESP hot-side	None	None	None	Multiple types
059	Impoundment	FA,BA	Bit	40109	Dry Bottom PC Boiler	tangential	ESP hot-side	None	None	None	Multiple types
061	Impoundment	FA	Bit	33104	Dry Bottom PC Boiler	tangential	Multiple types	None	None	None	Postcombustion SCR
062	Impoundment	FA	Bit	33104	Dry Bottom PC Boiler	tangential	Multiple types	None	None	None	Postcombustion SCR
064	Impoundment	FA	Bit	33104	Dry Bottom PC Boiler	tangential	Multiple types	None	None	None	Postcombustion SCR
069	Impoundment	FA,BA	Bit	33104	Dry Bottom PC Boiler	tangential	Multiple types	None	None	None	Postcombustion SCR
070	Impoundment	FA,BA	Bit	33104	Dry Bottom PC Boiler	tangential	Multiple types	None	None	None	Postcombustion SCR
079	Impoundment	FA,OA	Blend	22346	Dry Bottom PC Boiler	multiple types	ESP cold-side	None	None	Yes	Multiple types
082	Impoundment	FA,OA	Blend	22346	Dry Bottom PC Boiler	multiple types	ESP cold-side	None	None	Yes	Multiple types
083	Impoundment	FA	Blend	22347	Dry Bottom PC Boiler	tangential	ESP cold-side	None	None	Yes	Other
084	Impoundment	FA,OA	Blend	22346	Dry Bottom PC Boiler	multiple types	ESP cold-side	None	None	Yes	Multiple types
090	See Notes	FA	Mix	27413	Dry Bottom PC Boiler	multiple types	ESP cold-side	None	None	Yes	Multiple types
091	See Notes	FA	Mix	27413	Dry Bottom PC Boiler	multiple types	ESP cold-side	None	None	Yes	Multiple types
092	See Notes	FA	Mix	27413	Dry Bottom PC Boiler	multiple types	ESP cold-side	None	None	Yes	Multiple types

Table 3-2 (Continued)
Leachate Sample Attributes

Sample ID	Source	Byproduct	Source Fuel Type	Site	Source Plant PC Boiler Type	PC Boiler Firing	Source Plant Particulate Collection	Source Plant SO2 Control	Source Plant SO2 Sorbent	Source Plant Flue Gas Cond.	Source Plant NOx Control
093	Landfill	FA,BA	Subbit	27412	Dry Bottom PC Boiler	wall-fired opposed	ESP cold-side	None	None	None	Combustion-OFA
097	Landfill	FA	Subbit	50212	Dry Bottom PC Boiler	wall-fired	ESP cold-side	None	None	Yes	Multiple types
098	Landfill	FA,BA	Mix	50183	Dry Bottom PC Boiler	multiple types	Multiple types	None	None	Yes	Multiple types
099	Landfill	FA,BA	Mix	50183	Dry Bottom PC Boiler	multiple types	Multiple types	None	None	Yes	Multiple types
101	Landfill	FA,BA	Bit	50408	Dry Bottom PC Boiler	wall-fired	ESP cold-side	None	None	None	Combustion-none
102	Landfill	FA	Bit	50211	Dry Bottom PC Boiler	wall-fired front	Fabric filter	None	None	no data	Combustion-LNB
105	Impoundment	FGD	Lig	34186B	Dry Bottom PC Boiler	tangential	ESP cold-side	Wet-natural	Mg-Lime	None	Multiple types
106	Landfill	FGD,FA,BA	Lig	34186C	Dry Bottom PC Boiler	tangential	ESP cold-side	Wet-natural	Mg-Lime	None	Multiple types
107	Impoundment	FGD	Lig	34186B	Dry Bottom PC Boiler	tangential	ESP cold-side	Wet-natural	Mg-Lime	None	Multiple types
108	Landfill	FA	Lig	34186A	Dry Bottom PC Boiler	tangential	ESP cold-side	Wet-natural	Mg-Lime	None	Multiple types
111	Landfill	FA	Bit	49003B	Dry Bottom PC Boiler	wall-fired opposed	ESP cold-side	None	None	None	Combustion-LNB
112	Landfill	FA	Bit	49003B	Dry Bottom PC Boiler	wall-fired opposed	ESP cold-side	None	None	None	Combustion-LNB
113	Impoundment	FA	Bit	49003A	Dry Bottom PC Boiler	wall-fired opposed	ESP cold-side	None	None	Yes	Multiple types
114	Impoundment	FA	Bit	49003A	Dry Bottom PC Boiler	wall-fired opposed	ESP cold-side	None	None	Yes	Multiple types
115	Impoundment	FA	Bit	49003A	Dry Bottom PC Boiler	wall-fired opposed	ESP cold-side	None	None	Yes	Multiple types
116	Impoundment	FA	Bit	49003A	Dry Bottom PC Boiler	wall-fired opposed	ESP cold-side	None	None	Yes	Multiple types
118	Impoundment	FA,BA	Bit	35015B	Multiple types	multiple types	ESP cold-side	None	None	None	Combustion-LNB
119	Impoundment	FA,BA	Bit	35015B	Multiple types	multiple types	ESP cold-side	None	None	None	Combustion-LNB
120	Landfill	FGD, FA	Bit	35015A	Dry Bottom PC Boiler	tangential	ESP cold-side	Wet-natural	Mg-Lime	Yes	Combustion-LNB
121	Landfill	FGD, FA	Bit	35015A	Dry Bottom PC Boiler	tangential	ESP cold-side	Wet-natural	Mg-Lime	Yes	Combustion-LNB
122	Landfill	FGD, FA	Bit	35015A	Dry Bottom PC Boiler	tangential	ESP cold-side	Wet-natural	Mg-Lime	Yes	Combustion-LNB
123	Landfill	FA	Bit	20094A	Dry Bottom PC Boiler	wall-fired opposed	ESP multiple	None	None	None	Multiple types
124	Landfill	FA,BA	Bit	20094B	Dry Bottom PC Boiler	wall-fired opposed	ESP multiple	None	None	None	Multiple types
126	Impoundment	FA,BA	Subbit	43035	Dry Bottom PC Boiler	wall-fired opposed	ESP hot-side	None	None	None	Combustion-LNB
127	Impoundment	FA,BA	Subbit	43035	Dry Bottom PC Boiler	wall-fired opposed	ESP hot-side	None	None	None	Combustion-LNB
128	Landfill	FGD,FA	Lig	43034	Wet Bottom PC Boiler	wall-fired	ESP cold-side	Wet-inhib	Limestone	None	Multiple types
ES-1	Landfill	FGD,FA	Subbit	31192	Dry Bottom PC Boiler	tangential	Fabric filter	Wet-natural	Limestone	None	Other

Table 3-2 (Continued)
Leachate Sample Attributes

Sample ID	Source	Byproduct	Source Fuel Type	Site	Source Plant PC Boiler Type	PC Boiler Firing	Source Plant Particulate Collection	Source Plant SO2 Control	Source Plant SO2 Sorbent	Source Plant Flue Gas Cond.	Source Plant NOx Control
HN-1	Impoundment	FA,BA	Bit	13115B	Dry Bottom PC Boiler	tangential	ESP cold-side	None	None	Yes	Other
HN-2	Impoundment	FA,BA	Bit	13115B	Dry Bottom PC Boiler	tangential	ESP cold-side	None	None	Yes	Other
SX-1	Impoundment	FA	Blend	25410B	Cyclone		ESP cold-side	None	None	Yes	Combustion-OFA

Notes:
Ash at site 27413 (samples 090, 091, 092) was first sluiced, then managed dry.
QC and duplicate samples not listed

Abbreviations:
Bit = bituminous; Subbit = Subbituminous; Mix = CCP from different units burning different coals; Blend = CCP from a single unit burning two different fuels
PC = pulverized coal; ESP = electrostatic precipitator; OFA = overfired air; LNB = low-NOx burner
FA = fly ash; BA = bottom ash; EA = economizer ash; FGD = flue gas desulfurization sludge; OA = oil ash

Table 3-3
Sample Collection Methods

Sample ID	Site	Source	Byproduct	Point	Method
001	50210	Landfill	FA,BA	Leachate Well	Waterra Pump to Peristaltic
002	50213	Landfill	FA	Lysimeter	Bladder Pump
003	50213	Landfill	FA	Lysimeter	Bladder Pump
004	50183	Landfill	FA,BA	Leachate Collection System	Peristaltic Pump
005	50183	Landfill	FA,BA	Leachate Well	Waterra Pump to Peristaltic
006	23223A	Landfill	SDA	Leachate Collection System	Peristaltic Pump
007	23223B	Impoundment	FGD	Leachate Well	Bladder Pump
008	23223B	Impoundment	FGD	Leachate Well	Bladder Pump
009	23223B	Impoundment	FGD	Ash/Water Interface	Peristaltic Pump
010	23214	Landfill	FA	Leachate Collection System	Bailer to Peristaltic
012	14093	Impoundment	FA	Leachate Well	Waterra Pump to Peristaltic
013	14093	Impoundment	FA	Leachate Well	Peristaltic Pump
014	14093	Impoundment	FA	Leachate Well	Peristaltic Pump
015	25410A	Impoundment	FA,BA	Ash/Water Interface	Peristaltic Pump
016	25410A	Impoundment	FA,BA	Drive Point Piezometer	Peristaltic Pump
017	13115A	Impoundment	FA,BA	Ash/Water Interface	Peristaltic Pump
018	13115B	Impoundment	FA,BA	Leachate Well	Peristaltic Pump
019	13115A	Impoundment	FA	Sluice Line	Dip Sampler to Peristaltic Pump
020	13115A	Impoundment	FA,BA	Outfall	Peristaltic Pump
021	49003A	Impoundment	FA	Drive Point Piezometer	Peristaltic Pump
022	49003A	Impoundment	FA	Ash/Water Interface	Peristaltic Pump
023	49003A	Impoundment	FA	Drive Point Piezometer	Peristaltic Pump
024	49003B	Landfill	FA	Leachate Collection System	Dip Sampler to Peristaltic Pump
025	49003B	Landfill	FA	Leachate Collection System	Dip Sampler to Peristaltic Pump
026	49003A	Impoundment	FA	Outfall	Dip Sampler to Peristaltic Pump
027	35015A	Landfill	FGD, FA	Leachate Collection System	Dip Sampler to Peristaltic Pump
028	35015A	Landfill	FGD, FA	Leachate Collection System	Dip Sampler to Peristaltic Pump
029	35015A	Landfill	FGD, FA	Leachate Collection System	Dip Sampler to Peristaltic Pump
030	35015B	Impoundment	FA	Seep	Dip Sampler to Peristaltic Pump
031	35015B	Impoundment	FA	Drive Point Piezometer	Peristaltic Pump
032	35015B	Impoundment	FA,BA	Outfall	Peristaltic Pump
037	33106	Impoundment	FA	Drive Point Piezometer	Peristaltic Pump
038	33106	Impoundment	FA	T-Handle Probe	Peristaltic Pump
039	33106	Impoundment	FA	Drive Point Piezometer	Peristaltic Pump
042	33106	Impoundment	FA	Sluice Line	Peristaltic Pump
043	33106	Impoundment	FA	Sluice Line	Peristaltic Pump
044	33106	Impoundment	FA	Outfall	Peristaltic Pump
049	33106	Impoundment	FA,BA	Ash/Water Interface	Peristaltic Pump
051	40109	Impoundment	FA	Sluice Line	Peristaltic Pump
052	40109	Impoundment	FA	Drive Point Piezometer	Peristaltic Pump
053	40109	Impoundment	FA	T-Handle Probe	Peristaltic Pump
057	40109	Impoundment	FA,BA	Ash/Water Interface	Peristaltic Pump
059	40109	Impoundment	FA,BA	Outfall	Peristaltic Pump

Table 3-3 (Continued)
Sample Collection Methods

Sample ID	Site	Source	Byproduct	Point	Method
061	33104	Impoundment	FA	Drive Point Piezometer	Peristaltic Pump
062	33104	Impoundment	FA	Drive Point Piezometer	Peristaltic Pump
064	33104	Impoundment	FA	Sluice Line	Peristaltic Pump
069	33104	Impoundment	FA,BA	Ash/Water Interface	Peristaltic Pump
070	33104	Impoundment	FA,BA	Outfall	Peristaltic Pump
079	22346	Impoundment	FA,OA	Leachate Well	Peristaltic Pump
082	22346	Impoundment	FA,OA	Ash/Water Interface	Peristaltic Pump
083	22347	Impoundment	FA	Ash/Water Interface	Peristaltic Pump
084	22346	Impoundment	FA,OA	Leachate Well	Peristaltic Pump
090	27413	See Notes	FA	Leachate Well	Peristaltic Pump
091	27413	See Notes	FA	Leachate Well	Peristaltic Pump
092	27413	See Notes	FA	Leachate Well	Peristaltic Pump
093	27412	Landfill	FA,BA	Soil Boring	Core Extract
097	50212	Landfill	FA	Leachate Collection System	Peristaltic Pump
098	50183	Landfill	FA,BA	Leachate Collection System	Peristaltic Pump
099	50183	Landfill	FA,BA	Leachate Well	Waterra Pump to Peristaltic
101	50408	Landfill	FA,BA	Leachate Collection System	Peristaltic Pump
102	50211	Landfill	FA	Leachate Collection System	Peristaltic Pump
105	34186B	Impoundment	FGD	Ash/Water Interface	Peristaltic Pump
106	34186C	Landfill	FGD,FA,BA	Leachate Collection System	Dip Sampler to Peristaltic Pump
107	34186B	Impoundment	FGD	Sluice Line	Peristaltic Pump
108	34186A	Landfill	FA	Seep	Peristaltic Pump
111	49003B	Landfill	FA	Leachate Collection System	Dip Sampler to Peristaltic Pump
112	49003B	Landfill	FA	Leachate Collection System	Dip Sampler to Peristaltic Pump
113	49003A	Impoundment	FA	T-Handle Probe	Peristaltic Pump
114	49003A	Impoundment	FA	T-Handle Probe	Peristaltic Pump
115	49003A	Impoundment	FA	Ash/Water Interface	Peristaltic Pump
116	49003A	Impoundment	FA	Outfall	Dip Sampler to Peristaltic Pump
118	35015B	Impoundment	FA,BA	Ash/Water Interface	Peristaltic Pump
119	35015B	Impoundment	FA,BA	Outfall	Peristaltic Pump
120	35015A	Landfill	FGD, FA	Leachate Collection System	Dip Sampler to Peristaltic Pump
121	35015A	Landfill	FGD, FA	Leachate Collection System	Dip Sampler to Peristaltic Pump
122	35015A	Landfill	FGD, FA	Leachate Collection System	Dip Sampler to Peristaltic Pump
123	20094A	Landfill	FA	Soil Boring	Core Extract
124	20094B	Landfill	FA,BA	Soil Boring	Core Extract
126	43035	Impoundment	FA,BA	Seep	Dip Sampler to Peristaltic Pump
127	43035	Impoundment	FA,BA	Seep	Dip Sampler to Peristaltic Pump
128	43034	Landfill	FGD,FA	Leachate Collection System	Peristaltic Pump
ES-1	31192	Landfill	FGD,FA	Soil Boring	Core Extract

Table 3-3 (Continued)
Sample Collection Methods

Sample ID	Site	Source	Byproduct	Point	Method
HN-1	13115B	Impoundment	FA,BA	Soil Boring	Core Extract
HN-2	13115B	Impoundment	FA,BA	Soil Boring	Core Extract
SX-1	25410B	Impoundment	FA	Soil Boring	Core Extract

Notes:
Ash at site 27413 (samples 090, 091, 092) was first sluiced, then managed dry.
QC and duplicate samples not listed

Abbreviations:
FA = fly ash; BA = bottom ash; EA = economizer ash; FGD = flue gas desulfurization sludge; OA = oil ash

4
LEACHATE QUALITY AT CCP MANAGEMENT FACILITIES

Analytical data were entered in a database and reviewed for outliers; anomalous values were checked and corrected, if appropriate, by the Trent University laboratory. Data are summarized in this section; all results are listed in Appendix A.

Many of the data summaries that follow are based on box-whisker plots, which graphically show the distribution of concentrations for a given group of data (Figure 4-1). Non-detect values were plotted at their detection limit.

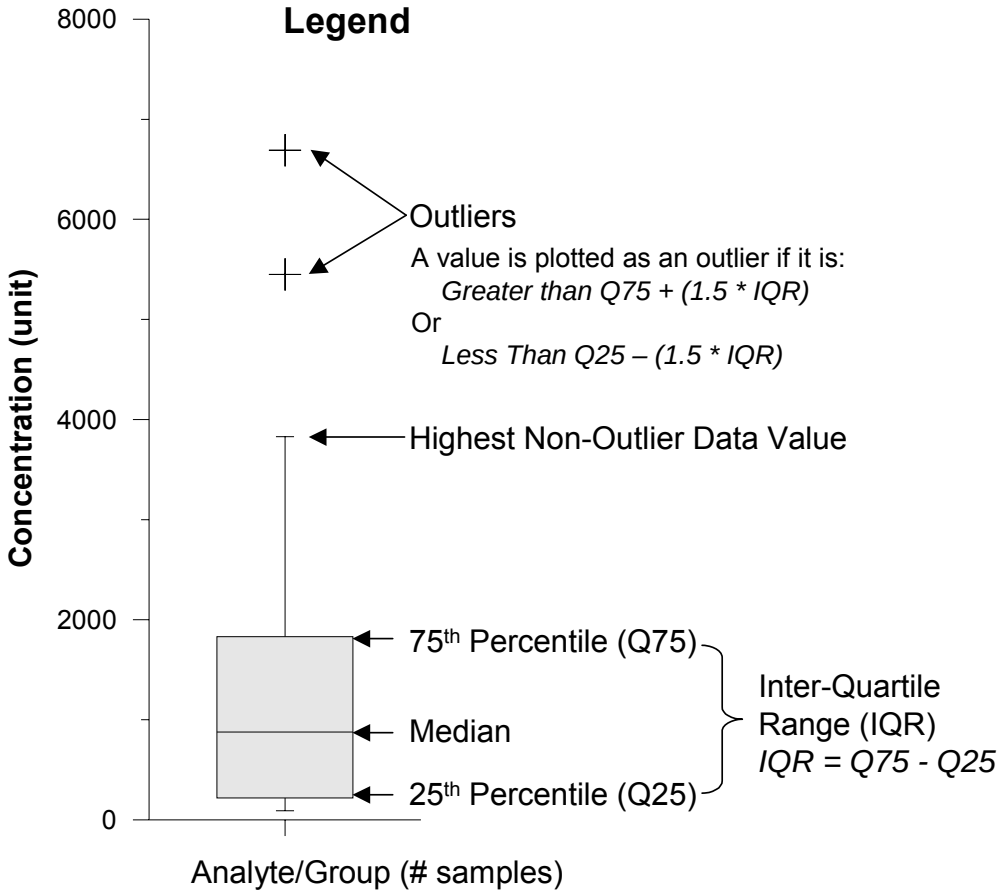

Figure 4-1
Legend for box-whisker plots

Major Constituents

Ash Leachate

The collected leachate samples were generally moderately to strongly oxidizing (positive Eh compared to the standard hydrogen electrode) and moderately to strongly alkaline (Figure 4-2). The subbituminous/lignite ash samples had a slightly higher median pH than bituminous ash, and the highest pH values were from sites receiving subbituminous/lignite ash. The lowest Eh and lowest pH samples were from impoundments.

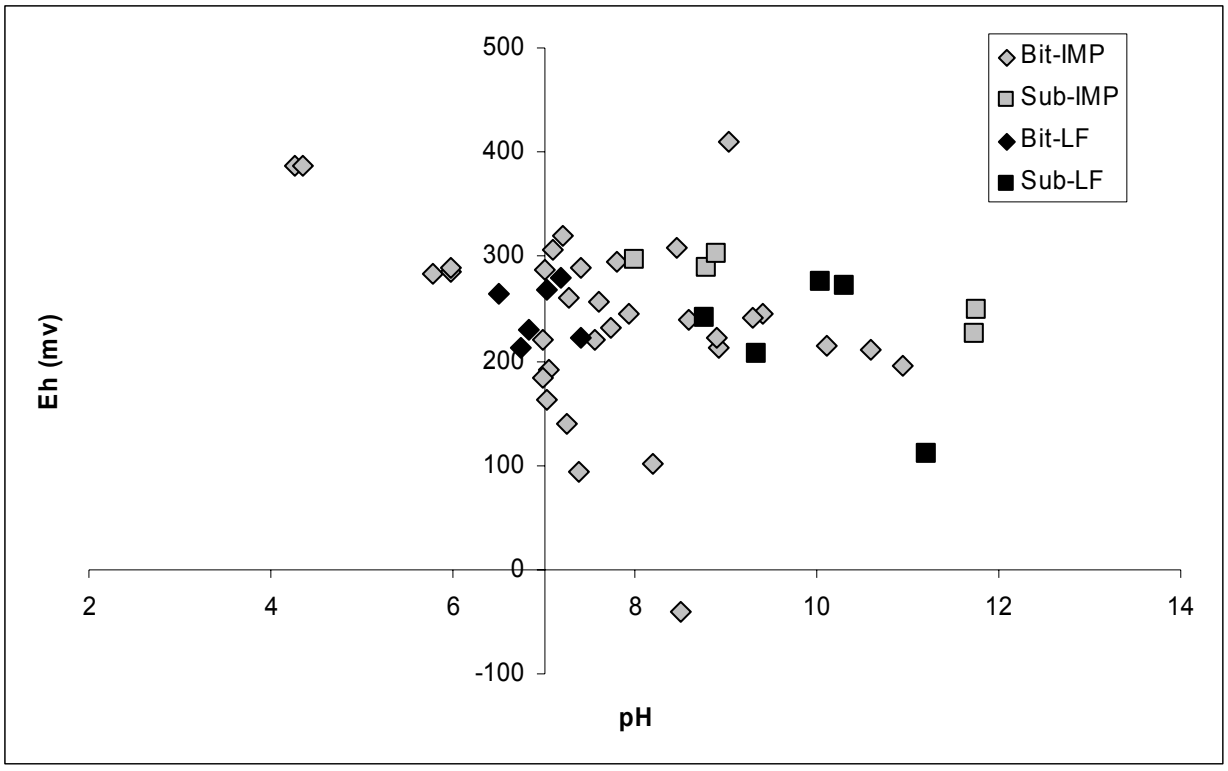

Figure 4-2
Eh-pH diagram for ash samples

Sulfate was the only constituent in the ash leachate samples with a median concentration greater than 100 mg/L (339 mg/L; Figure 4-3, Table 4-1). Most samples had concentrations greater than 100 mg/L, and more than 25 percent of the samples had concentrations greater than 1,000 mg/L. The highest concentration for any constituent in ash leachate was for sulfate in sample 002 (6,690 mg/L; Table 4-1), a leachate sample collected from a landfill receiving subbituminous coal ash.

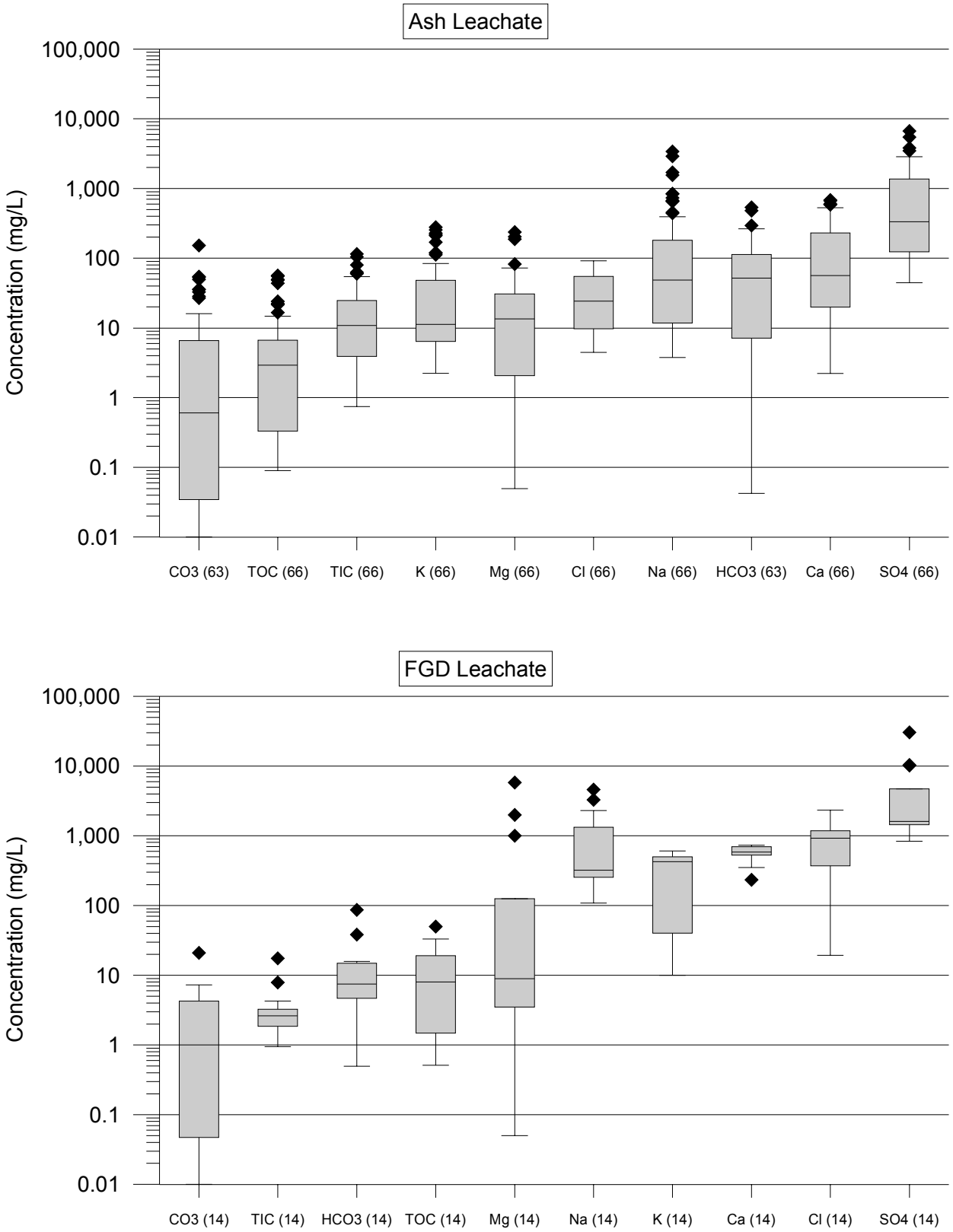

Figure 4-3
Ranges for major constituents in CCP leachate

More than 25 percent of the calcium, bicarbonate, and sodium concentrations in ash leachate were greater than 100 mg/L, and several sodium concentrations were greater than 1,000 mg/L, with the highest being 3,410 mg/L in sample 002.

Most of the ash leachate sample anion concentrations were dominated by sulfate (Figure 4-4). All of the exceptions were impoundment samples, three of which were porewater (samples 018, 061, and 084) while the other seven samples were pond, sluice, or outfall water. All except one of the exceptions had relatively low sulfate concentrations (two less than 200 mg/L and seven less than 100 mg/L), while sample 018 had a close to median sulfate concentration (339 mg/L) and a relatively high bicarbonate concentration (535 mg/L). All of the exceptions tended toward carbonate/bicarbonate type.

Cation concentrations in the leachate samples were usually dominated by calcium or calcium with varying percentages of sodium and magnesium when the source coal was bituminous, and by sodium when the source coal was subbituminous/lignite. Samples 017, 019, and 020 were exceptions to this relationship, having roughly equal percentages of the cations. The sodium-dominated subbituminous/lignite samples were collected from landfills, while samples 017, 019, and 020 were collected from an impoundment that receives more bottom ash than fly ash.

Table 4-1
Summary Statistics of CCP Leachate Analytical Results

	Ash Leachate Samples					FGD Leachate Samples				
	Count	Min	Median	Max	% BDL	Count	Min	Median	Max	% BDL
Ag (ug/L)	67	<0.2	<0.2	2.0	93%	14	<0.20	<0.20	<0.20	100%
Al (ug/L)	67	<2.0	114	44,400	16%	14	<24	179	890	14%
As (ug/L)	67	1.4	25	1,380	0%	14	11	28	230	0%
B (ug/L)	67	207	2,160	112,000	0%	14	1,450	9,605	98,500	0%
Ba (ug/L)	67	<18	108	657	4%	14	<30	73	158	7%
Be (ug/L)	67	<0.2	<0.4	8.6	94%	14	<0.20	<0.80	1.5	93%
Ca (mg/L)	66	<2.2	55	681	2%	14	234	589	730	0%
Cd (ug/L)	67	<0.2	1.5	65	12%	14	0.50	1.8	13	0%
Cl (mg/L)	66	4.5	25	92	0%	14	19	921	2,330	0%
Co (ug/L)	67	<0.04	1.0	133	31%	14	<0.028	1.0	78	36%
CO_3 (mg/L)	63	<0.01	0.60	152	13%	14	<0.010	1.0	21	21%
Cr (ug/L)	67	<0.2	0.60	5,100	45%	14	<0.20	<0.50	53	64%
Cu (ug/L)	67	<0.2	3.0	494	19%	14	<0.26	2.6	44	14%
Fe (ug/L)	67	<3	<50	25,600	52%	14	<4.6	<50	1,200	71%
H_2CO_3 (mg/L)	63	<0.01	<0.01	3.4	87%	14	<0.010	<0.010	0.041	93%
HCO_3 (mg/L)	63	0.042	53	535	0%	14	0.50	7.5	87	0%
Hg (ng/L)	22	0.25	3.8	61	0%	8	0.82	8.3	79	0%
K (mg/L)	66	<2.2	11	277	3%	14	10	425	609	0%
Li (ug/L)	67	<1.0	129	23,600	13%	14	<20	3,055	7,070	14%
Mg (mg/L)	66	<0.05	13	236	8%	14	<0.050	8.9	5,810	14%
Mn (ug/L)	67	<0.1	55	4,170	21%	14	<0.10	113	1,170	14%
Mo (ug/L)	67	<8.2	405	39,600	3%	14	164	341	60,800	0%
Na (mg/L)	66	3.8	52	3,410	0%	14	108	322	4,630	0%
Ni (ug/L)	67	<0.6	5.8	189	13%	14	<2.0	3.4	597	36%
Pb (ug/L)	67	<0.1	<0.20	8.0	73%	14	<0.14	<0.20	3.5	64%
Sb (ug/L)	67	<0.1	2.4	59	3%	14	<0.10	1.00	22	29%
Se (ug/L)	67	0.071	19	1,760	0%	14	1.1	6.2	2,360	0%
Si (ug/L)	67	221	4,645	19,000	0%	14	400	2,480	45,400	0%
SO_4 (mg/L)	66	45	339	6,690	0%	14	836	1,615	30,500	0%
Sr (ug/L)	67	<30	829	12,000	1%	14	1,500	5,230	16,900	0%
TIC (mg/L)	66	0.75	11	115	0%	14	0.95	2.6	18	0%
Tl (ug/L)	67	<0.1	0.36	18	46%	14	<0.10	<0.22	2.9	86%
TOC (mg/L)	66	<0.09	3.3	57	24%	14	0.51	8.0	50	0%
U (ug/L)	67	<0.01	1.2	61	19%	14	<0.010	0.20	16	36%
V (ug/L)	67	<0.42	45	5,020	3%	14	<0.69	4.1	400	21%
Zn (ug/L)	67	<1.5	5.0	289	46%	14	<2.0	<5.0	68	57%
DO (%)	61	0.10	35	165	0%	14	0.20	14	95	0%
ORP (mV)	63	-41	241	411	2%	14	1.5	201	356	0%
pH (SU)	64	4.3	7.9	12	0%	14	6.2	9.0	12	0%
EC (µmho/cm)	64	174	990	12,760	0%	14	2,190	6,461	26,140	0%
Temp (ºC)	64	10	21	36	0%	14	9.9	17	27	0%

Notes:
Dissolved oxygen (DO) is percent saturation

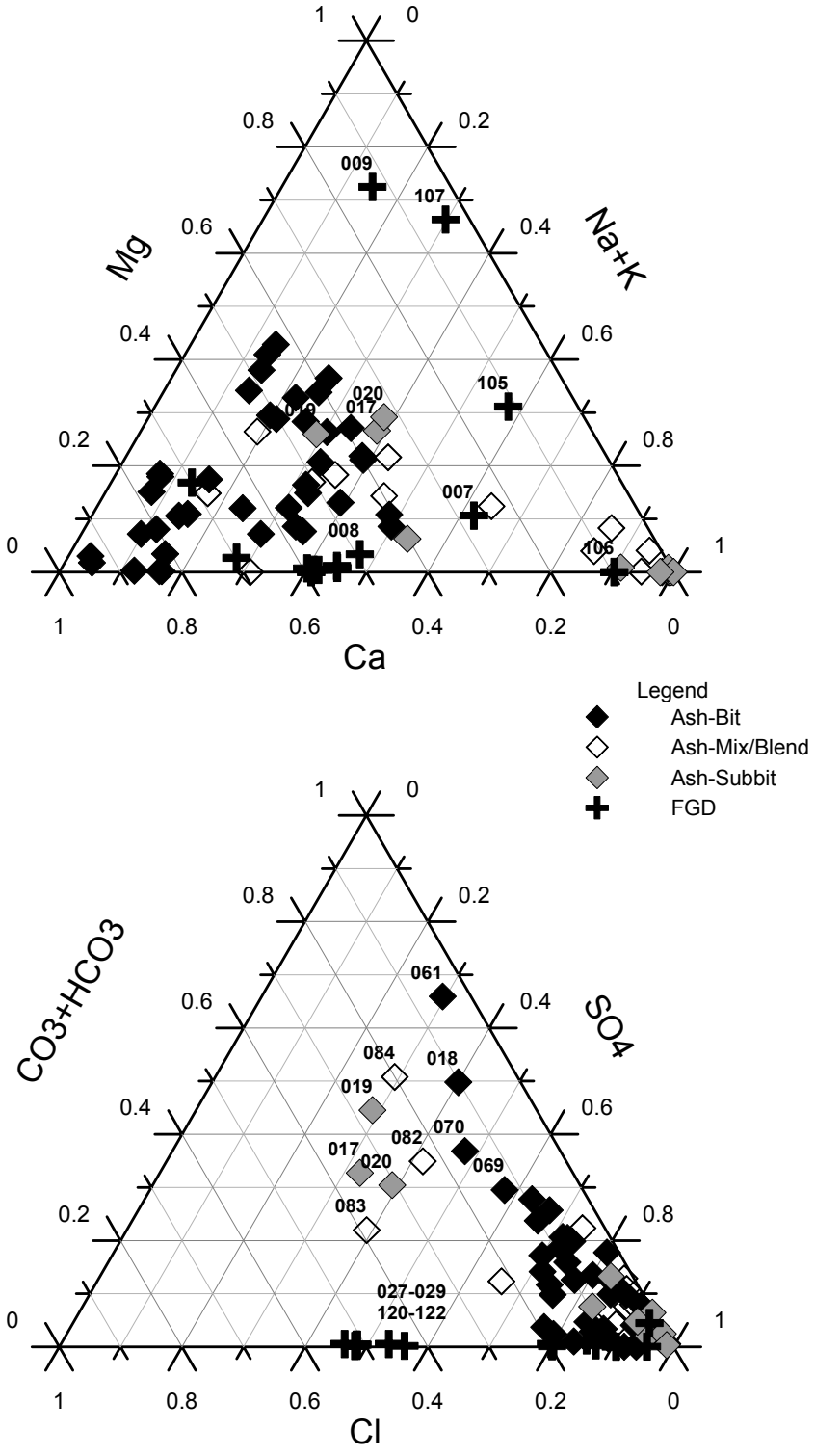

Figure 4-4
Ternary plots showing relative percentages of major constituents in ash leachate

FGD Leachate

Leachate samples collected from FGD product management sites (FGD leachates) were moderately to strongly oxidizing (positive Eh compared to the standard hydrogen electrode) and moderately to strongly alkaline (Figure 4-5). Landfill samples, as a group, were less oxic and more alkaline than impoundment samples, although the lowest Eh value was for an impoundment.

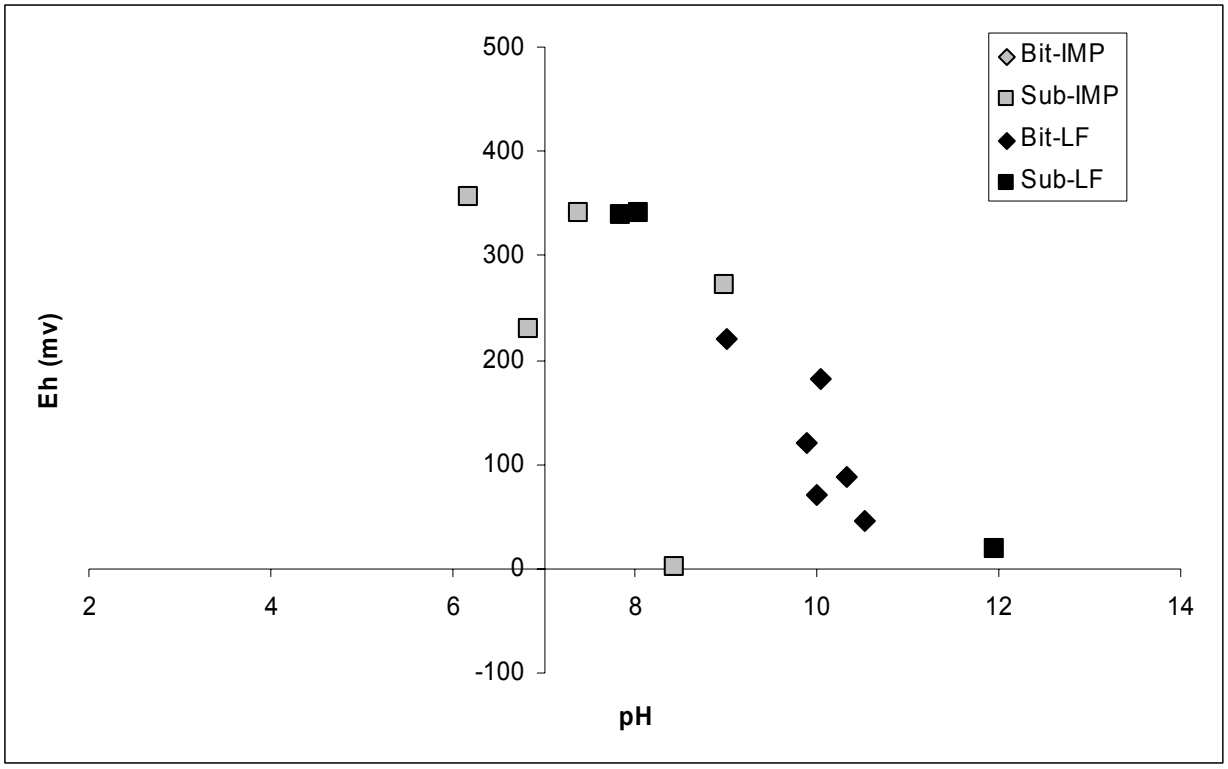

Figure 4-5
Eh-pH diagram for FGD leachate samples

Concentrations of most major constituents (specifically, calcium, chloride, potassium, sodium, and sulfate) in FGD leachate were higher than in ash leachate (Figure 4-3). The median sulfate concentrations was 1,615 mg/L, and the maximum sulfate concentration was 30,500 mg/L, which was the highest single analytical result returned from the field leachate sampling. The high sulfate concentration was obtained from an impoundment where sluice water is recirculated.[2]

[2] Two of the 14 FGD leachate samples were from impoundments where sluice water is recirculated; however, the median concentrations from FGD sites without recirculation are also significantly higher than the ash leachate medians.

More than 25 percent of the chloride and sodium concentrations were greater than 1,000 mg/L, and median concentrations of chloride, calcium, potassium, and sodium were greater than 100 mg/L. Overall, the FGD leachate samples have higher concentrations of chloride and potassium, relative to the other major constituents, than ash leachate.

All of the FGD leachate samples from plants burning subbituminous/lignite coal were dominated by sulfate (Figure 4-4), while the six samples (027-029, 120-122) from a plant that burned bituminous coal had equal percentages of sulfate and chloride—sulfate concentrations were relatively low in these samples.[3] This plant (35015A) has a wet FGD system that uses magnesium-lime as sorbent, similar to some of the other FGD systems from which leachate samples were collected (Table 3-1).

Cation ratios in FGD leachate samples varied considerably, even among samples collected from the same site, largely due to varying magnesium concentrations. For example, samples 007, 008, and 009, all from the 23223B site, ranged from calcium-sodium to magnesium-sodium, primarily based on a variation in magnesium concentrations. Samples 105 and 107, both from the 34186B site, exhibited a similar range in cation ratios, which was also based on varying magnesium concentrations. However, there was no clear relationship between FGD sorbent, coal type, and cation chemistry in the FGD leachate samples.

Minor and Trace Elements

Box-whisker plots of minor and trace elements in ash and FGD leachate are sorted by median concentration, from highest concentration on the right to lowest concentration on the left.

Ash Leachate

Silica and boron had median concentrations higher than 1,000 μg/L in the ash leachate field samples (Figure 4-6). Median concentrations of strontium, molybdenum, lithium, aluminum, and barium were greater than 100 μg/L (Figure 4-6), while median concentrations of chromium, beryllium, thallium, silver, lead, and mercury were lower than 1 μg/L (Figure 4-7). Silver, beryllium, and lead were rarely detected (26 percent of the samples or less).

[3] Due to the low number of samples, the FGD leachate results were not differentiated by source coal in Figure 4-4.

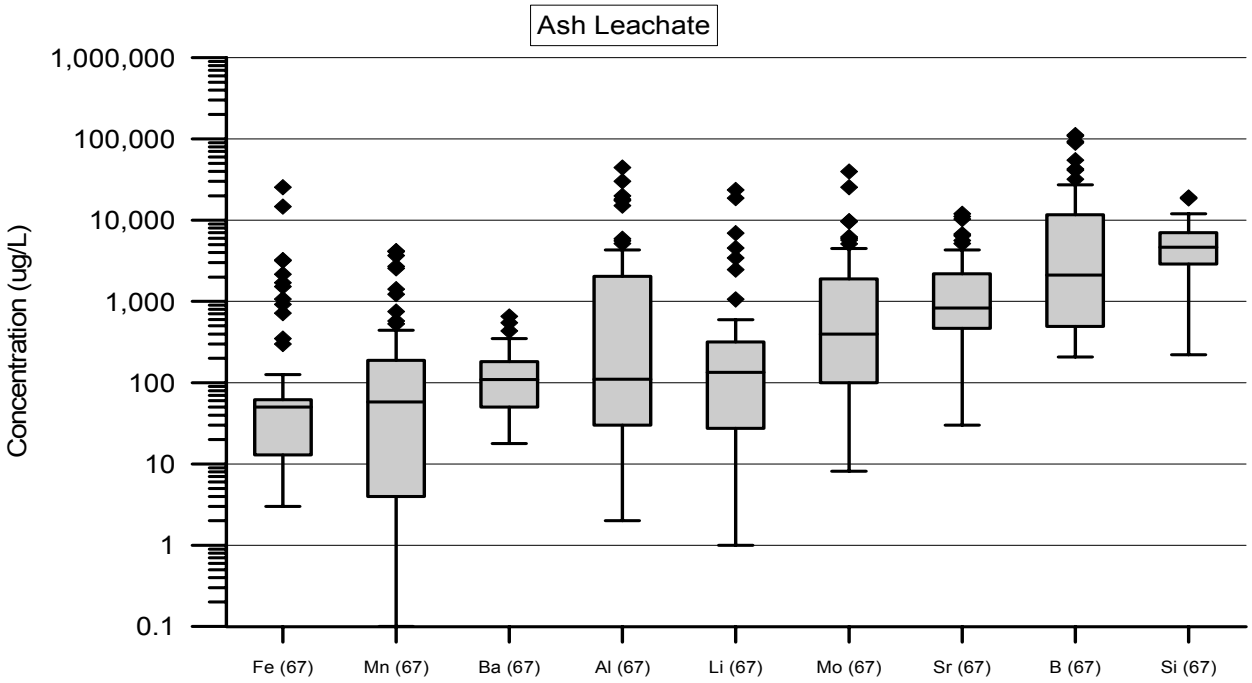

Figure 4-6
Ranges of minor constituents in ash leachate

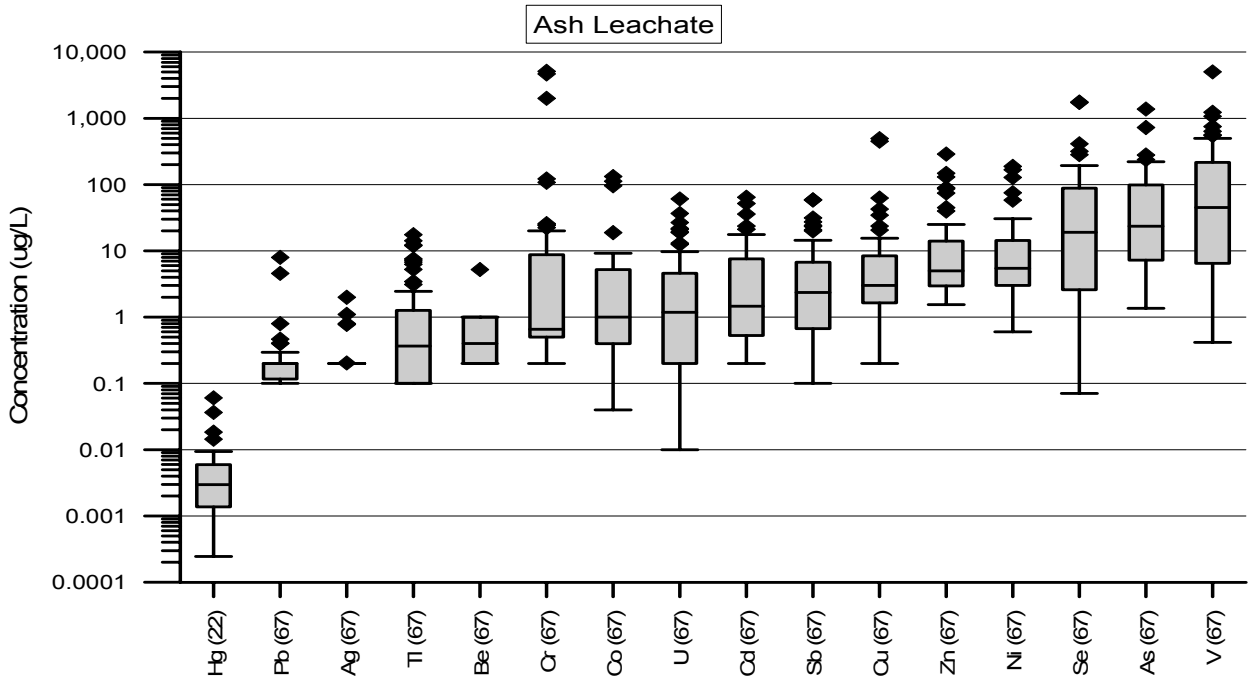

Figure 4-7
Ranges of trace constituents in ash leachate

FGD Leachate

Boron, strontium, lithium, and silica had median concentrations greater than 1,000 µg/L in the FGD field leachate samples (Figure 4-8). Median concentrations of molybdenum, aluminum, and manganese were greater than 100 µg/L (Figure 4-8), while median concentrations of chromium, beryllium, thallium, silver, lead, and mercury were lower than 1 µg/L (Figure 4-9). Silver was not detected in the 14 FGD leachate samples, and beryllium, chromium, iron, lead, and thallium, were detected in less than 40 percent of the samples (Table 4-1).

The relative concentrations of minor and trace elements in FGD leachate were somewhat different than in ash leachate. Median concentrations of boron, strontium, and lithium in FGD leachate were a factor of 3 or more higher than in ash leachate, while concentrations of selenium and vanadium were a factor of 3 or more higher in ash leachate than in FGD leachate (Figure 4-10). Median concentrations of uranium and thallium were also a factor of 3 or more higher in the ash leachate, but the concentrations were very low (1 µg/L or less) in both leachates.

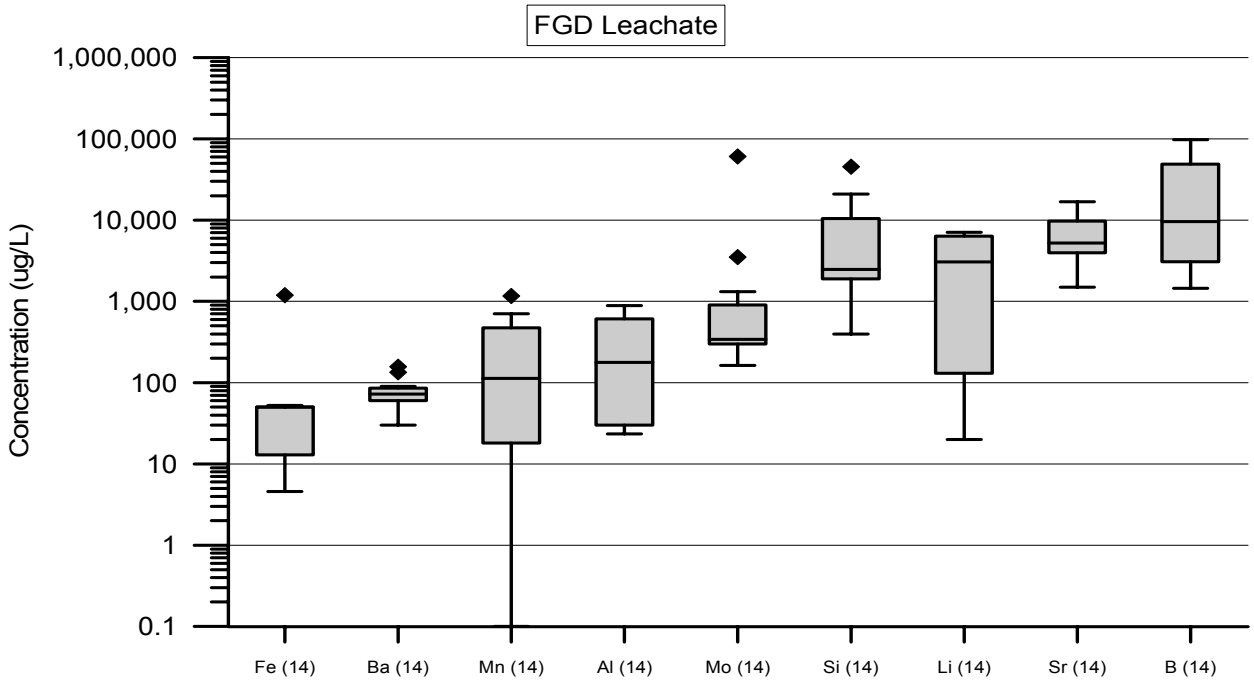

Figure 4-8
Ranges of minor constituents in FGD leachate

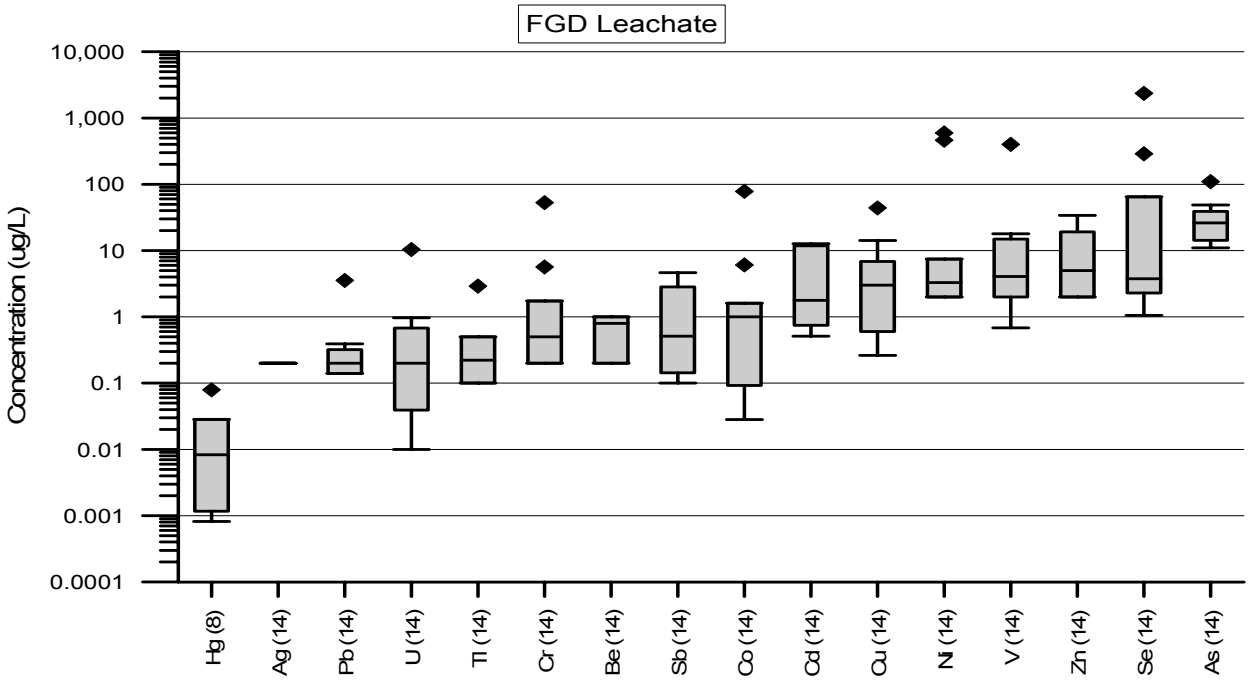

Figure 4-9
Ranges of trace constituents in FGD leachate

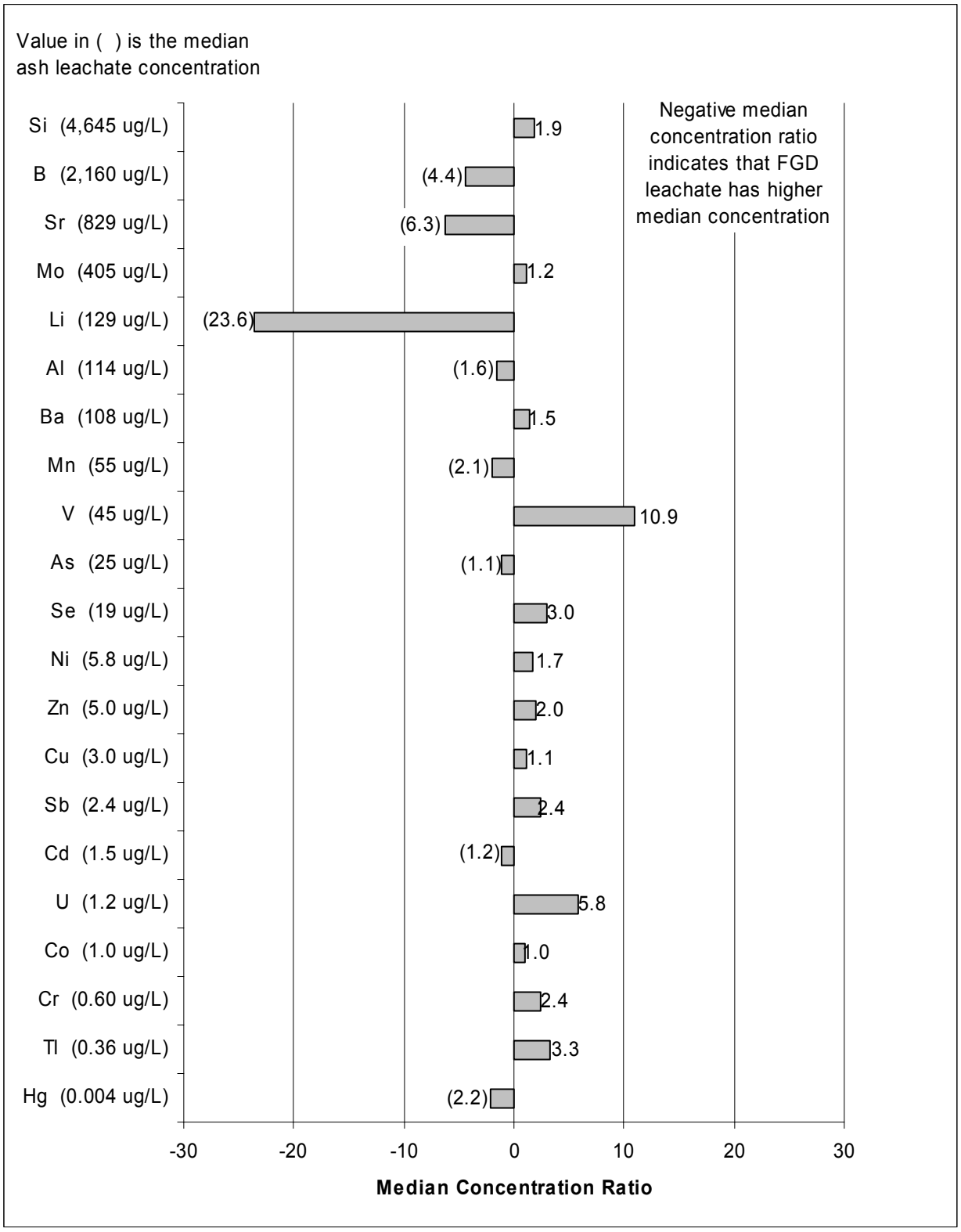

Figure 4-10
Comparison of median concentrations of minor and trace elements in ash and FGD leachate

Comparison of Ash Leachate Concentrations to Site and Plant Attributes

Leachate concentrations were compared as a function of source coal type and management method in order to evaluate the differences in leachate quality. Samples from multiple sites are required for such a comparison to be meaningful. As a result, this comparison focused on ash samples because five or more samples from two or more sites were available for each comparison (Table 4-2). Summary statistics listing the count, minimum, median, and maximum concentration of each analyte by management type (landfill, impoundment), and source coal (bituminous, subbituminous/lignite) are listed in Table 4-3 for ash leachate and Table 4-4 for FGD leachate.

Table 4-2
Sample (A) and Site (B) Categories

A. Sample Count		Source Coal					
		Bit	Blend	Lig	Mix	Subbit	total
Ash	Impoundment	36	7	0	0	5	48
	Landfill	6	0	1	5	4	16
	Other	0	0	0	3	0	3
	total	42	7	1	8	9	67
FGD	Impoundment	0	0	2	0	3	5
	Landfill	6	0	2	0	1	9
	total	6	0	4	0	4	14
	All	**48**	**7**	**5**	**8**	**13**	**81**

B. Site Count		Source Coal					
		Bit	Blend	Lig	Mix	Subbit	total
Ash	Impoundment	7	4	0	0	2	13
	Landfill	3	0	1	2	3	9
	Other	0	0	0	1	0	1
	total	10	4	1	3	5	23
FGD	Impoundment	0	0	1	0	1	2
	Landfill	1	0	2	0	1	4
	total	1	0	3	0	2	6
	All	**11**	**4**	**4**	**3**	**7**	**29**

Table 4-3
Statistical Summary of Ash Leachate Samples by Management Method and Coal Type

	Landfill				Landfill				Impoundment				Impoundment			
	Bituminous				Subbituminous/Lignite				Bituminous				Subbituminous/Lignite			
	Count	min	med	max	Count	min	med	max	Count	min	med	max	Count	min	med	max
Ag (ug/L)	6	<0.2	<0.2	<0.2	5	<0.2	<0.2	0.78	36	<0.2	<0.2	2.0	5	<0.2	<0.2	<0.2
Al (ug/L)	6	<2	7.5	52	5	81	2,680	17,500	36	<5.9	62	15,100	5	730	4,190	5,920
As (ug/L)	6	1.4	6.2	11	5	4.1	45	84	36	5.1	58	1,380	5	4.1	5.1	6.4
B (ug/L)	6	11,100	23,050	89,500	5	6,080	18,400	41,500	36	207	1,085	112,000	5	470	860	3,890
Ba (ug/L)	6	23	45	50	5	<18	18	63	36	<30	141	545	5	36	140	350
Be (ug/L)	6	<0.2	<0.2	<0.8	5	<0.2	<1	<1	36	<0.2	<0.4	8.6	5	<0.2	<1	<1
Ca (mg/L)	5	235	405	431	5	6.3	19	596	36	12	51	681	5	<2.5	43	81
Cd (ug/L)	6	4.6	10	36	5	7.6	11	52	36	<0.2	1.2	21	5	<0.3	<0.3	2.1
Cl (mg/L)	5	15	29	73	5	11	28	92	36	4.5	15	87	5	31	72	85
Co (ug/L)	6	0.072	9.1	113	5	<0.42	3.3	133	36	<0.2	1.5	22	5	<0.04	<1	1.1
CO_3 (mg/L)	5	0.025	0.11	0.18	5	2.5	50	152	34	<0.01	0.13	16	5	1.1	4.4	36
Cr (ug/L)	6	<0.2	0.17	20	5	0.48	2,000	5,100	36	<0.2	<0.5	29	5	0.66	2.8	108
Cu (ug/L)	6	<0.91	1.1	2.8	5	1.6	43	494	36	<0.38	1.9	452	5	2.4	7.1	12
Fe (ug/L)	6	<8	34	90	5	<3.0	<50	46	36	<5	10	14,700	5	<25	<50	<50
H_2CO_3 (mg/L)	5	<0.01	<0.01	0.020	5	<0.01	<0.01	<0.01	34	<0.01	<0.01	3.4	5	<0.01	<0.01	<0.01
HCO_3 (mg/L)	5	100	229	265	5	1.0	108	481	34	0.042	28	535	5	1.1	110	241
Hg (ng/L)	2	2.1	3.0	3.8	3	14	18	37	7	0.38	1.4	5.2	2	5.4	7.4	9.4
K (mg/L)	5	23	170	219	5	73	80	120	36	<2.2	9.2	277	5	5.5	7.7	40
Li (ug/L)	6	431	5,740	23,600	5	<4.4	<20	27	36	30	213	1,060	5	<7.0	<20	16
Mg (mg/L)	5	69	188	236	5	0.53	6.7	57	36	0.080	6.8	72	5	<0.05	21	28
Mn (ug/L)	6	72	2,060	4,110	5	<1.5	1.5	7.7	36	<0.2	72	4,170	5	<0.2	<4	14
Mo (ug/L)	6	751	3,280	9,630	5	2,680	5,720	25,400	36	8.2	214	6,030	5	<30	80	524
Na (mg/L)	5	80	188	455	5	840	1,700	3,410	36	3.8	19	72	5	53	56	653
Ni (ug/L)	6	3.0	18	189	5	2.2	8.0	75	36	<0.6	7.1	72	5	<0.6	3.7	7.1
Pb (ug/L)	6	<0.12	<0.14	0.12	5	<0.2	0.29	0.29	36	<0.1	<0.15	8.0	5	<0.14	<0.2	0.21
Sb (ug/L)	6	0.14	2.5	9.1	5	0.67	0.90	5.2	36	0.29	6.1	59	5	0.24	0.48	0.62
Se (ug/L)	6	0.67	49	91	5	6.6	413	1,760	36	0.071	13	283	5	1.8	2.5	181
Si (ug/L)	6	2,300	6,075	9,400	5	221	1,540	9,900	36	700	4,715	18,500	5	2,200	3,400	10,300

Table 4-3 (Continued)
Statistical Summary of Ash Leachate Samples by Management Method and Coal Type

	Landfill				Landfill				Impoundment				Impoundment			
	Bituminous				Subbituminous/Lignite				Bituminous				Subbituminous/Lignite			
	Count	min	med	max	Count	min	med	max	Count	min	med	max	Count	min	med	max
SO_4 (mg/L)	5	845	2,350	2,440	5	2,870	3,830	6,690	36	45	171	1,830	5	91	131	1,120
Sr (ug/L)	6	1,320	4,600	10,300	5	<30	303	12,000	36	170	671	5,610	5	530	649	1,830
TIC (mg/L)	5	24	55	80	5	1.7	32	105	36	0.75	5.5	115	5	5.9	22	49
Tl (ug/L)	6	<0.1	0.47	5.3	5	<0.1	<0.1	<0.5	36	<0.1	0.68	18	5	<0.1	<0.1	<0.1
TOC (mg/L)	5	1.3	4.1	4.6	5	5.3	49	55	36	<0.09	0.64	22	5	0.40	6.0	7.9
U (ug/L)	6	7.4	19	37	5	0.22	5.7	21	36	<0.1	0.70	61	5	<0.02	1.1	1.2
V (ug/L)	6	<0.83	3.1	44	5	3.6	635	5,020	36	2.6	39	754	5	10	17	236
Zn (ug/L)	6	<2	45	289	5	<2	<5	12	36	<2	8.7	90	5	<2	8.4	11
DO (%)	6	16	53	95	5	0.20	14	87	34	2.9	40	165	5	1.6	4.5	35
ORP (mV)	6	213	247	280	5	111	240	276	33	41	240	409	5	225	289	303
pH (SU)	6	6.5	6.9	7.4	5	8.8	10	11	34	4.3	7.6	11	5	8.0	8.9	12
EC (umho/cm)	6	2,000	3,682	4,915	5	6,174	7,690	12,760	34	174	578	2,980	5	680	990	4,020
Temp (°C)	6	14	15	17	5	11	17	22	34	10	22	32	5	16	30	36

Table 4-4
Statistical Summary of FGD Leachate Samples by Management Method and Coal Type

	Landfill				Landfill				Impoundment*			
	Bituminous				Subbituminous/Lignite				Subbituminous/Lignite			
	Count	min	med	max	Count	min	med	max	Count	min	med	max
Ag (ug/L)	6	<0.2	<0.2	<0.2	3	<0.2	<0.2	<0.2	5	<0.2	<0.2	<1
Al (ug/L)	6	<24	149	229	3	<26	26	608	5	31	610	890
As (ug/L)	6	11	28	49	3	12	14	110	5	17	29	230
B (ug/L)	6	1,450	2,950	3,260	3	7,310	11,900	15,600	5	26,800	50,200	98,500
Ba (ug/L)	6	58	63	80	3	70	86	134	5	<30	75	158
Be (ug/L)	6	<0.2	<0.5	<0.8	3	<0.2	<0.2	<1	5	<0.2	<1	1.5
Ca (mg/L)	6	669	704	730	3	234	351	528	5	524	570	600
Cd (ug/L)	6	0.51	0.83	1.9	3	0.75	3.8	13	5	0.50	6.6	12
Cl (mg/L)	6	911	1,170	1,260	3	19	98	859	5	345	572	2,330
Co (ug/L)	6	<0.028	<0.55	0.093	3	<0.11	0.11	1.6	5	<0.092	6.1	78
CO_3 (mg/L)	6	0.73	2.9	7.3	3	0.047	0.44	21	5	<0.01	<0.01	1.7
Cr (ug/L)	6	<0.2	<0.35	<0.5	3	0.46	0.91	5.7	5	<0.4	<1.7	53
Cu (ug/L)	6	<0.26	0.34	3.5	3	0.60	1.5	3.6	5	0.41	6.9	44
Fe (ug/L)	6	<13	<31.5	<50	3	<4.6	<25	4.6	5	<4.7	4.7	1,200
H_2CO_3 (mg/L)	6	<0.01	<0.01	<0.01	3	<0.01	<0.01	<0.01	5	<0.01	<0.01	0.041
HCO_3 (mg/L)	6	3.4	5.9	16	3	0.50	15	87	5	4.9	7.9	38
Hg (ng/L)	3	1.2	12	21	2	0.82	40	79	3	1.9	4.2	28
K (mg/L)	6	470	500	609	3	10	30	350	5	20	80	500
Li (ug/L)	6	5,890	6,415	7,070	3	<20	33	130	5	<20	1,050	3,390
Mg (mg/L)	6	<2.5	4.3	9.6	3	<0.05	8.2	77	5	23	1,000	5,810
Mn (ug/L)	6	16	50	202	3	<0.1	<4	197	5	113	564	1,170
Mo (ug/L)	6	180	316	368	3	310	910	3,520	5	164	570	60,800
Na (mg/L)	6	247	291	341	3	108	141	2,310	5	606	1,330	4,630
Ni (ug/L)	6	<2	<3	3.5	3	<2	4.3	7.5	5	3.3	153	597
Pb (ug/L)	6	<0.14	<0.17	<0.2	3	<0.14	<0.2	0.39	5	<0.2	0.32	3.5
Sb (ug/L)	6	<0.1	<0.22	0.14	3	1.3	2.3	4.7	5	0.72	4.6	22
Se (ug/L)	6	1.1	2.4	3.9	3	17	51	65	5	3.7	159	2,360
Si (ug/L)	6	1,810	1,950	3,000	3	2,600	3,940	21,000	5	400	10,500	45,400

Table 4-4 (Continued)
Statistical Summary of FGD Leachate Samples by Management Method and Coal Type

	Landfill				Landfill				Impoundment*			
	Bituminous				Subbituminous/Lignite				Subbituminous/Lignite			
	Count	min	med	max	Count	min	med	max	Count	min	med	max
SO_4 (mg/L)	6	1,350	1,510	1,620	3	836	1,450	4,710	5	2,080	10,200	30,500
Sr (ug/L)	6	3,520	4,095	4,500	3	5,960	9,140	9,730	5	1,500	11,700	16,900
TIC (mg/L)	6	0.95	2.5	3.3	3	3.0	4.3	18	5	1.7	2.4	7.9
Tl (ug/L)	6	<0.1	<0.42	0.34	3	<0.1	<0.1	<0.1	5	<0.1	<0.5	2.9
TOC (mg/L)	6	0.51	1.4	2.4	3	7.9	8.1	19	5	9.9	21	50
U (ug/L)	6	<0.022	<0.15	0.097	3	<0.01	0.97	10	5	<0.2	0.68	16
V (ug/L)	6	<0.69	0.98	4.5	3	4.0	6.8	400	5	<1.8	15	103
Zn (ug/L)	6	<2	<3.5	12	3	<2	5.4	19	5	<2	23	68
DO (%)	6	11	23	81	3	0.40	65	95	5	0.20	0.30	36
ORP (mV)	6	46	104	220	3	18	339	341	5	1.5	271	356
pH (SU)	6	9.0	10.0	10.5	3	7.8	8.0	12.0	5	6.2	7.4	9.0
EC (umho/cm)	6	5,550	6,211	6,897	3	2,190	2,870	11,560	5	4,770	12,950	26,140
Temp (°C)	6	12	16	16	3	19	19	21	5	9.9	19	27

* Impoundment category includes two samples from impoundments where water is recirculated

Management in Impoundments Versus Landfills

Concentration ranges for ash leachate in impoundments and landfills are compared in Table 4-5, and selected constituents are graphically illustrated in Figure 4-11 for ash from bituminous coal, and Figure 4-12 for ash from subbituminous/lignite coal. Graphical comparisons for all analyzed constituents are presented in Appendix B, Figures B-1 and B-2.

Table 4-5
Comparison of Ash Leachate Concentrations from Landfills and Impoundments

	Landfill Concentration Higher			Impoundment Concentration Higher	
	Strongly	Moderately	No Difference	Moderately	Strongly
Ca (mg/L)	◆		○		
Cl (mg/L)		◆	○		
CO_3 (mg/L)		○	◆		
HCO_3 (mg/L)	◆	○			
K (mg/L)	◆○				
Mg (mg/L)	◆		○		
Na (mg/L)	◆○				
SO_4 (mg/L)	◆○				
Ag (ug/L)			◆○		
Al (ug/L)			○		◆
As (ug/L)	○				◆
B (ug/L)	◆○				
Ba (ug/L)					○◆
Be (ug/L)			◆○		
Cd (ug/L)	◆○				
Co (ug/L)	◆○				
Cr (ug/L)	○		◆		
Cu (ug/L)	○			◆	
Fe (ug/L)			○	◆	
Hg (ng/L)	◆○				
Li (ug/L)	◆		○		
Mn (ug/L)	◆		○		
Mo (ug/L)	◆○				
Ni (ug/L)		◆○			
Pb (ug/L)		○		◆	
Sb (ug/L)	○			◆	
Se (ug/L)	○	◆			
Si (ug/L)			◆	○	
Sr (ug/L)	◆		○		
Tl (ug/L)			○	◆	
U (ug/L)	◆	○			
V (ug/L)	○				◆
Zn (ug/L)		◆	○		

Notes:
◆ = bituminous source coal ○ = subbituminous/lignite source coal
Strongly indicates that interquartile range of one dataset is higher than the other dataset, or median is one order of magnitude higher in one dataset
Moderately indicates that a portion of the interquartile range, and the median, of one dataset is higher than the other dataset.

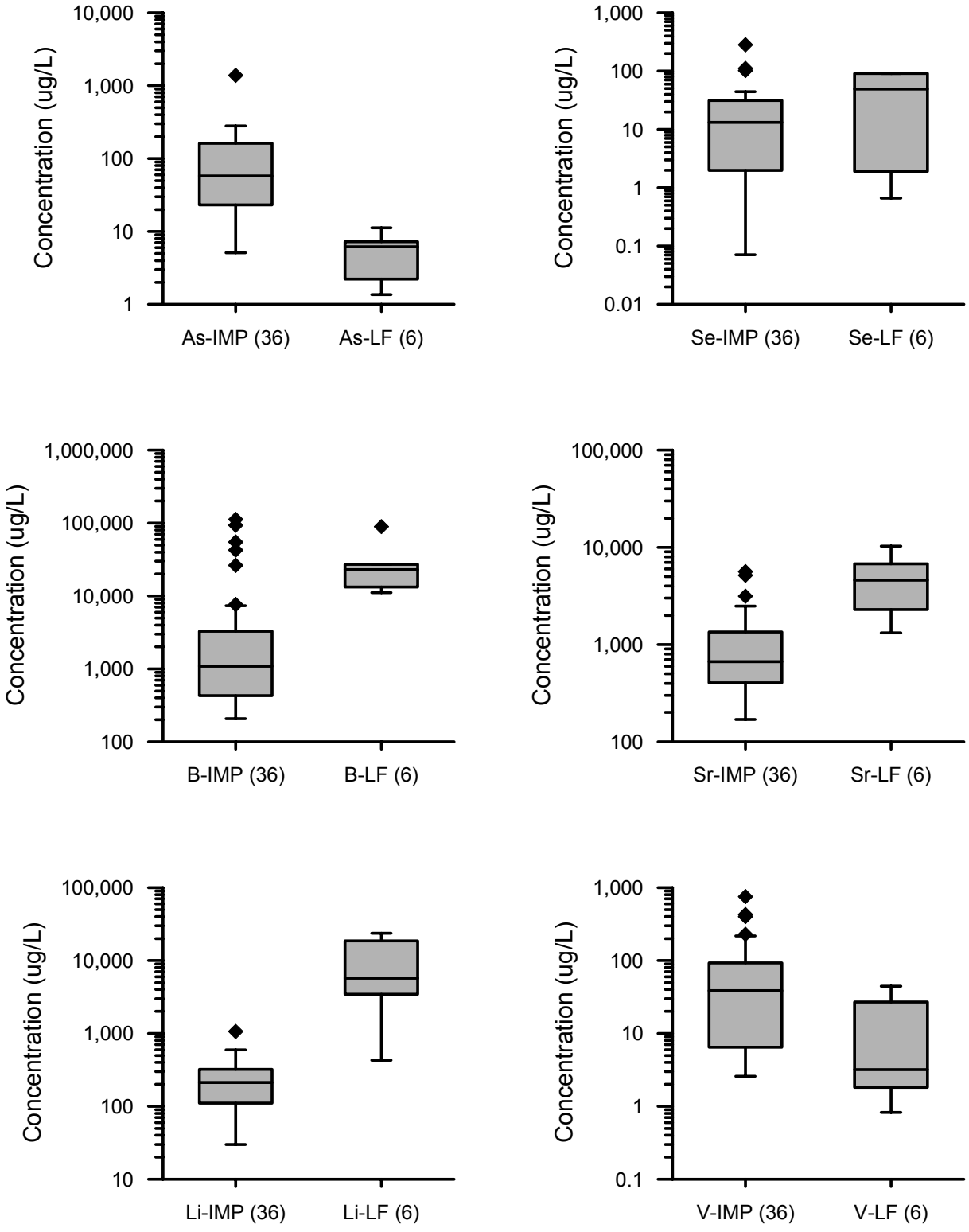

Figure 4-11
Comparison of field leachate concentrations for selected constituents: bituminous coal ash, landfill versus impoundment (See Appendix B for other parameters)

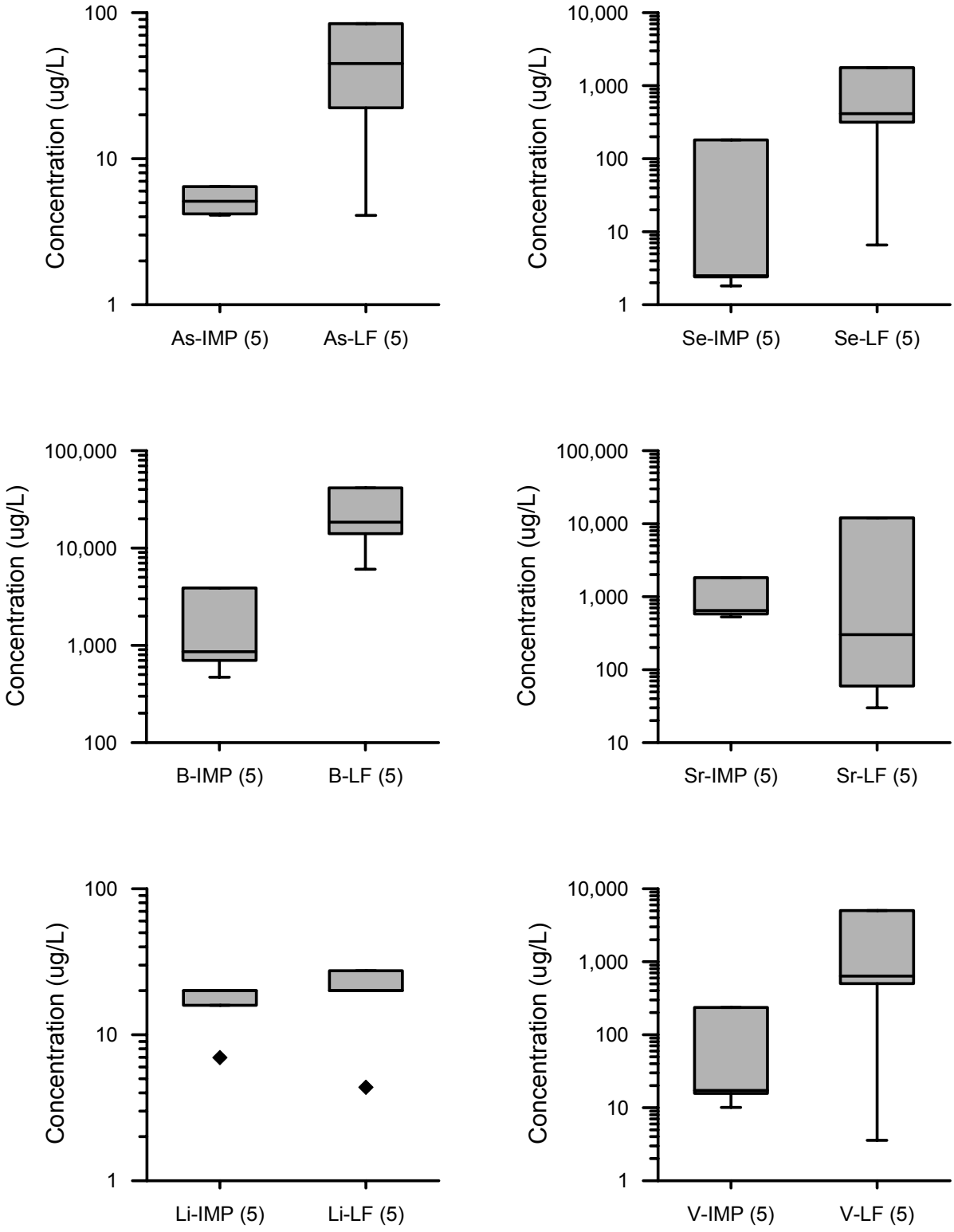

Figure 4-12
Comparison of field leachate concentrations for selected constituents: subbituminous/lignite coal ash, landfill versus impoundment (See Appendix B for other parameters)

Most constituents (22 out of the 34 analyzed) had higher concentration in the landfill leachate samples than in the impoundment leachate samples. The most significant factor contributing to this result is that the leachate in impoundments has a higher water to solid ratio than leachate in landfills, and is, in essence, more dilute. The pond water is more dilute due to the volume of water required to hydraulically transport ash, and the porewater in impoundments is often more dilute because constituents that are easily leached from the surface of the ash particles are washed off during sluicing.

Bituminous versus Subbituminous and Lignite Source Coal

Concentration ranges for ash leachate in impoundments and landfills are compared in Table 4-6, and selected constituents are graphically illustrated in Figure 4-13 for landfill leachate, and Figure 4-14 for impoundment leachate. All analyzed constituents are graphically illustrated in Appendix B, Figures B-3 and B-4.

The field leachate data demonstrate the dependence of several individual constituents on the source coal type. For major ions, leachate from bituminous coal ash had higher concentrations of calcium in both landfill and impoundment settings, while leachate from subbituminous/lignite coal had higher concentrations of carbonate and sodium in both management settings.

Minor and trace constituents for which concentrations in leachate from bituminous coal ash are higher than in leachate from subbituminous/lignite coal, regardless of management environment, are cobalt, lithium, manganese, nickel, antimony, thallium, and zinc (Table 4-6). The difference for lithium is particularly strong. This non-reactive element had a concentration range of 3,400 to 23,600 μg/L in landfill leachate from bituminous coal versus 5 to 27 μg/L in landfill leachate from subbituminous/lignite coal, and 30-1,060 μg/L (bituminous) versus 7 to 20 μg/L (subbituminous/lignite) in impoundment leachate (Figures 4-13 and 4-14). Manganese had similarly large concentration differences, particularly in the landfill environment. Thallium was only detected in leachate from bituminous coal ash (31 of 42 samples, 74 percent), and was not detected in leachate from subbituminous/lignite coal ash (0 of 10 samples).

Minor and trace constituents for which concentrations in leachate from subbituminous/lignite coal ash were higher than in leachate from bituminous coal, regardless of management environment, are aluminum, chromium, copper, and mercury (Table 4-6). The difference is most notable for aluminum and mercury, where the concentrations are an order of magnitude or more higher for both landfill and impoundment leachate.

Table 4-6
Comparison of Ash Leachate Concentrations for Bituminous and Lignite/Subbituminous Source Coal

	Bituminous Concentration Higher			Lig/Subbit Concentration Higher	
	Strongly	Moderately	No Difference	Moderately	Strongly
Ca (mg/L)	◆	O			
Cl (mg/L)			◆		O
CO_3 (mg/L)					O◆
HCO_3 (mg/L)			◆	O	
K (mg/L)		◆	O		
Mg (mg/L)	◆		O		
Na (mg/L)					O◆
SO_4 (mg/L)			O		◆
Ag (ug/L)			◆O		
Al (ug/L)					O◆
As (ug/L)	O				◆
B (ug/L)			O◆		
Ba (ug/L)			◆O		
Be (ug/L)			◆O		
Cd (ug/L)		O	◆		
Co (ug/L)		◆O			
Cr (ug/L)				O	◆
Cu (ug/L)				O	◆
Fe (ug/L)			◆O		
Hg (ng/L)					◆O
Li (ug/L)	◆O				
Mn (ug/L)	◆O				
Mo (ug/L)		O		◆	
Ni (ug/L)		◆O			
Pb (ug/L)			O	◆	
Sb (ug/L)	O	◆			
Se (ug/L)			O		◆
Si (ug/L)		◆	O		
Sr (ug/L)		◆	O		
Tl (ug/L)	O	◆			
U (ug/L)		◆	O		
V (ug/L)			O		◆
Zn (ug/L)	◆	O			

Notes:
◆ = Landfills O = Impoundments
Strongly indicates that interquartile range of one dataset is higher than the other dataset, or median is one order of magnitude higher in one dataset
Moderately indicates that a portion of the interquartile range, and the median, of one dataset is higher than the other dataset.

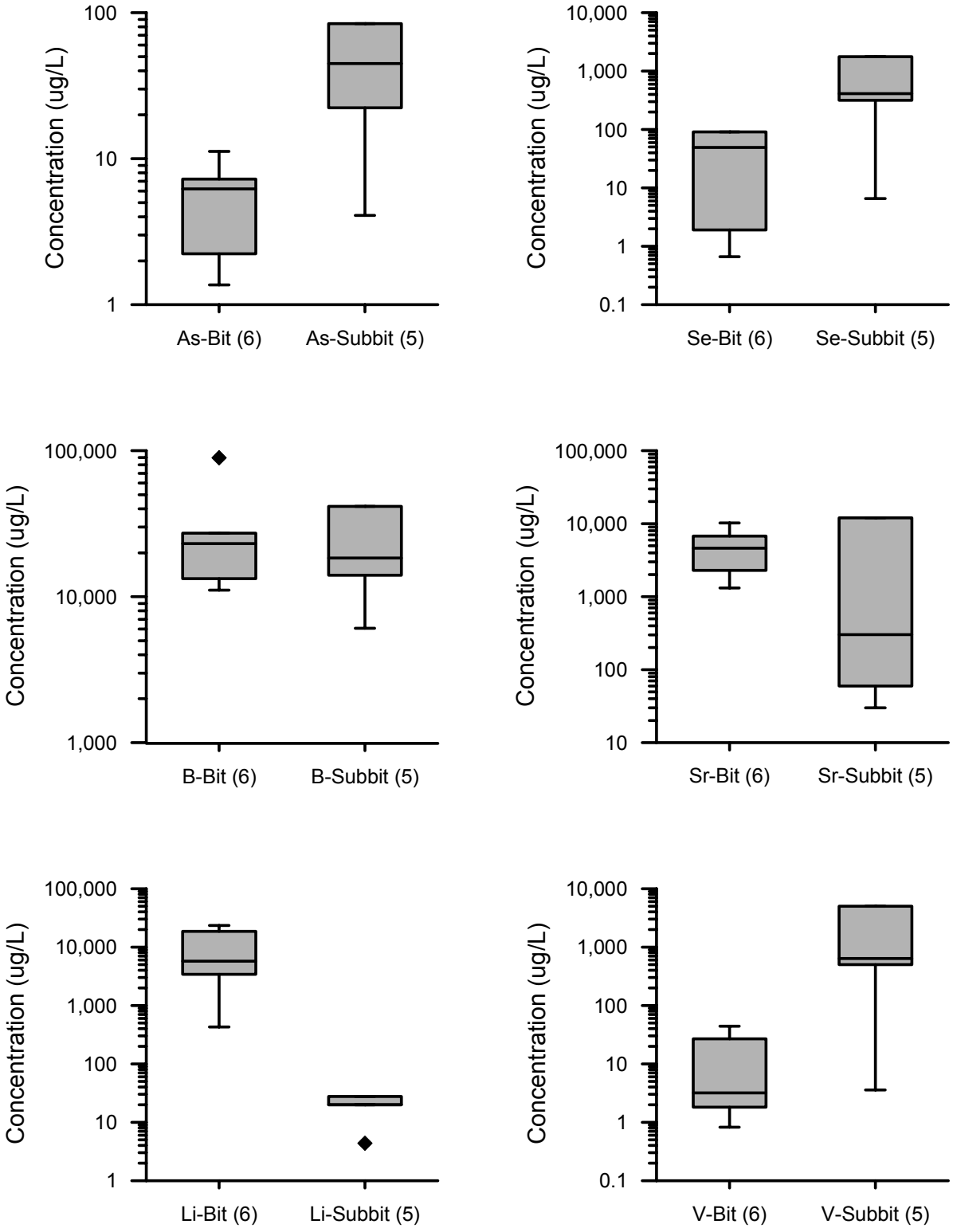

Figure 4-13
Comparison of field leachate concentrations for selected constituents: bituminous vs subbituminous/lignite coal ash, landfills (See Appendix B for other parameters)

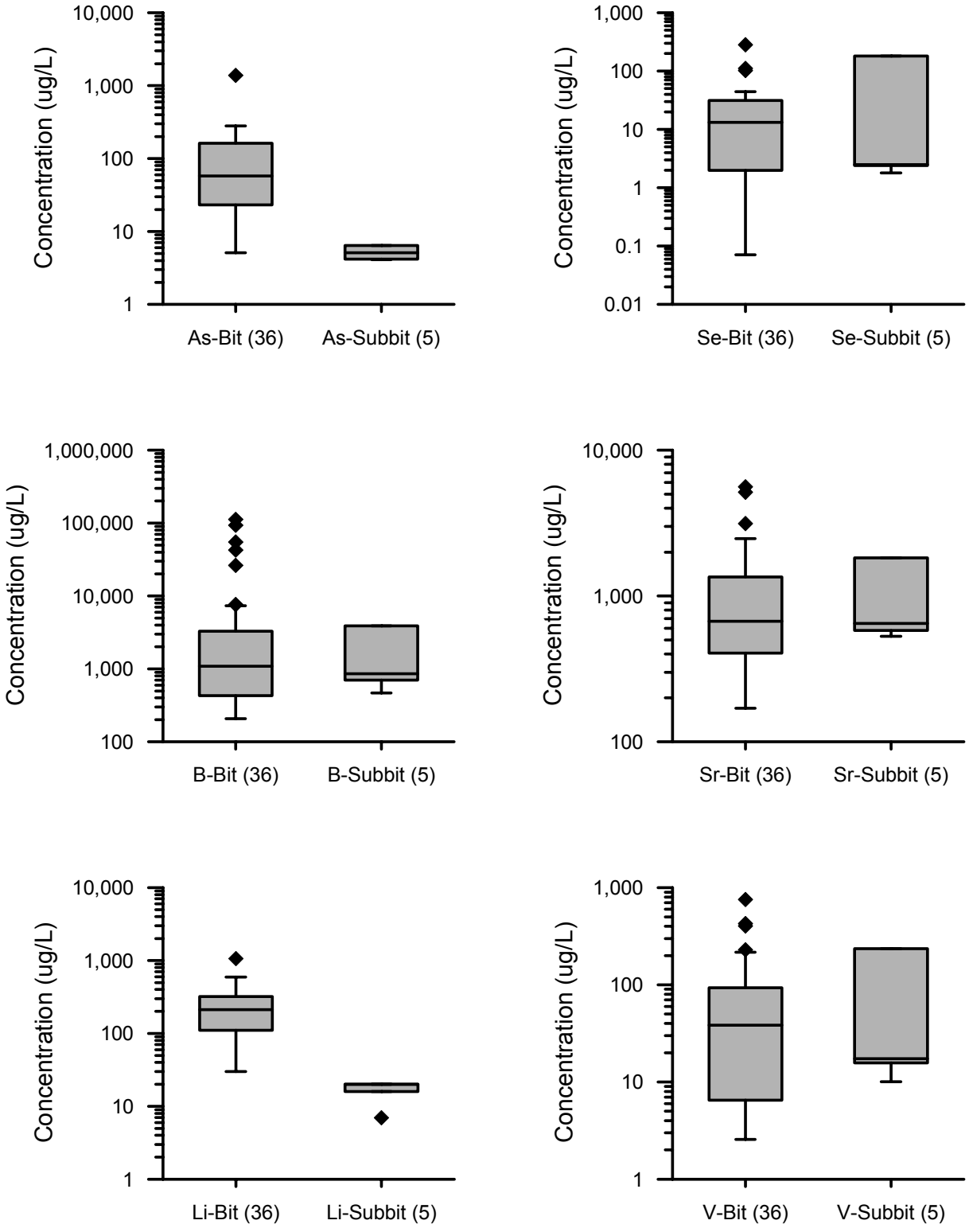

Figure 4-14
Comparison of field leachate concentrations for selected constituents: bituminous vs subbituminous/lignite coal ash, impoundments (See Appendix B for other parameters)

Key constituents for which a consistent difference between bituminous and subbituminous/lignite leachate were not found included:

- Arsenic: Concentrations in impoundments were significantly higher when the source coal was subbituminous/lignite, and concentrations in landfills were significantly higher when the source coal was bituminous. Site-specific pH and redox conditions play a significant role in arsenic leaching.
- Boron: The highest boron concentrations (50,000 to 112,000 µg/L) were in leachate from bituminous coal ash, while the highest subbituminous/lignite concentration was 41,000 µg/L. However, there were numerous samples from bituminous ash leachate with considerably lower concentration, and as a result, the medians and interquartile ranges for boron were similar for the two coal types.
- Selenium and Vanadium: Concentrations of these two elements were, for the most part, higher in leachate from subbituminous/lignite coal ash than in leachate from bituminous coal ash. However, there were several relatively high concentrations in bituminous ash impoundments that increased the median sufficiently so that there were no significant differences in the interquartile ranges.
- Strontium and Uranium: For landfill leachate, these elements had significantly higher concentration when the source coal was bituminous than when the source coal was subbituminous/lignite. In impoundment leachate, the bituminous median values were lower than the subbituminous/lignite median values, although the maximum concentrations were significantly higher in the bituminous samples.

Evaluation of Unique Samples

Several samples stand out as unique either due to relatively high concentrations of selected constituents or power plant attributes. Table 4-7 and Table 4-8, respectively, list the maximum concentration of each constituent analyzed in ash and FGD leachate, and whether or not this concentration is significantly higher than the next highest concentration from another site. Table 4-8 excludes samples 106 and 107, which are from an FGD impoundment where concentrations of most constituents are very high because sluice water is recirculated.

Table 4-7
Ash Leachate Samples with Maximum Concentrations

	Count	Max	Sample	Site	Next*	Comment
Ag (ug/L)	67	2.0	HN-1	13115B	1.1	The three highest silver concentrations came from core samples.
Al (ug/L)	67	44,400	016	25410A	30,000	This sample also had relatively high concentrations of B, Cd, K, Mo, Pb, Si, V, and Zn.
As (ug/L)	67	1,380	061	33104	727	No consistent correlations to site/plant attributes.
B (ug/L)	67	112,000	013	14093	109,000	Concentration not significantly higher than other samples.
Ba (ug/L)	67	657	092	27413	545	Concentration not significantly higher than other samples.
Be (ug/L)	67	8.6	043	33106	5.2	Only four beryllium detects; these occurred in four of the five samples with pH lower than 6.0.

Table 4-7 (Continued)
Ash Leachate Samples with Maximum Concentrations

	Count	Max	Sample	Site	Next*	Comment
Ca (mg/L)	66	681	012	14093	665	Concentration not significantly higher than other samples.
Cd (ug/L)	67	65	016	25410A	52	Two highest concentrations in samples from plants with cyclone boilers, both burn petroleum coke, 25410A also burns used tires.
Cl (mg/L)	66	92	097	50212	87	Concentration not significantly higher than other samples.
Co (ug/L)	67	133	002	50213	113	No consistent correlations to site/plant attributes.
CO_3 (mg/L)	63	152	003	50213	53	No consistent correlations to site/plant attributes.
Cr (ug/L)	67	5,100	002	50213	2,000	May be partially due to erosion of balls (30% Cr) that are used when pulverizing the coal at 50213 plant.
Cu (ug/L)	67	494	002	50213	452	Second lysimeter (003) at this site had a concentration of 62 µg/L.
Fe (ug/L)	67	25,600	079	22346	14,700	No consistent correlations to site/plant attributes.
H_2CO_3 (mg/L)	63	3.4	043	33106	2.8	Highest at sites with low pH.
HCO_3 (mg/L)	63	535	097	50212	535	Concentration not significantly higher than other samples.
Hg (ng/L)	22	61	098	50183	37	Resample concentration at this point was 6 ng/L.
K (mg/L)	66	277	HN-1	13115B	255	Concentration not significantly higher than other samples.
Li (ug/L)	67	23,600	111	49003B	6,940	Two leachate collection system points were sampled twice at this site. For both sample events, one returned high lithium concentration and one returned lower, although still high lithium concentrations. Similar pH, ORP and DO values.
Mg (mg/L)	66	236	111	49003B	188	Concentration not significantly higher than other samples.
Mn (ug/L)	67	4,170	018	13115B	4,110	Concentration not significantly higher than other samples.
Mo (ug/L)	67	39,600	016	25410A	25,400	Two highest concentrations in samples from plants with Cyclone boilers, both burn petroleum coke, 25410A also burns used tires.
Na (mg/L)	66	3,410	002	50213	1,700	Two highest concentrations in samples from this site.
Ni (ug/L)	67	189	111	49003B	128	Two leachate collection system points were sampled twice at this site. For both sample events, one returned high nickel concentration and one returned low nickel concentrations. Similar pH, ORP and DO values.
Pb (ug/L)	67	8.0	051	40109	4.6	Two of three samples with lead higher than 1 µg/L were also the only two samples with pH < 5. Other sample (016) had pH of 11.5.
Sb (ug/L)	67	59	023	49003A	27	Antimony concentrations at this site are unusually high.
Se (ug/L)	67	1,760	003	50213	428	Two highest concentrations in samples from this site.
Si (ug/L)	67	19,000	016	25410A	18,500	Concentration not significantly higher than other samples.
SO_4 (mg/L)	66	6,690	002	50213	3,830	Two highest concentrations in samples from this site
Sr (ug/L)	67	12,000	108	34186A	11,100	Concentration not significantly higher than other samples.
TIC (mg/L)	66	115	18	13115B	105	Concentration not significantly higher than other samples.
Tl (ug/L)	67	18	032	35015B	12	Concentration not significantly higher than other samples.
TOC (mg/L)	66	57	098	50183	55	Concentration not significantly higher than other samples.
U (ug/L)	67	61	023	49003A	37	Several other elements relatively high in this sample.
V (ug/L)	67	5,020	010	23214	1,230	Two highest concentrations in samples from plants with Cyclone boilers, both burn petroleum coke.
Zn (ug/L)	67	289	111	49003B	130	Two leachate collection system points were sampled twice at this site twice. For both sample events, one returned high zinc concentration and one returned low zinc concentrations. Similar pH, ORP and DO values.

* next highest concentration from a different site.

For ash leachates, samples from three sites had four to seven constituents with the highest concentration: 50213 (7), 25410A (4), and 49003B (4). 50213 site had the highest concentrations of Co, CO_3, Cr, Cu, Na, Se, and SO_4. The 50213 site is a landfill with pH range from 10.0 to 10.3. The power plant units associated with the 50213 site are dry-bottom PC boilers that have burned subbituminous coal during the active life of the site. Two smaller units have cold-side electrostatic precipitators, while a larger unit utilized a hot-side precipitator for most of the active life of the 50213 site and a fabric filter for the last two years. The larger unit has a low-NOx burner. Leachate was collected in two lysimeters that directly underlie the ash. The leachate at this site was alkaline, with a pH higher than 10. Relatively high ORP values, low iron concentrations, and oxidized forms of arsenic, selenium, and chromium indicate that redox conditions at this site were oxidizing. The only uncommon attributes of this site are the lysimeters used to collect the leachate and the hot-side precipitator. Two other sites received ash from hot-side precipitators (40109 and 43035). These sites did not have similarly high leachate concentrations, however they are both impoundments that receive ash derived from bituminous coal.

The high chromium concentrations at 50213 were attributed by the utility to high chromium concentration in the flue gas as a result of erosion of the balls used to pulverize the coal. Chromium volatilized in the flue gas may condense on the ash particles and then readily leach from the particles in the landfill environment. High concentrations of other elements may be due to limited dilution. The ash is not saturated at this site; instead, the lysimeters collect porewater that was in tight contact with the ash particles.

The 49003B site is also a landfill and had the highest concentrations of Li, Mg, Ni, and Zn, and a pH range from 6.5 to 7.0. The 49003B source power plant has no unusual attributes, yet concentrations of most elements at one of the two leachate collection system sample points were higher than median concentrations for the whole sample set.

The 25410A site is an impoundment and had the highest concentrations of Al, Cd, Mo, and Si, and a pH of 11.7. The 25410A plant is different from most plants in the study in that it burns a blend of fuels including pet coke and tires in a cyclone boiler. The elevated concentrations at the 25410A site may to be associated with either the cyclone boiler or the fuel mixture, or both.

Table 4-8 lists maximum concentrations in FGD leachate samples. In general, there were too few samples to conclusively correlate high or low concentrations to plant and site attributes.

Table 4-8
FGD Leachate Samples with Maximum Concentrations

	Count	Max.	Sample	Site	Next*	Comment
Ag (ug/L)	12	50183L ND				All values below detection limits,
Al (ug/L)	12	890	008	23223B	608	No consistent correlations to site/plant attributes.
As (ug/L)	12	110	106	34186C	49	High DO (95%), low ORP (18 mV), pH 12.
B (ug/L)	12	98,500	009	23223B	15,600	No consistent correlations to site/plant attributes.
Ba (ug/L)	12	134	106	34186C	90	Concentration not significantly higher than other samples.
Be (ug/L)	12	50183L ND				All values below detection limits,
Ca (mg/L)	12	730	029	35015A	577	Concentration not significantly higher than other samples.
Cd (ug/L)	12	13	106	34186C	12	No consistent correlations to site/plant attributes.
Cl (mg/L)	12	1,260	028	35015A	859	No consistent correlations to site/plant attributes.
Co (ug/L)	12	78	009	23223B	1.6	No consistent correlations to site/plant attributes.
CO_3 (mg/L)	12	21	106	34186C	7.3	High value pH related.
Cr (ug/L)	12	53	009	23223B	5.7	No consistent correlations to site/plant attributes.
Cu (ug/L)	12	44	008	23223B	3.6	No consistent correlations to site/plant attributes.
Fe (ug/L)	12	1,200	007	23223B	4.6	Only sample with pH below 7 (6.2)
H_2CO_3 (mg/L)	12	0.041	007	23223B	<0.01	Only sample with pH below 7 (6.2)
HCO_3 (mg/L)	12	87	006	23223A	16	No consistent correlations to site/plant attributes.
Hg (ng/L)	8	79	128	43034	28	Most oxidized FGD sample collected.
K (mg/L)	12	609	121	35015A	350	No consistent correlations to site/plant attributes.
Li (ug/L)	12	7,070	122	35015A	2,720	No consistent correlations to site/plant attributes.
Mg (mg/L)	12	1,990	009	23223B	77	No consistent correlations to site/plant attributes.
Mn (ug/L)	12	704	007	23223B	202	No consistent correlations to site/plant attributes.
Mo (ug/L)	12	60,800	007	23223B	3,520	No consistent correlations to site/plant attributes.
Na (mg/L)	12	2,310	106	34186C	1,330	No consistent correlations to site/plant attributes.
Ni (ug/L)	12	597	007	23223B	7.5	No consistent correlations to site/plant attributes.
Pb (ug/L)	12	3.5	007	23223B	0.39	Detects only for with lignite/subbituminous ash.
Sb (ug/L)	12	4.7	006	23223A	4.6	No consistent correlations to site/plant attributes.
Se (ug/L)	12	2,360	009	23223B	65	No consistent correlations to site/plant attributes.
Si (ug/L)	12	21,000	106	34186C	12,700	No consistent correlations to site/plant attributes.
SO_4 (mg/L)	12	10,400	009	23223B	4,710	No consistent correlations to site/plant attributes.
Sr (ug/L)	12	16,900	007	23223B	9,730	No consistent correlations to site/plant attributes.
TIC (mg/L)	12	18	006	23223A	4.3	No consistent correlations to site/plant attributes.
Tl (ug/L)	12	2.9	009	23223B	0.34	No consistent correlations to site/plant attributes.
TOC (mg/L)	12	21	007	23223B	19	No consistent correlations to site/plant attributes.
U (ug/L)	12	10	006	23223A	0.97	No consistent correlations to site/plant attributes.
V (ug/L)	12	400	106	34186C	18	No consistent correlations to site/plant attributes.
Zn (ug/L)	12	34	009	23223B	23	No consistent correlations to site/plant attributes.

* next highest concentration from a different site.

Typical plant components in this study included wet-bottom coal-fired PC units, cold-side ESPs, and wet FGD systems. Less common were plants with cyclone boilers, non-coal fuel sources, hot-side ESPs, and dry FGD systems. Results for these less common configurations are discussed below:

- Cyclone Boilers: The power plants associated with 23214, 25410A, and 25410B use cyclone boilers. Cyclone boilers tend to burn hotter than PC boilers, and also burn a wider variety of fuels. These plants are the only ones sampled that burn petroleum coke, and the fuel burned at 25410A and 25410B also includes used tires. Leachate sampled at these sites had higher than median concentrations of most elements, and the highest concentrations of cadmium, molybdenum, and vanadium. Vanadium is often associated with petroleum coke. The relatively high concentrations from these samples may reflect the effect of the cyclone boiler, or the fuel. Concentrations at one of the sample locations from 25410A and 25410B were often higher than at 23214, but not sufficiently so to indicate any effects from the tires on ash leachate composition.
- Hot-Side ESPs: The plants associated with the 40109, 43035, and 50213 sites have hot-side ESP's, while the other plants with ESPs are cold-side. The 40109 and 43035 samples did not stand out in terms of high or low concentration. These sites are impoundments and receive bituminous coal ash. As previously discussed, the 50213 site is a landfill and received subbituminous ash, and had relatively high concentrations of several constituents, including selenium. The high selenium concentration is unusual in that less selenium capture in ash is expected from plants with hot-side ESPs, due to the higher temperatures at the collection point. Presence in the leachate may indicate that the selenium captured in the hot-side is present in a relatively soluble form for the subbituminous coal ash. Similarly, the relatively high concentrations at the 50213 site may indicate increased leachability for the subbituminous ash collected at the hotter temperatures. However, this is only one site and more data from plants burning subbituminous coal with hot-side ESPs are needed to confirm this observation. The relatively low concentrations seen at the 40109 and 43035 sites may suggest that the 50213 data are specific to the particular plant, fuel, or management setting.
- Oil Ash: 22346 is the only site sampled where oil ash was managed with coal ash. The leachate from the ash sampled at this site did not stand out in terms of low or high concentration. Since oil ash is generally high in vanadium and nickel, this result suggests that either the effect of the oil ash is not appreciable due to its volume relative to the coal ash, or that the coal ash geochemically mitigates releases from the oil ash.
- Wet-Bottom PC Boiler: 43034 is the only plant that has a wet-bottom PC boiler. The leachate from the FGD byproduct sampled at this site did not stand out in terms of low or high concentration.
- Dry FGD System: 23223A is associated with the only power plant that used a spray dryer system; all other FGD samples came from power plants with wet FGD systems. With a few exceptions, the leachate from this site tended to have relatively low concentrations. The most notable exception was uranium, which had a concentration of 10 μg/L at this site and less than 1 μg/L at the other FGD sites.

5
SPECIATION OF ARSENIC, SELENIUM, CHROMIUM, AND MERCURY AT CCP MANAGEMENT FACILITIES

The mobility and toxicity of inorganic constituents is sometimes strongly dependent on their aqueous speciation. This is particularly true for arsenic, selenium, and chromium, which can be present at elevated concentrations in CCP leachate. Important species in leachate and groundwater are As(III) and As(V), Se (IV) and Se(VI), and Cr(III) and Cr(VI). Organic species for the other constituents (e.g., methylarsenic acid) were not considered in this study. Generally speaking, As(III) and Cr(VI) are more toxic and more mobile than As(V) and Cr(III); and Se(IV) is more toxic to most terrestrial and aquatic wildlife than the more mobile Se(VI). It is important to know the species present in leachate in order to assess potential impacts associated with these constituents. Although mercury is generally present only at very low concentrations in ash leachate and is very immobile in groundwater, the organic mercury species (monomethyl mercury) can bioaccumulate to toxic levels in the surface water environment and is therefore of interest.

Evaluation of Speciation Sample Preservation Methods

Speciation of arsenic and selenium in field samples with widely varying matrix characteristics such as the CCP leachate is challenging because preservation techniques and analytical interferences can have a significant impact on the results. Several preservation methods (HCl, cryofreezing, EDTA, HNO_3, none) were compared on sample splits from one site, and a comparison of speciation results for 32 split samples from several sites using two preservation methods (HCl and cryofreezing) are presented in Appendix C.

Results varied by sample, and suggested that, regardless of preservation method, a critically important factor was minimizing hold times. Species recovery was poorest for the samples collected in 2003 (samples 001 through 032) due to longer holding times for the frozen samples. Importantly, the split sample data collected during this study indicated that, even when overall species recovery was low, the relative predominance of reduced or oxidized species of arsenic and selenium were similar regardless of preservation method or laboratory used. Speciation results presented in the following sections are for samples that were preserved by cryofreezing in the field with liquid nitrogen.

Arsenic

Overview of Results

Total arsenic was detected at concentrations well above the detection limit in all collected water samples (n = 81 after removing all QA samples)[4], and at least one species was detected in all except two samples. Review of duplicate samples indicated that analytical results were usually reproducible, particularly when concentrations were greater than 1 µg/L (Table 5-1).

Excluding duplicates, 51 of the 81 samples contained detectable concentrations of arsenite, 73 samples had detectable concentrations of arsenate, and 30 samples contained detectable concentrations of arsenic species other than arsenite or arsenate. These other species are either monomethyl arsenate or soluble arsenic-sulfur (As-S) compounds. Both types of other arsenic species are technically As(V) compounds (i.e., they contain arsenic in the +5 oxidation state); although they were not grouped with As(V) because they potentially have different chemical and environmental characteristics.

Monomethyl arsenate is either formed by microbial methylation of inorganic arsenic or used as a biocide. However, contrary to the case of mercury, the methylated (i.e., organic) forms of arsenic are less toxic than the inorganic forms, and are therefore generally not regarded as a source of concern. The soluble As-S compounds are formed by reaction of arsenite and free sulfide in reducing waters, and there are also some studies suggesting that these species are less toxic than arsenite and arsenate. In all except two samples (which had relatively low total arsenic concentration), the other arsenic species constituted the minority of all arsenic present (<20 percent).

The arsenic speciation mass balance (the sum of all individual species determined in a given sample divided by the independently-determined total arsenic concentration) varied strongly, and was not always satisfactory. Less than half (35 of 81 samples) had a recovery greater than 80 percent (Figure 5-1). Reasons for this somewhat disappointing performance likely originate from the complexity of the studied samples. Species recovery for the 2004/2005 samples was better than for the 2003 samples due to reduced holding times and other laboratory refinements (Appendices C and D).

[4] QA samples include blanks and duplicates.

Table 5-1
Arsenic Speciation Data

Site	Sample	Source	CCP	Coal	Total As (ug/L)	As(III) (ug/L)	As(V) (ug/L)	As, other species (ug/L)	Sum of Species	% Recovery	% As(III)	% As(V)	% As (other)
50210	001	LF	FA,BA	Mix	20	<0.3	9.5	2.1	11.6	57%			
50213	002	LF	FA	Subbit	48	<6	47	<6	47.2	**98%**	0.0%	100.0%	0.0%
50213	003	LF	FA	Subbit	84	<6	69	<6	68.8	**82%**	0.0%	100.0%	0.0%
50183	004	LF	FA,BA	Mix	19	8.4	5.2	<0.3	13.5	73%			
50183	005	LF	FA,BA	Mix	3.0	<0.2	1.3	<0.2	1.3	45%			
23223A	006	LF	SDA	Subbit	12	<0.3	0.94	<0.3	0.9	8%			
23223B	007	IMP	FGD	Subbit	20	<2	<2	<2	0.0	0%			
23223B	008	IMP	FGD	Subbit	17	0.75	<0.5	<0.3	0.7	4%			
23223B	009	IMP	FGD	Subbit	29	<6	<10	<6	0.0	0%			
23214	010	LF	FA	Subbit	22	1.5	10	<0.6	11.5	52%			
14093	012	IMP	FA	Bit	238	97	66	<0.6	163.3	69%			
14093	013	IMP	FA	Bit	22	3.7	<0.5	<0.3	3.7	17%			
14093	*013D*	*Dup*	*FA*	*Bit*	*22*	*1.9*	*<0.5*	*<0.3*	*1.9*	*9%*			
14093	014	IMP	FA	Bit	163	1.9	86	0.86	88.6	54%			
25410A	015	IMP	FA,BA	Blend	24	<0.6	24	<0.6	23.6	**99%**	0.0%	100.0%	0.0%
25410A	016	IMP	FA,BA	Blend	69	<0.6	25	<0.6	24.7	36%			
13115A	017	IMP	FA,BA	Subbit	4.1	0.88	<0.08	0.069	1.0	23%			
13115B	018	IMP	FA,BA	Bit	23	0.42	5.2	<0.06	5.6	24%			
13115A	019	IMP	FA	Subbit	5.1	0.57	<0.08	<0.06	0.6	11%			
13115A	020	IMP	FA,BA	Subbit	4.2	1.0	0.53	0.15	1.7	40%			
49003A	021	IMP	FA	Bit	194	2.1	208	<0.3	210.0	**108%**	1.0%	99.0%	0.0%
49003A	022	IMP	FA	Bit	11	13	0.49	<0.06	13.0	**118%**	96.3%	3.7%	0.0%
49003A	023	IMP	FA	Bit	218	0.79	189	<0.3	189.5	**87%**	0.4%	99.6%	0.0%
49003B	024	LF	FA	Bit	11	0.36	<0.2	<0.2	0.4	3%			
49003B	025	LF	FA	Bit	6.5	1.4	<0.08	<0.06	1.4	21%			
49003A	026	IMP	FA	Bit	11	11	0.40	<0.2	11.6	**107%**	96.5%	3.5%	0.0%
35015A	027	LF	FGD, FA	Bit	39	13	4.8	1.3	19.4	49%			
35015A	028	LF	FGD, FA	Bit	30	2.4	1.7	0.20	4.3	14%			
35015A	029	LF	FGD, FA	Bit	49	1.7	8.9	0.35	10.9	22%			

Table 5-1 (Continued)
Arsenic Speciation Data

Site	Sample	Source	CCP	Coal	Total As (ug/L)	As(III) (ug/L)	As(V) (ug/L)	As, other species (ug/L)	Sum of Species	% Recovery	% As(III)	% As(V)	% As (other)
35015B	030	IMP	FA	Bit	43	3.5	29	0.35	33.4	79%			
35015B	031	IMP	FA	Bit	221	201	24	0.69	225.5	**102%**	89.2%	10.5%	0.3%
35015B	032	IMP	FA,BA	Bit	25	17	17	0.074	34.5	136%	50.8%	49.0%	0.2%
33106	037	IMP	FA	Bit	56	0.30	34		34.3	61%			
33106	038	IMP	FA	Bit	123	2.6	53		56.0	46%			
33106	039	IMP	FA	Bit	42	1.4	53		54.2	128%	2.6%	97.4%	ND
33106	042	IMP	FA	Bit	24	<0.1	19		19.2	**81%**	0.0%	100.0%	ND
33106	043	IMP	FA	Bit	75	<0.05	28		27.6	37%			
33106	044	IMP	FA	Bit	5.1	0.39	2.5		2.9	57%			
33106	*044D*	*Dup*	*FA*	*Bit*	*4.9*	*<0.04*	*2.3*		*2.3*	*48%*			
33106	049	IMP	FA,BA	Bit	5.4	<0.04	2.3	<0.04	2.3	43%			
40109	051	IMP	FA	Bit	38	0.70	15		15.7	41%			
40109	052	IMP	FA	Bit	164	23	7.7		30.5	19%			
40109	053	IMP	FA	Bit	279	108	82	0.70	191.0	68%			
40109	057	IMP	FA,BA	Bit	99	<0.2	93		92.5	**94%**	0.0%	100.0%	ND
40109	059	IMP	FA,BA	Bit	124	<0.2	127		126.6	**102%**	0.0%	100.0%	ND
40109	*059D*	*Dup*	*FA,BA*	*Bit*	*125*	*<0.2*	*119*		*118.5*	**95%**	0.0%	100.0%	ND
33104	061	IMP	FA	Bit	1,380	859	519		1,377.4	**100%**	62.4%	37.6%	ND
33104	062	IMP	FA	Bit	62	<0.2	37		37.5	61%			
33104	064	IMP	FA	Bit	178	<0.4	150		150.2	**84%**	0.0%	100.0%	ND
33104	069	IMP	FA,BA	Bit	100	<0.2	94		93.6	**94%**	0.0%	100.0%	ND
33104	070	IMP	FA,BA	Bit	143	<0.2	136		135.7	**95%**	0.0%	100.0%	ND
33104	*070D*	*Dup*	*FA,BA*	*Bit*	*144*	*<0.2*	*137*	*0.53*	*137.6*	**96%**	0.0%	99.6%	0.4%
22346	079	IMP	FA,OA	Blend	99	9.5	104		113.8	**115%**	8.3%	91.7%	ND
22346	*079D*	*Dup*	*FA,OA*	*Blend*	*97*	*9.9*	*73*		*82.5*	**85%**	12.0%	88.0%	ND
22346	082	IMP	FA,OA	Blend	23	0.21	15		14.7	64%			
22347	083	IMP	FA	Blend	6.2	0.23	2.4		2.6	43%			
22346	084	IMP	FA,OA	Blend	727	71	535		606.0	**83%**	11.8%	88.2%	ND

Table 5-1 (Continued)
Arsenic Speciation Data

Site	Sample	Source	CCP	Coal	Total As (ug/L)	As(III) (ug/L)	As(V) (ug/L)	As, other species (ug/L)	Sum of Species	% Recovery	% As(III)	% As(V)	% As (other)
27413	090	See Notes	FA	Mix	23	0.28	18	0.67	18.9	**84%**	1.5%	95.0%	3.5%
27413	091	See Notes	FA	Mix	11	<0.05	9.4	0.15	9.6	**89%**	0.0%	98.4%	1.6%
27413	092	See Notes	FA	Mix	3.3	<0.05	0.49	0.10	0.6	18%			
50212	097	LF	FA	Subbit	45	<0.1	36	<0.1	36.3	**81%**	0.0%	100.0%	0.0%
50183	098	LF	FA,BA	Mix	77	0.66	60	0.29	60.5	79%			
50183	099	LF	FA,BA	Mix	4.8	0.10	3.7	0.19	4.0	**84%**	2.6%	92.7%	4.7%
50408	101	LF	FA,BA	Bit	2.2	<0.1	0.23	0.62	0.9	38%			
50211	102	LF	FA	Bit	7.2	<0.05	6.3	<0.05	6.3	**88%**	0.0%	100.0%	0.0%
34186B	105	IMP	FGD	Lig	230	197	50	3.8	250.6	**109%**	78.4%	20.1%	1.5%
34186C	106	LF	FGD,FA,BA	Lig	110	16	63	5.8	84.7	77%			
34186C	*106D*	*Dup*	*FGD,FA,BA*	*Lig*	*112*	*14*	*77*	*5.2*	*96.3*	**86%**	14.3%	80.2%	5.4%
34186B	107	IMP	FGD	Lig	31	0.95	15	<0.2	16.1	52%			
34186A	108	LF	FA	Lig	4.1	0.37	2.3	<0.05	2.7	65%			
49003B	111	LF	FA	Bit	5.9	<0.1	3.4	<0.1	3.4	58%			
49003B	112	LF	FA	Bit	1.4	0.68	0.95	0.20	1.8	133%	37.1%	52.1%	10.8%
49003A	113	IMP	FA	Bit	102	0.75	118	0.17	118.7	**116%**	0.6%	99.2%	0.1%
49003A	114	IMP	FA	Bit	24	<0.1	20	<0.1	20.5	**87%**	0.0%	100.0%	0.0%
49003A	115	IMP	FA	Bit	8.3	3.1	5.3	<0.05	8.3	**100%**	36.7%	63.3%	0.0%
49003A	116	IMP	FA	Bit	8.2	1.0	7.4	0.083	8.5	**103%**	11.9%	87.2%	1.0%
35015B	118	IMP	FA,BA	Bit	41	0.66	45	0.15	46.3	**114%**	1.4%	98.3%	0.3%
35015B	*118D*	*Dup*	*FA,BA*	*Bit*	*40*	*0.18*	*46*	*0.11*	*45.9*	**116%**	0.4%	99.4%	0.2%
35015B	119	IMP	FA,BA	Bit	30	<0.05	31	0.29	30.8	**102%**	0.0%	99.1%	0.9%
35015A	120	LF	FGD, FA	Bit	27	7.2	11	9.3	27.9	**104%**	25.7%	41.0%	33.2%
35015A	121	LF	FGD, FA	Bit	11	1.3	6.0	0.57	7.9	72%			
35015A	122	LF	FGD, FA	Bit	26	7.6	8.3	6.0	21.9	**86%**	34.8%	37.8%	27.4%
43035	126	IMP	FA,BA	Subbit	5.2	<0.1	3.6	<0.1	3.6	69%			
43035	*126D*	*Dup*	*FA,BA*	*Subbit*	*4.9*	*<0.1*	*3.2*	*<0.1*	*3.2*	*66%*			
43035	127	IMP	FA,BA	Subbit	6.4	<0.2	4.0	<0.2	4.0	63%			
43034	128	LF	FGD,FA	Lig	14	10	2.8	0.45	13.3	**94%**	75.4%	21.2%	3.4%

Table 5-1 (Continued)
Arsenic Speciation Data

Site	Sample	Source	CCP	Coal	Total As (ug/L)	As(III) (ug/L)	As(V) (ug/L)	As, other species (ug/L)	Sum of Species	% Recovery	% As(III)	% As(V)	% As (other)
13115B	HN-1	IMP	FA,BA	Bit	60	<0.1	34	0.23	33.8	57%			
13115B	HN-2	IMP	FA,BA	Bit	21	<0.1	6.9	0.14	7.1	34%			
25410B	SX-1	IMP	FA	Blend	72	0.88	47	<0.1	47.8	66%			

Notes:
Ash at site 27413 (samples 090, 091, 092) was first sluiced, then managed dry.

Abbreviations:
Bit = bituminous; Subbit = Subbituminous; Mix = CCP from different units burning different coals; Blend = CCP from a single unit burning two different fuels
FA = fly ash; BA = bottom ash; EA = economizer ash; FGD = flue gas desulfurization sludge; OA = oil ash
LF = landfill; IMP = impoundment; DUP = duplicate sample
ND = not determined

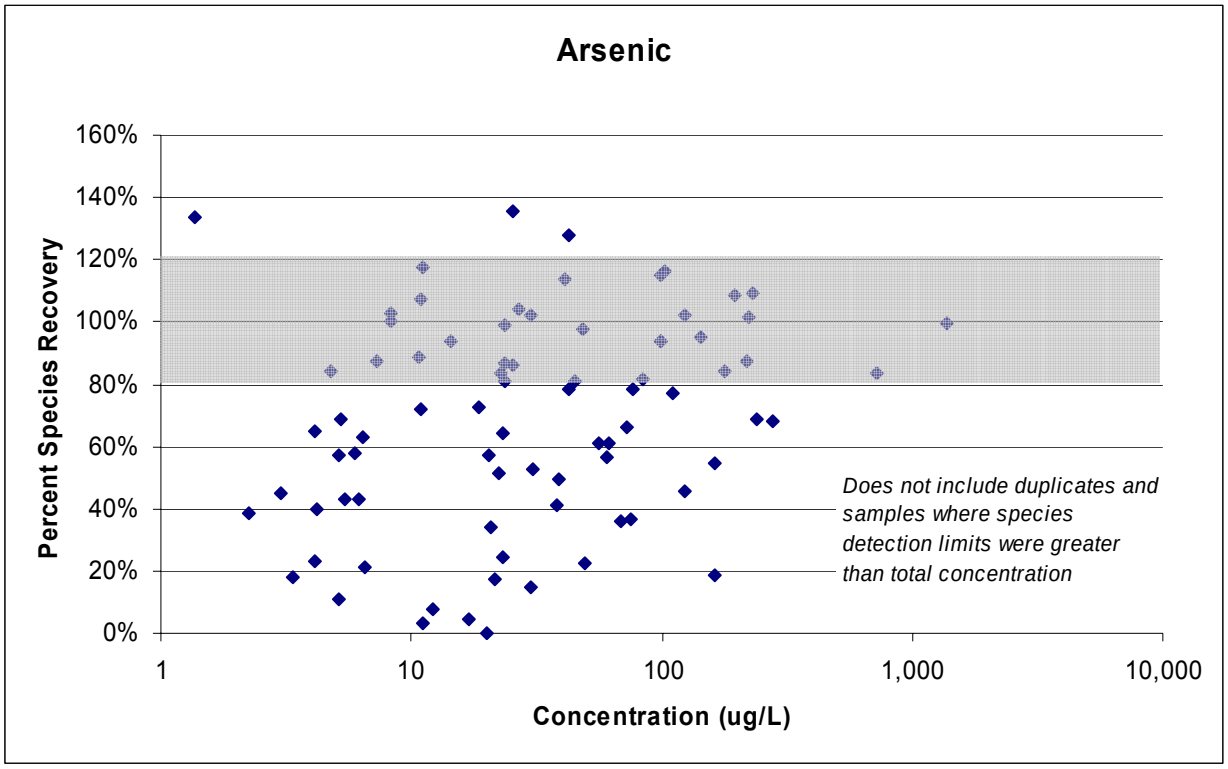

Figure 5-1
Arsenic species recovery

Comparison of Speciation to Site and Plant Attributes

Dominant species and relative percentages of the species were tabulated as a function of management method (landfill or impoundment) and source coal type. Relative species percentage was calculated for samples with greater than 80 percent recovery. The dominant species was determined based on the following criteria:

- For species recovery greater than 80 percent, a species was identified as dominant if its concentration was 60 percent or more of the sum of species.
- If species recovery was greater than 80 percent, and no species concentration was greater than 60 percent of the sum of species, then the sample was listed as "neutral".
- For species recovery less than 80 percent, a species was identified as dominant if its concentration was greater than 50 percent of the total concentration.[5]
- Samples with less than 80 percent species recovery in which no species concentration was greater than 50 percent of the total concentration were not tabulated.

[5] If the sum of species is 80 percent, and the species concentration is 50 percent of the total concentration, then that species accounts for at least 62.5 percent of the sum of species.

The relative percent of species recovery was tabulated for the 35 individual samples (not counting duplicates) in which the sum of species was greater than 80 percent of the total arsenic concentration (Table 5-1). For ash management sites (31 samples), the percentage of As(V) ranged from 3 to 100 percent with a median of 99 percent, the percentage of As(III) ranged from 0 to 96 percent with a median of 0.6 percent, and the percentage of other species ranged from 0 to 11 percent with a median of 0 percent. For FGD management sites (4 samples), the percentage of As(V) ranged from 20 to 41 percent with a median of 30 percent, the percentage of As(III) ranged from 26 to 78 percent with a median of 55 percent, and the percentage of other species ranged from 2 to 33 percent with a median of 15 percent. A more detailed tabulation by management method and source coal yields:

- For ash impoundments, the percentage of As(V) ranged from 3 to 100 percent for plants burning bituminous coal (20 samples), no samples from lignite/subbituminous plants had sufficient species recovery to calculate a ratio, and the percentage of As(V) ranged from 88 to 100 percent for sites receiving ash from units that burn a blend of bituminous and subbituminous coal (3 samples) (Figure 5-2).
- For ash landfills, the percentage of As(V) was 52 to 100 percent for plants burning bituminous coal (2 samples), 100 percent for plants burning lignite/subbituminous coal (3 samples), and 93 percent for a site that received ash from multiple units burning different coals (1 sample).
- One other ash management site (27413) where ash was originally sluiced, then landfilled, and where a mixture of coal sources were used, had 95 to 98 percent As(V) (2 samples).
- For FGD landfills, samples with greater than 80 percent species recovery had roughly equal percentages of As(III), As(V), and other arsenic species at sites receiving bituminous coal ash (2 samples), and a site receiving lignite ash had 72 percent As(III) (1 sample) (Figure 5-2).
- Similarly, an FGD impoundment/lignite sample had 72 percent As(III) (1 sample). There were no FGD impoundment/bituminous samples.

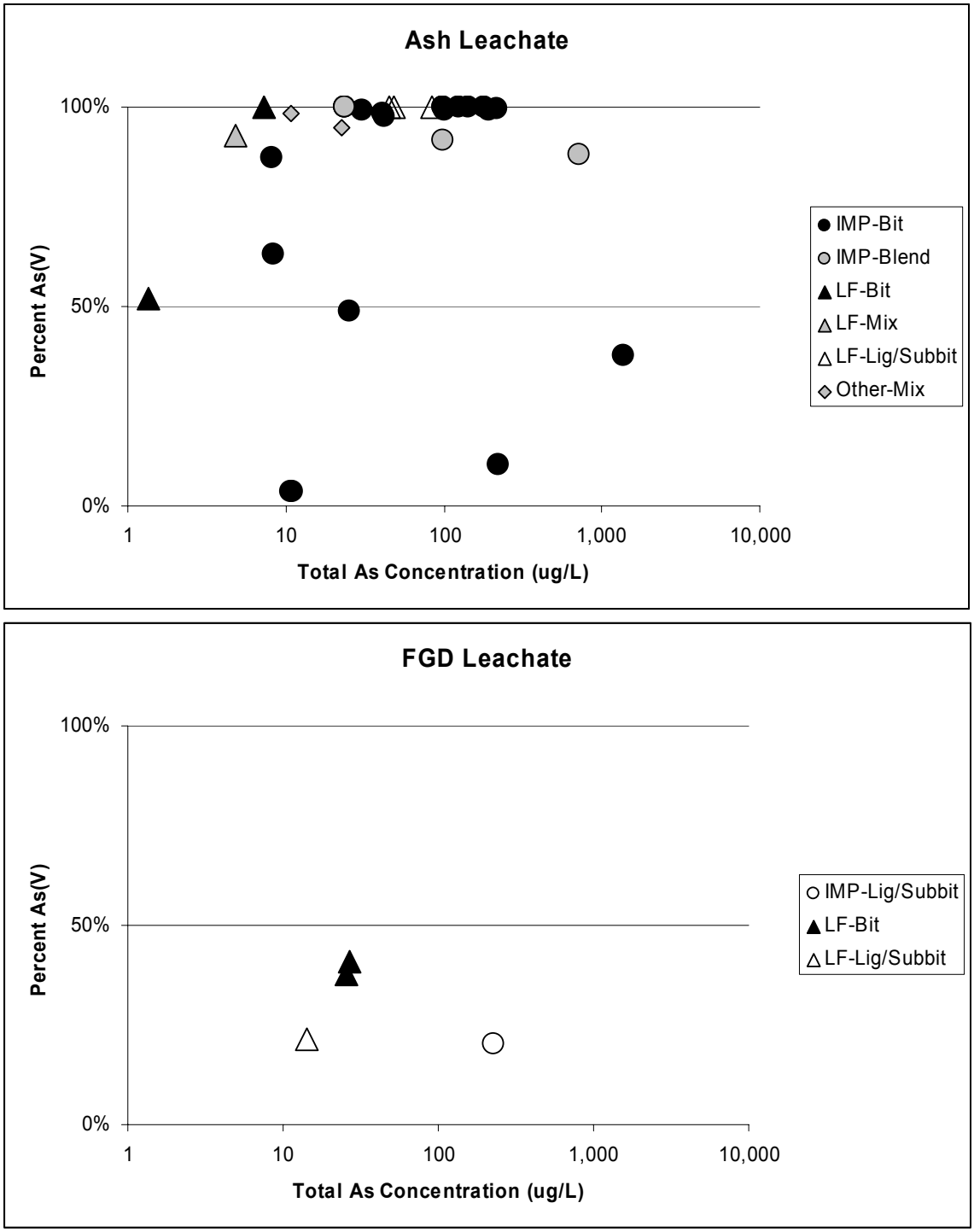

Figure 5-2
Relative percent of As(V) vs total As concentration

Results of the dominant species analysis corroborates the results of the relative species analysis, and indicates that ash leachate is dominated by As(V) (Table 5-2). As(III) is only dominant in

four samples from ash impoundment environments at sites where bituminous coal was burned, and in FGD leachate when bituminous coal was burned.

Table 5-2
Tabulation of Dominant Arsenic Species by Sample

Ash Samples	**Impoundment**	**Landfill**	***Total***
Ash – Bituminous	4 – 1 – 20 (36)	0 – 1 – 2 (6)	*4 – 2 – 22* *(42)*
Ash – Blend/Mix	0 – 0 – 5 (7)	0 – 0 – 2 (5)	*0 – 0 – 9** *(15*)*
Ash – Subbituminous/Lignite	0 – 0 – 2 (5)	0 – 0 – 4 (5)	*0 – 0 – 6* *(10)*
Total	*4 – 1 – 27* *(48)*	*0 – 1 – 8* *(16)*	*4 – 2 – 37** *(67*)*
FGD Samples	**Impoundment**	**Landfill**	***Total***
FGD – Bituminous		0 – 2 – 1 (6)	*0 – 2 – 1* *(6)*
FGD – Blend/Mix			
FGD – Subbituminous/Lignite	1 – 0 – 0 (5)	1 – 0 – 1 (3)	*2 – 0 – 1* *(8)*
Total	*1 – 0 – 0* *(5)*	*1 – 2 – 2* *(9)*	*2 – 2 – 2* *(14)*

Legend: number of samples in which → As(III) dominant - Neutral - As(V) dominant
(Total number of samples in group)

* Tabulation includes the samples from the 27413 site, which could not be characterized as landfill or impoundment.

The four ash leachate samples dominated by As(III) (022, 026, 031, and 061) came from three different sites (49003A, 35015B, and 33104), indicating that it is not a site-specific occurrence. Furthermore, other samples from each of the three sites were dominated by As(V), indicating that it is not a site-wide occurrence. Total arsenic concentration in the four samples dominated by As(III) ranged from 11 to 1,380 µg/L (Figure 5-3). The pH values of these samples were neutral to slightly alkaline (7.1 to 8.5 SU). Sample 031 had only 6 percent dissolved oxygen and a negative ORP value, indicative of reducing conditions. Most of the other samples with dissolved oxygen concentrations lower than 10 percent were not evaluated because species recovery was too low, and no other sample had a negative ORP value. Sample 061 had abundant dissolved oxygen (65 percent), although it also had a relatively low ORP value of 140 mV and a dissolved iron concentration of 2,170 µg/L, which may be indicative of reducing conditions. The total arsenic concentration for samples 031 and 061 were an order of magnitude or more higher than the other samples collected at these sites. Samples 022 and 026, both collected from the 49003A impoundment had field measurements indicative of oxic conditions, and total arsenic concentrations were at the low end of the range for samples collected at this site.

FGD leachate samples were evenly split between the reduced and oxidized species of arsenic. There was no correlation with pH, dissolved oxygen, or ORP. In fact, the two samples clearly dominated by As(V) (106 and 121) had lower ORP values than the two samples dominated by As(III) (105 and 128).

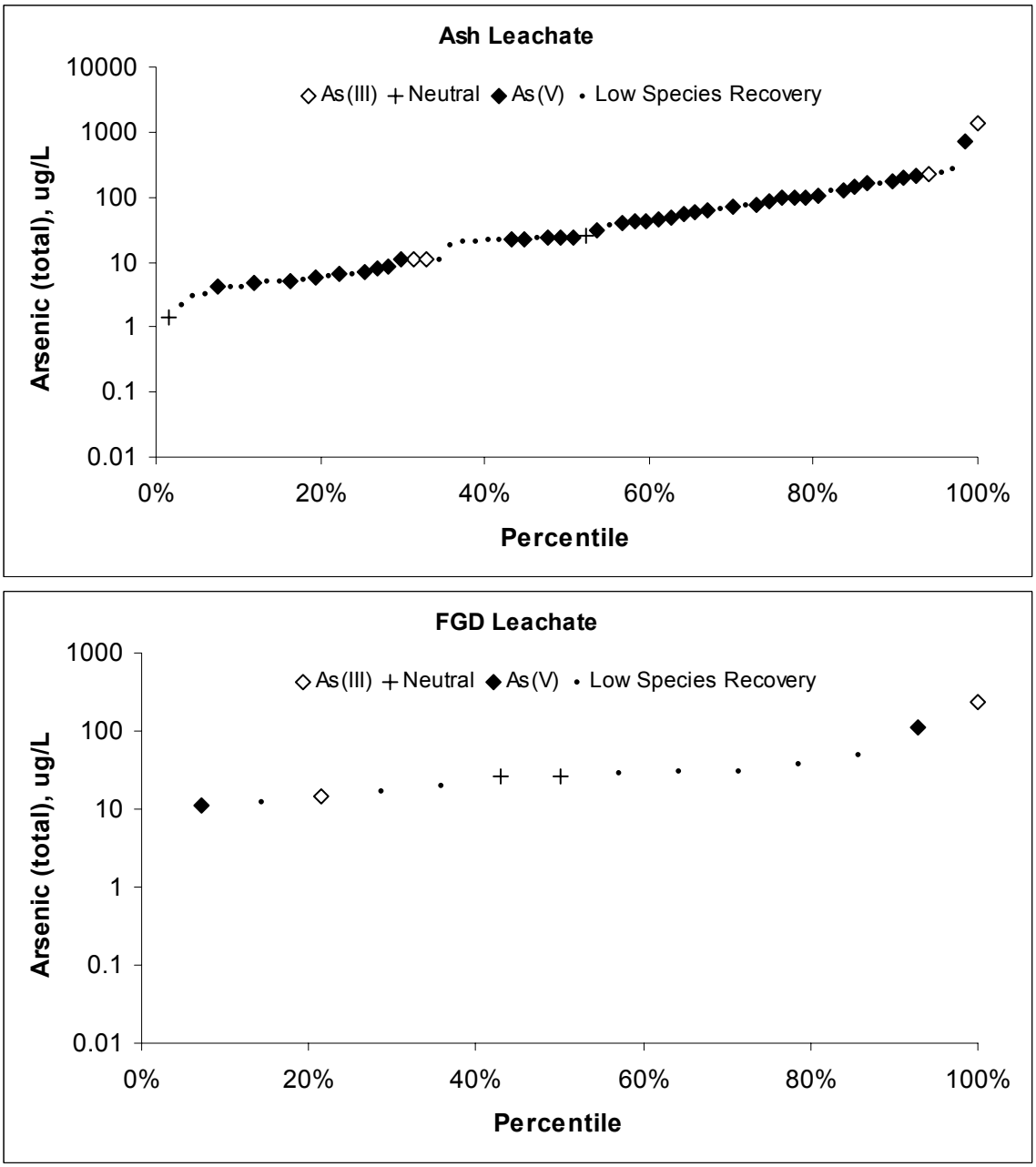

Figure 5-3
Species predominance as a function of total arsenic concentration in leachate.

Selenium

Overview of Results

Detectable concentrations of selenium were present in all 81 samples (Table 5-3). Review of duplicate sample results indicated that results were highly reproducible across the entire concentration range.

Selenite was detected in 58 of the 81 samples, and selenate was detected in 55 of the 81 samples. Two samples (107 and 128) contained other selenium species, which were theorized to be selenium-sulfur compounds.

Like arsenic, the selenium speciation mass balance varied strongly, and was not always satisfactory. Selenium had the same number of samples (35 of 81 samples) as arsenic with greater than 80 percent recovery (Figure 5-4); although the samples with poor species recovery were not always the same as arsenic.

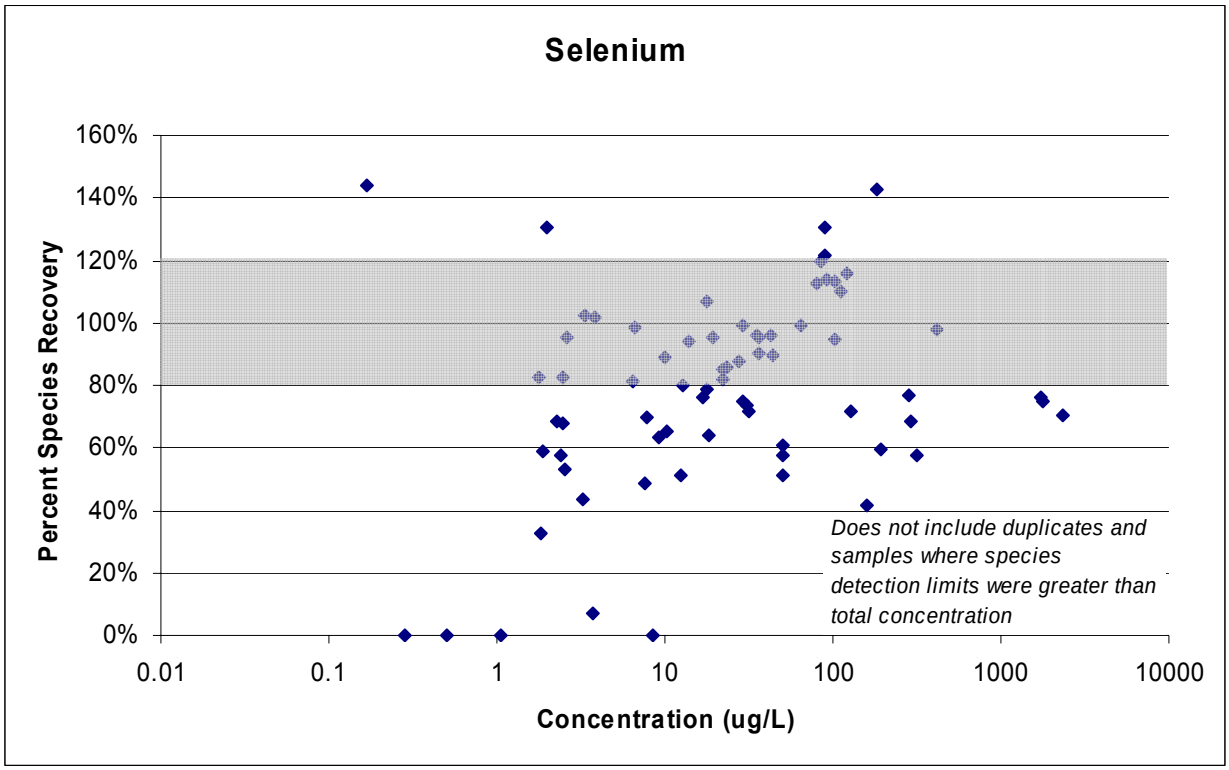

Figure 5-4
Selenium species recovery

Table 5-3
Selenium Speciation Data

Site	Sample	Source	CCP	Coal	Total Se (ug/L)	Se(IV) (ug/L)	Se(VI) (ug/L)	Se, other (ug/L)	Sum of Species	% Recovery	% Se(IV)	% Se(VI)	% Se (other)
50210	001	LF	FA,BA	Mix	127	8.3	83		91.3	72%			
50213	002	LF	FA	Subbit	1,730	19	1,300		1,318.6	76%			
50213	003	LF	FA	Subbit	1,760	76	1,240		1,315.9	75%			
50183	004	LF	FA,BA	Mix	50	8.1	22		30.3	61%			
50183	005	LF	FA,BA	Mix	7.6	3.1	0.57		3.7	49%			
23223A	006	LF	SDA	Subbit	17	1.6	11		12.8	76%			
23223B	007	IMP	FGD	Subbit	289	79	119		198.2	69%			
23223B	008	IMP	FGD	Subbit	3.7	<0.1	0.27		0.3	7%			
23223B	009	IMP	FGD	Subbit	2,360	<2	1,660		1,660.0	70%			
23214	010	LF	FA	Subbit	318	24	158		182.3	57%			
14093	012	IMP	FA	Bit	3.2	1.4	<0.2		1.4	43%			
14093	013	IMP	FA	Bit	0.28	<0.1	<0.1		0.0	0%			
14093	*013D*	*dup*	*FA*	*Bit*	*0.38*	*<0.1*	*<0.1*		*0.0*	*0%*			
14093	014	IMP	FA	Bit	1.8	0.59	<0.2		0.6	33%			
25410A	015	IMP	FA,BA	Blend	22	15	3.4		18.3	**82%**	81.2%	18.8%	ND
25410A	016	IMP	FA,BA	Blend	193	101	14		115.4	60%			
13115A	017	IMP	FA,BA	Subbit	2.4	0.26	1.1		1.4	57%			
13115B	018	IMP	FA,BA	Bit	0.50	<0.1	<0.2		0.0	0%			
13115A	019	IMP	FA	Subbit	1.8	0.14	1.3		1.5	**82%**	9.5%	90.5%	ND
13115A	020	IMP	FA,BA	Subbit	2.5	0.90	0.79		1.7	68%			
49003A	021	IMP	FA	Bit	6.5	5.3	<0.6		5.3	**81%**	100.0%	0.0%	ND
49003A	022	IMP	FA	Bit	31	20	2.2		22.7	74%			
49003A	023	IMP	FA	Bit	283	217	1.5		218.2	77%			
49003B	024	LF	FA	Bit	18	5.3	6.3		11.6	64%			
49003B	025	LF	FA	Bit	1.9	<0.1	1.1		1.1	59%			
49003A	026	IMP	FA	Bit	32	20	2.2		22.6	72%			
35015A	027	LF	FGD, FA	Bit	1.1	<0.3	<0.3		0.0	0%			
35015A	028	LF	FGD, FA	Bit	2.6	<0.3	1.4		1.4	53%			
35015A	029	LF	FGD, FA	Bit	2.3	<0.3	1.6		1.6	69%			

Table 5-3 (Continued)
Selenium Speciation Data

Site	Sample	Source	CCP	Coal	Total Se (ug/L)	Se(IV) (ug/L)	Se(VI) (ug/L)	Se, other (ug/L)	Sum of Species	% Recovery	% Se(IV)	% Se(VI)	% Se (other)
35015B	030	IMP	FA	Bit	44	27	12		39.5	**90%**	68.3%	31.7%	ND
35015B	031	IMP	FA	Bit	13	0.92	5.5		6.4	51%			
35015B	032	IMP	FA,BA	Bit	18	13	0.75		14.2	79%			
33106	037	IMP	FA	Bit	2.0	2.6	<1		2.6	131%	100.0%	0.0%	ND
33106	038	IMP	FA	Bit	0.13	<0.5	<1		0.0	0%			
33106	039	IMP	FA	Bit	0.17	0.24	<0.4		0.2	144%	100.0%	0.0%	ND
33106	042	IMP	FA	Bit	43	39	1.9		41.0	**96%**	95.3%	4.7%	ND
33106	043	IMP	FA	Bit	24	20	<1		20.2	**86%**	100.0%	0.0%	ND
33106	044	IMP	FA	Bit	14	11	1.7		13.1	**94%**	86.7%	13.3%	ND
33106	*044D*	*dup*	*FA*	*Bit*	*14*	*12*	*1.8*		*13.3*	***98%***	86.7%	13.3%	ND
33106	049	IMP	FA,BA	Bit	10	8.3	0.64		8.9	**89%**	92.8%	7.2%	ND
40109	051	IMP	FA	Bit	0.45	<0.5	<1		0.0	0%			
40109	052	IMP	FA	Bit	10	6.7	<4		6.7	65%			
40109	053	IMP	FA	Bit	1.2	<2	<4		0.0	0%			
40109	057	IMP	FA,BA	Bit	2.4	2.0	<1		2.0	**83%**	100.0%	0.0%	ND
40109	059	IMP	FA,BA	Bit	2.6	2.5	<1		2.5	**95%**	100.0%	0.0%	ND
40109	*059D*	*dup*	*FA,BA*	*Bit*	*2.6*	*2.2*	*<1*		*2.2*	***87%***	100.0%	0.0%	ND
33104	061	IMP	FA	Bit	4.3	<10	<20		0.0	0%			
33104	062	IMP	FA	Bit	112	90	32		122.5	**110%**	73.8%	26.2%	ND
33104	064	IMP	FA	Bit	103	97	<4		97.1	**95%**	100.0%	0.0%	ND
33104	069	IMP	FA,BA	Bit	36	33	1.7		34.8	**96%**	95.1%	4.9%	ND
33104	070	IMP	FA,BA	Bit	29	29	<4		28.8	**99%**	100.0%	0.0%	ND
33104	*070D*	*dup*	*FA,BA*	*Bit*	*29*	*28*	*<4*		*27.9*	***95%***	100.0%	0.0%	ND
22346	079	IMP	FA,OA	Blend	0.16	<0.2	<0.3		0.0	0%			
22346	*079D*	*dup*	*FA,OA*	*Blend*	*0.16*	*<0.2*	*<0.3*		*0.0*	*0%*			
22346	082	IMP	FA,OA	Blend	19	18	0.26		18.1	**95%**	98.6%	1.4%	ND
22347	083	IMP	FA	Blend	13	8.7	1.5		10.2	80%			
22346	084	IMP	FA,OA	Blend	0.57	<2	<3		0.0	0%			
27413	090	See Notes	FA	Mix	86	5.2	97		102.3	**120%**	5.1%	94.9%	ND
27413	091	See Notes	FA	Mix	122	3.6	138		141.9	**116%**	2.5%	97.5%	ND
27413	092	See Notes	FA	Mix	103	0.56	116		117.0	**113%**	0.5%	99.5%	ND

Table 5-3 (Continued)
Selenium Speciation Data

Site	Sample	Source	CCP	Coal	Total Se (ug/L)	Se(IV) (ug/L)	Se(VI) (ug/L)	Se, other (ug/L)	Sum of Species	% Recovery	% Se(IV)	% Se(VI)	% Se (other)
50212	097	LF	FA	Subbit	413	38	366		404.2	**98%**	9.4%	90.6%	ND
50183	098	LF	FA,BA	Mix	51	29	<2		29.3	58%			
50183	099	LF	FA,BA	Mix	2.0	<0.8	<2		0.0	0%			
50408	101	LF	FA,BA	Bit	91	<0.8	104		103.6	**114%**	0.0%	100.0%	ND
50211	102	LF	FA	Bit	80	5.3	85		90.8	**113%**	5.9%	94.1%	ND
34186B	105	IMP	FGD	Lig	8.5	<2	<4	<2	0.0	0%			
34186C	106	LF	FGD,FA,BA	Lig	65	<2	64	<2	64.4	**99%**	0.0%	100.0%	0.0%
34186C	*106D*	*dup*	*FGD,FA,BA*	*Lig*	*65*	*<2*	*65*	*<2*	*65.1*	***100%***	0.0%	100.0%	0.0%
34186B	107	IMP	FGD	Lig	159	<2	16	51	66.5	42%			
34186A	108	LF	FA	Lig	6.6	2.6	3.9	<0.5	6.5	**98%**	39.6%	60.4%	0.0%
49003B	111	LF	FA	Bit	91	39	72		110.3	122%	35.1%	64.9%	ND
49003B	112	LF	FA	Bit	0.67	<0.5	<1		0.0	0%			
49003A	113	IMP	FA	Bit	29	19	2.6		21.8	75%			
49003A	114	IMP	FA	Bit	0.071	<0.5	<1		0.0	0%			
49003A	115	IMP	FA	Bit	36	30	3.1		32.7	**90%**	90.7%	9.3%	ND
49003A	116	IMP	FA	Bit	35	31	3.3		34.0	**96%**	90.2%	9.8%	ND
35015B	118	IMP	FA,BA	Bit	18	18	1.3		18.9	**107%**	93.0%	7.0%	ND
35015B	*118D*	*dup*	*FA,BA*	*Bit*	*18*	*16*	*1.3*		*17.7*	***96%***	92.9%	7.1%	ND
35015B	119	IMP	FA,BA	Bit	28	23	1.7		24.4	**87%**	93.1%	6.9%	ND
35015A	120	LF	FGD, FA	Bit	3.3	1.8	1.5		3.4	**102%**	54.7%	45.3%	ND
35015A	121	LF	FGD, FA	Bit	3.9	1.1	2.8		3.9	**102%**	28.2%	71.8%	ND
35015A	122	LF	FGD, FA	Bit	1.1	<0.5	<1		0.0	0%			
43035	126	IMP	FA,BA	Subbit	89	13	103	<0.3	115.9	131%	10.8%	89.2%	0.0%
43035	*126D*	*dup*	*FA,BA*	*Subbit*	*88*	*13*	*104*	*<0.3*	*116.9*	*132%*	11.1%	88.9%	0.0%
43035	127	IMP	FA,BA	Subbit	181	12	245	<0.3	257.5	143%	4.8%	95.2%	0.0%
43034	128	LF	FGD,FA	Lig	51	17	6.7	1.8	25.9	51%			

Table 5-3 (Continued)
Selenium Speciation Data

Site	Sample	Source	CCP	Coal	Total Se (ug/L)	Se(IV) (ug/L)	Se(VI) (ug/L)	Se, other (ug/L)	Sum of Species	% Recovery	% Se(IV)	% Se(VI)	% Se (other)
13115B	HN-1	IMP	FA,BA	Bit	22	2.6	16		19.0	**85%**	13.9%	86.1%	ND
13115B	HN-2	IMP	FA,BA	Bit	9.2	<1	5.8		5.8	64%			
25410B	SX-1	IMP	FA	Blend	7.8	1.8	3.6		5.4	70%			

Notes:
Ash at site 27413 (samples 090, 091, 092) was first sluiced, then managed dry.

Abbreviations:
Bit = bituminous; Subbit = Subbituminous; Mix = CCP from different units burning different coals; Blend = CCP from a single unit burning two different fuels
FA = fly ash; BA = bottom ash; EA = economizer ash; FGD = flue gas desulfurization sludge; OA = oil ash
LF = landfill; IMP = impoundment; DUP = duplicate sample
ND = not determined

Comparison of Speciation to Site and Plant Attributes

Dominant species and relative percentages of the species were tabulated using the same procedure as for arsenic. For ash management sites (32 samples), the percentage of Se(IV) ranged from 0 to 100 percent with a median of 88 percent, the percentage of Se(VI) ranged from 0 to 100 percent with a median of 12 percent, and the percentage of other species was 0 percent for samples with greater than 80 percent species recovery. For FGD management sites (3 samples), the percentage of Se(IV) ranged from 0 to 55 percent with a median of 28 percent, the percentage of Se(VI) ranged from 45 to 100 percent with a median of 72 percent, and the percentage of other species was 0 percent. A more detailed tabulation by management method and source coal yields:

- For ash impoundments, the percentage of Se(VI) ranged from 0 to 86 percent for plants burning bituminous coal (19 samples), 89 to 95 percent for plants burning lignite/subbituminous coal (3 samples), and 1 to 19 percent for sites receiving ash from units that burn a blend of bituminous and subbituminous coal (2 samples) (Figure 5-5).
- For ash landfills, the percentage of Se(VI) was 65 to 100 percent for plants burning bituminous coal (3 samples), and 60 to 91 percent for plants burning lignite/subbituminous coal (2 samples).
- One other ash management site (27413) where ash was originally sluiced, then landfilled, and where a mixture of coal sources were used, had 95 to 99 percent Se(VI) (3 samples).
- For FGD landfills, the percentage of Se(VI) was 45 to 72 percent for plants burning bituminous coal (2 samples), and 100 percent for plants burning lignite/subbituminous coal (1 sample) (Figure 5-5).
- No FGD impoundment samples had greater than 80 percent species recovery.

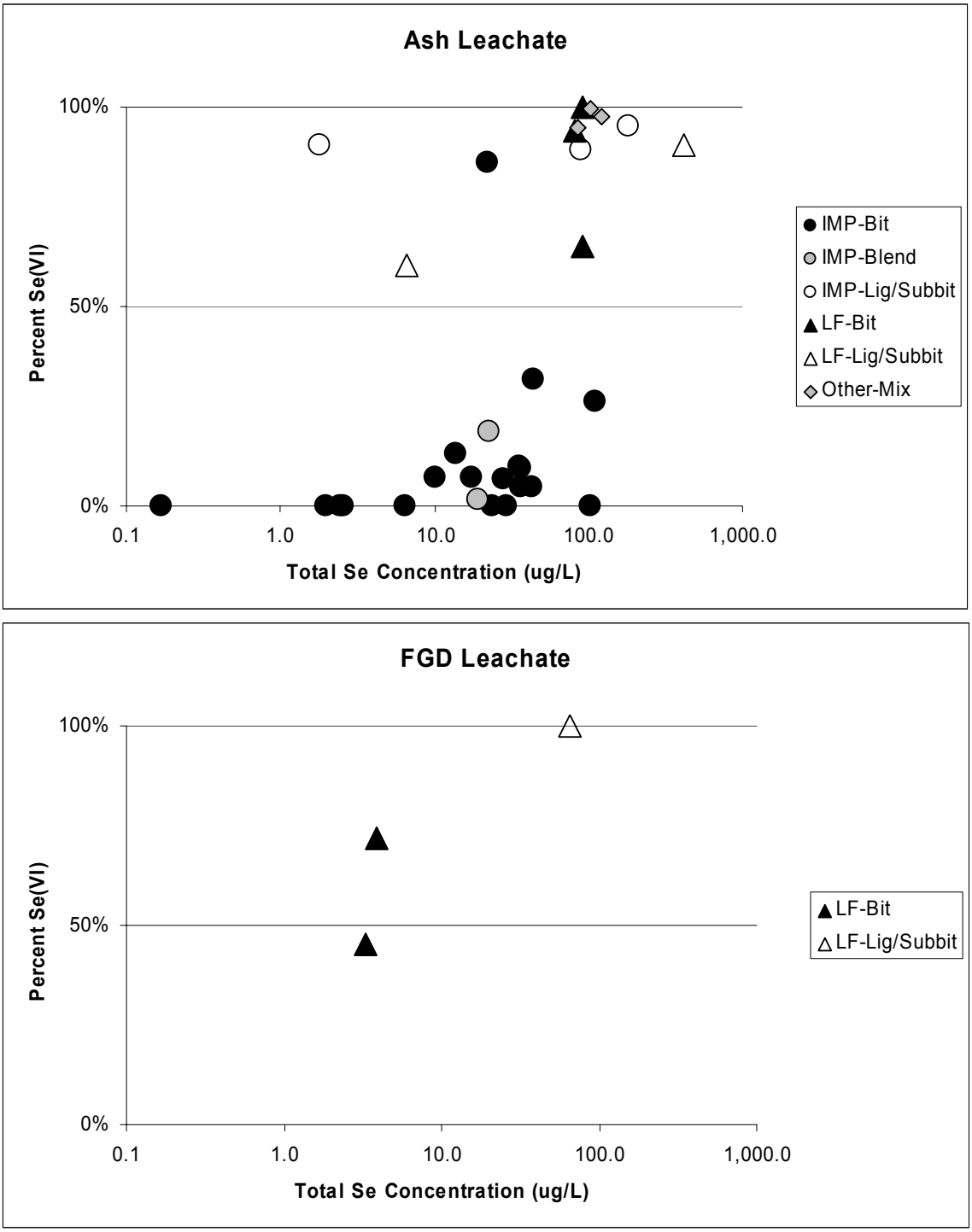

Figure 5-5
Relative percent of Se(VI) versus total Se concentration

Results of the dominant species analysis corroborates the relative percentage analysis and indicates that ash leachate is dominated by Se(IV) in impoundment settings when the source coal is bituminous or a mixture of bituminous and subbituminous, while Se(VI) is predominant in

landfill settings and when the source coal is subbituminous/lignite (Table 5-4). Most samples with relatively high concentration (>80 µg/L) were dominated by Se(VI) while samples with concentrations lower than 50 µg/L were mostly dominated by Se(IV) (Figure 5-6).

Table 5-4
Tabulation of Dominant Selenium Species by Sample

Ash Samples	**Impoundment**	**Landfill**	***Total***
Ash – Bituminous	24 – 0 – 2 (36)	0 – 0 – 4 (6)	*24 – 0 – 6* *(42)*
Ash – Blend/Mix	4 – 0 – 0 (7)	1 – 0 – 1 (5)	*5 – 0 – 4** *(15*)*
Ash – Subbituminous/Lignite	0 – 0 – 3 (5)	0 – 0 – 4 (5)	*0 – 0 – 7* *(10)*
Total	*28 – 0 – 5* *(48)*	*1 – 0 – 9* *(16)*	*29 – 0 – 17** *(67*)*
FGD Samples	**Impoundment**	**Landfill**	***Total***
FGD – Bituminous		0 – 1 – 3 (6)	*0 – 1 – 3* *(6)*
FGD – Blend/Mix			
FGD – Subbituminous/Lignite	0 – 0 – 1 (5)	0 – 0 – 2 (3)	*0 – 0 – 3* *(8)*
Total	*0 – 0 – 1* *(5)*	*0 – 1 – 5* *(9)*	*0 – 1 – 6* *(14)*

Legend: number of samples in which → Se(IV) dominant - Neutral - Se(VI) dominant
(Total number of samples in group)

* Tabulation includes the samples from the 27413 site, which could not be characterized as landfill or impoundment.

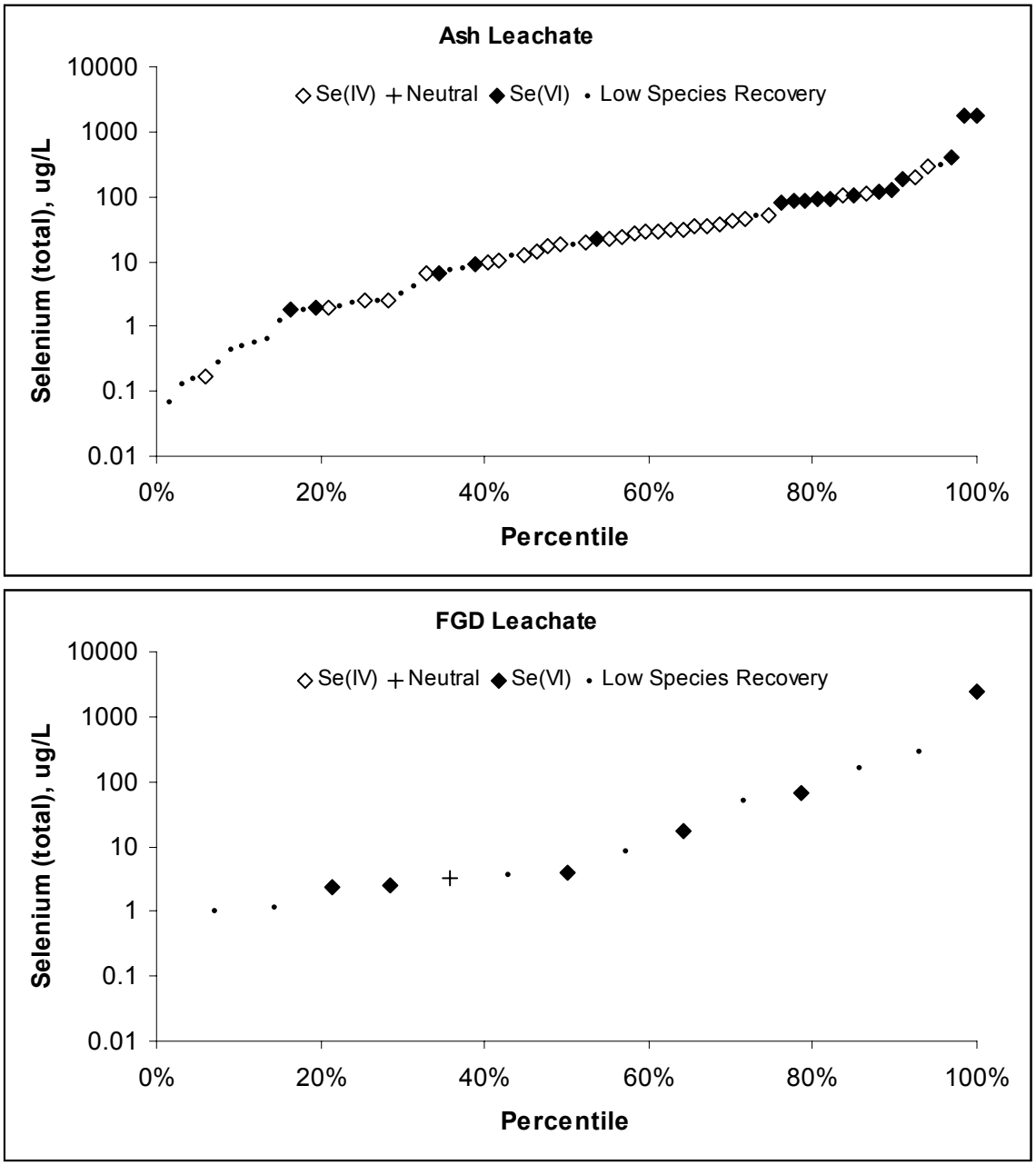

Figure 5-6
Species predominance as a function of total selenium concentration in leachate.

Chromium

Overview of Results

Chromium was detected in 42 of the 81 samples (Table 5-5). Chromium speciation was not always determined in samples for which total concentrations were non-detect or lower than 1 µg/L. Cr(III) analysis was performed for 45 samples, and 29 had detectable concentrations. Cr(VI) was analyzed in 58 samples and 37 had detectable concentrations. Review of duplicate samples indicated that chromium results were reproducible.

The speciation mass balance was good for total chromium concentrations greater than 5 µg/L: 16 of 19 samples with concentration greater than 5 µg/L had species recovery greater than 80 percent (Figure 5-7). The three other samples from this group had greater than 65 percent recovery.

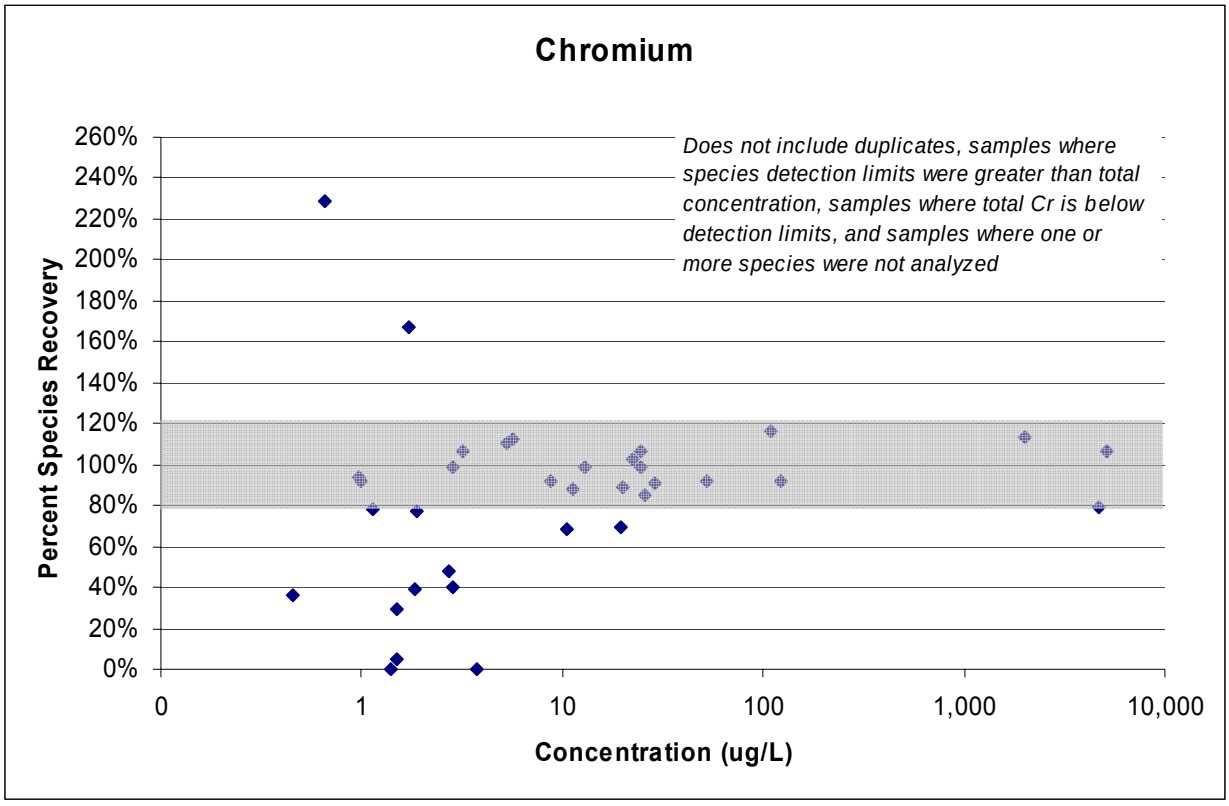

Figure 5-7
Chromium species recovery

Table 5-5
Chromium Speciation Data

Site	Sample	Source	Byproduct	Coal	Total Cr (ug/L)	Cr(III) (ug/L)	Cr(VI) (ug/L)	Sum of Species	% Recovery	% Cr(III)	% Cr(VI)
50210	001	LF	FA,BA	Mix	<0.5		2.2	2.20	*		
50213	002	LF	FA	Subbit	5,100	340	5,090	5,430.00	**106%**	6%	94%
50213	003	LF	FA	Subbit	4,670	190	3,530	3,720.00	80%		
50183	004	LF	FA,BA	Mix	8.8	<0.1	8.1	8.10	**92%**	0%	100%
50183	005	LF	FA,BA	Mix	0.66		1.5	1.50	229%	0%	100%
23223A	006	LF	SDA	Subbit	5.7	<0.1	6.4	6.40	**113%**	0%	100%
23223B	007	IMP	FGD	Subbit	1.7	<0.1	2.9	2.90	167%	0%	100%
23223B	008	IMP	FGD	Subbit	<0.5		<0.1	*	*		
23223B	009	IMP	FGD	Subbit	53	1.3	47	48.53	**92%**	3%	97%
23214	010	LF	FA	Subbit	26	<0.4	22	22.00	**85%**	0%	100%
14093	012	IMP	FA	Bit	<0.5		1.9	1.90	*		
14093	013	IMP	FA	Bit	<0.5		0.70	0.70	*		
14093	*013D*	*dup*	*FA*	*Bit*			*0.70*	*0.70*	*		
14093	014	IMP	FA	Bit	<0.5		0.50	0.50	*		
25410A	015	IMP	FA,BA	Blend	13	<0.4	13	12.80	**99%**	0%	100%
25410A	016	IMP	FA,BA	Blend	3.8	<0.1	<0.5	*	0%		
13115A	017	IMP	FA,BA	Subbit	2.8	<0.04	2.8	2.80	**98%**	0%	100%
13115B	018	IMP	FA,BA	Bit	<0.5		1.3	1.30	*		
13115A	019	IMP	FA	Subbit	0.96	<0.1	0.90	0.90	**94%**	0%	100%
13115A	020	IMP	FA,BA	Subbit	0.66		<0.05	*	0%		
49003A	021	IMP	FA	Bit	<0.5		<0.05	*	*		
49003A	022	IMP	FA	Bit	0.98	<0.04	0.90	0.90	**92%**	0%	100%
49003A	023	IMP	FA	Bit	<0.5		<0.5	*	*		
49003B	024	LF	FA	Bit	<0.5			*	*		
49003B	025	LF	FA	Bit	<0.5			*	*		
49003A	026	IMP	FA	Bit	1.1	<0.04	0.90	0.90	78%		
35015A	027	LF	FGD, FA	Bit	<0.5			*	*		
35015A	028	LF	FGD, FA	Bit	<0.5			*	*		
35015A	029	LF	FGD, FA	Bit	<0.5			*	*		

Table 5-5 (Continued)
Chromium Speciation Data

Site	Sample	Source	Byproduct	Coal	Total Cr (ug/L)	Cr(III) (ug/L)	Cr(VI) (ug/L)	Sum of Species	% Recovery	% Cr(III)	% Cr(VI)
35015B	030	IMP	FA	Bit	<0.5		<0.05	*	*		
35015B	031	IMP	FA	Bit	<0.5		<0.1	*	*		
35015B	032	IMP	FA,BA	Bit	1.4	<0.1	<0.05	*	0%		
33106	037	IMP	FA	Bit	<0.4	<0.01	<0.01	*	*		
33106	038	IMP	FA	Bit	<0.4	<0.01	<0.01	*	*		
33106	039	IMP	FA	Bit	<0.4	<0.01	<0.01	*	*		
33106	042	IMP	FA	Bit	<0.4	0.17	0.029	0.20	*		
33106	043	IMP	FA	Bit	29	26	<0.1	26.42	**91%**	100%	0%
33106	044	IMP	FA	Bit	<0.4	0.25	<0.01	0.25	*		
33106	*044D*	*dup*	*FA*	*Bit*	*<0.4*	*0.12*	*<0.01*	*0.12*	*		
33106	049	IMP	FA,BA	Bit	<0.4	0.074	<0.01	0.07	*		
40109	051	IMP	FA	Bit	11	9.9	<0.05	9.92	**88%**	100%	0%
40109	052	IMP	FA	Bit	<0.4	0.16	0.064	0.22	*		
40109	053	IMP	FA	Bit	<0.4	0.050	<0.01	0.05	*		
40109	057	IMP	FA,BA	Bit	1.9	1.1	0.41	1.47	77%		
40109	059	IMP	FA,BA	Bit	2.7	0.011	1.3	1.29	48%		
40109	*059D*	*dup*	*FA,BA*	*Bit*	*2.5*	*<0.01*	*1.2*	*1.23*	*49%*		
33104	061	IMP	FA	Bit	<0.4	0.27	<0.01	0.27	*		
33104	062	IMP	FA	Bit	10	0.95	6.2	7.19	69%		
33104	064	IMP	FA	Bit	22	0.044	23	23.02	**103%**	0%	100%
33104	069	IMP	FA,BA	Bit	3.2	0.46	3.0	3.44	**107%**	13%	87%
33104	070	IMP	FA,BA	Bit	5.3	0.63	5.3	5.91	**111%**	11%	89%
33104	*070D*	*dup*	*FA,BA*	*Bit*	*5.4*	*0.62*	*5.2*	*5.78*	***106%***	*11%*	*89%*
22346	079	IMP	FA,OA	Blend	<0.2	<0.02	<0.006	*	*		
22346	*079D*	*dup*	*FA,OA*	*Blend*	*<0.2*	*<0.02*	*<0.006*	*	*		
22346	082	IMP	FA,OA	Blend	25	1.2	23	24.19	**98%**	5%	95%
22347	083	IMP	FA	Blend	20	2.4	15	17.66	**89%**	14%	86%
22346	084	IMP	FA,OA	Blend	<0.2	0.039	<0.006	0.04	*		
27413	090	See Notes	FA	Mix	0.75			*	*		
27413	091	See Notes	FA	Mix	<0.2			*	*		
27413	092	See Notes	FA	Mix	122	2.8	109	111.61	**91%**	2%	98%

Table 5-5 (Continued)
Chromium Speciation Data

Site	Sample	Source	Byproduct	Coal	Total Cr (ug/L)	Cr(III) (ug/L)	Cr(VI) (ug/L)	Sum of Species	% Recovery	% Cr(III)	% Cr(VI)
50212	097	LF	FA	Subbit	2,000	40	2,230	2,270.00	**114%**	2%	98%
50183	098	LF	FA,BA	Mix	2.8	0.16	0.99	1.15	40%		
50183	099	LF	FA,BA	Mix	<0.2			*	*		
50408	101	LF	FA,BA	Bit	1.5	<0.08	0.075	0.07	5%		
50211	102	LF	FA	Bit	20	0.42	13	13.70	70%		
34186B	105	IMP	FGD	Lig	<0.4			*	*		
34186C	106	LF	FGD,FA,BA	Lig	0.91			*	*		
34186C	*106D*	*dup*	*FGD,FA,BA*	*Lig*	*0.88*			*	*		
34186B	107	IMP	FGD	Lig	<2			*	*		
34186A	108	LF	FA	Lig	0.48			*	*		
49003B	111	LF	FA	Bit	0.54			*	*		
49003B	112	LF	FA	Bit	<0.2			*	*		
49003A	113	IMP	FA	Bit	<0.2			*	*		
49003A	114	IMP	FA	Bit	0.31			*	*		
49003A	115	IMP	FA	Bit	1.5	0.34	0.092	0.43	29%		
49003A	116	IMP	FA	Bit	1.8	0.40	0.31	0.71	39%		
35015B	118	IMP	FA,BA	Bit	<0.2			*	*		
35015B	*118D*	*dup*	*FA,BA*	*Bit*	*<0.2*			*	*		
35015B	119	IMP	FA,BA	Bit	0.23			*	*		
35015A	120	LF	FGD, FA	Bit	<0.2			*	*		
35015A	121	LF	FGD, FA	Bit	<0.2			*	*		
35015A	122	LF	FGD, FA	Bit	<0.2			*	*		
43035	126	IMP	FA,BA	Subbit	108	4.1	121	125.04	**116%**	3%	97%
43035	*126D*	*dup*	*FA,BA*	*Subbit*	*109*	*2.1*	*122*	*124.39*	***114%***	*2%*	*98%*
43035	127	IMP	FA,BA	Subbit	24	0.53	26	26.03	**107%**	2%	98%
43034	128	LF	FGD,FA	Lig	0.46	0.16	<0.02	0.16	36%		

Table 5-5 (Continued)
Chromium Speciation Data

Site	Sample	Source	Byproduct	Coal	Total Cr (ug/L)	Cr(III) (ug/L)	Cr(VI) (ug/L)	Sum of Species	% Recovery	% Cr(III)	% Cr(VI)
13115B	HN-1	IMP	FA,BA	Bit	<0.5			*	*		
13115B	HN-2	IMP	FA,BA	Bit	<0.5			*	*		
25410B	SX-1	IMP	FA	Blend	<0.5		<0.1	*	*		

Notes:
Ash at site 27413 (samples 090, 091, 092) was first sluiced, then managed dry.
* indicates that sum of species was not calculated because individual species were not analyzed or not detected, **or** % recovery was not calculated because the total chromium concentration was below detection limits or individual species were not analyzed.

Abbreviations:
Bit = bituminous; Subbit = Subbituminous; Mix = CCP from different units burning different coals; Blend = CCP from a single unit burning two different fuels
FA = fly ash; BA = bottom ash; EA = economizer ash; FGD = flue gas desulfurization sludge; OA = oil ash
LF = landfill; IMP = impoundment; DUP = duplicate sample
ND = not determined

Comparison of Speciation to Site and Plant Attributes

For ash leachate samples with greater than 80 percent species recovery (20 samples), the percentage of Cr(III) ranged from 0 to 100 percent, with a median of 2 percent and the range of Cr(VI) was 0 to 100 percent with a median of 98 percent. For FGD leachate (3 samples), Cr(III) ranged from 0 to 3 percent with a median of 0 percent and Cr(VI) ranged from 97 to 100 percent with a median of 100 percent (Figure 5-8).

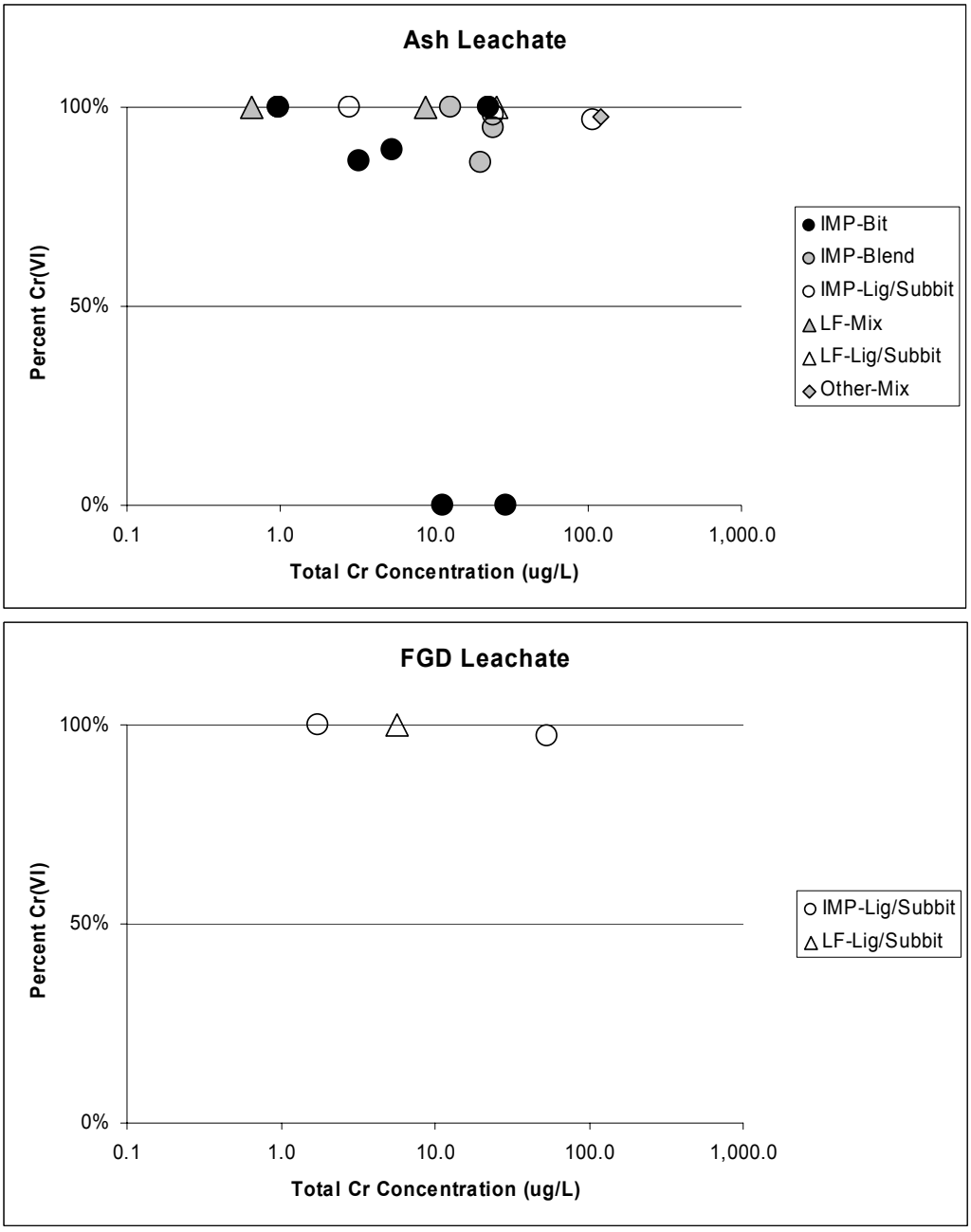

Figure 5-8
Percent Cr(VI) versus total Cr concentration

Using the same approach as for arsenic and selenium, the dominant chromium species was determined in 27 samples, and 24 of these were dominated by Cr(VI). The only samples dominated by Cr(III) were obtained from impoundments where the source coal was bituminous (Table 5-6). Two of these samples had very low pH (<4.5) and the other had relatively low concentration. There was no apparent relationship of between chromium speciation and total concentration (Figure 5-9).

The predominance of Cr(VI) matches geochemical expectations, because nearly all leachate samples are neutral to alkaline, and Cr(VI) is very soluble under such conditions, while Cr(III) would precipitate or bind strongly to mineral surfaces. The notable exceptions were samples 043 and 051, which only contained soluble Cr(III), and sample 057 which had a mixture of Cr(III) and Cr(V)), but also had a relatively low total concentration (1.9 µg/L). Samples 043 and 051 had the lowest pH values measured in the study (4.26 and 4.35, respectively; 1.5 pH units lower than the next lowest sample). Under the strongly acidic pH of these samples, the solubility of Cr(III) and Cr(VI) is reversed.

Five samples (002, 003, 092, 097, and 126) had Cr(VI) concentrations greater than 100 µg/L, and three of those samples (002, 003, and 097) had concentrations > 1,000 µg/L. All five samples were strongly alkaline (pH > 9.4) and oxidizing (Eh > 200 mV), and four are known to have had subbituminous coal as the CCP source (the coal source for sample 092 was uncertain).

Table 5-6
Tabulation of Dominant Selenium Species by Sample

Ash Samples	**Impoundment**	**Landfill**	***Total*****
Ash – Bituminous	3 – 0 – 6 (15)	0 – 0 – 1 (3)	*3 – 0 – 7* *(18)*
Ash – Blend/Mix	0 – 0 – 3 (4)	0 – 0 – 2 (3)	*0 – 0 – 6** *(9*)*
Ash – Subbituminous/Lignite	0 – 0 – 4 (5)	0 – 0 – 4 (5)	*0 – 0 – 8* *(10)*
Total	*3 – 0 – 13* *(24)*	*0 – 0 – 7* *(11)*	*3 – 0 – 21** *(37*)*
FGD Samples	**Impoundment**	**Landfill**	***Total*****
FGD – Bituminous			
FGD – Blend/Mix			
FGD – Subbituminous/Lignite	0 – 0 – 2 (2)	0 – 0 – 1 (3)	*0 – 0 – 3* *(5)*
Total	0 – 0 – 2 (2)	0 – 0 – 1 (3)	*0 – 0 – 3* *(5)*

Legend: number of samples in which → Cr(III) dominant - Neutral - Cr(VI) dominant
(Total number of samples in group)

* Tabulation includes two samples from the 27413 site, which could not be characterized as landfill or impoundment.
** Sum of total ash and FGD samples is less than 81 because only 42 samples had detectable chromium concentrations.

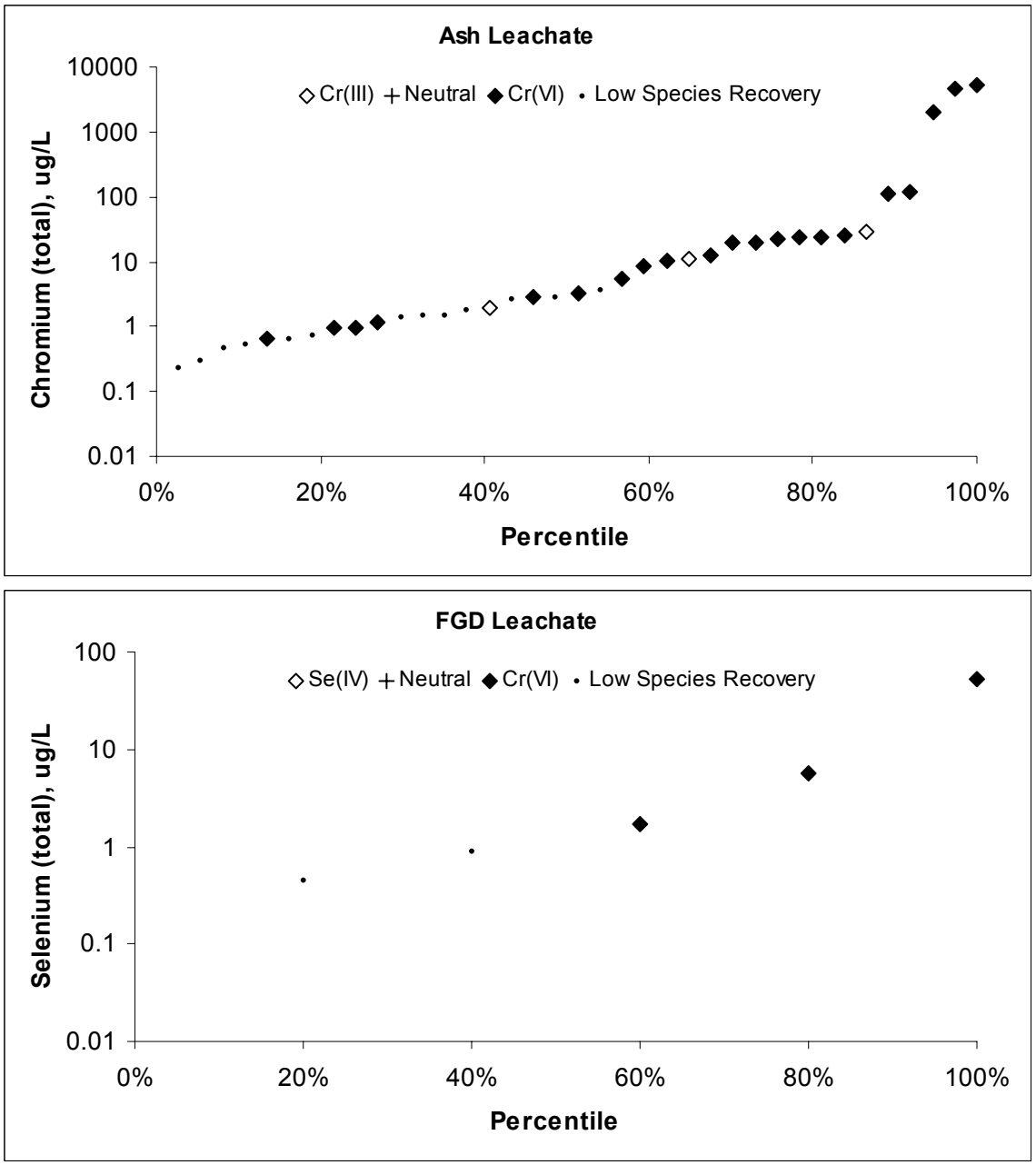

Figure 5-9
Species predominance as a function of total chromium concentration in leachate.

Mercury

Mercury speciation was determined on 31 samples, not counting duplicates (Table 5-7). Dimethyl mercury (DMM) was not determined on four of these samples, either because no sample was collected (due to logistic issues) or because the sample was lost during analysis (due to the fact that the employed analytical technique only allows one analysis attempt per sample). In addition, there was no particulate methyl mercury ($MeHg_{part}$) for one sample due to a field equipment problem; and dissolved methyl mercury and particulate mercury were not analyzed in

another sample due to insufficient sample volume. The two duplicate samples showed poor reproducibility of results.

Table 5-7
Mercury Species Data

Site	Sample	Source	CCP	Coal	Hg_{diss} (ng/L)	DMM (ng/L)	$MeHg_{diss}$ (ng/L)	Hg_{part} (ng/L)	$MeHg_{part}$ (ng/L)
50210	001	LF	FA,BA	Mix		0.055			0.028
50213	002	LF	FA	Subbit	14	0.0051	0.11	254	0.032
50213	003	LF	FA	Subbit	18	<0.005	0.091	26	<0.01
50183	004	LF	FA,BA	Mix	5.9	<0.005	0.26	<1	0.036
50183	005	LF	FA,BA	Mix	2.1	0.0097	0.12	44	0.086
23223A	006	LF	SDA	Subbit	0.82	<0.005	0.54	25	0.092
23223B	007	IMP	FGD	Subbit	1.9	0.0074	<0.02	16	0.022
23223B	008	IMP	FGD	Subbit	4.2	<0.005	0.068	<1	0.013
23223B	009	IMP	FGD	Subbit	28		<0.02	121	0.015
49003A	021	IMP	FA	Bit	1.4	<0.005	0.034	155	0.020
49003A	022	IMP	FA	Bit	1.00	<0.005	0.027	53	0.027
49003A	023	IMP	FA	Bit	1.4	<0.005	<0.02	14	0.026
49003A	026	IMP	FA	Bit	0.38	<0.005	<0.02	17	<0.01
35015A	027	LF	FGD, FA	Bit	21	<0.005	1.6	4.3	<0.01
35015A	028	LF	FGD, FA	Bit	1.2	<0.005	0.18	13	<0.01
35015A	029	LF	FGD, FA	Bit	12	<0.005	0.70	59	0.011
35015B	030	IMP	FA	Bit	0.80	0.022	0.063	<1	0.11
35015B	031	IMP	FA	Bit	5.2	0.050	6.7	30	
35015B	032	IMP	FA,BA	Bit	1.4	0.032	0.047	186	0.055
22346	079	IMP	FA,OA	Blend	0.25	<0.005	<0.02	5.8	0.058
22346	*079D*	*dup*	*FA,OA*	*Blend*	*0.48*	*<0.005*	*0.053*	*3.0*	*0.052*
22346	082	IMP	FA,OA	Blend	5.9	<0.005	0.046	18	0.027
22347	083	IMP	FA	Blend	2.1	0.040	0.17	22	0.16
22346	084	IMP	FA,OA	Blend	0.58	<0.005	0.056	4.6	0.027
50212	097	LF	FA	Subbit	37	*	0.22	16	0.054
50183	098	LF	FA,BA	Mix	61	*	0.76	11	0.015
50183	099	LF	FA,BA	Mix	5.7	*	0.033	13	<0.01
50408	101	LF	FA,BA	Bit	2.1	*	<0.02	3.0	0.010
50211	102	LF	FA	Bit	3.8	*	0.12	52	<0.01
43035	126	IMP	FA,BA	Subbit	9.4		0.17	3.1	0.024
43035	*126D*	*dup*	*FA,BA*	*Subbit*	*2.0*		*0.21*	*6.1*	*0.024*
43035	127	IMP	FA,BA	Subbit	5.4		0.028	3.0	0.018
43034	128	LF	FGD,FA	Lig	79		6.4	100	0.059

Notes:
* Failed QC due to high concentration in the equipment blank sample.

Abbreviations:
Bit = bituminous; Subbit = Subbituminous; Mix = CCP from different units burning different coals; Blend = CCP from a single unit burning two different fuels
FA = fly ash; BA = bottom ash; EA = economizer ash; FGD = flue gas desulfurization sludge; OA = oil ash
LF = landfill; IMP = impoundment; DUP = duplicate sample

Total Hg_{diss} was detected in all 30 samples where collected, with concentrations ranging from 0.25 to 79 ng/L. Particulate mercury was detected in 27 of 30 samples.

DMM results were detectable in only 8 of the 22 samples that passed QC, and detected concentrations were lower than 0.06 ng/L. Samples 097 through 102 reported considerably higher DMM concentrations than the other samples; however, the second highest concentration was from equipment blank sample 084 (0.81 ng/L). As a result, DMM samples 097 through 102, which were collected on a single trip, failed to meet QC criteria, and were not reported here. There was no apparent difference in DMM concentration by coal type or management method.

$MeHg_{diss}$ was detected in 24 of 30 samples where analyzed, and concentrations ranged from non-detect to 6.7 ng/L. Only three samples had a $MeHg_{diss}$ concentration greater than 1 ng/L. The site with the highest concentration, 35015A, yielded two other samples with concentrations lower than 0.1 ng/L. There was no clear difference in $MeHg_{diss}$ concentrations by coal type, but there was a tendency for landfill leachate to yield higher concentrations than impoundment leachate.

Methylated vs. Inorganic Mercury

The relative methyl mercury fraction of the total mercury concentration was calculated as:

$$f(MeHg)\ [\%] = 100 \bullet [MeHg_{diss} + DMM)]/Hg_{diss}$$

DMM was added to the $MeHg_{diss}$ concentrations, because it is likely that any DMM present in the collected MeHg samples would have been volatilized by the time the samples were analyzed. There was no apparent correlation between the concentrations of total mercury and methylated mercury compounds (Figure 5-10). Furthermore, methylated mercury compounds constitute only a small fraction of the total mercury concentration in the studied waters, usually less than 5 percent (Figure 5-10). This is in agreement with most previous environmental mercury speciation studies. Only samples 006 and 031 had more than 15.2 percent $MeHg_{diss}$. Sample 006 had extremely low (<1 ng/L) Hg_{diss} and $MeHg_{diss}$ concentrations, while the $MeHg_{diss}$ concentration in sample 031 is suspect because: 1) it is higher than the total mercury (Hg_{diss}) concentration; and 2) it is two orders of magnitude higher than in two other samples (030 and 032) collected at that site on the same day (Table 5-7).

Dissolved vs. Particulate Mercury

Particulate mercury (Hg_{part} and $MeHg_{part}$) is a measure of the mercury on colloids in the water, which accumulate on the filter during sampling. As such, the particulate concentrations are dependent both on the mass of mercury on the particles and the mass of solids collected on the filters. It is of interest because mercury bound to colloids, which can move with groundwater, may be transported more quickly than mercury dissolved in water, which may sorb to the soil under the pH range typical of most groundwater.

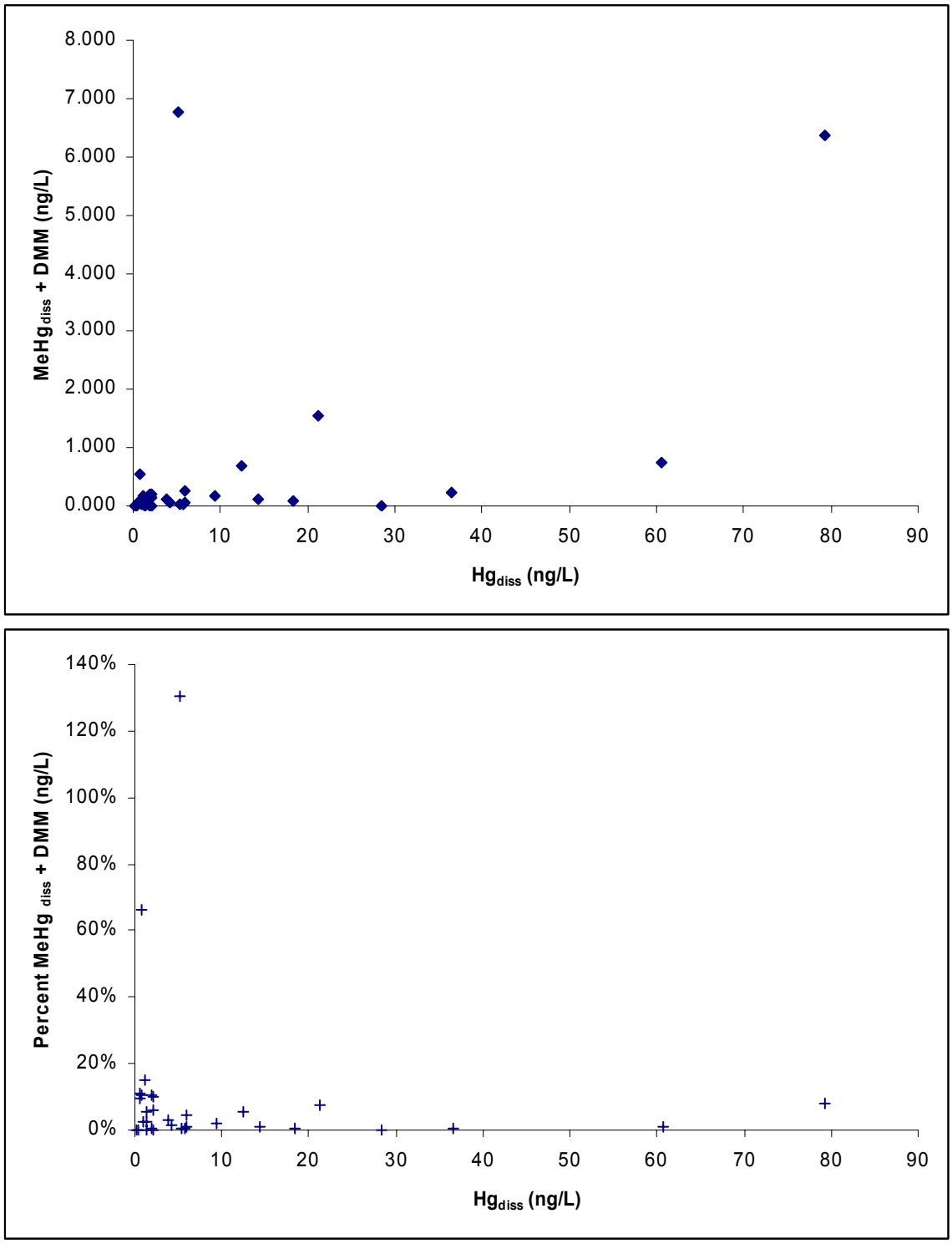

Figure 5-10
Comparison of organic and inorganic mercury concentrations

The Hg_{part} concentrations in the field leachate samples were low, ranging from <1 to 254 ng/L (Table 5-7). The highest concentration (sample 002) was obtained from a lysimeter at Site 50213, where subbituminous fly ash was managed. A second lysimeter at the same site had a particulate concentration of 26 ng/L. Conversely, the Hg_{diss} concentration associated with these two samples did not exhibit the variability of the particulate concentrations. There was no overall relationship between Hg_{part} and Hg_{diss} concentration (Figure 5-11), nor was there a relationship between $MeHg_{part}$ and $MeHg_{diss}$ (Figure 5-12).

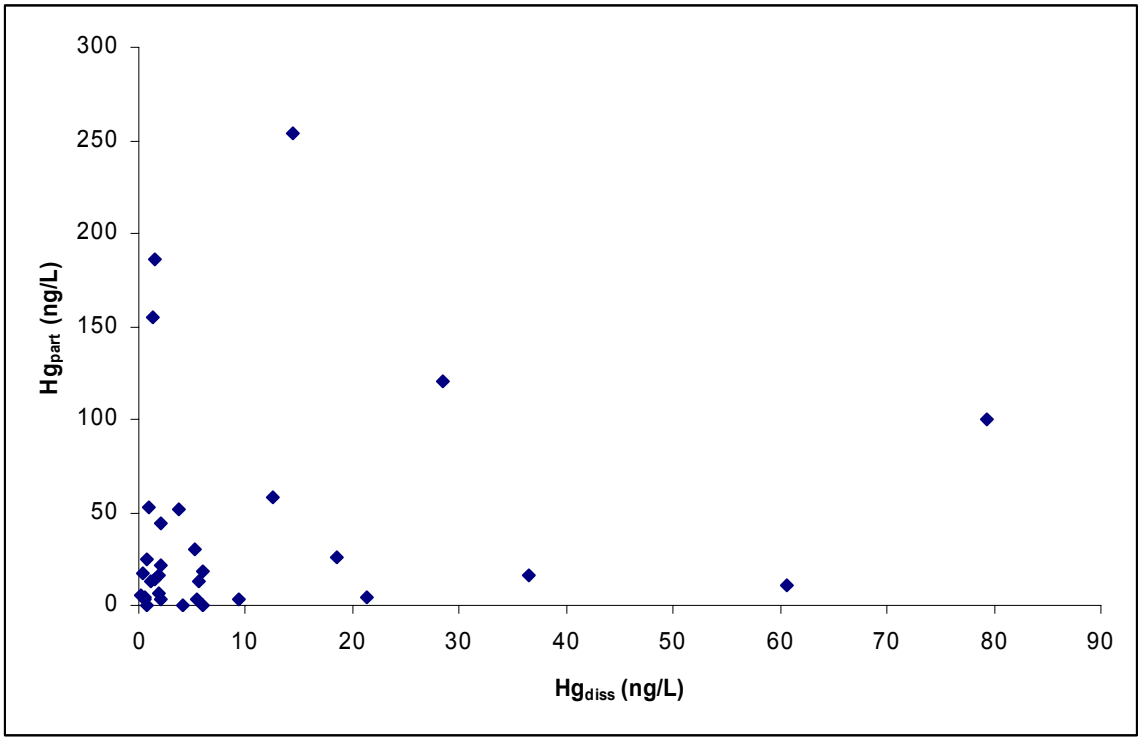

Figure 5-11
Dissolved versus particulate mercury concentrations

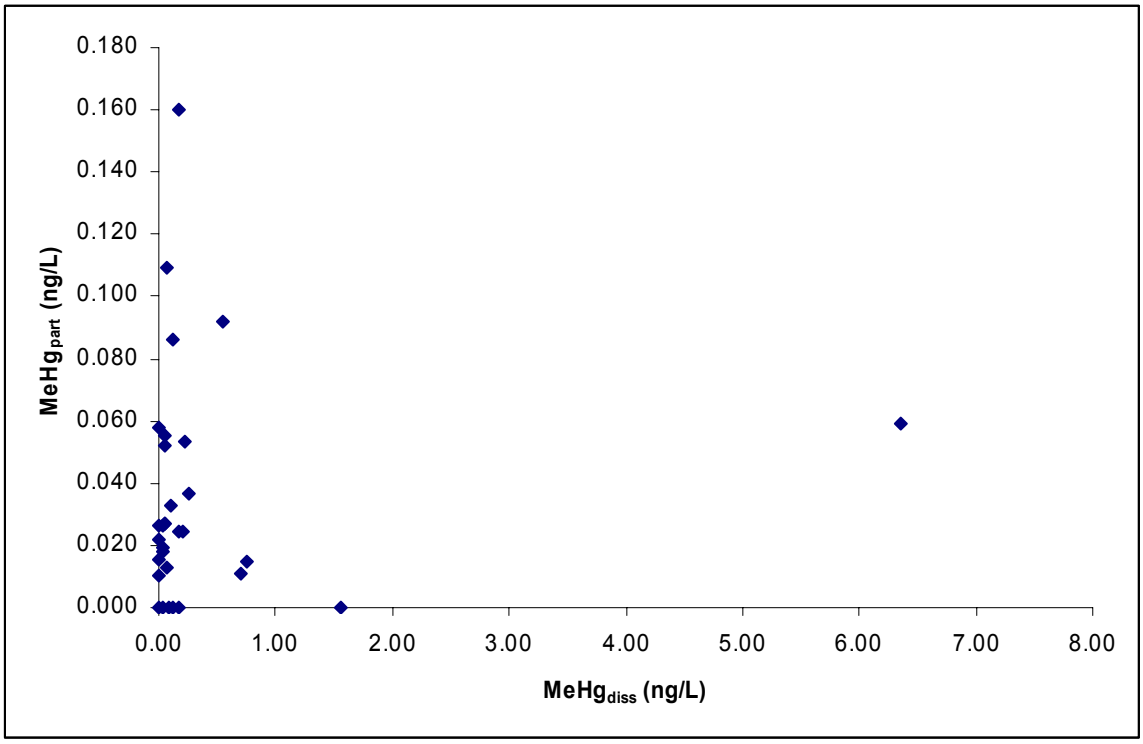

Figure 5-12
Dissolved versus particulate methyl mercury concentrations

6
CONCLUSIONS

The following conclusions are based on 81 field leachate samples collected at 29 CCP management sites. Due to their unique characteristics, coal ash leachate (67 samples) and FGD leachate (14 samples) were treated separately.

Chemical Composition of Coal Ash Field Leachate Samples

- Most leachate samples were moderately to strongly oxidizing and moderately to strongly alkaline. The subbituminous/lignite ash samples had higher median pH (10.0) than bituminous ash (6.9). Several samples with relatively low Eh and pH were collected from impoundments.
- The anion chemistry of coal ash leachate samples is dominated by sulfate. The median concentration of this constituent was 339 mg/L; this was the only constituent in the leachate with a median concentration greater than 100 mg/L.
- Major cation chemistry was strongly influenced by the type of coal burned at the power plant. Ash leachate derived from bituminous coal was dominated by calcium and magnesium, while ash leachate derived from subbituminous/lignite coal was dominated by sodium.
- Silica and boron had the highest median concentrations (4,645 and 2,160 µg/L, respectively) of the minor and trace constituents. Median concentrations of strontium, molybdenum, lithium, aluminum, and barium were greater than 100 µg/L. Conversely, median concentrations of chromium, beryllium, thallium, silver, lead, and mercury were lower than 1 µg/L; with silver, beryllium, and lead being rarely detected (detected in 7, 6, and 27 percent of the samples, respectively).
- Most constituents (22 out of the 34 analyzed) had higher concentrations in landfill leachate samples than in impoundment leachate samples.
- Leachate samples derived from bituminous coal ash had higher concentrations of calcium, magnesium, cobalt, lithium, manganese, nickel, antimony, thallium, and zinc than leachate from subbituminous coal ash. Lithium and manganese had concentrations an order of magnitude higher in the bituminous ash leachate samples, while thallium was only detected in leachate from bituminous ash.
- Leachate from subbituminous/lignite coal ash had higher concentrations of carbonates, chloride, sodium, sulfate, aluminum, chromium, copper, and mercury than leachate from bituminous coal. The difference was most notable for

aluminum and mercury, where the concentrations were higher by an order of magnitude or more.

Chemical Composition of FGD Leachate Field Samples

- The FGD leachate samples were moderately to strongly oxidizing, and moderately to strongly alkaline. Landfill samples, as a group, were less oxic and more alkaline than impoundment samples, although the lowest Eh value was for an impoundment.
- Concentrations of most major constituents (specifically, calcium, chloride, potassium, sodium, and sulfate) in FGD leachate were higher than in ash leachate. The median sulfate concentration was 1,615 mg/L, and the maximum sulfate concentration was 30,500 mg/L, which was the highest single analytical result returned from the field leachate sampling. The high sulfate concentration was obtained from an impoundment where sluice water is recirculated.
- More than 25 percent of the chloride and sodium concentrations were greater than 1,000 mg/L, and median concentrations of chloride, calcium, potassium, and sodium were greater than 100 mg/L.
- The FGD leachate samples had higher percentages of chloride and potassium than the ash leachate samples.
- Anion concentrations were largely dominated by sulfate. Major cation concentrations (calcium, magnesium, potassium, sodium) were variable, with samples from the same site having different cation chemistry.
- The relative concentrations of minor and trace elements in FGD leachate were somewhat different than in ash leachate. Median concentrations of boron, strontium, and lithium in FGD leachate were a factor of 3 or more higher than in ash leachate, while concentrations of selenium, vanadium, uranium, and thallium in ash leachate were higher than in FGD leachate by a factor of 3 or more.
- Boron (9,605 µg/L), strontium (5,230 µg/L), lithium (3,055 µg/L), and silica (2,480 µg/L) had median concentrations greater than 1,000 µg/L in the FGD field leachate samples. Median concentrations of molybdenum, aluminum, and manganese were greater than 100 µg/L, while median concentrations of chromium, beryllium, thallium, silver, lead, and mercury were lower than 1 µg/L. Silver was not detected in the 14 FGD leachate samples, while beryllium (7 percent detects), chromium (36 percent), iron (29 percent), lead (36 percent), and thallium (14 percent), were usually not detected.

Speciation Analysis in Field Leachate Samples

Arsenic

- Arsenic concentrations in ash leachate ranged from 1.4 to 1,380 µg/L, with a median of 25 µg/L.

- The dominant arsenic species was determined in 43 samples. Most ash leachate samples (37) were dominated by As(V). As(III) was only dominant in four samples from impoundments where bituminous coal ash was managed. Two samples had equal amounts of arsenic species.
- Arsenic concentration in FGD leachate ranged from 11 to 230 μg/L, with a median of 28 μg/L.
- The dominant arsenic species was determined in 6 FGD leachate samples. Two were dominated by As(V), two were dominated by As(III), and two samples had equal amounts of the species.

Selenium

- Selenium concentration in ash leachate ranged from 0.07 to 1,760 μg/L, with a median of 19 μg/L.
- The dominant selenium species was determined in 46 leachate samples. Most ash leachate samples (29) were dominated by Se(IV). Se(VI) was dominant in 17 samples. Se(IV) dominated in impoundment settings when the source coal was bituminous or a mixture of bituminous and subbituminous, while Se(VI) was predominant in landfill settings and when the source coal was subbituminous/lignite. Most samples with relatively high concentration (>80 μg/L) were dominated by Se(VI) while samples with concentrations lower than 50 μg/L were mostly dominated by Se(IV).
- Selenium concentration in FGD leachate ranged from 1.1 to 2,360 μg/L, with a median of 6.2 μg/L.
- The dominant selenium species was determined in 7 FGD leachate samples. Six were dominated by Se(VI), one had similar percentages of both species, and none were dominated by Se(IV).

Chromium

- Chromium concentration in ash leachate ranged from <0.2 to 5,100 μg/L, with a median of 0.60 μg/L.
- The dominant chromium species was determined in 27 ash leachate samples. Most ash leachate samples (24) were dominated by Cr(VI). Cr(III) was dominant in three samples, two of which had acidic pH.
- Chromium concentration in FGD leachate ranged from <0.2 to 53 μg/L, with a median concentration below detection limits.
- The dominant chromium species was determined in three FGD leachate samples, and all three were dominated by Cr(VI).

Mercury

- Mercury concentrations in 22 ash leachate samples were very low, ranging from 0.25 to 61 ng/L, with a median concentration of 3.8 ng/L. Mercury concentrations in 8 FGD leachate samples were also very low, ranging from 0.82 to 79 ng/L, with a median concentration of 8.3 ng/L.
- The organic species of mercury always had low concentration, usually less than 5 percent of the total mercury concentration. Monomethyl mercury concentrations ranged from <0.02 to 6.7 ng/L, with a median concentration of 0.08 ng/L. Dimethyl mercury concentrations ranged from <0.02 to 0.06 ng/L, with a median concentration of <0.02 ng/L. There was no relationship between inorganic and organic mercury concentrations.
- There was no clear relationship between organic mercury concentrations and coal type, although there was a tendency for landfill leachate to yield slightly higher concentrations than impoundment leachate.

Effects of Power Plant Attributes on CCP Leachate Composition

- Power plants that have cyclone boilers and burn petroleum coke produced leachate samples with higher than median concentrations of most elements, and the highest concentrations of cadmium, molybdenum, and vanadium.
- There was no definitive relationship on leachate quality associated with hot-side and cold-side ESPs. Three sites receiving ash from hot-side ESPs were sampled. A landfill yielded the highest concentrations of Co, CO_3, Cr, Cu, Na, Se, and SO_4 of the sampled ash sites. However two impoundments did not show evidence of high concentrations.
- Oil ash was managed with coal ash at one site. The leachate from the ash sampled at this site did not show any evidence of low or high concentration for any elements.
- Most constituents in leachate from the single plant with a spray-dryer FGD system had lower concentration than leachate samples from the wet FGD systems used at other plants.

7
REFERENCES

EPRI, 1994. *Chemical Attenuation Reactions of Selenium*, Palo Alto, CA, Report TR-103535.

EPRI, 2000a. *Environmental Chemistry of Arsenic: A Literature Review*, Palo Alto, CA, Report 100585.

EPRI, 2000b. *Field Evaluation of the Comanagement of Utility Low-Volume Wastes with High-Volume Coal Combustion By-Products: HA Site.* Final Report 1000720, October 2000.

EPRI, 2003a. *Combustion By-Product Environmental Analysis System*, Palo Alto, CA, Report 1005263.

EPRI, 2003b. *Field Evaluation of Comanagement of Utility Low-Volume Wastes with High-Volume By-Products: MO Site*, Palo Alto, CA, Report 1005267.

EPRI, 2004. *Chemical Attenuation Coefficients for Arsenic Species Using Soil Samples from Selected Power Plant Sites*, Palo Alto, CA, Report 1005505.

Gürleyük, H. and D. Wallschläger, 2001. *Determination of Chromium Species Using Suppressed Ion Chromatography-Inductively-Coupled Plasma-Mass Spectrometry*, J. Anal. At. Spectrom. **16**, 926-930.

Hintelmann, H. and N. Ogrinc, 2003. *Determination of Stable Mercury Isotopes by ICP/MS and Their Application in Environmental Studies*, in: Cai, Y. & Braids, O.C. (eds.): Biogeochemistry of environmentally important trace elements, ACS Symposium Series 835, American Chemical Society, 321-338.

Lindberg, S.E., G. Southworth, E.M. Prestbo, D. Wallschläger, M.A. Bogle, and J. Price, 2004. *Gaseous Methyl- and Inorganic Mercury in Landfill Gas from Landfills in Florida, Minnesota, Delaware and California*, accepted for publication in Atmos. Environ.

Puls, R.W and M.J. Barcelona, 1995. *Low-Flow (Minimal Drawdown) Ground-Water Sampling Procedures*, U.S. Environmental Protection Agency, EPA Ground Water Issue, EPA540-S-95-504.

Wallschläger, D. and R. Roehl, 2001. *Determination of Inorganic Selenium Speciation in Waters by Ion Chromatography-Inductively-Coupled Plasma-Mass Spectrometry Using Eluant Elimination with a Membrane Suppressor*, J. Anal. At. Spectrom. **16**, 922-925.

Wallschläger, D., R.T. Wilkin, and R.G. Ford, 2005. *Soluble Arsenic-Thio Species in Sulfidic Waters*, submitted to Environ. Sci. Technol.

A
ANALYTICAL RESULTS

Table A-1
Hydrochemistry and Trace Elements

		001	002	003	004	005	006	007	008	009	010	012	QA-1	013
Chloride	mg/L	86.2	25	11	26	6.5	19	572	371	345	28	9	< 0.01	27.3
Sulfate	mg/L	909	6,690	5,450	1,960	350	1,450	3,150	2,080	10,400	3,830	1,650	0.47	1,700
Sodium	mg/L	443	3,410	2,910	672	93	108	1,330	606	743	1,700	30	0.4	55
Potassium	mg/L	255	80	80	20	< 5	10	80	20	40	118	< 20	< 0.2	75
Magnesium	mg/L	< 1	0.59	0.53	70	15	77	125	23	1,990	8	13	0.10	36
Calcium	mg/L	10	19	9	218	70	528	524	563	577	139	681	0.53	584
TOC	mg/L	13.9	55.1	49.8	43.9	4.5	8.1	20.5	16.2	9.9	5.3	1.9	0.4 (a)	6.3
TIC	mg/L	6.9	32.2	63.1	29.7	11.9	17.5	2.4	2.7	1.7	1.7	2.0	1.56	16.6
Temperature	°C	20.2	21.5	15.4	14.9	21.3	18.7	17.6	26.9	25.6	17.3	22.6	n/a	21.3
Spec. Cond.	mS/cm	3.5	12.8	11.2	3.8	0.8	2.9	8.3	4.8	13.0	7.7	2.7	n/a	2.9
Diss. Oxygen	% sat.	0.1	0.2	0.2	0.2	0.2	0.4	0.2	0.3	0.3	14	5	n/a	4
pH	pH	11.6	10.0	10.3	9.3	7.4	8.0	6.2	8.4	7.4	11.2	9.4	n/a	8.2
ORP (corr.)	mV	209	276	271	276	411	341	356	1	342	111	245	n/a	102
Lithium	ug/L	2,460	< 20	< 20	< 20	< 20	< 20	170	< 20	2,720	< 20	80	< 20	100
Beryllium	ug/L	< 1	< 1	< 1	< 1	< 1	< 1	< 1	< 1	< 1	< 1	< 1	< 4	< 1
Boron	ug/L	2,120	18,400	31,900	10,800	1,410	15,600	81,500	49,000	98,500	14,000	93,400	< 50	112,000
Aluminum	ug/L	18,100	2,680	17,500	< 30	< 30	< 30	610	890	190	980	530	< 30	< 30
Silicon	ug/L	6,900	5,800	1,200	6,100	6,400	2,600	10,500	400	12,700	9,900	1,500	< 100	18,500
Vanadium	ug/L	373	1,070	635	45	< 2	4	15	< 2	18	5,020	195	< 2	4
Manganese	ug/L	< 4	7	< 4	751	577	< 4	704	113	564	< 4	22	< 4	2,560
Iron	ug/L	< 50	< 50	< 50	< 50	< 50	< 50	1,200	< 50	< 50	< 50	< 50	< 50	14,700
Cobalt	ug/L	< 1	133	9	< 1	< 1	< 1	6	< 1	78	< 1	< 1	< 1	7
Nickel	ug/L	< 3	75	8	14	4	4	597	5	463	8	4	< 20	15
Copper	ug/L	11	494	62	6	3	4	14	44	7	15	< 3	< 3	< 3
Zinc	ug/L	< 5	< 5	< 5	< 5	6	19	23	< 5	34	12	12	< 30	45
Strontium	ug/L	800	60	< 30	930	80	9,140	16,900	14,900	11,700	3,900	2,250	< 30	1,260
Molybdenum	ug/L	9,740	5,720	6,200	1,200	440	310	60,800	570	320	25,400	740	< 30	100
Silver	ug/L	< 0.2	< 0.2	< 0.2	< 0.2	< 0.2	< 0.2	< 0.2	< 0.2	< 0.2	< 0.2	< 0.2	< 1	0.2
Cadmium	ug/L	17.7	8.8	7.6	1.9	0.8	0.7	12.3	11.8	4.2	51.9	1.5	< 2	0.4
Antimony	ug/L	0.9	0.8	0.7	0.6	< 0.3	4.7	2.8	0.7	4.6	1.0	6.7	< 3	0.7
Barium	ug/L	50	< 30	< 30	110	40	70	50	< 30	90	50	40	< 30	< 30
Thallium	ug/L	< 0.1	< 0.5	< 0.5	< 0.1	< 0.1	< 0.1	< 0.5	< 0.1	2.9	< 0.1	< 0.1	<0.01	0.6
Lead	ug/L	< 0.2	< 0.2	< 0.2	< 0.2	< 0.2	< 0.2	3.5	0.3	< 0.2	0.3	< 0.2	< 1	< 0.2
Uranium	ug/L	< 0.2	0.2	9.8	1.3	< 0.2	10.4	0.7	< 0.2	0.7	0.3	1.8	< 1	3.3

Table A-1 (Continued)
Hydrochemistry and Trace Elements

		013D	014	QA-2	015	016	SX-1	017	018	019	020	HN-1	HN-2	021
Chloride	mg/L	27.5	32.8	0.05	25.3	54.8	22.2	72.0	63.4	84.8	75.9	29.2	45.4	18.0
Sulfate	mg/L	1,610	1,370	0.40	782	910	1,530	91.4	339	124	131	1,260	810	193
Sodium	mg/L	56	17	0.9	60	731	52	53	57	56	54	72	53	31
Potassium	mg/L	74	26	< 0.2	20	229	38	8	9	6	6	277	48	11
Magnesium	mg/L	39	7	0.63	33	20	7	21	36	28	23	3	21	13
Calcium	mg/L	544	591	1.34	255	15	529	46	231	81	43	302	291	48
TOC	mg/L	6.2	3.9	0.6 (a)	5.3	24.0	16.6	6.7	14.2	6.0	0.4 (a)	21.5	22.5	1.2 (a)
TIC	mg/L	16.7	35.1	1.47	15.4	5.60	11.3	22.4	115.0	48.7	24.8	2.48	2.94	8.03
Temperature	°C	n/a	20.5	32	31.7	30.6	n/a	29.7	18.3	35.5	29.6	n/a	n/a	20.8
Spec. Cond.	mS/cm	n/a	2.6	0.0	1.6	5.1	n/a	0.7	1.6	1.0	0.7	n/a	n/a	0.6
Diss. Oxygen	% sat.	n/a	5.5	3	3.7	2.9	n/a	1.6	2.9	3.4	4.5	n/a	n/a	29.5
pH	pH	n/a	9.3	5.3	9.3	11.7	n/a	8.8	7.4	8.0	8.9	n/a	n/a	7.9
ORP (corr.)	mV	n/a	240	515	339	124	n/a	289	94	296	303	n/a	n/a	245
Lithium	ug/L	n/a	110	< 20	100	60	50	< 20	30	< 20	< 20	1,060	60	310
Beryllium	ug/L	n/a	< 1	< 4	< 1	< 1	< 0.8	< 1	< 1	< 1	< 1	< 0.8	< 0.8	< 0.8
Boron	ug/L	n/a	54,900	< 50	3,890	109,000	24,200	860	26,300	470	700	2,350	42,700	850
Aluminum	ug/L	n/a	300	< 30	100	44,400	< 150	1,920	80	4,190	730	< 150	< 150	80
Silicon	ug/L	n/a	1,500	< 100	8,800	19,000	2,400	3,000	10,300	3,400	2,200	3,400	3,300	5,400
Vanadium	ug/L	n/a	36	< 2	550	1,230	11	16	6	10	17	206	41	217
Manganese	ug/L	n/a	25	< 4	< 4	8	52	< 4	4,170	14	< 4	< 4	< 4	67
Iron	ug/L	n/a	< 50	< 50	< 50	1,530	< 50	< 50	3,190	< 50	< 50	< 50	< 50	300
Cobalt	ug/L	n/a	< 1	< 1	3	2	< 1	< 1	2	1	< 1	< 1	< 1	< 1
Nickel	ug/L	n/a	5	< 20	16	128	< 3	5	8	7	4	10	7	4
Copper	ug/L	n/a	< 3	< 3	< 3	21	< 3	12	35	8	7	7	5	6
Zinc	ug/L	n/a	40	< 30	< 5	130	25	8	7	9	11	16	< 5	6
Strontium	ug/L	n/a	3,140	< 30	4,300	1,200	2,690	530	640	580	720	930	680	730
Molybdenum	ug/L	n/a	6,030	< 30	420	39,600	3,010	80	100	< 30	< 30	1,910	500	710
Silver	ug/L	n/a	< 0.2	< 1	< 0.2	< 0.2	1.1	< 0.2	< 0.2	< 0.2	< 0.2	2.0	0.8	< 0.2
Cadmium	ug/L	n/a	21.2	< 2	1.0	64.7	14.0	< 0.3	0.4	< 0.3	< 0.3	8.5	1.5	1.2
Antimony	ug/L	n/a	2.0	< 3	1.4	2.4	1.3	0.5	0.6	0.6	0.5	3.4	1.6	31.4
Barium	ug/L	n/a	40	< 30	350	140	80	140	100	350	220	80	60	240
Thallium	ug/L	n/a	< 0.1	<0.01	2.5	0.3	3.1	< 0.1	0.1	< 0.1	< 0.1	< 0.5	< 0.5	1.5
Lead	ug/L	n/a	< 0.2	< 1	< 0.2	4.6	0.8	< 0.2	< 0.2	0.21	< 0.2	0.4	0.4	< 0.2
Uranium	ug/L	n/a	1.1	< 1	3.7	0.7	12.5	1.1	4.6	1.2	1.2	< 0.2	0.7	2.7

Table A-1 (Continued)
Hydrochemistry and Trace Elements

		022	023	024	025	026	027	028	029	030	031	032	034	035
Chloride	mg/L	17.8	28.4	23	15.3	17.9	932	1,260	1,200	33.8	87	55.9	< 0.01	< 0.01
Sulfate	mg/L	217	248	2,350	845	219	1,620	1,610	1,510	948	1,830	386	< 0.05	< 0.05
Sodium	mg/L	42	33	188	80	43	285	341	297	25	60	32	< 0.1	< 0.1
Potassium	mg/L	9	8	170	40	9	470	580	500	20	50	10	< 0.2	< 0.2
Magnesium	mg/L	14	28	203	82	14	3	10	4	39	35	50	< 0.05	< 0.05
Calcium	mg/L	43	79	405	235	43	671	722	730	332	665	124	< 0.05	< 0.05
TOC	mg/L	0.5 (a)	2.2	1.3 (a)	4.1	0.9 (a)	1.9	0.5 (a)	1.4 (a)	0.5 (a)	11.0	0.6 (a)	0.1 (a)	0.1 (a)
TIC	mg/L	2.49	27.3	54.5	79.9	1.04	1.00	3.25	0.95	10.4	1.53	12.9	0.43 (a)	0.46 (a)
Temperature	°C	21.6	17.4	15.6	15.2	22.2	16.3	16.1	15.5	15.4	15.6	13.9	23.0	23.6
Spec. Cond.	mS/cm	0.6	0.7	4.0	2.0	0.6	5.6	6.6	6.1	1.8	3.0	1.0	0.003	0.002
Diss. Oxygen	% sat.	39.1	17.6	16	15.8	22.4	11.8	10.6	17.1	29.6	6.1	14.5	84.7	71.1
pH	pH	7.1	7.0	7.0	6.5	7.2	10.0	9.0	9.9	8.5	8.5	7.8	5.67	5.40
ORP (corr.)	mV	307	287	268	264	319	71	220	121	308	-41	295	335	306
Lithium	ug/L	360	120	18,600	3,430	320	6,920	5,890	6,260	100	410	240	<0.1	<0.1
Beryllium	ug/L	< 0.8	< 0.8	< 0.8	< 0.8	< 0.8	< 0.8	< 0.8	< 0.8	< 0.8	< 0.8	< 0.8	<0.04	<0.04
Boron	ug/L	430	1,970	22,400	11,100	420	1,450	3,260	2,820	3,280	7,610	2,210	0.9	1.4
Aluminum	ug/L	40	90	< 30	< 30	40	190	< 30	130	190	140	< 30	0.4	0.8
Silicon	ug/L	3,600	3,400	9,400	5,400	3,300	3,000	1,900	2,000	700	3,700	5,400	6.7	18.4
Vanadium	ug/L	70	427	4	< 2	63	< 2	< 2	4	18	4	12	0.10	0.06
Manganese	ug/L	104	149	3,650	4,110	104	18	202	62	41	269	92	<0.02	0.05
Iron	ug/L	< 50	120	80	90	< 50	< 50	< 50	< 50	< 50	< 50	< 50	0.4	0.4
Cobalt	ug/L	8	2	96	8	8	< 1	< 1	< 1	< 1	1	3	<0.02	<0.02
Nickel	ug/L	19	9	167	6	21	3	< 3	< 3	3	8	17	0.08	0.09
Copper	ug/L	8	8	< 3	< 3	< 3	< 3	3	< 3	16	< 3	24	0.46	0.47
Zinc	ug/L	21	11	148	< 5	14	< 5	12	< 5	90	13	15	<0.3	0.7
Strontium	ug/L	430	1,990	6,460	2,290	400	3,520	3,980	4,300	990	2,480	360	<0.4	<0.4
Molybdenum	ug/L	410	500	3,870	2,420	400	180	350	300	140	210	120	<0.1	<0.1
Silver	ug/L	< 0.2	< 0.2	< 0.2	< 0.2	< 0.2	< 0.2	< 0.2	< 0.2	< 0.2	< 0.2	< 0.2	<0.02	<0.02
Cadmium	ug/L	1.1	1.0	9.1	5.1	1.6	0.5	0.8	0.6	< 0.3	0.5	1.2	<0.02	<0.02
Antimony	ug/L	24.3	59.1	4.9	0.5	23.5	< 0.3	< 0.3	< 0.3	5.0	2.7	3.8	<0.02	<0.02
Barium	ug/L	190	110	50	50	190	60	60	80	80	60	160	<0.2	<0.2
Thallium	ug/L	12.0	1.3	1.5	0.4	12.3	< 0.5	< 0.5	< 0.5	3.4	< 0.1	17.6	<0.02	<0.02
Lead	ug/L	< 0.2	< 0.2	< 0.2	< 0.2	< 0.2	< 0.2	< 0.2	< 0.2	< 0.2	< 0.2	< 0.2	0.03	<0.02
Uranium	ug/L	< 0.2	60.8	13.0	19.3	< 0.2	< 0.2	< 0.2	< 0.2	5.3	2.0	1.0	<0.01	<0.01

Table A-1 (Continued)
Hydrochemistry and Trace Elements

		036	037	038	039	042	043	044	044D	049	050	051	052	053
Chloride	mg/L	< 0.01	8.8	9.7	9.4	9.7	7.1	9.8	9.1	9.8	< 0.01	5.3	7.6	8.1
Sulfate	mg/L	< 0.05	123	121	101	57	111	70	70	53	< 0.05	111	128	176
Sodium	mg/L	< 0.1	3.8	3.9	4.7	8.6	8.5	8.3	8.3	7.0	0.1	11.8	6.8	5.6
Potassium	mg/L	< 0.2	2.2	2.3	5.3	5.2	7.0	5.0	5.0	4.0	< 0.2	13.6	11.1	9.2
Magnesium	mg/L	< 0.05	6.91	6.61	3.08	2.06	2.58	2.66	2.67	2.53	< 0.05	1.81	0.08	0.12
Calcium	mg/L	< 0.05	45.8	45.3	36.1	12.4	19.9	15.4	15.5	13.2	0.09	14.4	58.4	69.5
TOC	mg/L	0.1 (a)	< 0.09	< 0.09	< 0.09	< 0.09	< 0.09	< 0.09	< 0.09	< 0.09	0.1 (a)	< 0.09	0.8 (a)	0.7 (a)
TIC	mg/L	0.48 (a)	10.4	10.5	6.66	2.01	1.03	0.75 (a)	0.68 (a)	2.18	0.44 (a)	0.92	3.30	4.96
Temperature	°C	23.6	22	22.7	24.2	29.4	32	32	31.5	25.8	24.5	26.5	27.1	26.7
Spec. Cond.	mS/cm	0.001	0.379	0.381	0.317	0.178	0.293	0.209	0.210	0.174	0.009	0.287	0.588	0.468
Diss. Oxygen	% sat.	77	35	27.6	33.5	84.1	75.7	67.9	80.2	77.6	72	82.4	56	40.6
pH	pH	5.66	7.05	7.04	6.98	5.79	4.26	5.97	6.03	5.97	4.92	4.35	10.59	8.92
ORP (corr.)	mV	299	192	163	184	283	388	285	289	290	300	387	211	212
Lithium	ug/L	<0.1	82	81	125	179	239	146	145	99	<0.1	520	561	595
Beryllium	ug/L	<0.04	<0.4	<0.4	<0.4	1.6	8.6	0.8	1.3	<0.4	<0.04	5.2	<0.4	<0.4
Boron	ug/L	3.1	1390	1240	917	426	838	429	489	265	43.3	272	4620	7370
Aluminum	ug/L	1.0	15	14	6	148	3730	66	72	14	3.5	2150	15100	2010
Silicon	ug/L	21.5	7960	7660	7000	4700	5780	4730	5100	4670	15.3	5840	1890	1030
Vanadium	ug/L	0.10	13.8	6.9	2.6	70.8	35.6	9.6	9.5	5.6	0.21	4.7	754.4	62.4
Manganese	ug/L	0.67	248	244	261	42.7	77.5	86.1	88.6	79.4	23.4	113	0.4	5.9
Iron	ug/L	1.0	921	1700	1070	6	722	18	28	7	8.2	3240	16	30
Cobalt	ug/L	<0.02	1.7	0.7	<0.2	11.5	21.6	8.7	9.0	5.2	0.05	18.9	<0.2	0.2
Nickel	ug/L	0.45	7.2	4.2	2.4	37.8	71.9	26.7	27.5	13.6	2.98	58.2	<0.6	1.5
Copper	ug/L	0.55	0.5	1.0	<0.4	8.7	152	12.0	11.2	1.9	1.13	452	1.8	8.4
Zinc	ug/L	0.7	<3	<3	<3	58.1	80.4	35.6	32.9	18.3	5.6	74.6	<3	5.7
Strontium	ug/L	<0.4	1350	1360	1120	170	247	272	262	209	<0.4	806	5150	5610
Molybdenum	ug/L	<0.1	1110	1060	287	127	35	54	54	60	0.2	8	246	360
Silver	ug/L	<0.02	<0.2	<0.2	<0.2	<0.2	<0.2	<0.2	<0.2	<0.2	<0.02	<0.2	<0.2	<0.2
Cadmium	ug/L	<0.02	4.6	4.1	1.2	1.3	1.9	0.7	0.8	0.5	<0.02	2.4	0.8	2.3
Antimony	ug/L	<0.02	4.6	2.4	0.3	13.9	17.8	8.7	8.8	7.1	<0.02	5.9	14.4	2.6
Barium	ug/L	<0.2	125	169	77	75	131	180	181	195	<0.2	545	250	87
Thallium	ug/L	<0.02	<0.2	<0.2	<0.2	0.7	4.2	1.6	1.5	0.7	<0.02	6.3	0.4	0.3
Lead	ug/L	<0.02	<0.1	<0.1	<0.1	0.2	1.9	0.2	<0.1	<0.1	<0.02	8.0	<0.1	0.5
Uranium	ug/L	<0.01	0.2	0.1	<0.1	<0.1	0.5	<0.1	<0.1	<0.1	<0.01	1.0	0.1	1.7

Table A-1 (Continued)
Hydrochemistry and Trace Elements

		057	059	059D	060	061	062	064	069	070	070D	077	078	079
Chloride	mg/L	5.6	4.5	4.6	< 0.01	7.1	15.8	5.0	7.3	12.1	9.7	< 0.01	< 0.01	77.2
Sulfate	mg/L	52	55	55	< 0.05	61	117	150	45	50	51	< 0.05	< 0.05	315
Sodium	mg/L	8.1	8.5	8.5	< 0.1	9.5	11.4	7.3	6.0	10.8	10.8	< 0.1	< 0.1	63
Potassium	mg/L	5.8	6.4	6.4	< 0.2	6.4	9.6	9.4	3.6	5.0	4.9	< 0.2	< 0.2	13
Magnesium	mg/L	1.53	1.37	1.43	< 0.05	4.97	0.11	1.49	2.16	1.78	1.81	< 0.05	< 0.05	19.5
Calcium	mg/L	16.8	16.8	16.5	0.20	55.1	76.5	58.1	19.0	26.0	26.3	< 0.05	< 0.05	95.3
TOC	mg/L	< 0.09	< 0.09	< 0.09	< 0.09	< 0.09	< 0.09	< 0.09	< 0.09	< 0.09	< 0.09	0.4 (a)	0.2 (a)	0.3 (a)
TIC	mg/L	6.02	5.07	4.99	0.43 (a)	38.3	3.98	3.92	6.04	9.44	9.55	0.34 (a)	0.28 (a)	20.6
Temperature	°C	28.5	31.2	n/a	25.7	27.6	29	30	27.7	29.4	28.9	28.6	27.0	19.5
Spec. Cond.	mS/cm	0.189	0.195	n/a	0.003	0.433	0.765	0.455	0.182	0.244	0.247	0.001	0.002	1.076
Diss. Oxygen	% sat.	89.2	165.1	n/a	90.2	65.3	37.9	67.7	63.5	67.9	68.3	64.3	74.3	28.0
pH	pH	7.66	9.04	n/a	5.4	7.25	10.95	10.12	7.57	8.91	9.1	5.07	5.58	6.75
ORP (corr.)	mV	n/a	409	na	277	140	196	214	220	223	220	263	236	114
Lithium	ug/L	267	293	288	<0.1	155	243	430	140	160	167	<0.05	<0.05	134
Beryllium	ug/L	<0.4	<0.4	<0.4	<0.04	<0.4	<0.4	<0.4	<0.4	<0.4	<0.4	<0.01	<0.01	<0.2
Boron	ug/L	300	351	309	1.2	2600	494	476	231	207	236	7.1	6.8	1110
Aluminum	ug/L	111	356	366	1.8	58	3900	2310	29	468	519	2.3	2.3	<2
Silicon	ug/L	5120	5010	5190	8.6	11100	6870	4760	7450	7190	6920	509	513	10100
Vanadium	ug/L	31.3	34.4	34.6	0.18	5.6	176.9	229.6	61.3	93.1	94.2	0.22	0.21	0.4
Manganese	ug/L	1.6	0.6	0.8	0.04	395	<0.2	<0.2	22.0	0.4	0.7	7.50	4.84	190
Iron	ug/L	6	26	25	0.7	2170	17	13	<5	27	46	12.9	2.28	25600
Cobalt	ug/L	<0.2	<0.2	<0.2	<0.02	0.3	<0.2	<0.2	1.3	<0.2	<0.2	0.007	0.003	0.18
Nickel	ug/L	2.3	1.7	1.4	<0.6	4.0	<0.6	0.9	5.4	0.6	<0.6	<0.03	<0.03	<0.6
Copper	ug/L	1.3	2.0	1.8	0.5	<0.4	1.2	0.5	0.7	1.8	2.1	0.30	0.27	<0.2
Zinc	ug/L	<3	4.0	<3	0.4	<3	<3	<3	<3	<3	<3	0.4	0.4	1.5
Strontium	ug/L	545	547	576	<0.4	1840	1010	478	340	258	263	3.37	3.39	2190
Molybdenum	ug/L	62	63	61	<0.1	95	173	217	78	61	63	<0.02	<0.02	135
Silver	ug/L	<0.2	<0.2	<0.2	<0.02	<0.2	<0.2	<0.2	<0.2	<0.2	<0.2	<0.01	<0.01	<0.2
Cadmium	ug/L	<0.2	0.4	<0.2	<0.02	0.3	0.6	0.6	0.3	<0.2	<0.2	<0.01	<0.01	<0.2
Antimony	ug/L	6.2	5.6	5.5	<0.02	0.7	8.2	27.4	9.5	7.6	7.9	<0.005	0.005	<0.1
Barium	ug/L	182	171	166	<0.2	226	194	319	156	124	132	<0.1	<0.1	99.2
Thallium	ug/L	1.0	0.9	0.9	<0.02	0.5	<0.2	0.3	1.0	0.4	0.4	<0.005	<0.005	<0.1
Lead	ug/L	<0.1	<0.1	<0.1	<0.02	<0.1	<0.1	<0.1	<0.1	<0.1	<0.1	0.04	0.02	<0.1
Uranium	ug/L	0.5	1.2	1.3	<0.01	1.4	<0.1	0.7	0.3	2.2	2.2	<0.001	<0.001	1.91

Table A-1 (Continued)
Hydrochemistry and Trace Elements

		079D	082	083	084	088	089	090	091	092	TEB	094	095	096 (1)
Chloride	mg/L	77.9	72.0	68.4	67.9	< 0.01	0.37	11.8	5.35	4.67	0.22	0.06	0.04	92.4
Sulfate	mg/L	315	174	92.8	135	< 0.05	1.50	324	393	448	0.65	< 0.05	< 0.05	2,850
Sodium	mg/L	63	68	45	38	0.7	0.9	182	277	109	0.6	< 0.1	< 0.1	1,560
Potassium	mg/L	14	5	4	6	< 0.2	0.2	113	84	67	1.2	< 0.2	< 0.2	74
Magnesium	mg/L	19.4	19.1	12.6	30.8	< 0.05	0.35	0.15	< 0.05	< 0.05	< 0.05	< 0.05	< 0.05	9
Calcium	mg/L	98.0	79.1	34.4	105	< 0.05	0.72	11.9	2.22	287	1.30	< 0.05	< 0.05	9
TOC	mg/L	0.8 (a)	2.6	4.7	< 0.09	0.4 (a)	0.5 (a)	12.8	4.3	3.4	0.4 (a)	0.3 (a)	0.3 (a)	49.8
TIC	mg/L	19.7	35.9	11.9	60.5	0.28 (a)	1.20	13.8	7.62	0.85	1.37	0.21 (a)	0.23 (a)	128
Temperature	°C	18.0	30.2	25.9	19.2	n/a	n/a	17.2	16.8	15.9	n/a	12.4	13.7	16.1
Spec. Cond.	mS/cm	1.068	0.911	0.547	0.927	n/a	n/a	1.59	2.33	1.427	n/a	0.002	0.005	7.295
Diss. Oxygen	% sat.	21.0	65.1	100.0	40.7	n/a	n/a	n/a	n/a	n/a	n/a	84	73.3	67
pH	pH	6.84	8.64	9.36	7.78	n/a	n/a	10.86	11.52	11.17	n/a	6.2	5.44	7.29
ORP (corr.)	mV	87	241	217	198	n/a	n/a	246	288	346	n/a	227	261	223
Lithium	ug/L	134	60	27	139	<0.05	4	2	5	11	1.25	<0.05	<0.05	5
Beryllium	ug/L	<0.2	<0.2	<0.2	<0.2	<0.01	0.011	<0.2	<0.2	<0.2	<0.01	<0.01	<0.01	<0.2
Boron	ug/L	1200	442	1020	4310	89.6	215	1800	495	1080	240	1.1	0.7	5650
Aluminum	ug/L	<2	1080	2030	41	1.1	92.9	19900	30000	5140	38.6	7.8	1.3	1700
Silicon	ug/L	9970	4210	1050	2300	3780	6740	4200	4390	2460	7100	11.5	9.2	1400
Vanadium	ug/L	0.5	103	49.3	11.5	0.09	1.23	365	562	156	1.07	0.13	0.15	473
Manganese	ug/L	191	2.0	1.0	91.1	1.50	9.97	0.9	<0.1	<0.1	6.1	0.5	0.22	1.5
Iron	ug/L	25200	<3	<3	62.0	52.7	271	29.7	<8	<8	140	5.4	0.51	25.3
Cobalt	ug/L	0.18	0.80	0.53	0.81	<0.001	0.17	0.12	0.04	0.40	0.301	<0.001	<0.001	3.27
Nickel	ug/L	<0.6	3.6	4.4	4.6	<0.05	6.29	14	4	<1	12	0.06	0.08	7
Copper	ug/L	1.4	3.8	2.1	<0.2	0.33	2.02	1.4	0.5	1.4	1.2	1.4	2.5	30.0
Zinc	ug/L	2.5	<2	3.0	<2	<0.1	6.9	<2	<2	<2	2.9	3.3	4.3	<2
Strontium	ug/L	2140	828	1010	2520	9.48	82.6	830	1610	11100	135	0.31	0.11	311
Molybdenum	ug/L	132	21.9	27.7	283	0.04	0.83	1890	1390	658	0.75	0.02	<0.01	4510
Silver	ug/L	<0.2	<0.2	<0.2	<0.2	<0.01	<0.01	<0.2	<0.2	<0.2	<0.01	<0.01	<0.01	<0.2
Cadmium	ug/L	<0.2	<0.2	0.3	0.7	<0.005	0.037	6.1	4.8	2.8	0.04	0.02	0.01	15.0
Antimony	ug/L	<0.1	1.1	2.9	1.1	0.021	0.074	2.3	0.5	0.2	0.082	0.007	<0.005	0.8
Barium	ug/L	93.6	434	294	176	<0.2	10.7	89.3	259	657	29.7	0.6	<0.2	20
Thallium	ug/L	<0.1	0.5	<0.1	0.4	<0.005	<0.005	<0.1	<0.1	<0.1	0.021	<0.005	<0.005	<0.1
Lead	ug/L	<0.1	<0.1	0.2	<0.1	0.01	0.17	<0.1	<0.1	<0.1	0.03	0.09	0.06	<0.1
Uranium	ug/L	1.95	2.66	1.23	26.8	<0.0005	0.17	0.39	<0.01	0.01	0.02	<0.0005	<0.0005	5.53

Table A-1 (Continued)
Hydrochemistry and Trace Elements

		096D (1)	097	098	099	100	101	102	103	104	105	106	106D	107
Chloride	mg/L	92.5	91.7	38.7	27.3	0.07	37.2	73.0	0.01	0.02	1,080	859	715	2,330
Sulfate	mg/L	2,870	2,870	1,800	1,510	0.08	1,610	2,410	< 0.05	0.12	10,200	4,710	4,430	30,500
Sodium	mg/L	1,560	1,560	837	651	1.3	117	455	0.2	0.1	3,270	2,310	2,210	4,630
Potassium	mg/L	77	73	31	6	< 0.2	23	219	< 0.2	< 0.2	380	350	350	500
Magnesium	mg/L	10	7	44	16	< 0.05	188	69	< 0.05	< 0.05	1,000	< 0.05	< 0.05	5,810
Calcium	mg/L	11	6	52	73	0.17	392	431	< 0.05	< 0.05	600	234	228	570
TOC	mg/L	50.1	48.7	56.8	14.7	0.4 (a)	4.6	3.3	0.1 (a)	0.1 (a)	33.1	19.1	18.6	50.1
TIC	mg/L	128	105	39.7	14.1	0.28 (a)	27.8	24.3	0.16 (a)	0.27 (a)	7.88	4.27	4.36	1.85
Temperature	°C	16.5	17.4	12.9	15.1	13.4	16.9	15.8	n/a	6.6	9.94	19.0	19.0	19.18
Spec. Cond.	mS/cm	7.379	7.340	4.282	3.451	0.003	3.363	4.915	n/a	0.072	18.85	11.56	11.56	26.14
Diss. Oxygen	% sat.	61.1	69.4	27.5	37	81.1	86.1	94.7	n/a	64.5	36	95	95	2
pH	pH	7.71	9.35	8.58	7.91	5.94	6.74	7.41	n/a	9.54	8.99	11.96	11.96	6.83
ORP (corr.)	mV	224	206	39	103	238	213	222	n/a	288	271	18	18	230
Lithium	ug/L	5	4	63	<1	<0.05	431	6940	<0.05	<0.05	1050	130	132	3390
Beryllium	ug/L	<0.2	<0.2	<0.2	<0.2	<0.01	<0.2	<0.2	<0.01	<0.01	<0.2	<0.2	<0.2	1
Boron	ug/L	5950	6080	11700	2590	0.8	89500	23700	<0.1	0.2	26800	7310	7460	50200
Aluminum	ug/L	1700	4300	117	42	3	52	<2	2.3	2.7	31	608	618	708
Silicon	ug/L	1340	1540	4620	4410	25.7	6750	3940	5.9	17.9	2280	21000	22000	45400
Vanadium	ug/L	477	500	159	3.8	0.10	0.8	44.3	0.25	0.33	1.8	400	403	103
Manganese	ug/L	1.4	1.5	59.8	1230	0.39	1420	72.3	0.33	2.32	473	<0.1	0.1	1170
Iron	ug/L	20.1	46.3	<8	126	0.52	12.1	<8	2.05	1.36	4.7	4.6	6.6	52.4
Cobalt	ug/L	3.31	3.28	0.88	0.29	<0.001	9.19	0.07	<0.001	0.008	0.09	0.11	0.07	13.0
Nickel	ug/L	7	8	9	2	0.18	31	3	<0.03	0.25	3.3	7.5	8.0	153
Copper	ug/L	29.9	42.8	1.7	1.5	1.60	2.8	1.6	0.51	0.55	0.4	0.6	0.5	2
Zinc	ug/L	<2	<2	<2	<2	5	86	<2	0.2	0.7	<2	<2	<2	68
Strontium	ug/L	293	303	1700	93	0.72	1320	10300	0.67	3.88	6980	9730	10000	1500
Molybdenum	ug/L	4450	4480	2580	2070	0.05	751	9630	<0.04	<0.04	164	3520	3560	1320
Silver	ug/L	<0.2	<0.2	<0.2	<0.2	<0.01	<0.2	<0.2	<0.01	<0.01	<0.2	<0.2	<0.2	<1
Cadmium	ug/L	13.1	13.0	7.7	6.1	0.028	4.6	35.9	0.005	<0.005	0.5	12.8	11.8	6.6
Antimony	ug/L	0.8	0.9	0.7	0.2	0.013	0.1	4.4	0.013	<0.005	9.4	2.3	2.2	22.3
Barium	ug/L	16	18	34	66	0.7	23	48	<0.1	0.2	75	134	138	158
Thallium	ug/L	<0.1	<0.1	<0.1	<0.1	<0.005	<0.1	<0.1	<0.005	<0.005	<0.1	<0.1	<0.1	<0.5
Lead	ug/L	0.2	0.3	0.3	0.2	<0.1	0.1	0.1	0.017	<0.005	0.2	0.4	0.5	0.8
Uranium	ug/L	5.41	5.66	1.87	0.19	<0.0005	36.6	7.38	<0.0007	<0.0007	6.47	<0.01	0.04	16.0

Table A-1 (Continued)
Hydrochemistry and Trace Elements

		108	109	110	111	112	113	114	115	116	117	118	118D	119
Chloride	mg/L	84	0.29	0.17	28.5	n/a	13.4	19.6	16.9	16.8	< 0.01	66.2	66.3	64.8
Sulfate	mg/L	3,490	< 0.05	0.10	2,440	n/a	203	210	166	163	< 0.05	462	467	441
Sodium	mg/L	840	0.2	< 0.1	190	n/a	21	28	31	32	0.3	36	37	36
Potassium	mg/L	120	< 0.2	< 0.2	210	n/a	11	11	9	10	< 0.2	13	13	9
Magnesium	mg/L	57	< 0.05	< 0.05	236	n/a	22	20	17	16	< 0.05	72	74	67
Calcium	mg/L	596	< 0.05	< 0.05	405	n/a	49	53	45	38	< 0.05	121	123	123
TOC	mg/L	10.3	0.4 (a)	0.2 (a)	4.1	n/a	1.8	1.4 (a)	1.4 (a)	1.5	0.3 (a)	3.9	4.3	4.1
TIC	mg/L	18.8	0.86	0.73 (a)	59.9	n/a	14.2	16.7	1.57	2.48	0.75 (a)	19.2	19.4	21.6
Temperature	°C	10.6	n/a	n/a	15.05	14.2	20.98	22.03	16.0	15.5	n/a	14.65	14.4	10.48
Spec. Cond.	mS/cm	6.174	n/a	n/a	4.529	2.765	0.643	0.673	0.567	0.564	n/a	1.348	1.355	1.319
Diss. Oxygen	% sat.	87	n/a	n/a	58.7	46.7	28.4	15.1	87	98.4	n/a	80.7	120	122.8
pH	pH	8.76	n/a	n/a	7.18	6.83	7.74	6.99	7.28	7.41	n/a	7.6	7.49	8.6
ORP (corr.)	mV	240	n/a	n/a	280	229	231	220	261	289	n/a	257	244	240
Lithium	ug/L	27	<0.05	<0.05	23600	4540	347	187	318	312	<0.05	253	264	162
Beryllium	ug/L	<0.2	<0.01	<0.01	<0.2	<0.2	<0.2	<0.2	<0.2	<0.2	<0.01	<0.2	<0.2	<0.2
Boron	ug/L	41500	0.9	2.0	27200	13300	1480	931	444	450	0.7	2200	2120	1700
Aluminum	ug/L	81	3.5	3.4	27	17	42	51	17	25	4.3	18	13	28
Silicon	ug/L	221	26.1	42.2	7440	2300	2840	12000	2890	2970	42.4	3710	3840	2870
Vanadium	ug/L	3.6	0.14	0.14	26.9	1.8	402	45.2	53.6	54.3	0.18	3.8	3.5	6.5
Manganese	ug/L	7.7	0.57	4.48	2700	531	147	445	59.3	58.1	0.40	155	167	59.6
Iron	ug/L	3.0	3.7	0.9	<13	55.4	<13	349	<13	<13	0.4	<13	<13	<13
Cobalt	ug/L	0.42	<0.001	0.039	113	8.91	1.76	5.36	7.15	7.05	0.039	3.76	3.53	1.58
Nickel	ug/L	2.2	<0.1	0.2	189	5	<2	6	14	14	<0.1	15	14	8
Copper	ug/L	1.6	0.64	0.96	1.3	0.9	0.4	1.6	9.8	8.8	0.53	2.5	3.0	1.9
Zinc	ug/L	<2	0.7	1.0	289	4	<2	6	16	13	0.8	11	9	<2
Strontium	ug/L	12000	0.59	40.5	6750	2740	662	771	405	411	0.61	507	513	465
Molybdenum	ug/L	2680	0.02	0.11	5100	2690	1280	264	340	336	0.02	131	128	88.7
Silver	ug/L	0.8	<0.01	<0.01	<0.2	<0.2	<0.2	<0.2	<0.2	<0.2	<0.01	<0.2	<0.2	<0.2
Cadmium	ug/L	10.6	0.02	0.01	23.6	11.8	5.6	1.4	2.0	2.0	<0.005	1.4	1.0	0.6
Antimony	ug/L	5.2	<0.005	0.006	9.1	0.6	58.5	4.4	20.0	20.7	<0.005	3.1	2.8	2.5
Barium	ug/L	63	<0.1	0.6	40	43	105	62	182	177	0.6	150	153	118
Thallium	ug/L	<0.1	<0.005	<0.005	5.3	0.6	0.8	0.3	7.6	7.3	<0.005	14.2	11.0	6.8
Lead	ug/L	0.3	0.028	0.008	<0.14	<0.14	<0.14	<0.14	<0.14	<0.14	0.013	<0.14	<0.14	<0.14
Uranium	ug/L	21.1	<0.0008	0.001	18.9	21.8	7.91	0.20	0.15	0.17	<0.0008	1.75	1.73	2.02

Table A-1 (Continued)
Hydrochemistry and Trace Elements

		120	121	122	125	126	126D	127	128
Chloride	mg/L	1,150	1,190	911	0.09	42.5	42.7	31	98
Sulfate	mg/L	1,350	1,510	1,430	< 0.05	507	509	1,120	836
Sodium	mg/L	255	303	247	0.1	393	393	653	141
Potassium	mg/L	500	609	486	< 0.2	20	20	40	30
Magnesium	mg/L	5	6	< 2.5	< 0.05	< 0.05	< 0.05	< 0.05	8
Calcium	mg/L	710	698	669	< 0.05	< 2.5	< 2.5	13	351
TOC	mg/L	1.5	1.3 (a)	2.4	0.6 (a)	6.0	5.8	7.9	7.9
TIC	mg/L	2.81	2.53	2.37	0.39 (a)	5.90	5.89	7.40	3.03
Temperature	°C	16.16	13.65	12.02	12.08	16.75	17.02	16.4	20.5
Spec. Cond.	mS/cm	6.322	6.897	5.906	0.013	2.57	2.76	4.02	2.19
Diss. Oxygen	% sat.	81.3	29.8	77.8	46	35	35	13.1	65
pH	pH	10.33	10.04	10.53	6.04	11.75	11.75	11.74	7.84
ORP (corr.)	mV	87	181	46	373	249	241	225	339
Lithium	ug/L	6470	6360	7070	<0.05	7	8	16	33
Beryllium	ug/L	<0.2	<0.2	<0.2	<0.01	<0.4	<0.4	<0.2	<0.2
Boron	ug/L	3080	3160	1560	2.7	3070	2890	3890	11900
Aluminum	ug/L	167	24	229	4.2	5590	5620	5920	26
Silicon	ug/L	1890	1810	2360	1.1	9450	8860	10300	3940
Vanadium	ug/L	4.5	0.7	1.3	0.29	122	120	236	6.8
Manganese	ug/L	38.1	113	15.5	0.14	<0.4	<0.4	<0.2	197
Iron	ug/L	<13	<13	<13	0.3	<25	<25	<25	<25
Cobalt	ug/L	0.05	0.09	0.03	0.022	<0.04	<0.04	0.20	1.61
Nickel	ug/L	3	<2	<2	<0.1	<0.6	<0.6	<2	<2
Copper	ug/L	0.3	0.4	1.4	0.04	4.2	3.9	2.4	1.5
Zinc	ug/L	<2	<2	<2	0.2	<2	<2	<2	5
Strontium	ug/L	4500	4210	3860	0.63	649	648	1830	5960
Molybdenum	ug/L	333	368	223	0.02	220	223	524	910
Silver	ug/L	<0.2	<0.2	<0.2	<0.01	<0.2	<0.2	<0.2	<0.2
Cadmium	ug/L	1.9	1.6	0.8	<0.005	1.0	1.0	2.1	3.8
Antimony	ug/L	0.1	0.1	<0.1	<0.005	0.4	0.4	0.2	1.3
Barium	ug/L	78	65	58	0.4	36	34	64	86
Thallium	ug/L	0.3	<0.1	<0.1	<0.005	<0.1	<0.1	<0.1	<0.1
Lead	ug/L	<0.14	<0.14	<0.14	<0.007	<0.14	<0.14	<0.14	<0.14
Uranium	ug/L	0.02	0.10	0.04	<0.0008	<0.02	<0.02	<0.02	0.97

Table A-1 (Continued)
Hydrochemistry and Trace Elements

Footnotes:
(1) = Samples 096 and 096D are samples of leachate that were treated with CO2 prior to analysis.
(a) = sample concentration less than 5 times blank
n/a = not analyzed

Table A-2
Speciation

	Sample ID	001	002	003	004	005	006	007	008	009	010	012	QA-1
As, diss.	ug/L	20.4	48.4	84	18.6	3.0	12.2	20.1	16.9	28.9	22.3	238	0.11
As(III), diss.	ug/L	< 0.3	< 6	< 6	8.4	< 0.2	< 0.3	< 2	0.7 (a)	< 6	1.5 (a)	97.0	< 0.02
As(V), diss.	ug/L	9.5	47	69	5.2	1.3	0.9 (a)	< 2	< 0.5	< 10	10	66	< 0.03
As, other	ug/L	2.1	< 6	< 6	< 0.3	< 0.2	< 0.3	< 2	< 0.3	< 6	< 0.6	< 0.6	< 0.02
Cr, diss.	ug/L	< 0.5	5,100	4,670	8.8	0.7	5.7	2	< 0.5	52.9	25.8	< 0.5	< 3
Cr(III), diss.	ug/L	n/a	340	190	< 0.1	n/a	< 0.1	< 0.1	n/a	1	< 0.4	n/a	n/a
Cr(VI), diss.	ug/L	2.2	5,090	3,530	8.1	1.5	6.4	2.9	< 0.1	47	22	1.9	< 0.05
Se, diss.	ug/L	127	1,730	1,760	49.9	7.6	16.8 (b)	289	3.7 (b)	2,360	318	3.24	0.10 (a)
Se(IV), diss.	ug/L	8.3	19	76	8.1	3.15	1.6	79.5	< 0.1	< 2	24.4	1.4	< 0.02
Se(VI), diss.	ug/L	83.0	1,300	1,240	22.1	0.57	11.2	119	0.27 (a)	1,660	158	< 0.2	< 0.03
Se, other	ug/L	n/a	n/a	n/a	n/a	n/a	n/a	n/a	n/a	n/a	n/a	n/a	n/a
$Hg_{diss.}$	ng/L	n/a	14.4	18.4	5.9	2.1 (a)	0.8 (a)	1.9 (a)	4.2 (a)	28.4	n/a	n/a	n/a
$Hg_{part.}$	ng/L	n/a	254	26	< 1	44	25 (a)	16 (a)	< 1	121	n/a	n/a	n/a
$MeHg_{diss.}$	ng/L	n/a	0.11	0.09 (a)	0.26	0.12	0.54	< 0.02	0.07 (a)	< 0.02	n/a	n/a	n/a
$MeHg_{part.}$	ng/L	0.03 (a)	0.03 (a)	< 0.01	0.04 (a)	0.09	0.09	0.02 (a)	0.01 (a)	0.02 (a)	n/a	n/a	n/a
DMM	ng/L	0.055	0.005	< 0.005	< 0.005	0.010	< 0.005	0.007	< 0.005	n/a	n/a	n/a	n/a

Table A-2 (Continued)
Speciation

Sample ID		013	013D	014	QA-2	015	016	SX-1	017	018	019	020	HN-1	HN-2
As, diss.	ug/L	21.6	22	163	0.12	23.8	68.6	72.0	4.11	23.1	5.11	4.19	59.8	20.6
As(III), diss.	ug/L	3.7	1.9	1.9	0.02 (a)	< 0.6	< 0.6	0.9	0.88	0.42	0.57	1.00	< 0.1	< 0.1
As(V), diss.	ug/L	< 0.5	< 0.5	86	< 0.03	24	25	46.9	<0.08	5.22	<0.08	0.53	33.6	6.9
As, other	ug/L	< 0.3	< 0.3	0.9 (a)	< 0.02	< 0.6	< 0.6	< 0.1	0.1	< 0.06	< 0.06	0.1	0.2	0.1
Cr, diss.	ug/L	< 0.5	n/a	< 0.5	< 3	12.9	3.8	< 0.5	3	< 0.5	1.0	0.7	< 0.5	< 0.5
Cr(III), diss.	ug/L	n/a	n/a	n/a	n/a	< 0.4	< 0.1	n/a	< 0.04	n/a	< 0.1	n/a	n/a	n/a
Cr(VI), diss.	ug/L	0.7	0.7	0.5	< 0.05	12.8	< 0.5	< 0.1	2.8	1.3	0.9	< 0.05	n/a	n/a
Se, diss.	ug/L	0.28 (b)	0.38 (b)	1.81 (b)	0.10 (a)	22.4	193	7.77	2.4	0.50 (b)	1.8	2.5	22.2	9.15
Se(IV), diss.	ug/L	< 0.1	< 0.1	0.6 (a)	< 0.02	14.9	101	2 (a)	0.3 (a)	< 0.1	0.1 (a)	0.9	3 (a)	< 1
Se(VI), diss.	ug/L	< 0.1	< 0.1	< 0.2	< 0.03	3.4	14.3	4 (a)	1.1	< 0.2	1.3	0.8	16	6
Se, other	ug/L	n/a	n/a	n/a	n/a	n/a	n/a	n/a	n/a	n/a	n/a	n/a	n/a	n/a
$Hg_{diss.}$	ng/L	n/a	n/a	n/a	n/a	n/a	n/a	n/a	n/a	n/a	n/a	n/a	n/a	n/a
$Hg_{part.}$	ng/L	n/a	n/a	n/a	n/a	n/a	n/a	n/a	n/a	n/a	n/a	n/a	n/a	n/a
$MeHg_{diss.}$	ng/L	n/a	n/a	n/a	n/a	n/a	n/a	n/a	n/a	n/a	n/a	n/a	n/a	n/a
$MeHg_{part.}$	ng/L	n/a	n/a	n/a	n/a	n/a	n/a	n/a	n/a	n/a	n/a	n/a	n/a	n/a
DMM	ng/L	n/a	n/a	n/a	n/a	n/a	n/a	n/a	n/a	n/a	n/a	n/a	n/a	n/a

Table A-2 (Continued)
Speciation

	Sample ID	021	022	023	024	025	026	027	028	029	030	031	032	034
As, diss.	ug/L	194	11.1	218	11.2	6.47	10.8	39.1	30.0	48.9	42.5	221	25.4	< 0.02
As(III), diss.	ug/L	2.1	12.5	0.8 (a)	0.4 (a)	1.35	11.2	13.2	2.4	1.7	3.5	201	17.5	< 0.01
As(V), diss.	ug/L	208	0.49	189	<0.2	<0.08	0.4 (a)	4.8	1.7	8.9	29.5	23.6	16.9	< 0.8
As, other	ug/L	< 0.3	< 0.06	< 0.3	< 0.2	< 0.06	< 0.2	1.3	0.2	0.3	0.4	0.7	0.1	n/a
Cr, diss.	ug/L	< 0.5	1.0	< 0.5	< 0.5	< 0.5	1.1	< 0.5	< 0.5	< 0.5	< 0.5	< 0.5	1.4	0.08
Cr(III), diss.	ug/L	n/a	< 0.04	n/a	n/a	n/a	< 0.04	n/a	n/a	n/a	n/a	n/a	< 0.1	0.06
Cr(VI), diss.	ug/L	< 0.05	0.9	< 0.5	n/a	n/a	0.9	n/a	n/a	n/a	< 0.05	< 0.1	< 0.05	< 0.01
Se, diss.	ug/L	6.5	30.7	283	18.2	1.9 (b)	31.5	1.05 (b)	2.56 (b)	2.29	44.1	12.5	18.0	< 0.02
Se(IV), diss.	ug/L	5.3	20.5	217	5.3	< 0.1	20.4	< 0.3	< 0.3	< 0.3	27.0	0.9 (a)	13.5	< 0.1
Se(VI), diss.	ug/L	< 0.6	2.2	1.5	6.3	1.1	2.2	< 0.3	1.4	1.6	12.5	5.5	0.7	< 0.2
Se, other	ug/L	n/a	n/a	n/a	n/a	n/a	n/a	n/a	n/a	n/a	n/a	n/a	n/a	n/a
$Hg_{diss.}$	ng/L	1.4 (a)	1.0 (a)	1.4 (a)	n/a	n/a	0.4 (a)	21.3	1.2 (a)	12.4	0.8 (a)	5.2	1.4 (a)	n/a
$Hg_{part.}$	ng/L	155	53	14 (a)	n/a	n/a	17 (a)	4 (a)	13 (a)	59	< 1	30	186	n/a
$MeHg_{diss.}$	ng/L	0.03 (a)	0.03 (a)	< 0.02	n/a	n/a	< 0.02	1.56	0.18	0.70	0.06 (a)	6.71	0.05 (a)	n/a
$MeHg_{part.}$	ng/L	0.02 (a)	0.03 (a)	0.03 (a)	n/a	n/a	< 0.01	< 0.01	< 0.01	0.01 (a)	0.11	n/a	0.05	n/a
DMM	ng/L	< 0.005	< 0.005	< 0.005	n/a	n/a	< 0.005	< 0.005	< 0.005	< 0.005	0.022	0.050	0.032	n/a

Table A-2 (Continued)
Speciation

Sample ID		035	036	037	038	039	042	043	044	044D	049	050	051	052
As, diss.	ug/L	< 0.02	0.03 (a)	56.0	123	42.3	23.7	75.2	5.1	4.9	5.4	0.12	38.1	164
As(III), diss.	ug/L	< 0.01	< 0.01	0.30	2.63	1.39	< 0.1	< 0.05	0.39	< 0.04	< 0.04	< 0.01	0.70 (a)	22.8
As(V), diss.	ug/L	< 0.8	< 0.8	34	53	53	19 (a)	28	3 (a)	2 (a)	2 (a)	< 0.8	15	8 (a)
As, other	ug/L	n/a	n/a	n/a	n/a	n/a	n/a	n/a	n/a	n/a	< 0.04	n/a	n/a	n/a
Cr, diss.	ug/L	0.07	0.14	< 0.4	< 0.4	< 0.4	< 0.4	29.2	< 0.4	< 0.4	< 0.4	0.80	11.3	< 0.4
Cr(III), diss.	ug/L	0.07	0.07	< 0.01	< 0.01	< 0.01	0.17	26.4	0.25	0.12	0.07	0.84	9.92	0.16
Cr(VI), diss.	ug/L	< 0.01	< 0.01	< 0.01	< 0.01	< 0.01	0.03 (a)	< 0.1	< 0.01	< 0.01	< 0.01	< 0.01	< 0.05	0.06
Se, diss.	ug/L	< 0.02	0.02 (a)	1.98 (b)	0.13 (a)	0.17 (a)	42.6	23.5 (b)	13.9	13.6	10.0	0.02 (a)	0.45 (b)	10.2
Se(IV), diss.	ug/L	< 0.1	< 0.1	2.6	< 0.5	0.2 (a)	39.1	20.2	11.4	11.5	8.3	< 0.1	< 0.5	7
Se(VI), diss.	ug/L	< 0.2	< 0.2	< 1	< 1	< 0.4	1.9	< 1	1.7	1.8	0.6 (a)	< 0.2	< 1	< 4
Se, other	ug/L	n/a	n/a	n/a	n/a	n/a	n/a	n/a	n/a	n/a	n/a	n/a	n/a	n/a
$Hg_{diss.}$	ng/L	n/a	n/a	n/a	n/a	n/a	n/a	n/a	n/a	n/a	n/a	n/a	n/a	n/a
$Hg_{part.}$	ng/L	n/a	n/a	n/a	n/a	n/a	n/a	n/a	n/a	n/a	n/a	n/a	n/a	n/a
$MeHg_{diss.}$	ng/L	n/a	n/a	n/a	n/a	n/a	n/a	n/a	n/a	n/a	n/a	n/a	n/a	n/a
$MeHg_{part.}$	ng/L	n/a	n/a	n/a	n/a	n/a	n/a	n/a	n/a	n/a	n/a	n/a	n/a	n/a
DMM	ng/L	n/a	n/a	n/a	n/a	n/a	n/a	n/a	n/a	n/a	n/a	n/a	n/a	n/a

Table A-2 (Continued)
Speciation

Sample ID		053	057	059	059D	060	061	062	064	069	070	070D	077	078
As, diss.	ug/L	279	98.6	124	125	< 0.02	1,380	61.5	178	99.5	143	144	< 0.008	0.017 (a)
As(III), diss.	ug/L	108	< 0.2	< 0.2	< 0.2	< 0.01	859	< 0.2	< 0.4	< 0.2	< 0.2	< 0.2	< 0.04	< 0.04
As(V), diss.	ug/L	82	93	127	119	< 0.8	519	37	150	94	136	137	< 0.8	< 0.8
As, other	ug/L	0.7	n/a	n/a	n/a	n/a	n/a	n/a	n/a	n/a	n/a	0.53	n/a	n/a
Cr, diss.	ug/L	< 0.4	1.9	2.7	2.5	0.10	< 0.4	10.5	22.4	3.2	5.3	5.4	0.02	0.02
Cr(III), diss.	ug/L	0.05	1.06	0.01 (a)	< 0.01	0.05	0.27	0.95	0.04 (a)	0.46	0.63	0.62	<0.02	0.02
Cr(VI), diss.	ug/L	< 0.01	0.41	1.28	1.23	< 0.01	< 0.01	6.24	23.0	2.98	5.28	5.17	<0.006	<0.006
Se, diss.	ug/L	1.24 (b)	2.44	2.58 (b)	2.55	< 0.02	4.31	112	103	36.4	29.1	29.4	< 0.008	< 0.008
Se(IV), diss.	ug/L	< 2	2.0	2.5	2.2	< 0.1	<10	90.4	97	33.1	29	28	< 0.04	< 0.04
Se(VI), diss.	ug/L	< 4	< 1	< 1	< 1	< 0.2	<20	32.1	< 4	1.7 (a)	< 4	< 4	< 0.06	< 0.06
Se, other	ug/L	n/a	n/a	n/a	n/a	n/a	n/a	n/a	n/a	n/a	n/a	n/a	n/a	n/a
$Hg_{diss.}$	ng/L	n/a	n/a	n/a	n/a	n/a	n/a	n/a	n/a	n/a	n/a	n/a	1.9 (a)	2.5 (a)
$Hg_{part.}$	ng/L	n/a	n/a	n/a	n/a	n/a	n/a	n/a	n/a	n/a	n/a	n/a	3 (a)	4 (a)
$MeHg_{diss.}$	ng/L	n/a	n/a	n/a	n/a	n/a	n/a	n/a	n/a	n/a	n/a	n/a	< 0.02	0.06 (a)
$MeHg_{part.}$	ng/L	n/a	n/a	n/a	n/a	n/a	n/a	n/a	n/a	n/a	n/a	n/a	0.15	0.09
DMM	ng/L	n/a	n/a	n/a	n/a	n/a	n/a	n/a	n/a	n/a	n/a	n/a	< 0.005	< 0.005

Table A-2 (Continued)
Speciation

Sample ID		079	079D	082	083	084	088	089	090	091	092	TEB	094	095
As, diss.	ug/L	99.1	97.0	23.0	6.19	727	0.076 (a)	0.896	22.6	10.8	3.33	0.922	0.035 (a)	0.046 (a)
As(III), diss.	ug/L	9.5	9.9	0.2 (a)	0.23	71	n/a	n/a	0.28	< 0.05	< 0.05	0.01 (a)	< 0.01	< 0.01
As(V), diss.	ug/L	104	73	15	2.4 (a)	535	n/a	n/a	18.0	9.4	0.5	0.09	< 0.02	< 0.02
As, other	ug/L	n/a	n/a	n/a	n/a	n/a	n/a	n/a	0.67	0.15 (a)	0.10 (a)	n/a	n/a	n/a
Cr, diss.	ug/L	< 0.2	< 0.2	24.6	19.9	< 0.2	0.22	1.22	0.7	< 0.2	122	0.49	0.03	< 0.01
Cr(III), diss.	ug/L	<0.02	<0.02	1.25	2.43	0.04 (a)	n/a	n/a	n/a	n/a	3 (a)	n/a	n/a	n/a
Cr(VI), diss.	ug/L	<0.006	<0.006	22.9	15.2	<0.006	n/a	n/a	n/a	n/a	109	n/a	n/a	n/a
Se, diss.	ug/L	0.16 (a)	0.16 (a)	19.1	12.8	0.57 (b)	0.010 (a)	0.194 (b)	85.5	122	103	0.094 (a)	0.037 (a)	0.063 (a)
Se(IV), diss.	ug/L	< 0.2	< 0.2	17.9	8.72	< 2	n/a	n/a	5.2	3.6	0.6 (a)	< 0.05	< 0.05	< 0.05
Se(VI), diss.	ug/L	< 0.3	< 0.3	0.3 (a)	1.5 (a)	< 3	n/a	n/a	97	138	116	< 0.05	< 0.05	< 0.05
Se, other	ug/L	n/a	n/a	n/a	n/a	n/a	n/a	n/a	n/a	n/a	n/a	n/a	n/a	n/a
$Hg_{diss.}$	ng/L	0.2 (a)	0.5 (a)	5.9	2.1 (a)	0.6 (a)	n/a	n/a	n/a	n/a	n/a	n/a	1.9 (a)	0.9 (a)
$Hg_{part.}$	ng/L	6 (a)	3 (a)	18 (a)	22 (a)	5 (a)	n/a	n/a	n/a	n/a	n/a	n/a	15 (a)	6 (a)
$MeHg_{diss.}$	ng/L	< 0.02	0.05 (a)	0.05 (a)	0.17	0.06 (a)	n/a	n/a	n/a	n/a	n/a	n/a	0.03 (a)	0.06 (a)
$MeHg_{part.}$	ng/L	0.06	0.05	0.03 (a)	0.16	0.03 (a)	n/a	n/a	n/a	n/a	n/a	n/a	< 0.01	0.02 (a)
DMM	ng/L	< 0.005	< 0.005	< 0.005	0.040	< 0.005	n/a	n/a	n/a	n/a	n/a	n/a	n/a	0.808

Table A-2 (Continued)
Speciation

Sample ID		096 [1]	096D [1]	097	098	099	100	101	102	103	104	105	106	106D
As, diss.	ug/L	38.3	37.8	44.9	76.9	4.80	0.200	2.23	7.24	0.009 (a)	0.031 (a)	230	110	112
As(III), diss.	ug/L	< 0.1	< 0.1	< 0.1	0.66	0.10 (a)	< 0.01	< 0.1	< 0.05	< 0.01	< 0.01	197	15.9	13.8
As(V), diss.	ug/L	28.2	28.4	36.3	59.5	3.7	< 0.02	0.2 (a)	6.3	0.11	0.08	50.3	63.0	77.3
As, other	ug/L	< 0.1	< 0.1	< 0.1	0.29	0.19	n/a	0.62	< 0.05	n/a	n/a	3.83	5.78	5.22
Cr, diss.	ug/L	1,990	1,980	2,000	2.8	< 0.2	0.03	1.5	19.6	< 0.02	< 0.02	< 0.4	0.9	0.9
Cr(III), diss.	ug/L	120	140	40 (a)	0.2	n/a	n/a	< 0.08	0.4 (a)	n/a	n/a	n/a	n/a	n/a
Cr(VI), diss.	ug/L	2,050	2,030	2,230	0.99	n/a	n/a	0.07	13.3	n/a	n/a	n/a	n/a	n/a
Se, diss.	ug/L	428	427	413	50.7	2.04 (b)	0.047 (a)	91.0	80.5	0.008 (a)	0.008 (a)	8.5 (b)	64.8	65.1
Se(IV), diss.	ug/L	37.3	37.6	38.2	29.3	< 0.8	< 0.05	< 0.8	5.3	< 0.05	< 0.05	< 2	< 2	< 2
Se(VI), diss.	ug/L	363	367	366	< 2	< 2	< 0.05	104	85	< 0.05	< 0.05	< 4	64	65
Se, other	ug/L	n/a	n/a	n/a	n/a	n/a	n/a	n/a	n/a	< 0.05	< 0.05	< 2	< 2	< 2
$Hg_{diss.}$	ng/L	29.5	32.2	36.5	60.6	5.7	1.5 (a)	2.1 (a)	3.8 (a)	n/a	n/a	n/a	n/a	n/a
$Hg_{part.}$	ng/L	23 (a)	10 (a)	16 (a)	11 (a)	13 (a)	3 (a)	3 (a)	52	n/a	n/a	n/a	n/a	n/a
$MeHg_{diss.}$	ng/L	0.22	0.20	0.22	0.76	0.03 (a)	< 0.02	< 0.02	0.12	n/a	n/a	n/a	n/a	n/a
$MeHg_{part.}$	ng/L	0.03 (a)	0.03 (a)	0.05	0.01 (a)	< 0.01	0.01 (a)	0.01 (a)	< 0.01	n/a	n/a	n/a	n/a	n/a
DMM	ng/L	0.216	0.335	0.262	0.035	0.265	n/a	0.565	2.47	n/a	n/a	n/a	n/a	n/a

Table A-2 (Continued)
Speciation

Sample ID		107	108	109	110	111	112	113	114	115	116	117	118	118D
As, diss.	ug/L	30.6	4.09	0.014 (a)	0.055 (a)	5.94	1.36	102	23.5	8.32	8.24	0.015 (a)	40.8	39.5
As(III), diss.	ug/L	1.0	0.37	< 0.01	< 0.01	< 0.1	0.7	0.8	< 0.1	3.05	1.01	< 0.01	0.66	0.18
As(V), diss.	ug/L	15.1	2.3	< 0.02	0.05 (a)	3.4	0.9	118	20.5	5.3	7.4	< 0.02	45.5	45.6
As, other	ug/L	< 0.2	< 0.05	n/a	n/a	< 0.1	0.2	0.2	< 0.1	< 0.05	0.08	n/a	0.15	0.11
Cr, diss.	ug/L	<2	0.5	0.02	0.03	0.5	< 0.2	< 0.2	0.3	1.5	1.8	0.03	< 0.2	< 0.2
Cr(III), diss.	ug/L	n/a	n/a	n/a	n/a	n/a	n/a	n/a	n/a	0.34	0.40	n/a	n/a	n/a
Cr(VI), diss.	ug/L	n/a	n/a	n/a	n/a	n/a	n/a	n/a	n/a	0.09	0.31	n/a	n/a	n/a
Se, diss.	ug/L	159	6.56 (b)	0.013 (a)	0.021 (a)	90.5	0.67 (b)	29.3	0.07 (a)	36.1	35.4	0.010 (a)	17.6	18.5
Se(IV), diss.	ug/L	< 2	2.6	< 0.05	< 0.05	38.7	< 0.5	19.2	< 0.5	29.6	30.7	< 0.05	17.5	16.5
Se(VI), diss.	ug/L	16	3.9	< 0.05	< 0.05	72	< 1	3 (a)	< 1	3	3	< 0.05	1.3 (a)	1.3 (a)
Se, other	ug/L	51	< 0.5	n/a	n/a	n/a	n/a	n/a	n/a	n/a	n/a	n/a	n/a	n/a
$Hg_{diss.}$	ng/L	n/a	n/a	n/a	n/a	n/a	n/a	n/a	n/a	n/a	n/a	n/a	n/a	n/a
$Hg_{part.}$	ng/L	n/a	n/a	n/a	n/a	n/a	n/a	n/a	n/a	n/a	n/a	n/a	n/a	n/a
$MeHg_{diss.}$	ng/L	n/a	n/a	n/a	n/a	n/a	n/a	n/a	n/a	n/a	n/a	n/a	n/a	n/a
$MeHg_{part.}$	ng/L	n/a	n/a	n/a	n/a	n/a	n/a	n/a	n/a	n/a	n/a	n/a	n/a	n/a
DMM	ng/L	n/a	n/a	n/a	n/a	n/a	n/a	n/a	n/a	n/a	n/a	n/a	n/a	n/a

Table A-2 (Continued)
Speciation

	Sample ID	119	120	121	122	125	126	126D	127	128
As, diss.	ug/L	30.2	26.8	11.0	25.5	< 0.009	5.20	4.86	6.42	14.3
As(III), diss.	ug/L	< 0.05	7.2	1.3	7.6	< 0.02	< 0.1	< 0.1	< 0.2	10.1
As(V), diss.	ug/L	30.5	11.4	6.0	8.3	< 0.4	4 (a)	3 (a)	4 (a)	3 (a)
As, other	ug/L	0.29	9.3	0.6	6.0	< 0.02	< 0.1	< 0.1	< 0.2	0.4
Cr, diss.	ug/L	0.2	< 0.2	< 0.2	< 0.2	0.05	108	109	24.4	0.5
Cr(III), diss.	ug/L	n/a	n/a	n/a	n/a	0.04	4.15 (a)	2.13 (a)	0.5 (a)	0.16
Cr(VI), diss.	ug/L	n/a	n/a	n/a	n/a	0.02 (a)	121	122	25.5	< 0.02
Se, diss.	ug/L	27.9	3.30 (b)	3.86 (b)	1.13 (b)	< 0.005	88.7	88.3	181	50.9
Se(IV), diss.	ug/L	22.8	1.8	1.1 (a)	< 0.5	< 0.06	12.5	13.0	12.3	17.4
Se(VI), diss.	ug/L	1.7	2 (a)	3 (a)	< 1	< 0.3	103	104	245	7
Se, other	ug/L	n/a	n/a	n/a	n/a	< 0.3	< 0.3	< 0.3	< 0.3	1.8
$Hg_{diss.}$	ng/L	n/a	n/a	n/a	n/a	3.1 (a)	9.4	2.0 (a)	5.4	79.3
$Hg_{part.}$	ng/L	n/a	n/a	n/a	n/a	3 (a)	3 (a)	6 (a)	3 (a)	100
$MeHg_{diss.}$	ng/L	n/a	n/a	n/a	n/a	0.16	0.17	0.21	0.03 (a)	6.36
$MeHg_{part.}$	ng/L	n/a	n/a	n/a	n/a	0.02 (a)	0.02 (a)	0.02 (a)	0.02 (a)	0.06
DMM	ng/L	n/a	n/a	n/a	n/a	n/a	n/a	n/a	n/a	n/a

Footnotes:
(1) = Samples 096 and 096D are samples of leachate that were treated with CO_2 prior to analysis.
(a) sample concentration less than 5 times blank
(b) isotope ratios do not match
n/a = not analyzed

B
BOX PLOTS COMPARING ASH LEACHATE CONCENTRATIONS BY SITE AND PLANT ATTRIBUTES

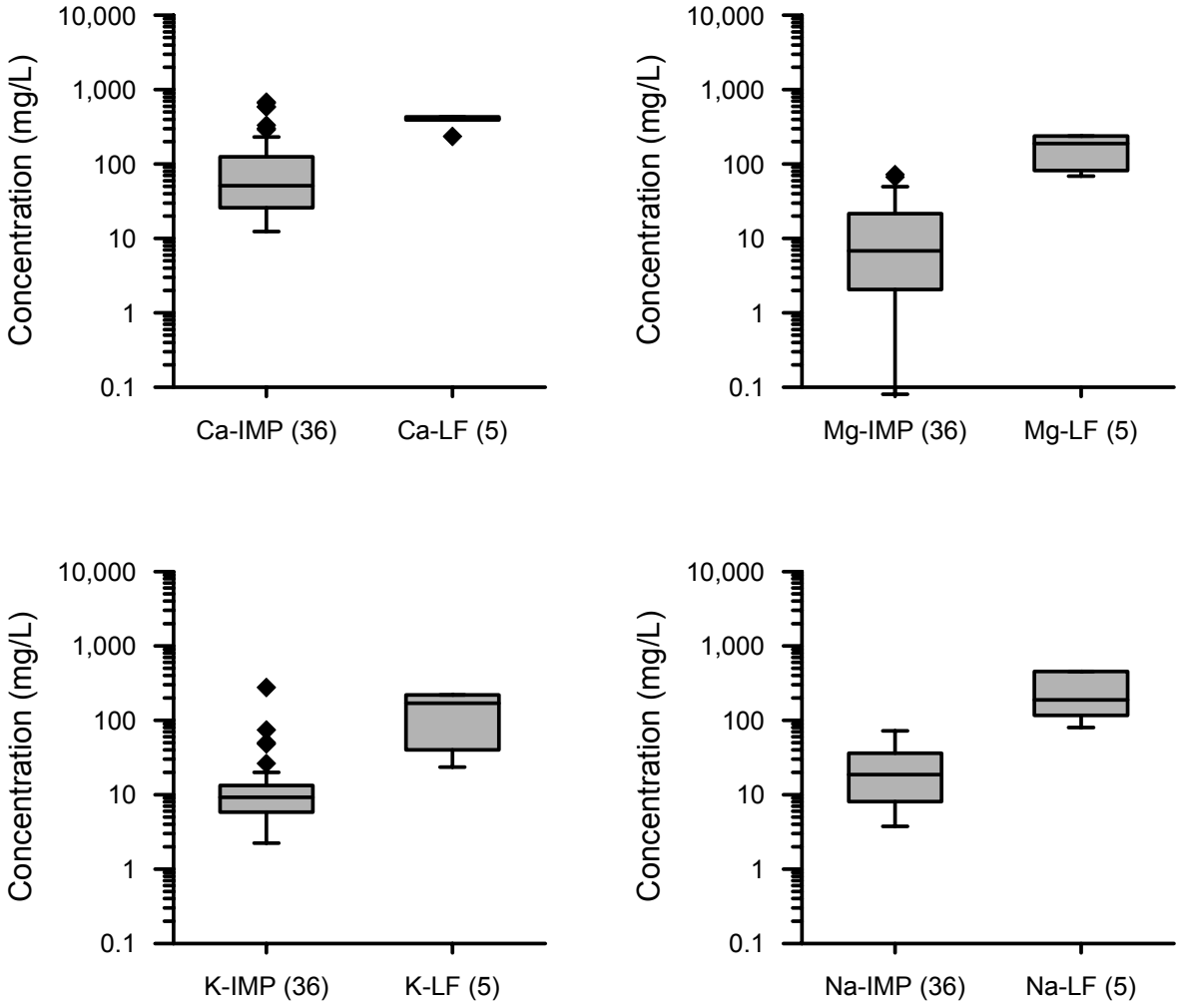

Figure B-1
Comparison of field leachate concentrations: bituminous coal ash, landfill versus impoundment

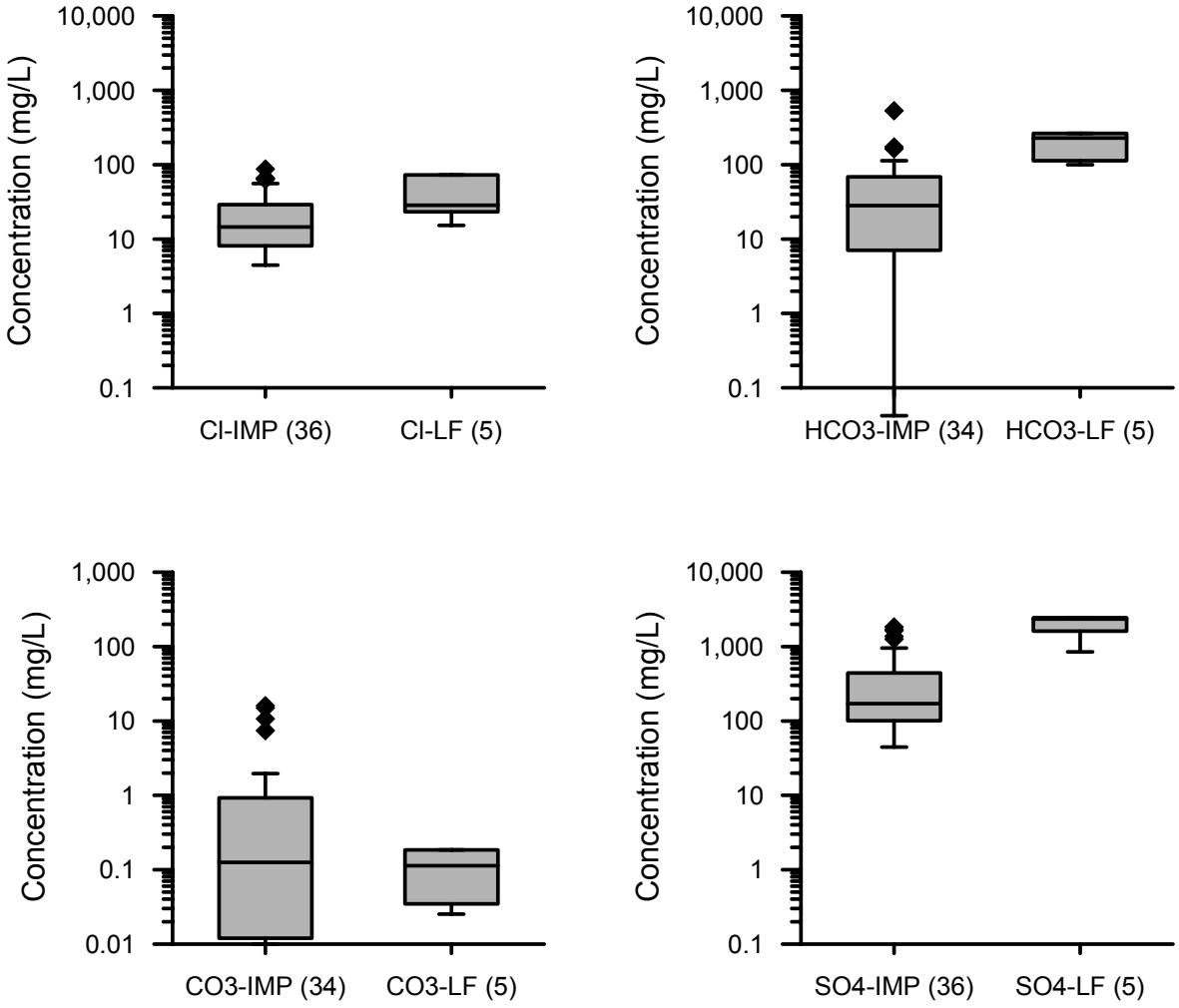

Figure B-1 (Continued)
Comparison of field leachate concentrations: bituminous coal ash, landfill versus impoundment

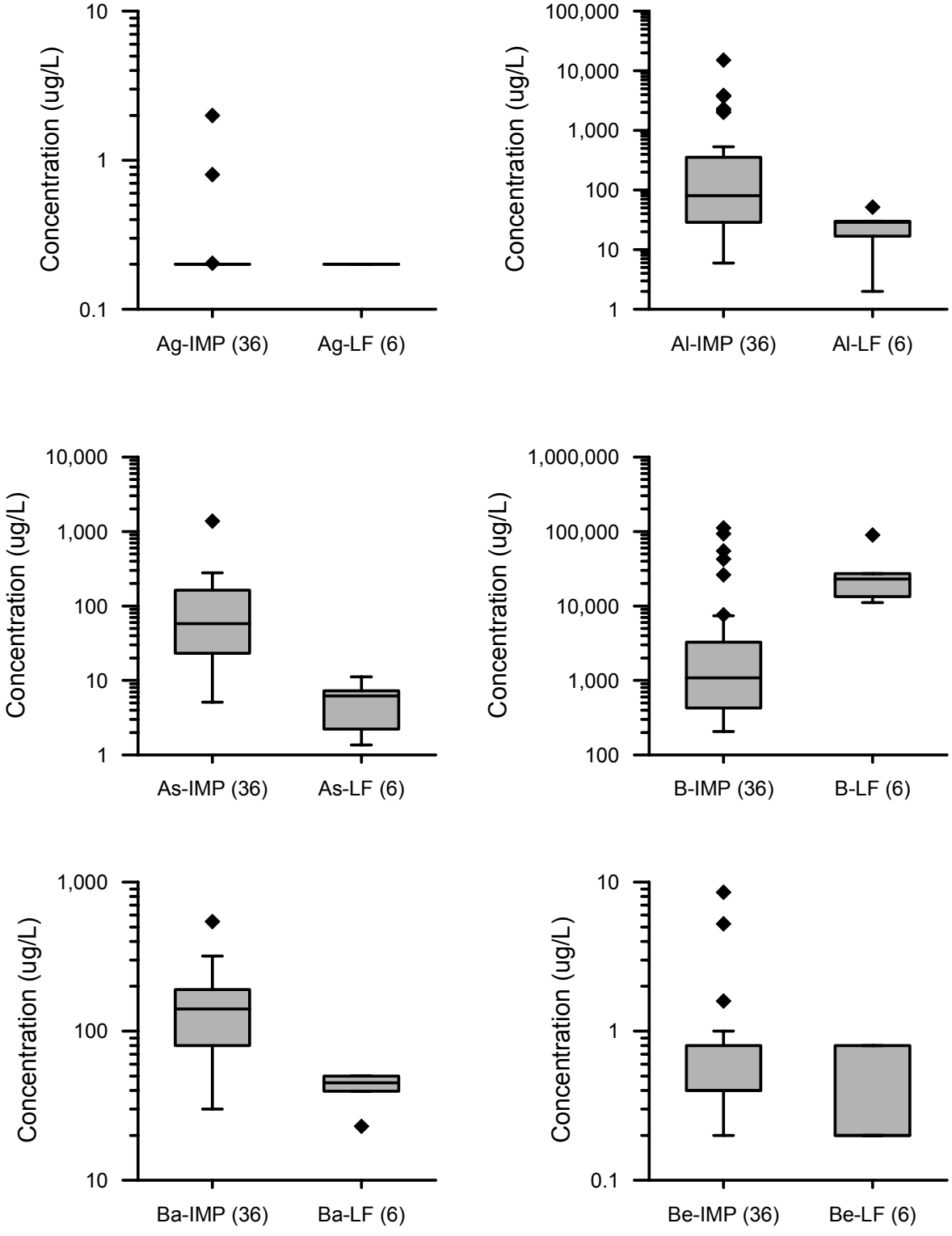

Figure B-1 (Continued)
Comparison of field leachate concentrations: bituminous coal ash, landfill versus impoundment

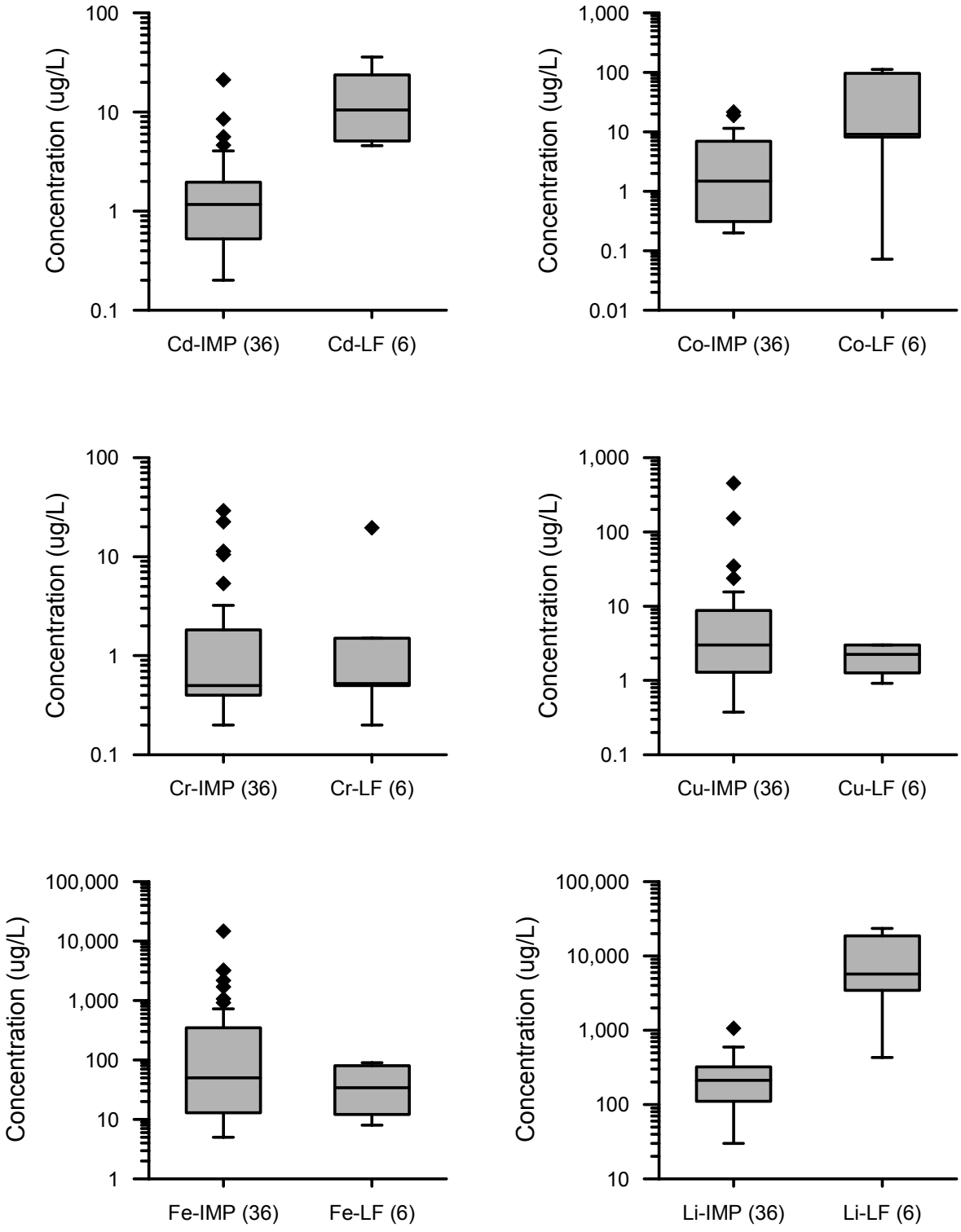

Figure B-1 (Continued)
Comparison of field leachate concentrations: bituminous coal ash, landfill versus impoundment

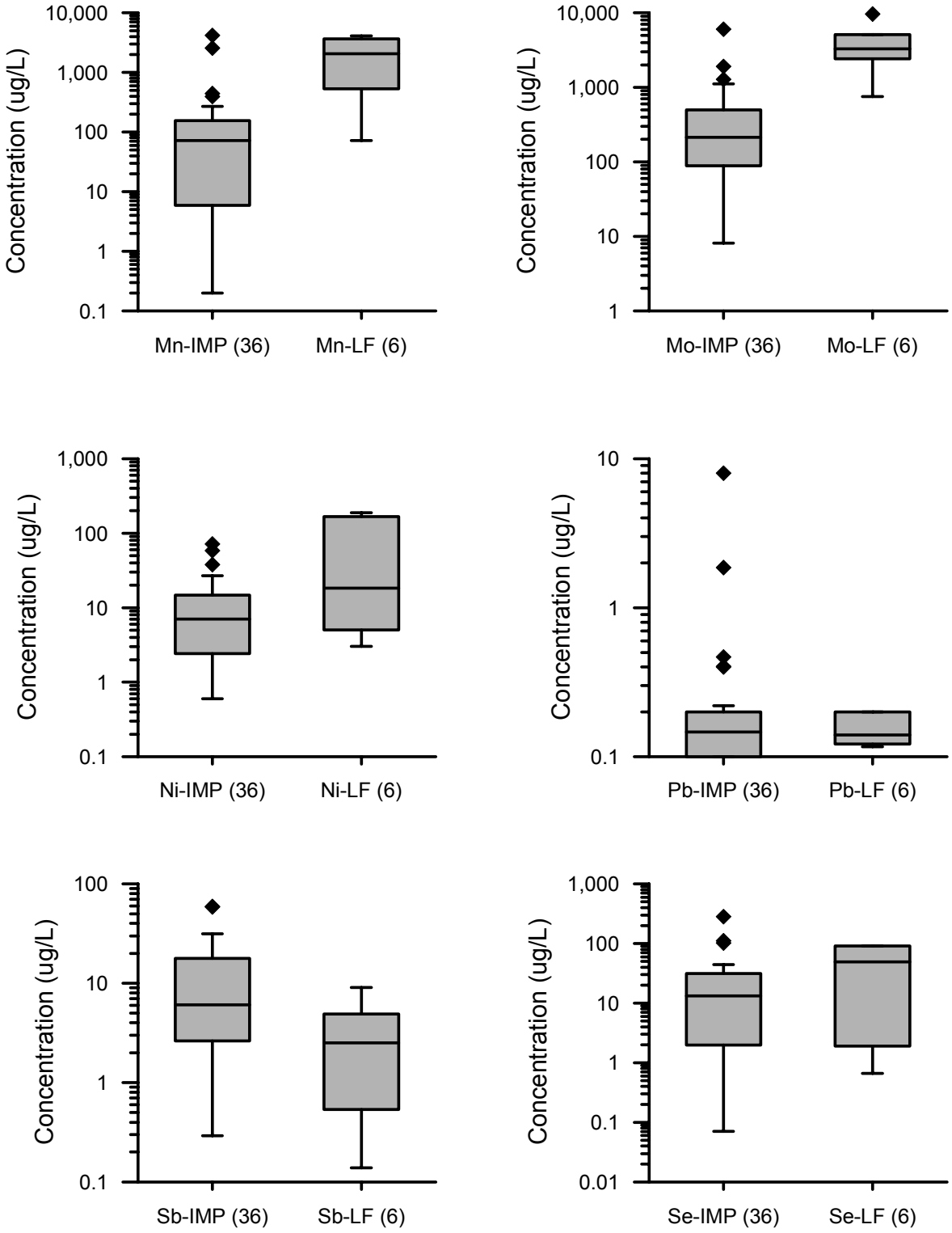

Figure B-1 (Continued)
Comparison of field leachate concentrations: bituminous coal ash, landfill versus impoundment

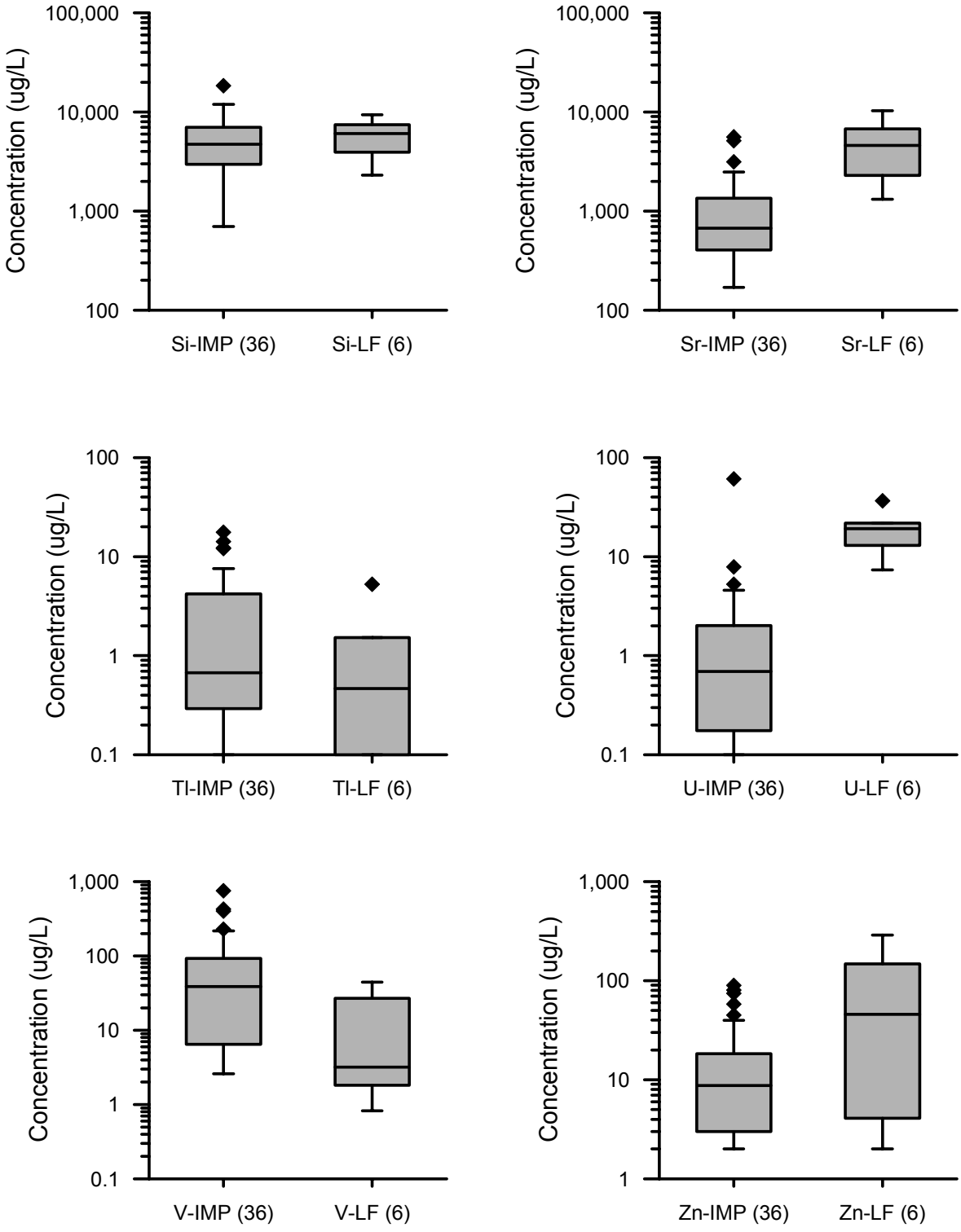

Figure B-1 (Continued)
Comparison of field leachate concentrations: bituminous coal ash, landfill versus impoundment

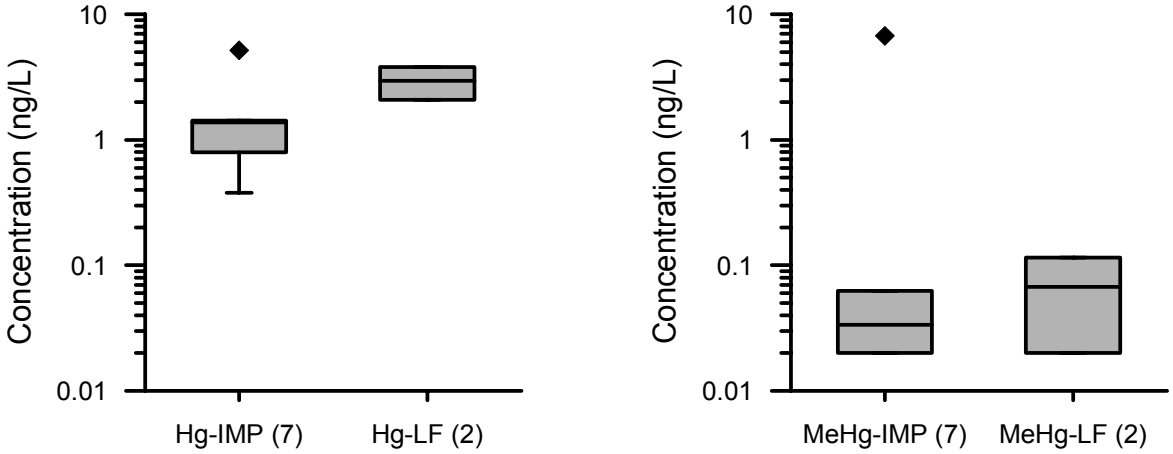

Figure B-1 (Continued)
Comparison of field leachate concentrations: bituminous coal ash, landfill versus impoundment

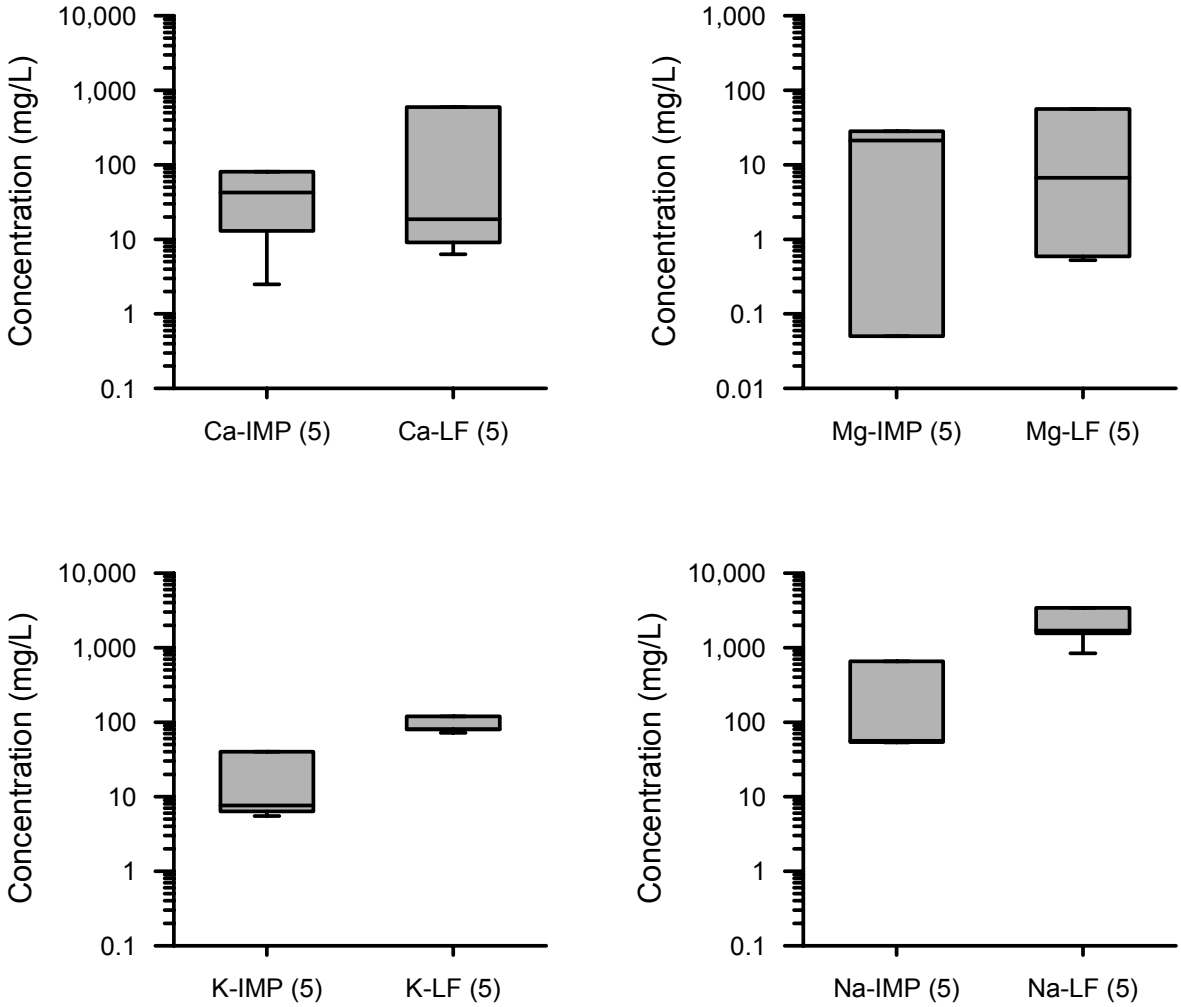

Figure B-2
Comparison of field leachate concentrations: subbituminous/lignite coal ash, landfill versus impoundment

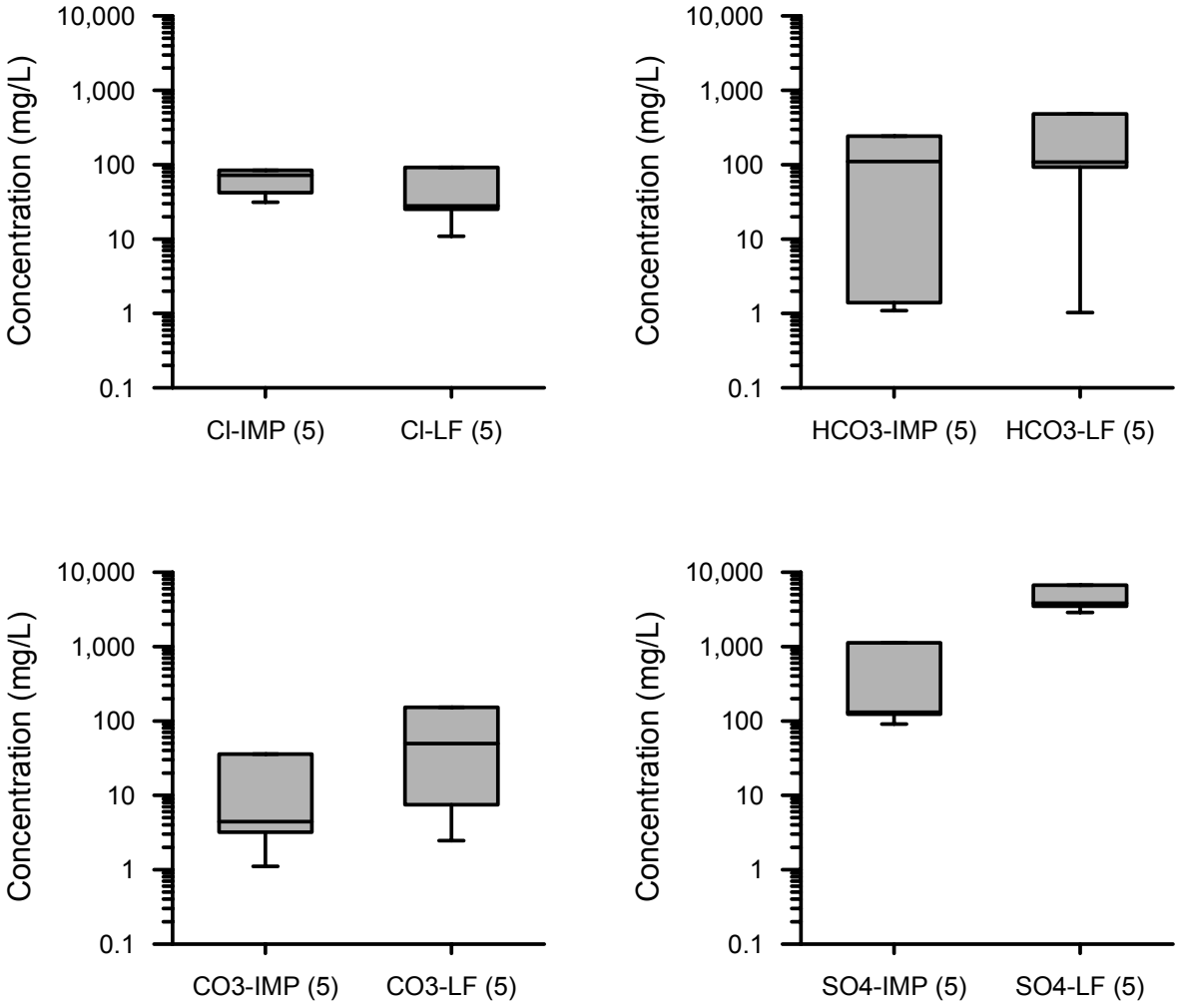

Figure B-2 (Continued)
Comparison of field leachate concentrations: subbituminous/lignite coal ash, landfill versus impoundment

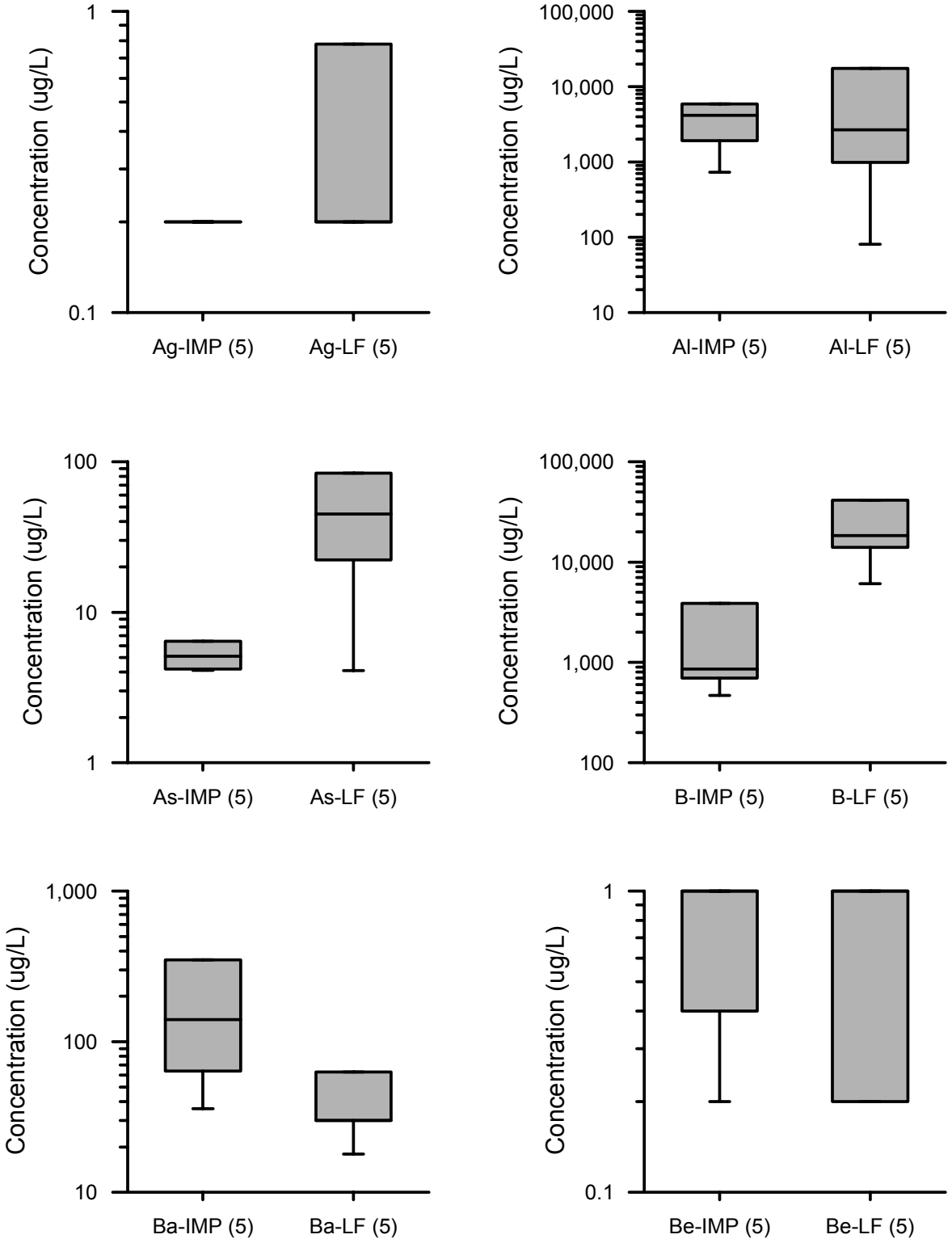

Figure B-2 (Continued)
Comparison of field leachate concentrations: subbituminous/lignite coal ash, landfill versus impoundment

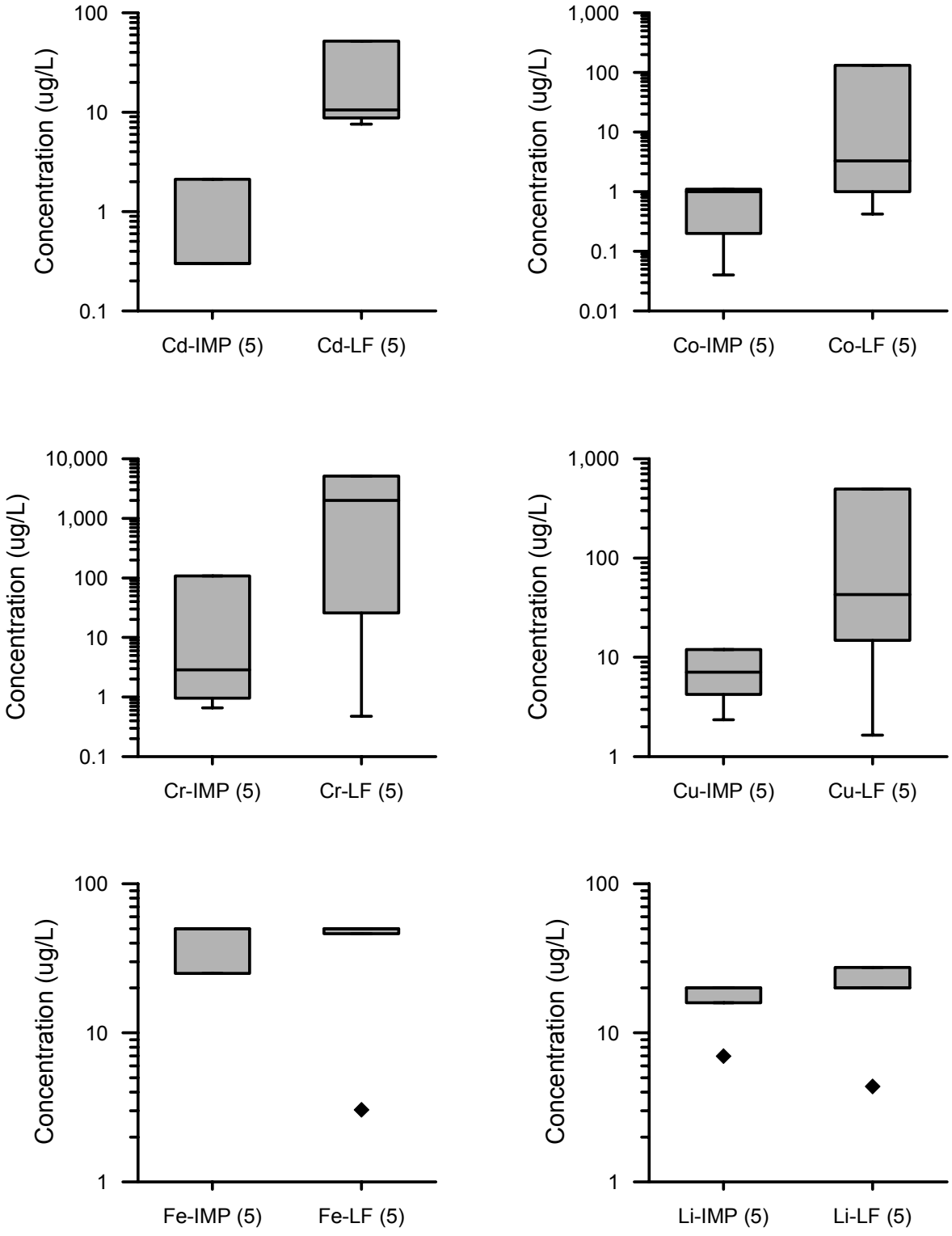

Figure B-2 (Continued)
Comparison of field leachate concentrations: subbituminous/lignite coal ash, landfill versus impoundment

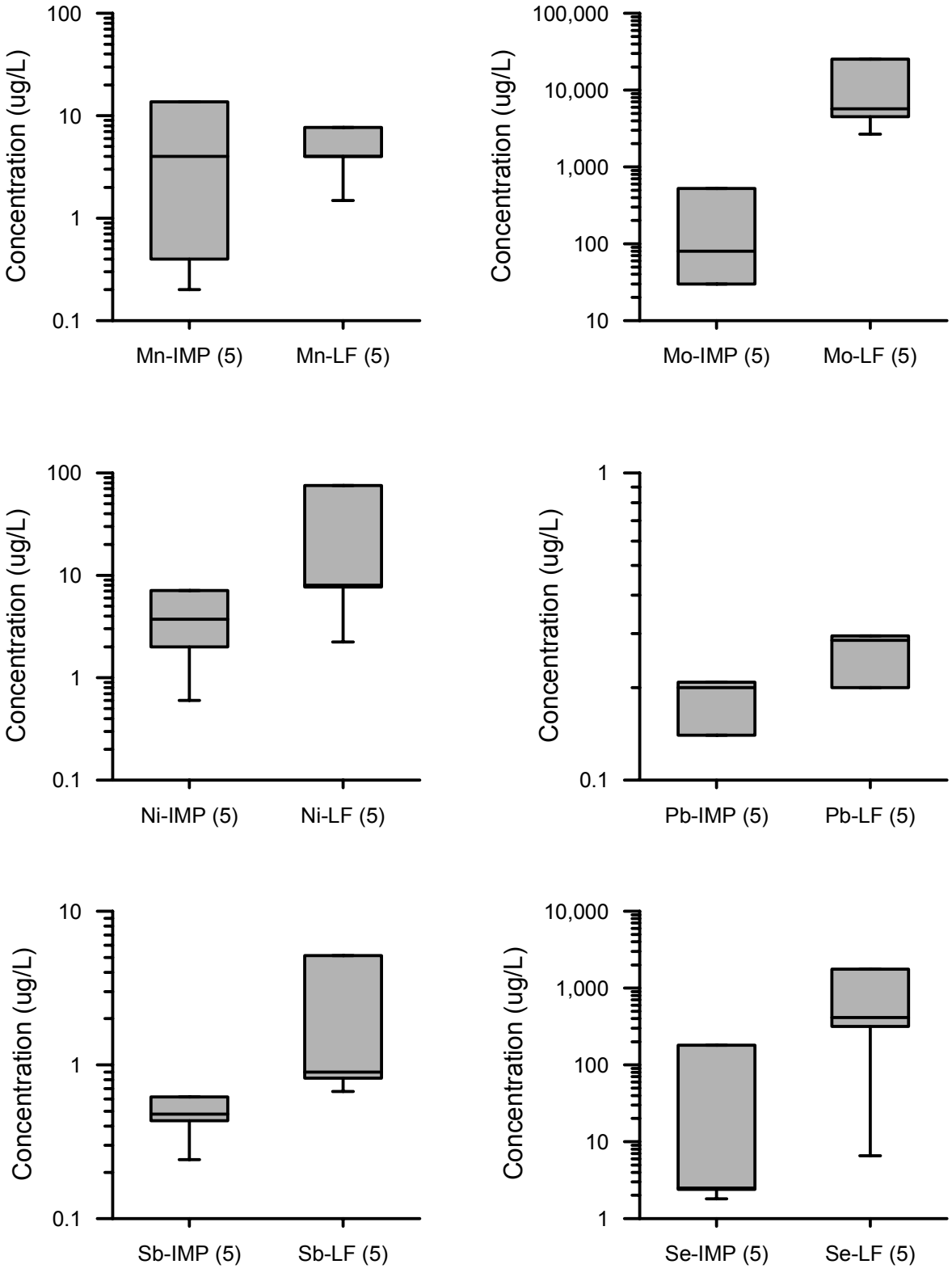

Figure B-2 (Continued)
Comparison of field leachate concentrations: subbituminous/lignite coal ash, landfill versus impoundment

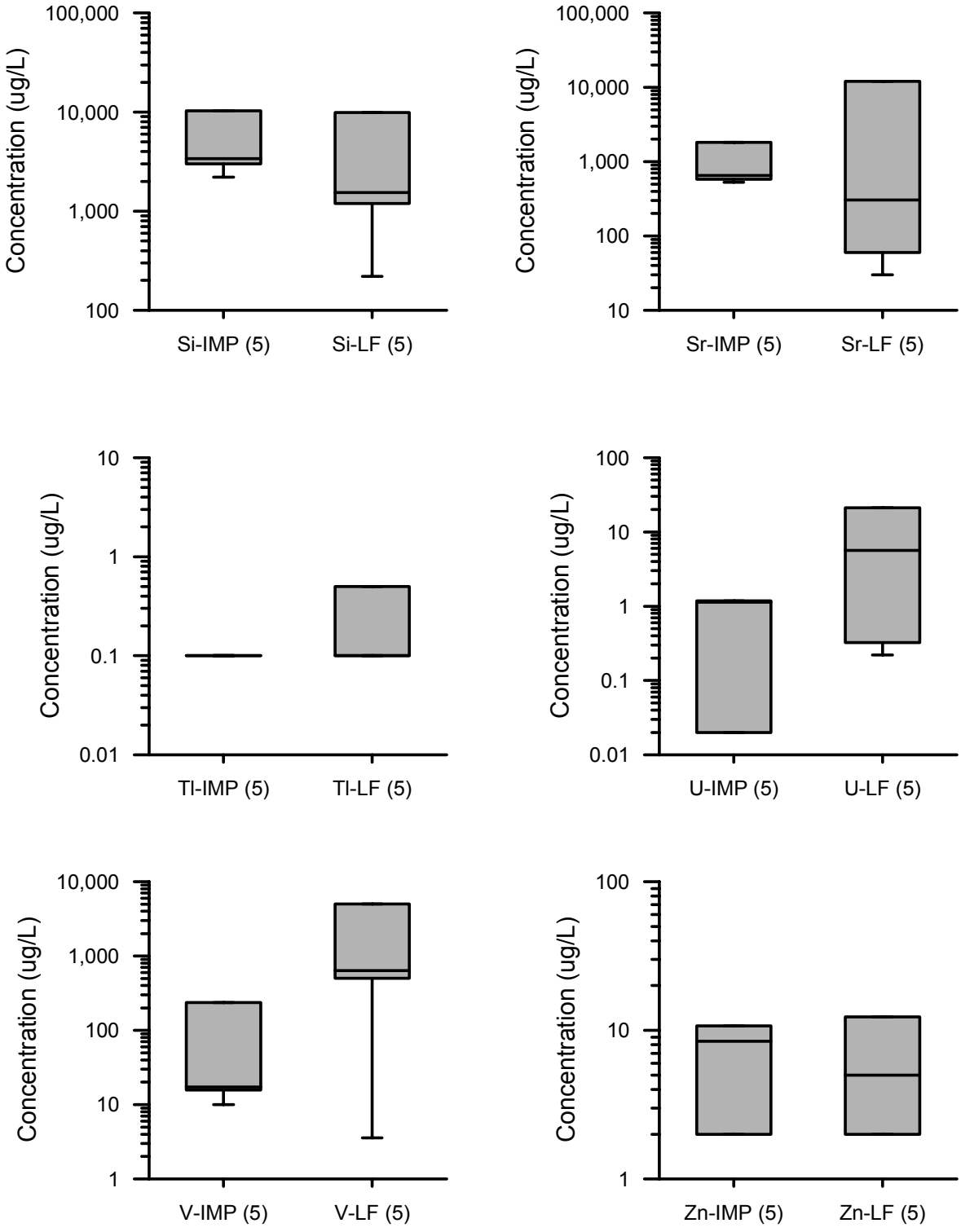

Figure B-2 (Continued)
Comparison of field leachate concentrations: subbituminous/lignite coal ash, landfill versus impoundment

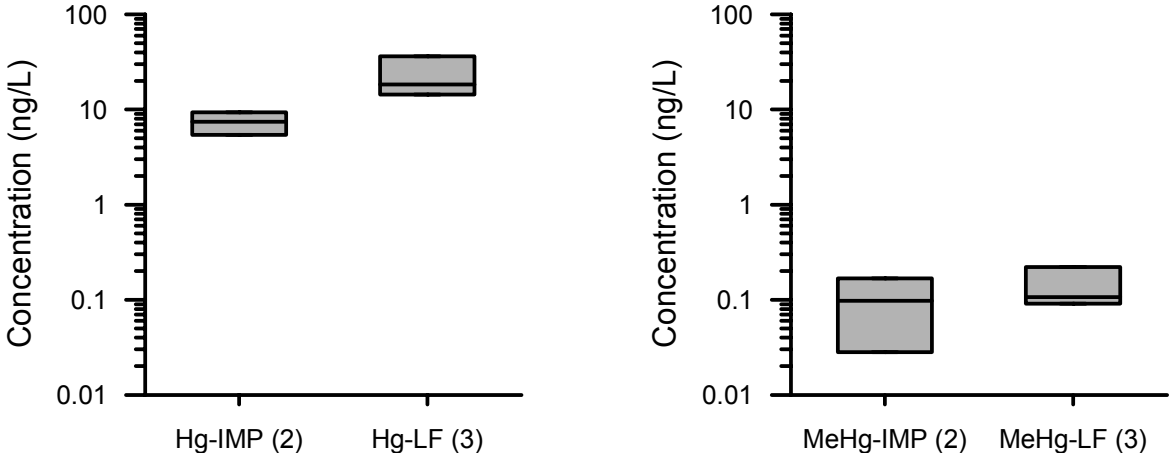

Figure B-2 (Continued)
Comparison of field leachate concentrations: subbituminous/lignite coal ash, landfill versus impoundment

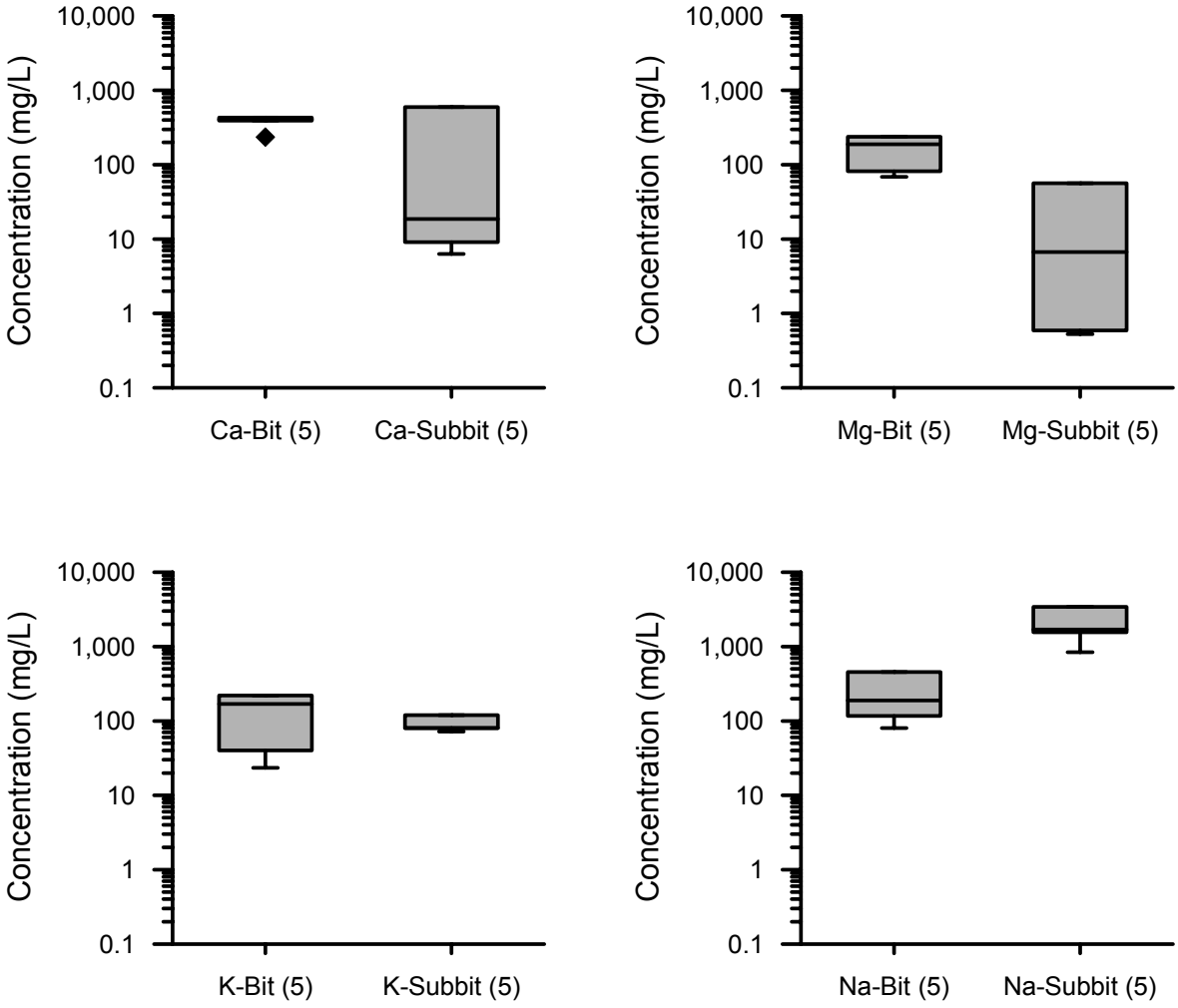

Figure B-3
Comparison of field leachate concentrations: bituminous vs. subbituminous/lignite coal ash, landfills

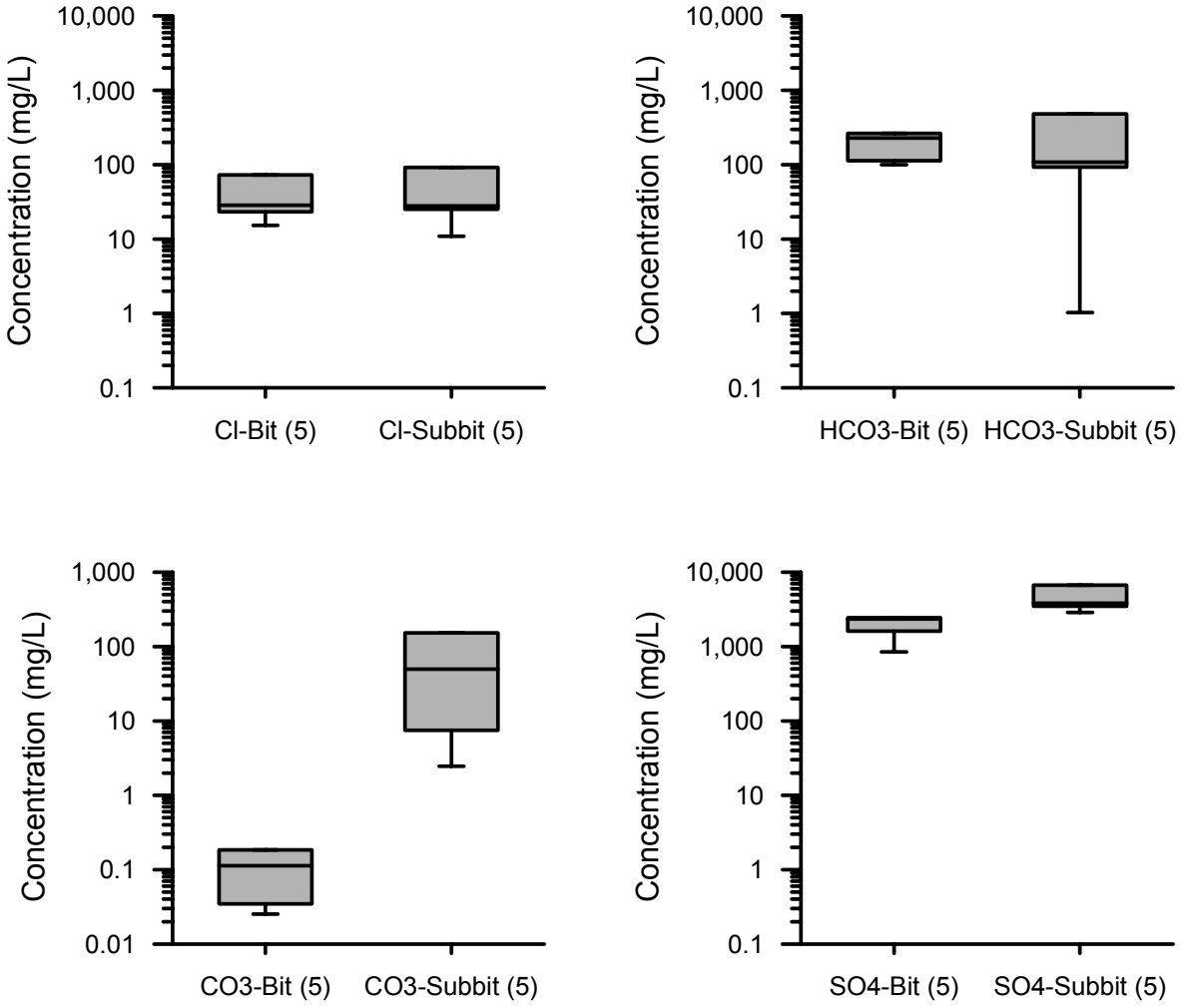

Figure B-3 (Continued)
Comparison of field leachate concentrations: bituminous vs. subbituminous/lignite coal ash, landfills

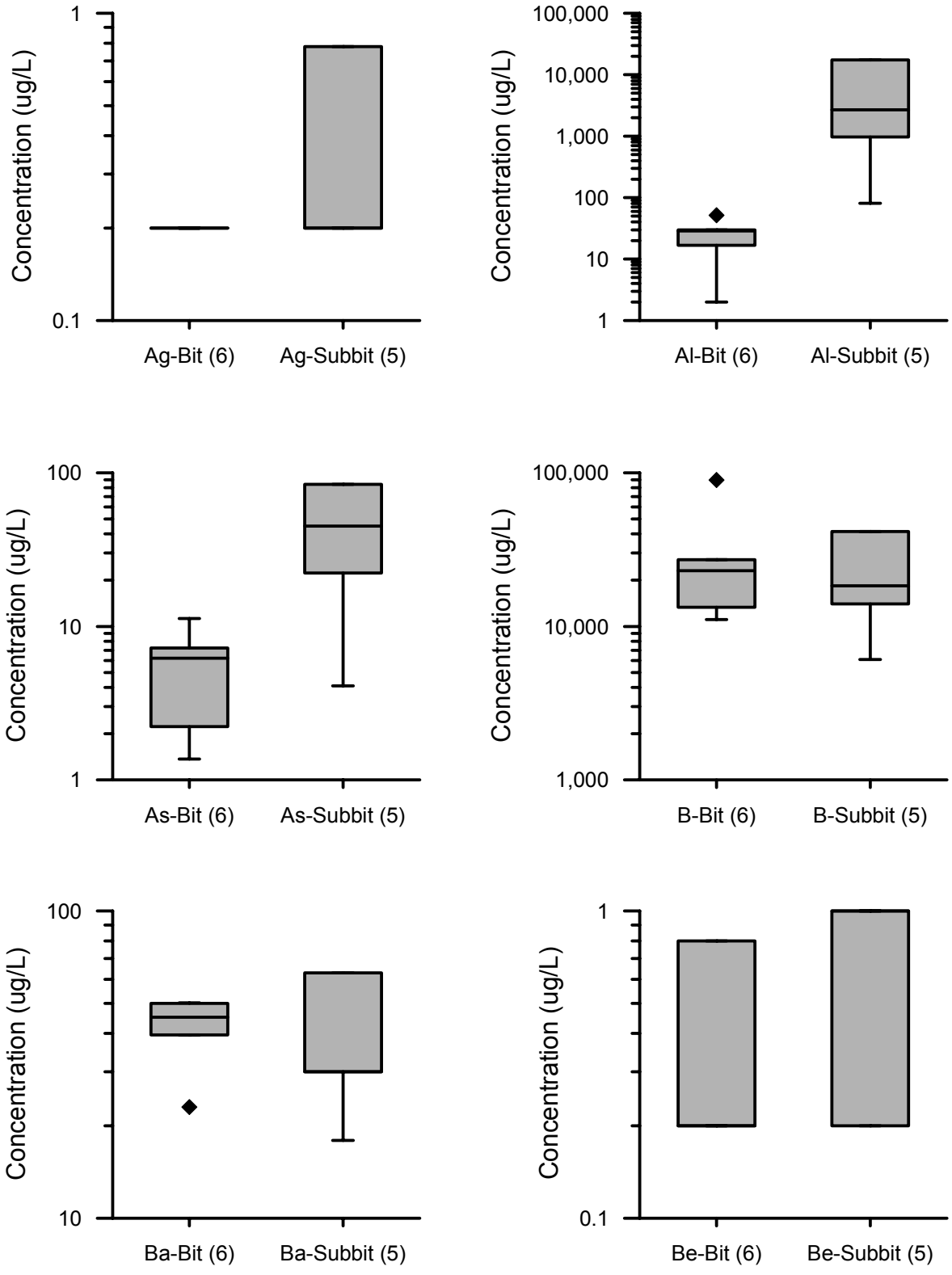

Figure B-3 (Continued)
Comparison of field leachate concentrations: bituminous vs. subbituminous/lignite coal ash, landfills

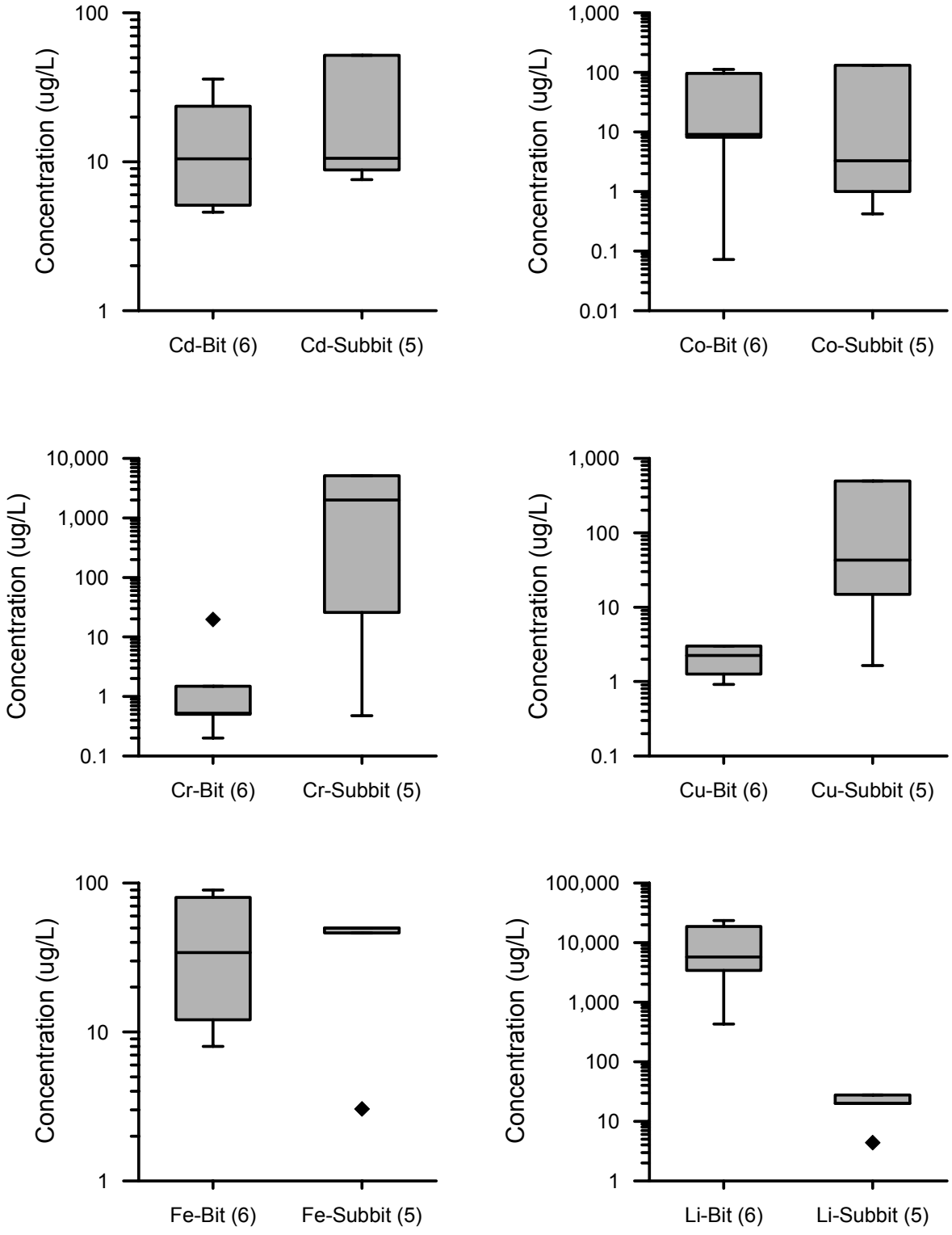

Figure B-3 (Continued)
Comparison of field leachate concentrations: bituminous vs. subbituminous/lignite coal ash, landfills

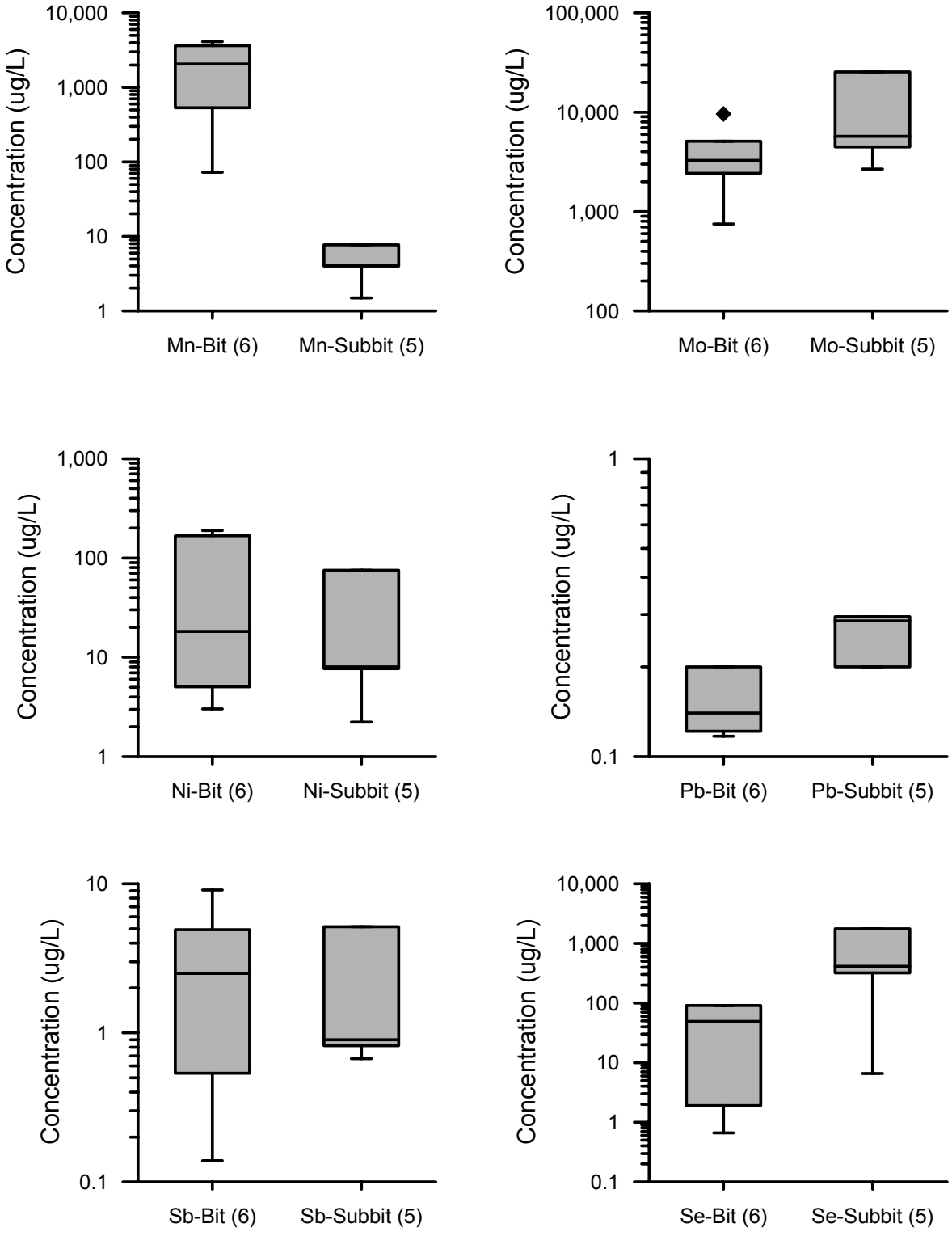

Figure B-3 (Continued)
Comparison of field leachate concentrations: bituminous vs. subbituminous/lignite coal ash, landfills

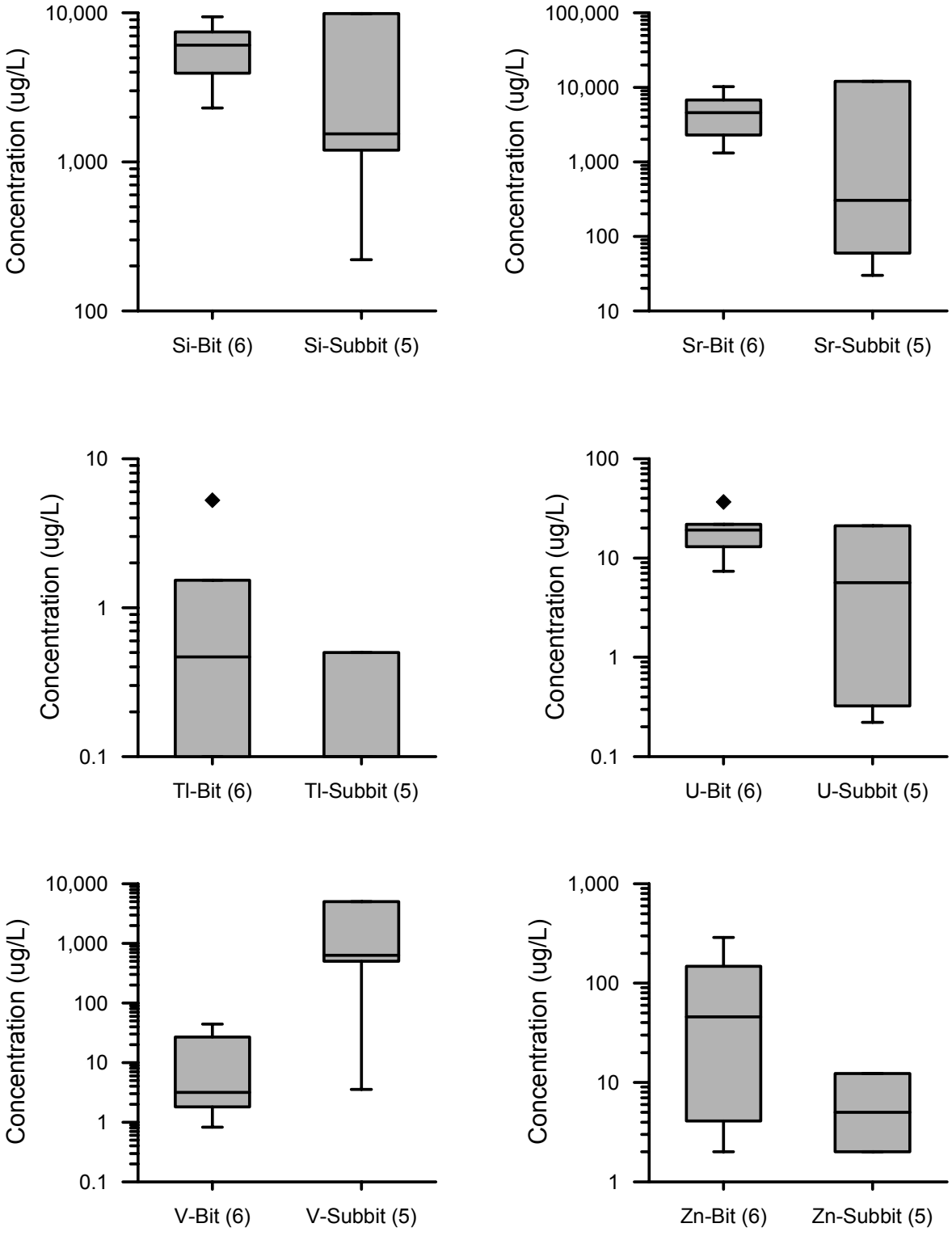

Figure B-3 (Continued)
Comparison of field leachate concentrations: bituminous vs. subbituminous/lignite coal ash, landfills

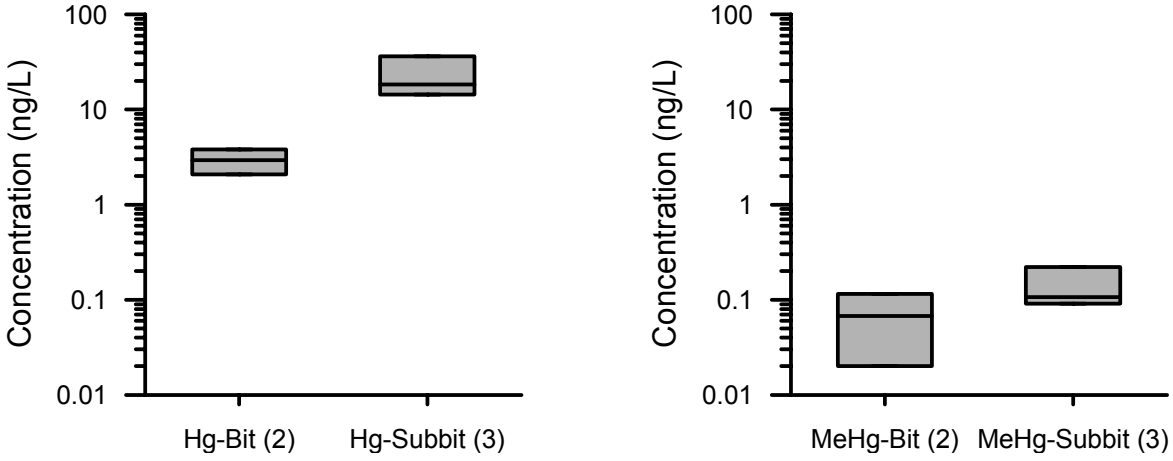

Figure B-3 (Continued)
Comparison of field leachate concentrations: bituminous vs. subbituminous/lignite coal ash, landfills

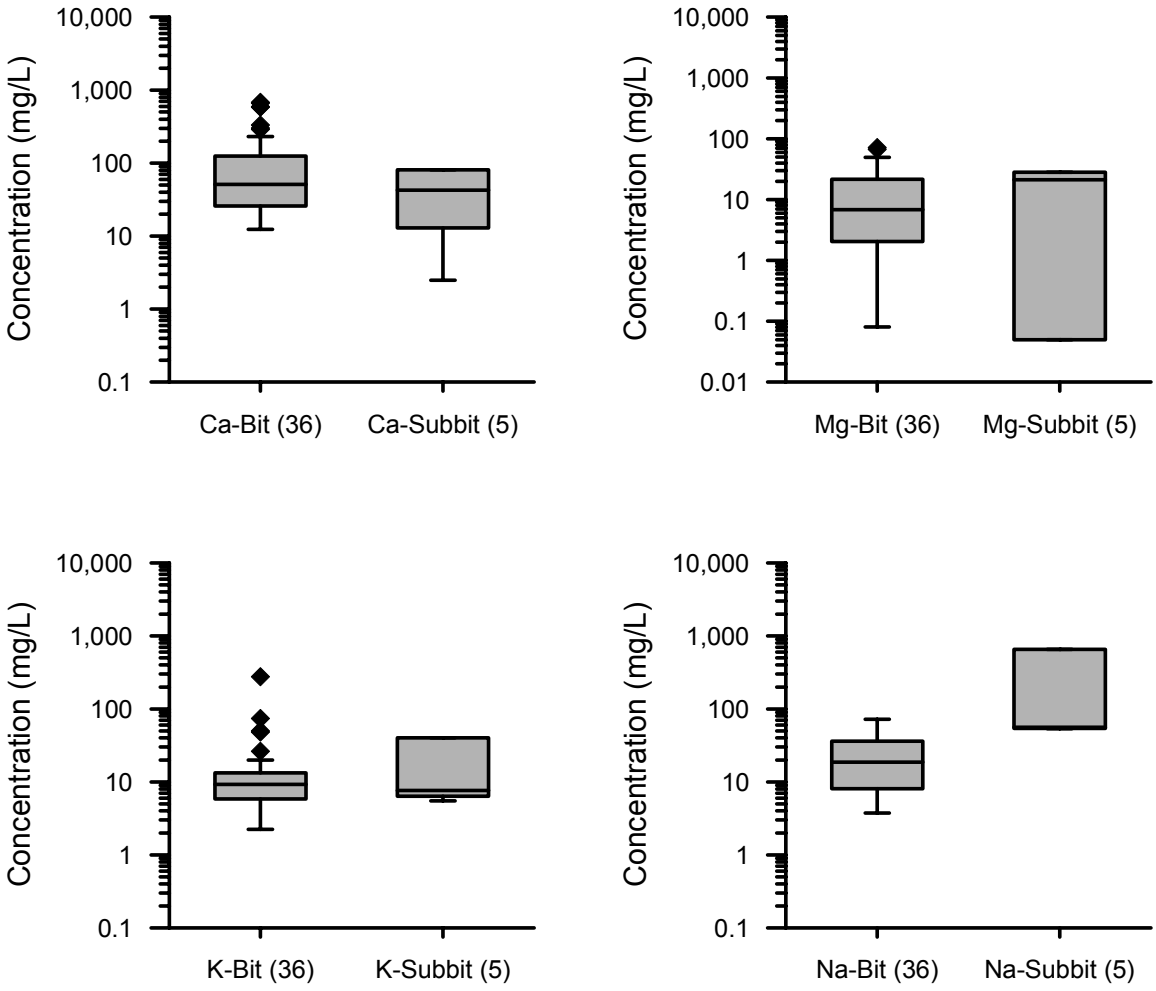

Figure B-4
Comparison of field leachate concentrations: bituminous vs. subbituminous/lignite coal ash, impoundments

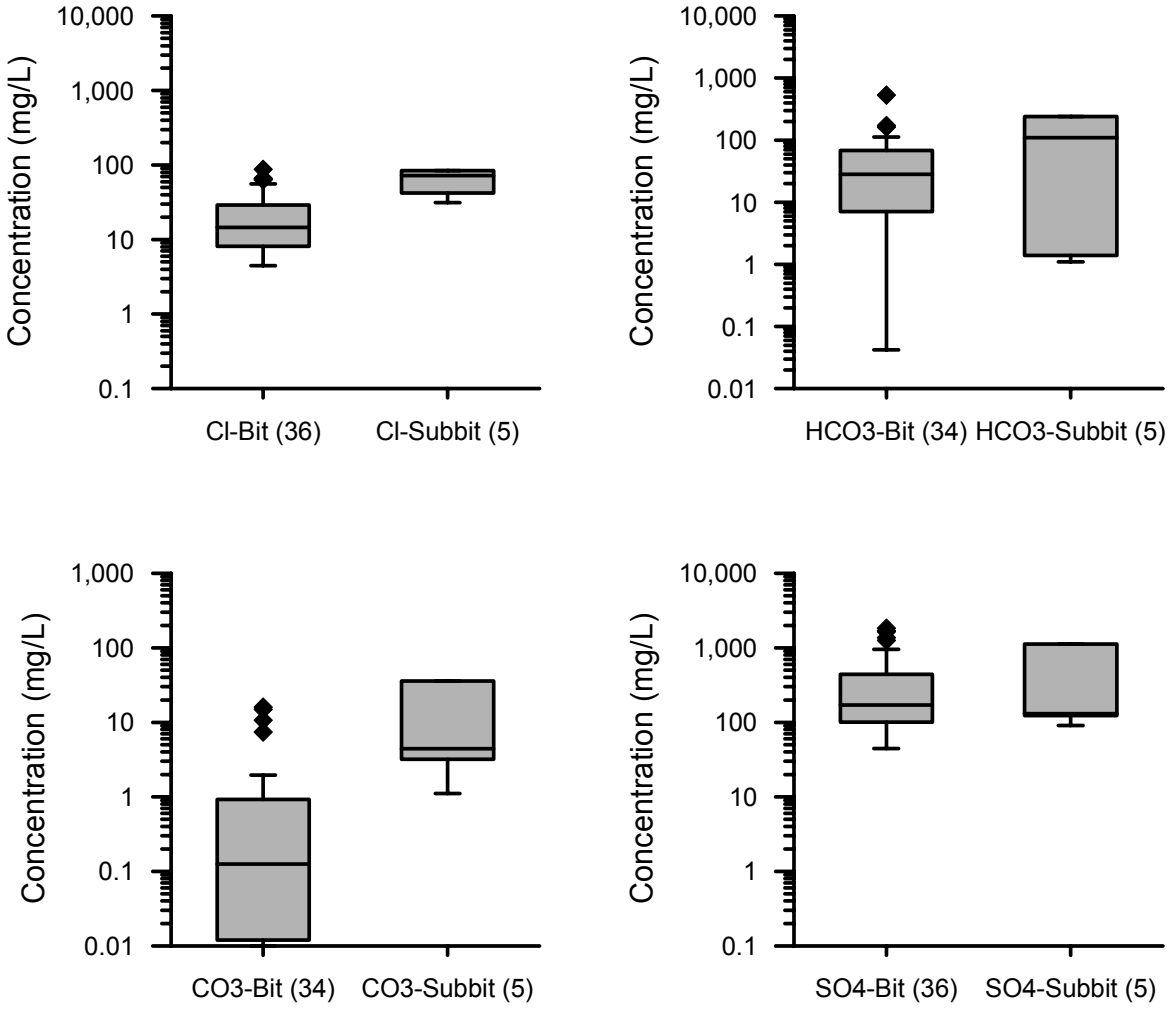

Figure B-4 (Continued)
Comparison of field leachate concentrations: bituminous vs. subbituminous/lignite coal ash, impoundments

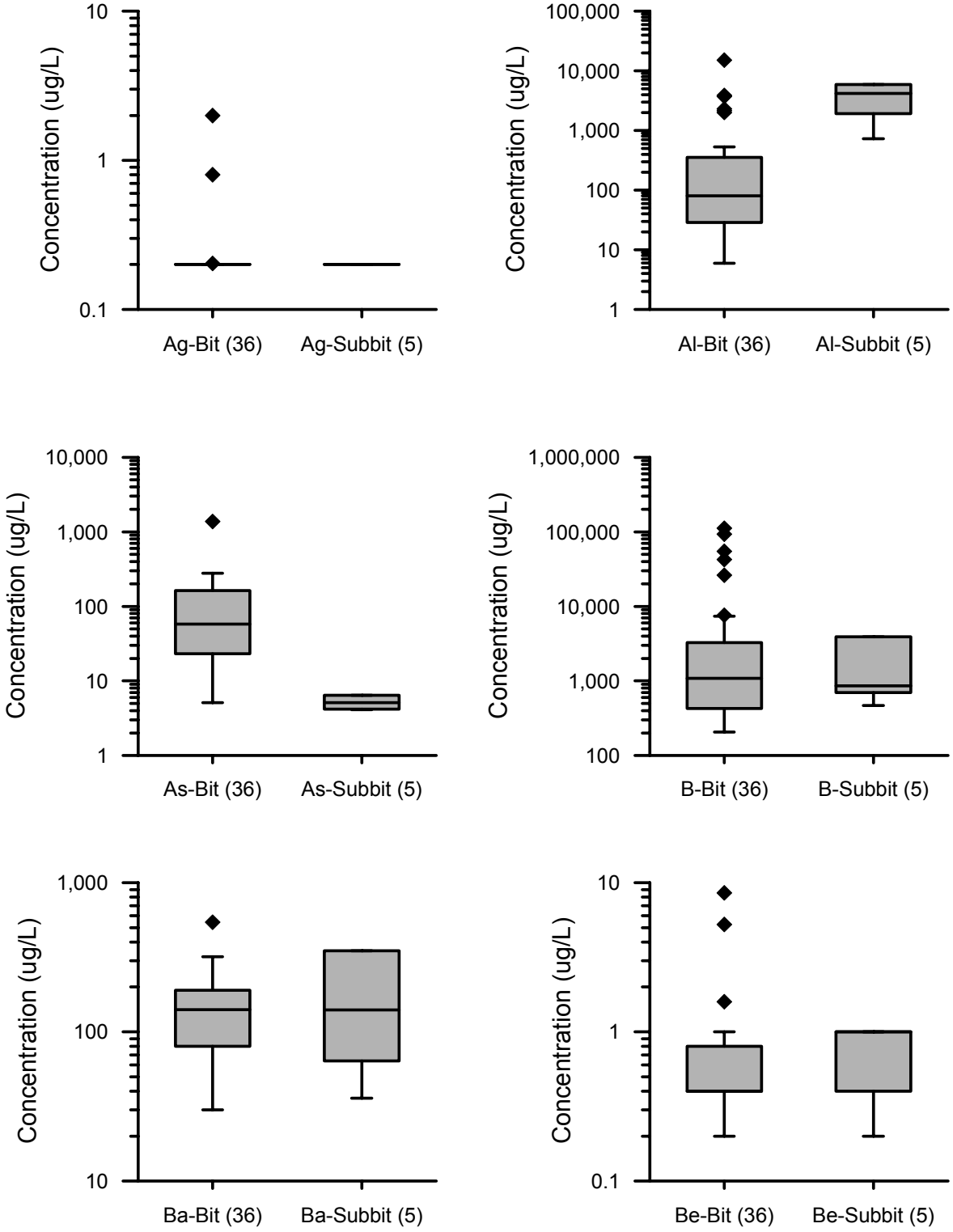

Figure B-4 (Continued)
Comparison of field leachate concentrations: bituminous vs. subbituminous/lignite coal ash, impoundments

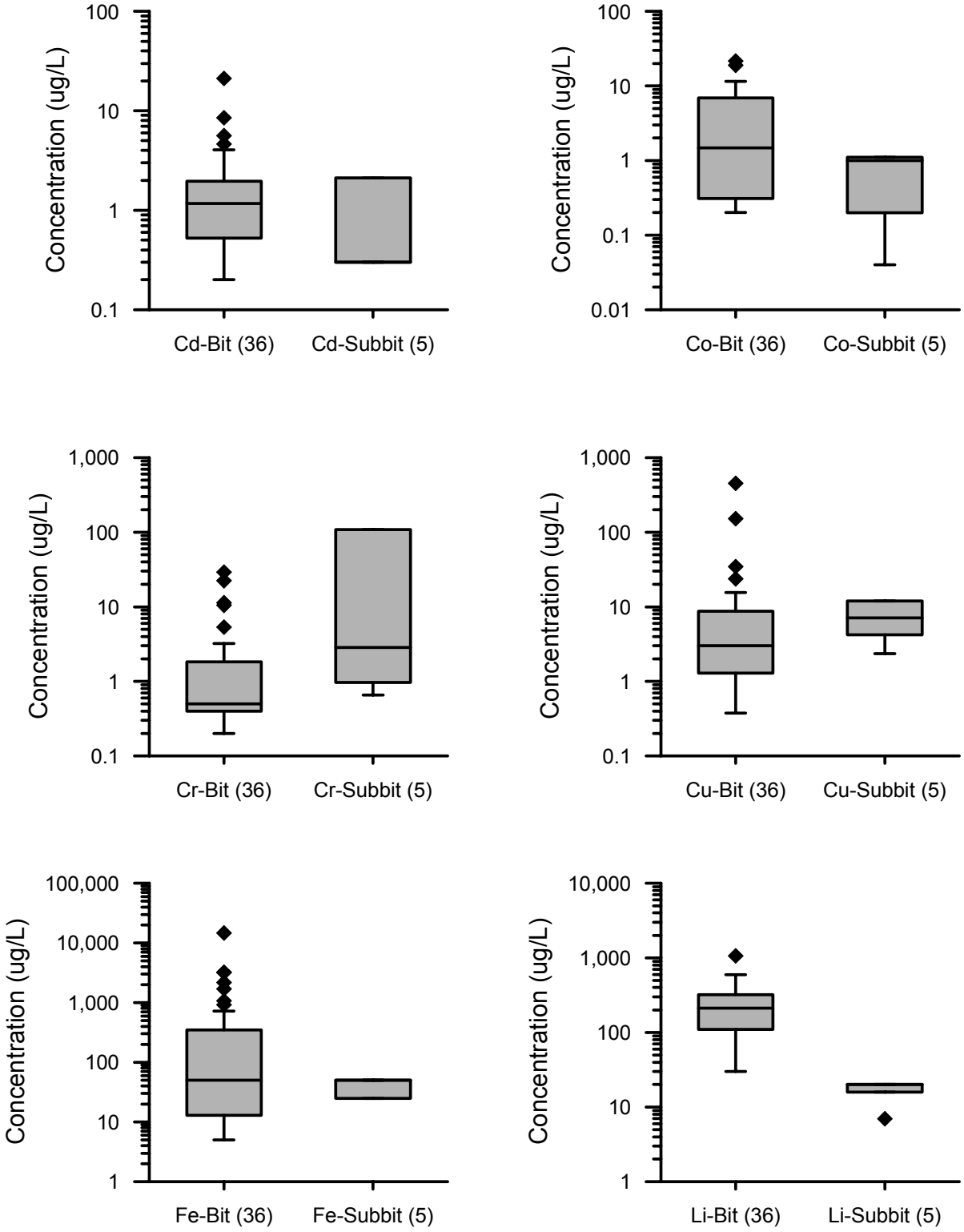

Figure B-4 (Continued)
Comparison of field leachate concentrations: bituminous vs. subbituminous/lignite coal ash, impoundments

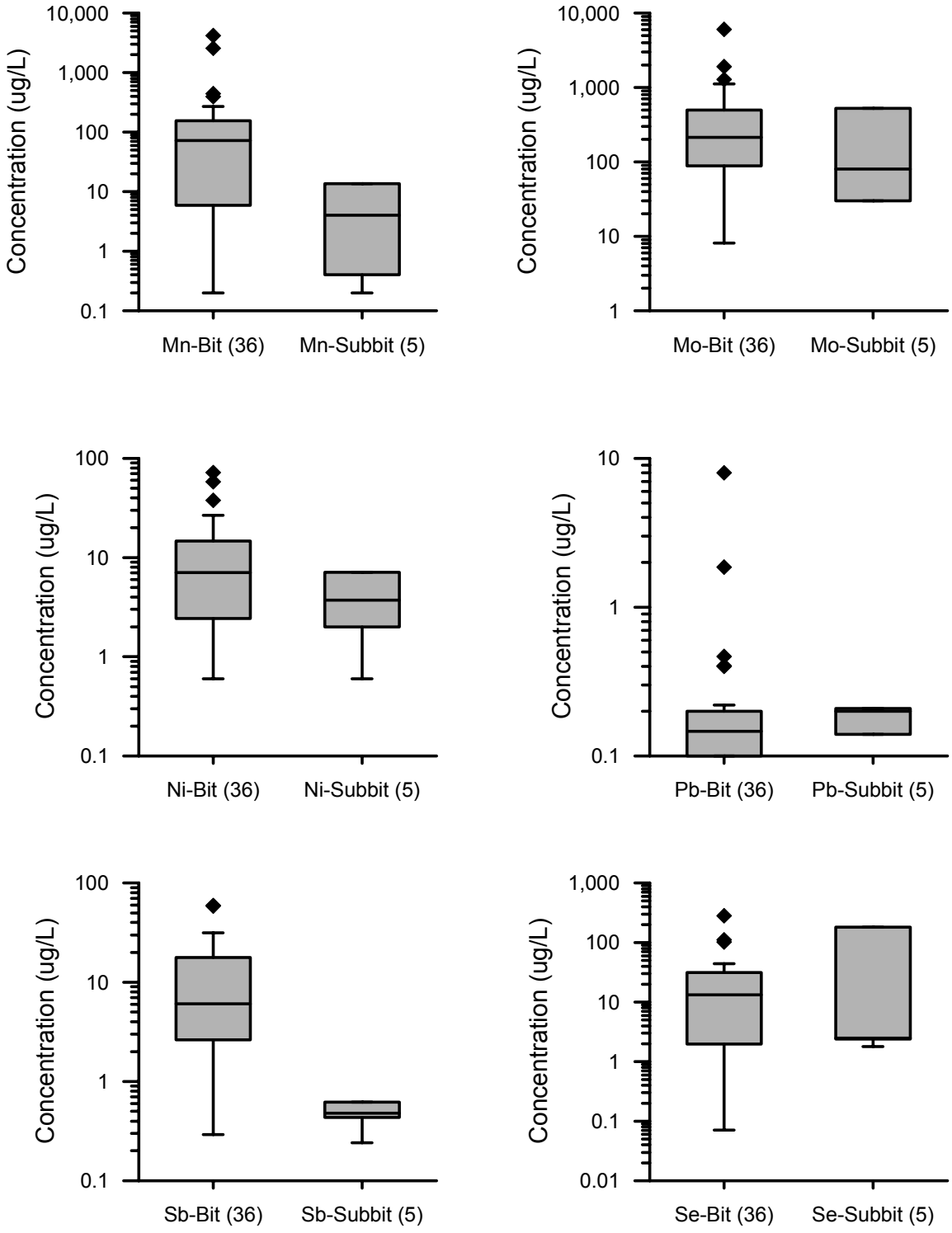

Figure B-4 (Continued)
Comparison of field leachate concentrations: bituminous vs. subbituminous/lignite coal ash, impoundments

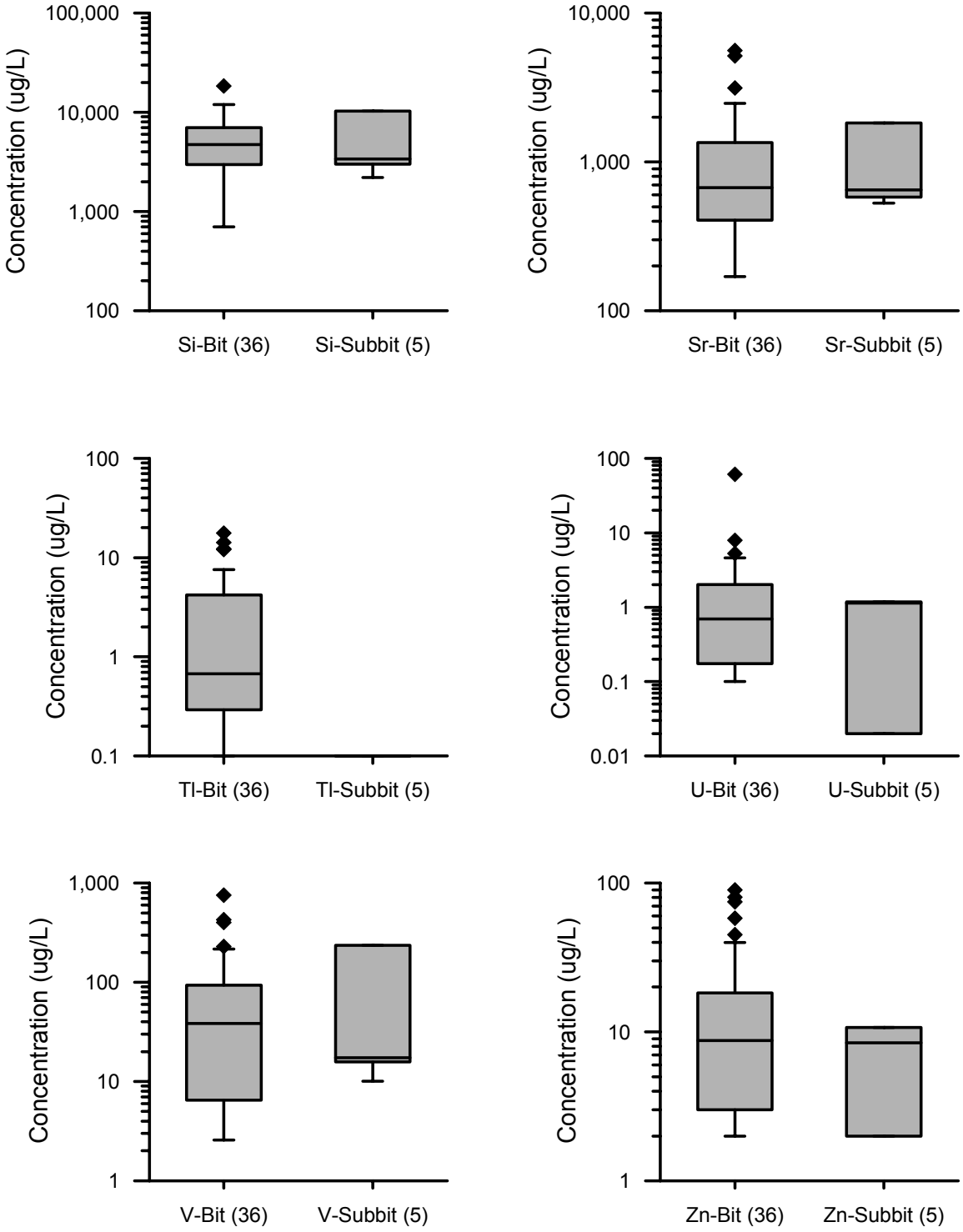

Figure B-4 (Continued)
Comparison of field leachate concentrations: bituminous vs. subbituminous/lignite coal ash, impoundments

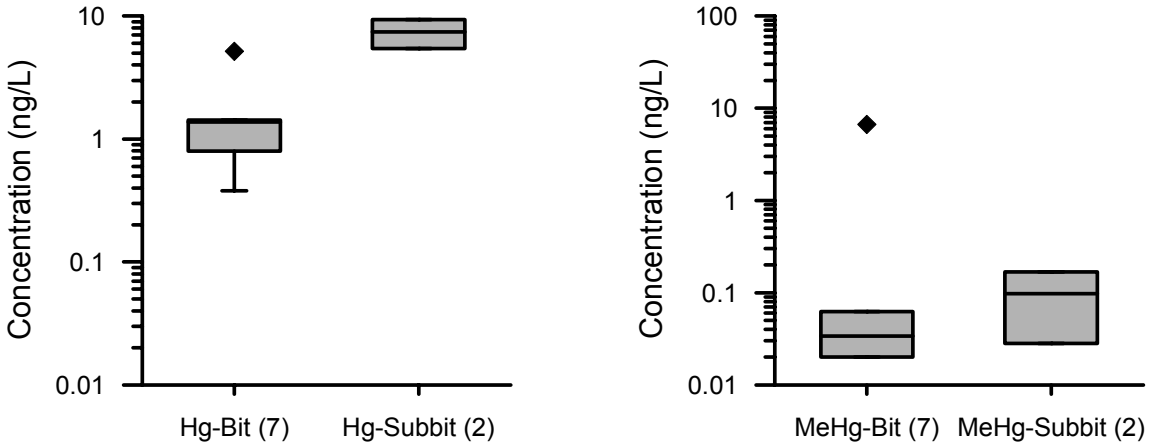

Figure B-4 (Continued)
Comparison of field leachate concentrations: bituminous vs. subbituminous/lignite coal ash, impoundments

C
EVALUATION OF ARSENIC, SELENIUM, AND CHROMIUM SAMPLE PRESERVATION AND ANALYSIS METHODS

Cryofreezing Overview

Cryofreezing was used as the default sample preservation strategy for the speciation samples in this project for two reasons:

- Recent research has shown that both arsenic and selenium form soluble sulfur species in sulfidic waters, which are decomposed and precipitated under acidic conditions, thereby completely altering the original speciation information. This would have affected all samples that contain detectable concentrations of "other" arsenic or selenium species, although in most cases, these "other" species constituted less than 10 percent of the total concentration of the element, and so the associated error would have been relatively small. However, six samples (five arsenic and one selenium) contained "other" species at fractions > 10 percent of the corresponding total arsenic or selenium concentration. Since it wasn't known in advance how strongly sulfidic the sampled waters would be, and field observations confirmed (via smell) that some samples had significant concentrations of free reduced sulfur compounds, cryofreezing was used instead of acidification to prevent decomposition of soluble arsenic- and selenium-sulfur compounds.
- It is well established that Cr(VI) gets reduced by dissolved organic matter in acidified samples during storage. Since nearly all samples containing elevated chromium concentrations had Cr(VI) as their major species, this could have led to significantly altered chromium speciation results. Again, cryofreezing circumvents the issue of pH change during storage. This was confirmed in a test of preservation methods performed in 2004 (after analytical issues had been observed in 2003); while the cryofrozen split yielded almost exclusively Cr(VI), acidified splits yielded lower Cr(VI) concentrations (Table C-2) and increasing Cr(III) concentrations over time. This already led to an altered chromium speciation pattern immediately after sample receipt, but yielded a completely reversed speciation result after several weeks of storage. For this reason, Cr(VI) is typically preserved under strongly alkaline conditions, but for the present project, this would have created other analytical issues related to the precipitation of Cr(III) and major trace elements (e.g. iron and manganese), and was thus avoided.

Unfortunately, during the analysis of samples collected in 2003, it was observed that the cryofreezing approach created another, unanticipated problem, during storage. When the cryofrozen samples were thawed prior to analysis, varying degrees of white-yellowish

precipitates were observed in many samples, which did not re-dissolve at room temperature (over a time frame of weeks). When speciation analyses of these samples were conducted, a significant gap in the mass balance (= total element concentration – sum of its individual species) of arsenic and/or selenium was observed; chromium was not significantly affected by this issue. It was theorized that these precipitates were calcium sulfate or carbonate, and geochemical model calculations confirmed that the solubility of these minerals was exceeded in many samples.

To test if the precipitates contained the "missing" fractions of arsenic (for which the mass balance discrepancies were worse than for selenium), the precipitates were digested in nitric acid, and the resulting solutions analyzed for arsenic released from the precipitates. Table C-1 shows that for some samples, the "missing" fraction of arsenic was apparently indeed bound to the observed precipitates, but there are more samples than that for which this did not confirm the postulated loss mechanism. Additionally, significant mass balance discrepancies were also observed in samples containing no visible precipitates. Therefore, while this storage artifact was certainly responsible for incomplete arsenic or selenium speciation mass balance in some samples, it was definitely not the only process involved, and possibly not even the major one. Dissolution of the precipitates in nitric acid changes arsenic speciation, so it remains unclear if any one species of arsenic was selectively or preferentially removed from solution during the formation of the precipitates.

Formation of these precipitates was only observed in samples collected in 2003, because those samples were stored for a long period (up to 6 months) prior to analysis. By comparison, samples collected in 2004 and 2005 were typically analyzed for their arsenic and selenium speciation within four weeks after collection, and the sum of species in these samples was closer to the total concentration than in the 2003 samples. Consequently, it seems likely that the formation of precipitates resulted from excessively long cryofrozen storage, and can be avoided by keeping storage time to one month or less. Attempts to "recreate" the precipitates were unsuccessful (on a time scale of weeks), so no further attempts were made to resolve the issue and correct the speciation mass balance for samples with precipitates.

Table C-1
Arsenic Speciation Mass Balance, Including Losses To Precipitates Formed During Cryofrozen Storage, For Leachate Samples Collected In 2003

Sample ID	Lab ID	Total As	As(III)	As(V)	other As species	precipitated As	mass balance without precipitated As [%]	mass balance including precipitated As [%]
001	1	20.4	< 0.3	9.5	2.1	7.04	57	91
002	2	48.4	< 6	47	< 6	1.10	98	100
003	3	84	< 6	69	< 6	7.50	82	91
004	4	18.6	8.4	5.2	< 0.3	0.59	73	76
005	5	3.0	< 0.2	1.3	< 0.2	0.08(a)	45	47
006	6	12.2	< 0.3	0.9(a)	< 0.3	<0.05	8	8
007	7	20.1	< 2	< 2	< 2	0.07(a)	0	0
008	8	16.9	0.7(a)	< 0.5	< 0.3	0.07(a)	4	5
009	9	28.9	< 6	< 10	< 6	0.09(a)	0	0
010	10	22.3	1.5(a)	10	< 0.6	0.46	52	54
011	11	4.8	< 0.2	0.6	< 0.2	0.26	12	17
012	12	238	97.0	66	< 0.6	38.1	69	85
013	13	21.6	3.7	< 0.5	< 0.3	11.8	17	72
013D	13A	22	1.9	< 0.5	< 0.3	NA	9	9
014	14	163	1.9	86	0.9(a)	25.1	54	70
015	15	23.8	< 0.6	24	< 0.6	1.72	99	106
016	16	68.6	< 0.6	25	< 0.6	23.4	36	70
SX-1	core 3	72.0	0.9	46.9	< 0.1	1.16	66	68
017	17	4.11	0.88	<0.08	0.1	0.26	23	30
018	18	23.1	0.42	5.22	< 0.06	17.8	24	101
019	19	5.11	0.57	<0.08	< 0.06	0.36	11	18
020	20	4.19	1.00	0.53	0.1	0.14(a)	40	43
HN-1	core 1	59.8	< 0.1	33.6	0.2	5.65	57	66
HN-2	core 2	20.6	< 0.1	6.9	0.1	1.64	34	42
021	21	194	2.1	208	< 0.3	2.38	108	110
022	22	11.1	12.5	0.49	< 0.06	0.11(a)	118	119
023	23	218	0.8(a)	189	< 0.3	12.4	87	93
024	24	11.2	0.4(a)	<0.2	< 0.2	1.47	3	16
025	25	6.47	1.35	<0.08	< 0.06	1.04	21	37
026	26	10.8	11.2	0.4(a)	< 0.2	0.11(a)	107	108
027	27	39.1	13.2	4.8	1.3	2.31	49	55
028	28	30.0	2.4	1.7	0.2	0.17(a)	14	15
029	29	48.9	1.7	8.9	0.3	4.01	22	31
030	30	42.5	3.5	29.5	0.4	0.58	79	80
031	31	221	201	23.6	0.7	3.65	102	103
032	32	25.4	17.5	16.9	0.1	0.43	136	137

(a) = sample concentration less than 5 times blank
Concentrations in µg/L

Due to the large heterogeneity of the collected sample set, additional issues related to speciation preservation were observed in individual samples. Some samples showed obvious loss of total arsenic, selenium, and/or chromium upon acidification, which was verified by analyzing total arsenic, total selenium, and total chromium in the cryofrozen speciation samples (and finding significantly higher concentrations). For those samples, the formation of a brownish flocculate was usually observed in the acidified splits, which is probably due to precipitation of humic acids (which are soluble under the original alkaline conditions present in most samples, but insoluble at acidic pH). Evidently, the precipitates removed a fraction of total arsenic, selenium, or chromium from solution, which would have led to a speciation mass balance > 100 percent (barring other analytical issues). In such cases, the corresponding total element concentration measured in the cryofrozen split was used instead of the one in the acidified sample. By contrast, there were also a number of samples in which the formation of brownish precipitates was observed in the non-acidified splits taken for major anion and cation analysis. This reflects the precipitation of iron (oxy)hydroxide minerals caused by oxidation of high Fe(II) concentrations present in reducing waters. This problem was avoided by acidification, unless the process was so rapid that it began as the sample was being pumped and filtered.

In conclusion, the preservation for arsenic and selenium speciation by acidification does not appear suitable for the whole collected sample set, and must certainly be avoided for chromium speciation. Cryofreezing appears to be suitable in principle, but the sample storage time must be minimized to avoid irreversible formation of precipitates. Finally, it appears that the collected sample set is too heterogeneous for any one procedure that will preserve arsenic, selenium, and chromium speciation in all samples reliably; therefore, it might be necessary to collect multiple splits in parallel that are preserved differently.

Evaluation of Preservation Arsenic, Chromium, and Selenium Speciation by Preservation Method

The field team returned to the location of sample 002 and collected replicate samples for analysis of preservatives and differences associated with analytical laboratories. Five preservation techniques were used: no preservation, hydrochloric acid (HCl) in opaque bottles, hydrochloric acid in foil-wrapped (dark) bottles, ethylenediaminetetraacetic acid (EDTA), and nitric acid (HNO_3). Sample 002 is geochemically characterized by alkaline pH (>10), ORP of > 200, low dissolved oxygen (0.2%), low iron (<50 µg/L), and high sulfate (> 6,000 mg/L) concentration.

Results varied by analyte, preservation method, and laboratory (Table C-2). Chromium was most strongly effected. Concentrations of Cr(VI) in the acid-preserved samples were less than one-half of the concentration determined in the cryofrozen and unpreserved samples. This analysis clearly suggests that acid-preservation is not an appropriate technique for Cr(IV) in this geochemical environment.

Selenium concentrations were least affected by preservation technique. The poorest result was for the cryofrozen sample (sample 002), in which the sum of species was 76 percent of the total selenium concentration. This sample was collected in 2003 and subject to the issues described

above associated with long hold times. The only apparent laboratory related relationship was for Se(IV); which was below detection limits in all samples other than the cryofrozen sample analyzed by laboratory 1, and detected at concentrations ranging from 76 to 94 µg/L by laboratory 2.

Table C-2
Arsenic, Selenium, and Chromium Speciation Using Different Preservatives

	As (III)	As (V)	As (other)	Σ As species	Total Arsenic	% Recovery
Field blank	<5	0.02	NA	NA	0.24	NA
Unpreserved, Lab 1	<5	27.1	6.4	33.5	58.1	58
Unpreserved, Lab 2	4.1	63	NA	67	73	92
Cryofrozen, Lab 1	<6	47	<6	47	48.4	97
0.5% HCl preserved, Lab 1	<5	30.8	9.7	40.5	54.7	74
0.5% HCl preserved, Lab 2	4.9	95	NA	100	82	122
0.5% HCl+ dark preserved, Lab 1	<5	32.2	4.6	36.8	54.9	67
0.5% HCl+ dark preserved, Lab 2	NA	NA	NA	NA	NA	NA
EDTA preserved, Lab 2	4.0	72	NA	76	71	107
0.5% HNO_3 preserved, Lab 1	<5	5.1	2.4	7.5	51.7	15
0.5% HNO_3 preserved, Lab 2	3.7	65	NA	69	82	84
	Cr (III)	**Cr(VI)**	**Cr (other)**	**Σ Cr species**	**Total Chromium**	**% Recovery**
Field blank	NA	<0.1	NA	NA	0.11	NA
Unpreserved, Lab 1	NA	4138	NA	NA	5204	NA
Unpreserved, Lab 2	NA	NA	NA	NA	NA	NA
Cryofrozen, Lab 1	340	5090	NA	5430	5100	106
0.5% HCl preserved, Lab 1	NA	2161	NA	NA	5217	NA
0.5% HCl preserved, Lab 2	NA	NA	NA	NA	NA	NA
0.5% HCl+ dark preserved, Lab 1	NA	1314	NA	NA	5242	NA
0.5% HCl+ dark preserved, Lab 2	NA	NA	NA	NA	NA	NA
EDTA preserved, Lab 2	NA	NA	NA	NA	NA	NA
0.5% HNO_3 preserved, Lab 1	NA	1760	NA	NA	5161	NA
0.5% HNO_3 preserved, Lab 2	NA	NA	NA	NA	NA	NA
	Se(IV)	**Se(VI)**	**Se (Other)**	**Σ Se species**	**Total Selenium**	**% Recovery**
Field blank	<0.05	<0.05	NA	<0.05	0.14	--
Unpreserved, Lab 1	<25	1432	16	1448	1312	110
Unpreserved, Lab 2	94	1270	NA	1364	1400	97
Cryofrozen, Lab 1	19	1300	NA	1319	1730	76
0.5% HCl preserved, Lab 1	<25	1348	27	1375	1426	96
0.5% HCl preserved, Lab 2	91	1423	NA	1514	1500	101
0.5% HCl+ dark preserved, Lab 1	<25	1349	14	1363	1424	96
0.5% HCl+ dark preserved, Lab 2	NA	NA	NA	NA	NA	NA
EDTA preserved, Lab 2	87	1478	NA	1565	1400	112
0.5% HNO_3 preserved, Lab 1	<25	1307	NA	1307	1392	94
0.5% HNO_3 preserved, Lab 2	76	1416	NA	1492	1400	107

Samples collected 4/6/04 except Cryofrozen sample collected 8/5/03
Lab 2 did not analyze chromium
NA=not analyzed

Arsenic concentrations were most variable. First, there was a significant difference by laboratory. Laboratory 1 returned total arsenic concentrations between 52 and 58 mg/L (excluding the cryofrozen sample, which was collected on a different date), while laboratory 2 returned total arsenic concentrations between 71 and 82 mg/L. Laboratory 2 also achieved greater species recovery (84 to 122%) than laboratory 1 (15 to 97 percent). For laboratory 2, all preservation methods proved acceptable for preservation of arsenic species. For laboratory 1, only the cryofrozen sample yielded better than 80 percent species recovery. Significantly, all preservation methods identified As(V) as the species with highest concentration.

This test was performed on samples from a geochemical environment where the oxidized species would be expected in leachate samples, and results cannot be extrapolated to other environments, particularly those where the reduced species may be expected. However, the results show that several different preservation methods are capable of identifying the predominant species of arsenic and selenium in water samples from a high pH, high ORP, low oxygen, low iron, high sulfate environment. However, only cryofreezing adequately preserved chromium species.

Comparison of Cryofrozen and Hydrochloric Acid-Preserved Replicate Samples

Splits of 32 field leachate samples[6] were preserved in the field with HCl and forwarded to a separate laboratory (laboratory 2) for analysis of arsenic and selenium species. Analyses were performed as described in Section 2.

Arsenic

For arsenic, the cryofrozen sample sets[7] typically had lower total concentration than the acid-preserved samples (Figure C-1); however, since the total concentration analyses by both labs were performed on acid-preserved samples, this difference is laboratory related, rather than preservative-related. The percentage difference in total concentration was greatest when values were lower than 10 µg/L; the average difference for samples with concentration greater than 10 µg/L was 27 percent. The difference may be due to a correction applied by laboratory 2 to account for chloride interference.

The sum of arsenic species was compared to the independently measured total arsenic to determine the species recovery. For both sets of samples, the species recovery was typically closer to 100 percent when the total concentration was greater than 10 µg/L. In most cases, the cryofrozen sample had a higher species recovery, and was closer to 100 percent species recovery, than the acid-preserved sample (Figure C-1).

[6] The split sample comparison included one sample (085) that was taken at one of the field sites for another study, and is not otherwise included in this evaluation. The acid-preserved splits of samples 084 and 085 were not analyzed for selenium species.

[7] The cryofrozen sample sets included acid-preserved samples for total analysis and frozen samples for species analysis.

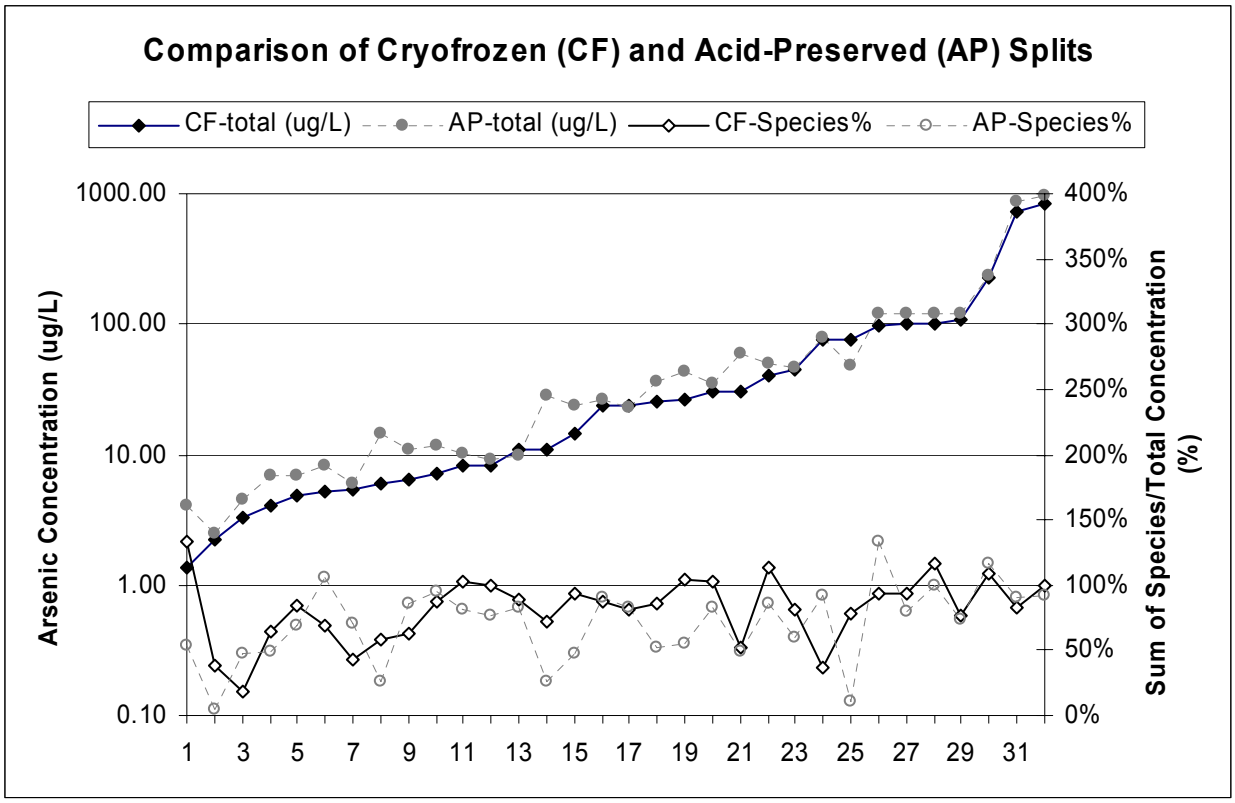

Figure C-1
Comparison of total arsenic concentration and of percent species recovery for cryofrozen and acid-preserved sample splits

The dominant species in each sample split was determined based on the following criteria:

- For species recovery greater than 80 percent, a species was identified as dominant if its concentration was 60 percent or more of the sum of species.
- If species recovery was greater than 80 percent, and no species concentration was greater than 60 percent of the sum of species, then the sample was listed as "neutral".
- For species recovery less than 80 percent, a species was identified as dominant if its concentration was greater than 50 percent of the total concentration.[8]
- Samples with less than 80 percent species recovery in which no species concentration was greater than 50 percent of the total concentration were not tabulated.

Based on this approach, 27 of the 32 cryofrozen samples, and 22 of the 32 acid-preserved samples can be classified as dominated by As(III), dominated by As(V), or neutral (Table C-3). In 17 of the 20 common splits (where the dominant species could be determined in both samples), the two preservation techniques yielded similar results. In the three splits with

[8] If the sum of species is 80 percent, and the species concentration is 50 percent of the total concentration, then that species accounts for at least 62.5 percent of the sum of species.

different results, As(V) was dominant in the cryofrozen sample and As(III) in the acid-preserved sample. Two of these three samples had total arsenic concentration lower than 5 μg/L; the other was sample 106, which had an arsenic concentration of 110 μg/L.

Table C-3
Dominant Arsenic Species in Split Samples

Cryofrozen								Acid-Preserved					
Split	% As(III)	% As(V)	% other	% recov.	DS	Total As		Split	% As(III)	% As(V)	% recov.	DS	Total As
T112	50%	70%	14%	133%	V	1.36		W112	54%	0%	54%	(III)	4.04
T101	0%	10%	28%	38%		2.23		W101	0%	0%	4%		2.50
T92	0%	15%	3%	18%		3.34		W92	0%	47%	47%		4.52
T108	9%	56%	0%	65%	(V)	4.09		W108	0%	48%	48%		6.91
T99	2%	78%	4%	84%	V	4.80		W99	69%	0%	69%	(III)	6.79
T126	0%	69%	0%	69%	(V)	5.20		W126	0%	106%	106%	V	8.32
T49	0%	43%	0%	43%		5.40		W49	20%	51%	71%	(V)	5.94
T111	0%	58%	0%	58%	(V)	5.94		W111	0%	27%	27%		14.32
T127	0%	63%	0%	63%	(V)	6.42		W127	0%	86%	86%	V	10.77
T102	0%	88%	0%	88%	V	7.24		W102	0%	94%	94%	V	11.74
T116	12%	90%	1%	103%	V	8.24		W116	10%	71%	81%	V	10.26
T115	37%	63%	0%	100%	V	8.32		W115	0%	77%	77%	(V)	9.08
T91	0%	88%	1%	89%	V	10.76		W91	0%	83%	83%	V	9.98
T121	12%	54%	5%	72%	(V)	11.00		W121	0%	26%	26%		28.36
T128	71%	20%	3%	94%	III	14.27		W128	44%	4%	48%		24.00
T114	0%	87%	0%	87%	V	23.53		W114	9%	81%	90%	V	26.50
T42	0%	81%	0%	81%	V	23.70		W42	8%	75%	83%	V	23.26
T122	30%	32%	24%	86%	neutral	25.54		W122	44%	8%	52%		36.28
T120	27%	43%	35%	104%	neutral	26.79		W120	44%	12%	56%		43.46
T119	0%	101%	1%	102%	V	30.20		W119	3%	79%	82%	V	34.74
T107	3%	49%	0%	52%		30.64		W107	2%	47%	48%		60.00
T118	2%	112%	0%	114%	V	40.78		W118	18%	67%	85%	V	48.94
T97	0%	81%	0%	81%	V	44.89		W97	0%	60%	60%	(V)	46.96
T43	0%	37%	0%	37%		75.20		W43	59%	32%	92%	neutral	77.76
T98	1%	77%	0%	79%	(V)	76.85		W98	10%	0%	10%		47.96
T57	0%	94%	0%	94%	V	98.60		W57	0%	133%	133%	V	120.00
T69	0%	94%	0%	94%	V	99.50		W69	0%	80%	80%	(V)	120.00
T113	1%	115%	0%	116%	V	101.98		W113	23%	76%	99%	V	120.00
T106	14%	57%	5%	77%	(V)	109.83		W106	71%	2%	73%	(III)	122.32
T105	85%	22%	2%	109%	III	229.95		W105	112%	5%	116%	III	233.00
T84	10%	74%	0%	83%	V	726.90		W84	8%	83%	90%	V	870.00
T85	59%	38%	3%	99%	neutral	829.10		W85	52%	41%	93%	neutral	950.00

DS indicates the dominant species in the sample, ( ) indicates that total species recovery was less than 80%, but one species was greater than 50%
Shading indicates samples where the dominant species could be determined in both splits.

Sample 106 was recirculated FGD system water, presenting a highly alkaline (pH near 12) and more concentrated matrix that may have confounded the analyses. Other complicating factors with sample 106 included high dissolved oxygen (95%) yet low ORP (18 mV), and low dissolved iron (4.6 μg/L).

Selenium

For selenium, the cryofrozen sample sets[9] typically had lower total concentration than the acid-preserved samples (Figure C-2). This difference, which, like arsenic, is laboratory related, was greatest when total concentration was lower than 10 µg/L; the average difference for samples with concentration greater than 10 µg/L was 25 percent.

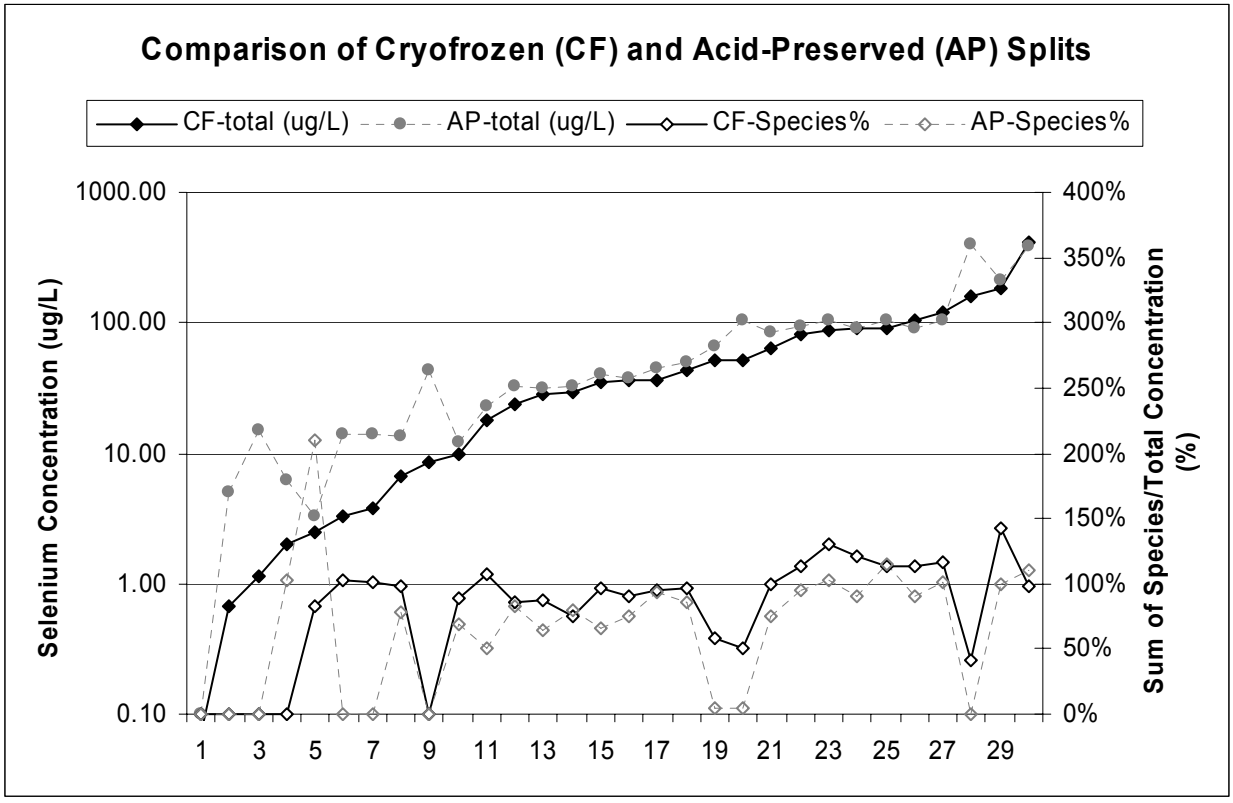

Figure C-2
Comparison of total selenium concentration and of percent species recovery for cryofrozen and acid-preserved sample splits

The sum of species for both sets of samples was closer to 100 percent when the total concentration was greater than 10 µg/L. The cryofrozen split typically had higher species recovery than the acid-preserved split; although in some cases, particularly at concentrations near and greater than 100 µg/L, the cryofrozen split recovery was greater than 100 percent and the acid-preserved split recovery was closer to 100 percent. For concentrations greater than 10 µg/L, species recovery correlated well between the two preservation methods (Figure C-2).

[9] The cryofrozen sample sets included acid-preserved samples for total analysis and frozen samples for species analysis.

The dominant selenium species was determined using the same approach as for arsenic. Based on this approach, 23 of the 30 cryofrozen sample splits, and 20 of the 30 acid-preserved sample splits can be classified as dominated by Se(IV), dominated by Se(VI), or neutral (Table C-4).

Table C-4
Dominant Selenium Species in Split Samples

Cryofrozen								Acid-Preserved					
Split	% Se(IV)	% Se(VI)	% other	% recov.	DS	Total As		Split	% Se(IV)	% Se(VI)	% recov.	DS	Total As
T114	0%	0%	0%	0%		0.07		W114	0%	0%	0%		0.10
T112	0%	0%	0%	0%		0.67		W112	0%	0%	0%		5.00
T122	0%	0%	0%	0%		1.13		W122	0%	0%	0%		15.00
T99	0%	0%	0%	0%		2.04		W99	103%	0%	103%	IV	6.12
T57	83%	0%	0%	83%	IV	2.44		W57	210%	0%	210%	IV	3.23
T120	56%	46%	0%	102%	neutral	3.30		W120	0%	0%	0%		14.00
T121	29%	73%	0%	102%	VI	3.86		W121	0%	0%	0%		14.00
T108	39%	59%	0%	98%	neutral	6.56		W108	38%	39%	77%		13.32
T105	0%	0%	0%	0%		8.47		W105	0%	0%	0%		43.00
T49	83%	6%	0%	89%	IV	10.00		W49	70%	0%	70%	(IV)	12.01
T118	100%	7%	0%	107%	IV	17.62		W118	51%	0%	51%	(IV)	23.00
T43	86%	0%	0%	86%	IV	23.50		W43	83%	0%	83%	IV	32.54
T119	81%	6%	0%	87%	IV	27.95		W119	65%	0%	65%	(IV)	32.00
T113	66%	9%	0%	75%	(IV)	29.27		W113	79%	0%	79%	(IV)	33.00
T116	87%	9%	0%	96%	IV	35.35		W116	66%	0%	66%	(IV)	40.00
T115	82%	8%	0%	90%	IV	36.10		W115	75%	0%	75%	(IV)	37.00
T69	91%	5%	0%	96%	IV	36.40		W69	87%	7%	93%	IV	44.54
T42	92%	5%	0%	96%	IV	42.60		W42	80%	6%	86%	IV	49.94
T98	58%	0%	0%	58%	(IV)	50.74		W98	5%	0%	5%		65.98
T128	34%	13%	3%	51%		50.90		W128	0%	5%	5%		106.36
T106	0%	99%	0%	99%	VI	64.79		W106	3%	73%	76%	(VI)	85.44
T102	7%	106%	0%	113%	VI	80.48		W102	5%	89%	94%	VI	95.40
T126	14%	117%	0%	131%	VI	88.70		W126	14%	88%	102%	VI	104.34
T111	43%	79%	0%	122%	VI	90.54		W111	38%	53%	91%	neutral	91.00
T101	0%	114%	0%	114%	VI	91.00		W101	0%	115%	115%	VI	104.48
T92	1%	113%	0%	113%	VI	103.36		W92	0%	90%	90%	VI	90.86
T91	3%	113%	0%	116%	VI	122.22		W91	0%	102%	102%	VI	102.84
T107	0%	10%	32%	42%		159.00		W107	0%	0%	0%		400.00
T127	7%	136%	0%	143%	VI	180.60		W127	5%	95%	100%	VI	210.00
T97	9%	89%	0%	98%	VI	412.50		W97	16%	95%	111%	VI	380.00

DS indicates the dominant species in the sample, ( ) indicates that total species recovery was less than 80%, but one species was greater than 50%
Shading indicates samples where the dominant species could be determined in both splits.

In 18 of the 19 common splits (where the dominant species could be determined in both samples), the two preservation techniques yielded similar results. The only exception was sample 111, which was dominated by Se(VI) in the cryofrozen split and was neutral in the acid split. However, both samples had more Se(VI) than Se(IV). The species breakdown for sample 111 was 43 percent Se(IV) and 79 percent Se(VI) in the cryofrozen sample, and 38 percent Se(IV) and 53 percent Se(VI) in the acid-preserved sample. Sample 111 had neutral pH (7.2),

was oxic (280 mV ORP and 59 percent dissolved oxygen), and did not exhibit a sulfur odor; as a result, the acid-preserved sample would not be expected to undergo precipitation of soluble sulfur species.

Summary

In summary, there are conditions under which one of the preservation methods may be more appropriate than the other. However, the split sample data collected during this study indicate that the preservation method does not affect results sufficiently to alter interpretation of the dominant species present in the sample..

D
LABORATORY ANALYTICAL ISSUES PERTAINING TO SPECIATION ANALYSIS

Determination of Total Arsenic, Selenium, and Chromium Concentrations

The determination of total chromium (TCr) by ICP-MS worked very well. Good agreement was obtained between the two isotopes ^{52}Cr and ^{53}Cr, as well as between the two instruments used (ICP-DRC-MS and ICP-DF-MS). Therefore, there is a high degree of confidence in the reported total chromium results, and they are not a reason if the speciation mass balance for chromium did not work out in any sample, which usually only happened in samples with low total chromium concentrations. Unfortunately, the determination of total arsenic and selenium by ICP-MS is more complicated than that of total chromium, and consequently, the quality of these data is somewhat impaired in certain samples, as discussed below. The problems associated with the determination of total arsenic and selenium by ICP-MS stem mostly from molecular interferences that overlap with the mass of the measured arsenic or selenium isotopes, and thus yield artificially-increased results. These interferences are caused either by constituents of the measured water samples or by molecules formed in the argon plasma used in ICP-MS analyses. To illustrate this problem, the method used for total selenium determination in the collected water samples is explained below.

In ICP-MS analyses, it is desirable to use the major isotope of the trace element of interest for its quantification, because it yields the highest signal, which usually translates into the lowest detection limit. Additionally, at least one other isotope of the same element should be measured, and if the concentrations determined in the sample by using two (or more) different isotopes agree well, then there is a high degree of confidence that this result is correct and not impaired by any significant molecular interferences. For selenium, the main isotope is ^{80}Se, but this isotope is impossible to measure by conventional ICP-MS instruments, because the argon plasma generates a large amount of the dimeric ion $^{40}Ar_2^+$, which has the same nominal mass as the ^{80}Se isotope, and the two signals cannot be separated. Although some publications suggest that ICP-DF-MS can resolve the overlap between analyte and interference for this example when it's used in the high resolution mode, the particular ICP-DF-MS instrument used by laboratory 1 did not achieve this separation consistently, and an ICP-DRC-MS instrument was used to address this issue, which was successful. The ICP-DRC-MS approach uses a cell with a reactive gas (here methane, CH_4) to break up the interference (by collision yielding two Ar atoms of mass 40) between the plasma and the mass spectrometer, while the analyte ^{80}Se remains unaffected, and can thus be determined free of the inference. However, in the collected water samples, there are additional interferences that complicate this approach. High bromide concentrations in the samples lead to the formation of the molecule $^{1}H^{79}Br^+$, which also has the nominal mass 80, but cannot be eliminated effectively by the reaction gas methane. Therefore, a second reaction gas

(ammonia, NH_3) was added, which undergoes a chemical reaction with HBr, and thus forms reaction products that have masses other than 80, so ^{80}Se can be measured in waters containing bromide.

The minor isotopes used for confirmation of results obtained using the main isotope usually have different interferences than the main isotope, so if the results obtained for different isotopes agree, it is generally accepted that all known interferences have been removed efficiently, as intended during the method development. In the case of selenium, the control isotopes used were ^{78}Se and ^{82}Se, and it turns out that ^{78}Se has an interference from the plasma ($^{40}Ar^{38}Ar^{+}$), but not from bromide, while ^{82}Se has an interference from bromide ($^{1}H^{81}Br^{+}$), but not form the plasma, so the control strategy for these two interferences works very well. Unfortunately, due to the fact that the studied waters were often very complex and generally very different from site to site, there were additional interferences in some samples that could not be resolved by the described approach. While some additional interferences were identified, and their influence on the measured total selenium results was compensated for as much as possible (for example, it was found that copper formed ammonia clusters $Cu(NH_3)^{+}$ in the DRC, which interfered with the measurement of ^{80}Se and ^{82}Se), there remained some samples that either contained interferences that were not identifiable, or where known interferences exceeded the compensation capacity of the developed analytical method. In those cases, the total selenium concentrations determined using the three different selenium isotopes disagreed beyond the normal range of analytical error, and such results were flagged[10] in the results table (Appendix A). For such samples, the lowest total selenium concentration obtained with any selenium isotope was usually reported, because the molecular interferences are by nature positive (i.e. they mimic selenium), so the lowest result should be the least (or not) interfered.

Figure D-1 shows the agreement between the results obtained for the three measured selenium isotopes as a function of the total selenium concentration: With the exception of three samples, the total selenium concentrations determined using each of the three individual isotopes agree within the analytical uncertainty (± 10 percent) for samples containing total selenium greater than 5 µg/L. Generally, the agreement between the three selenium isotopes is good when total selenium concentrations are higher, and gets worse towards lower concentrations, because a certain amount of an interference caused by the sample matrix would have a bigger impact if the actual selenium signal is small, and because the analytical uncertainty itself increases with decreasing concentration. For those three samples with higher total selenium concentrations where the isotope agreement is not good, the reason probably lies in a combination of complex matrix (high salinity and trace element concentrations) and comparably low total selenium concentration (i.e. too low to resolve the interferences by dilution), although the actual reasons for these discrepancies likely vary from sample to sample, and were not explored further in this project. To eliminate this problem in future similar studies, it would be necessary to either add hydride generation (HG) as a sample introduction technique, which selectively volatilizes the selenium into the plasma while most of the other sample constituents stay behind in the liquid phase and are not introduced into the plasma (so they cannot produce interferences), or switch to a different detection technique altogether (e.g. atomic fluorescence spectrometry, AFS). There are also other potential analytical issues associated with HG and AFS, and there is no guarantee that these approaches would have resolved all problems for the present sample set.

[10] Identified in Table A-2 using flag (b), "isotope ratios do not match"

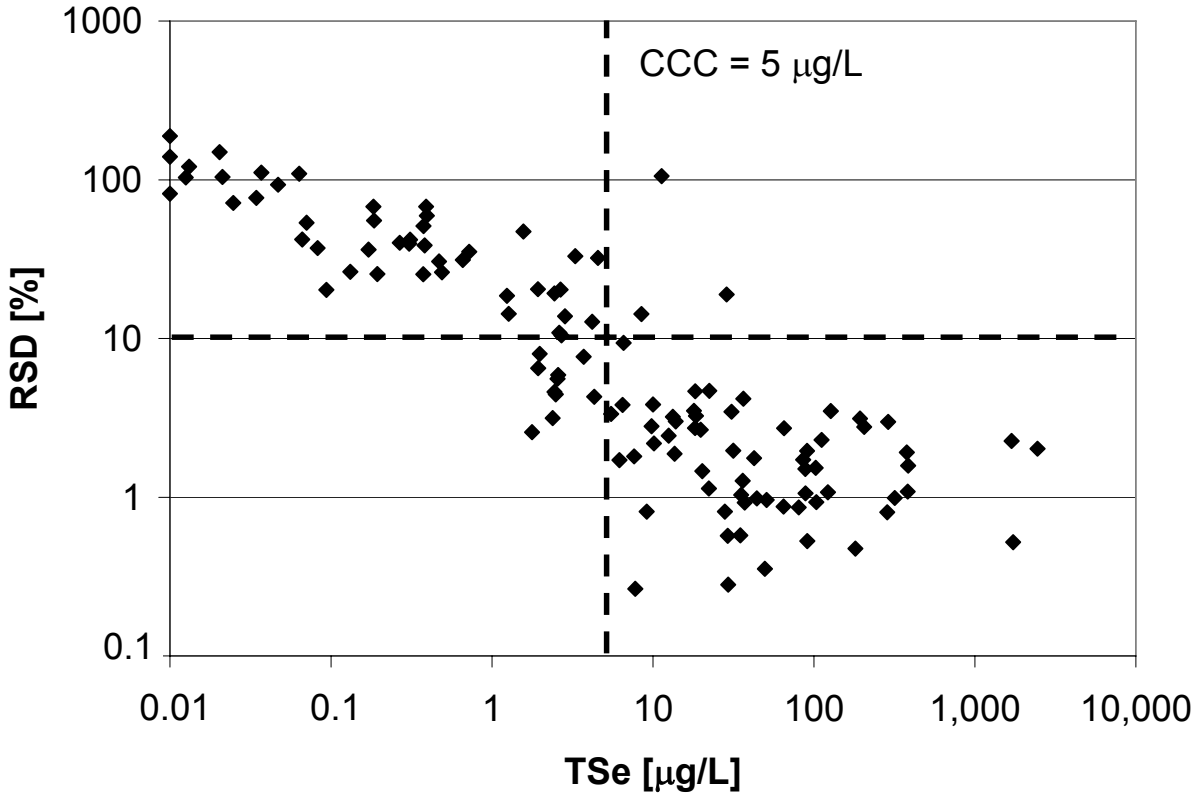

Figure D-1
Agreement between total selenium concentrations determined using the isotopes ^{78}Se, ^{80}Se and ^{82}Se in all collected water samples (expressed as percent relative standard deviation between the three individual results)

Besides interferences that affect individual selenium isotopes during the ICP-MS measurement, there are also matrix effects that affect all selenium isotopes at once, which relate to processes such as the sample introduction into the ICP-MS and the ionization of selenium in the plasma. The sample flow rate in ICP-MS measurements of bulk samples is regulated by the (constant) rotation speed and tubing diameter of a peristaltic pump, but the uptake of the sample into the plasma depends on its nebulization in the spray chamber; this process is assumed to be constant, and the fraction of the pumped sample nebulized is typically around 3 percent (so 97 percent of the sample goes to waste and is not measured). Parameters like the sample's viscosity or salinity can alter the nebulization process, and thus lead to higher or lower nebulization efficiency, thereby affecting the selenium signal obtained, which is proportional to the total amount of sample introduced into the plasma. To recognize and correct for such interferences, one or more internal standards (IS) are used, which are other trace elements spiked to the samples at a known concentration before analysis. The idea behind this is that a change in the sample introduction efficiency would affect the IS to the same degree as the analytes, and could thereby be compensated for mathematically.

The only condition that the IS needs to fulfill to be used for this correction approach is that it cannot be present in the samples in a measurable/significant concentration (so that the IS signal should always be constant if there were no sample uptake variations); for this reason, "exotic" elements like platinum group metals are commonly used for this purpose. In this project, rhodium was routinely used as the primary IS for total selenium measurements, and indium was used as a secondary IS to identify if there were problems associated with the rhodium measurement in any given sample. Several other commonly used IS elements were tried as well, but yielded less satisfactory results, usually because they occurred in the analyzed water samples in significant concentrations. The same was true to a lesser degree for indium, so it was not always usable as an IS, whereas rhodium generally fulfilled the absence condition. However, two additional problems were encountered related to the IS approach, which have not been reported in the literature before, and therefore were unanticipated and had to be recognized and dealt with during this project.

First, it was observed that certain matrix elements present in the studied waters produced interferences in the DRC process that mimicked one of the IS elements (for example, the strontium isotope ^{86}Sr forms an ammonia cluster $Sr(NH_3)^+$ in the DRC, which has the same nominal mass as the only rhodium isotope ^{103}Rh). This increases the apparent IS signal and suggests increased sample introduction efficiency for the particular sample, and since the analyte signal is normalized to the IS signal, leads to artificially decreased total selenium concentrations. This interference was recognized by the fact that the secondary IS was not elevated, and compensated for as much as possible by varying instrument parameter like the DRC gas flow rates and Rpa and Rpq (two DRC settings), but could not be eliminated altogether without compromising the efficiency with which the DRC removes the main interferences on the analytes (as discussed above). No alternate IS was found that fulfilled the absence condition and was not affected by this phenomenon, so more research is needed in this respect to find a way to compensate for this problem. One way to address the issue is the method of standard addition, where an interfered sample is measured repeatedly with varying amounts of the analyte added prior to analysis, but this procedure is impractical in routine operation, because every sample would need to be analyzed multiple times.

Secondly, it was noticed that the signal for either IS element increased unspecifically when high concentrations of a matrix element with similar or higher mass were present in the sample, e.g. barium (mass 137) increasing the IS signal for rhodium (mass 103) and indium (mass 115). This effect is the opposite of a well-known process in mass spectrometry called "space-charge effect", and could thus be referred to as "inverse space-charge effect". It was beyond the scope of this project to investigate the reasons for this observation, and the effect could not be eliminated by changing instrumental parameters, although it was moderated by increasing the acceleration voltage for the ions through the DRC. Like the previous interference, this issue causes an artificially-increased IS signal and thus leads to reduced total selenium concentrations. Contrary to interferences that lead to decreased sample introduction efficiency (and thereby to elevated apparent total selenium concentrations), these two effects would result in a positive speciation mass balance discrepancy (i.e. recovery > 100 percent), so since most samples showed a negative deviation in their selenium speciation mass balance, these two types of interferences did apparently not affect many of the measured samples; they may, however, explain why the sum of selenium species in some samples was significantly > 100 percent.

The second type of interference that is commonly compensated for by using internal standards relates to the ionization efficiency of the analyte in the plasma. This is a particular problem for selenium and arsenic, which have very high first ionization energies, and are ionized incompletely (25-50 percent) in the ICP. Major constituents of the matrix can alter the properties of the plasma, and thereby change the degree of ionization for these elements (and consequently their signal intensity); typical examples include major cations like sodium, which are easily ionized and thereby decrease the "energy" of the plasma, leading to reduced arsenic and selenium ionization, and organic carbon, which appears to enhance the ionization of arsenic and selenium by unknown mechanisms. Again, the IS could be used to compensate for these effects, but only if it shows a similar response to such interferences as the analytes of interest. This "similarity condition" is much harder to fulfill than the absence condition, and it's nearly impossible to fulfill them both perfectly for a large and inhomogeneous sample set, such as the present one. Of all tested IS elements, rhodium yielded that best results, but it has a significantly lower ionization energy than both arsenic and selenium, so that the analyte signals may have been suppressed in some samples without an effect on the IS. Again the result would be an artificially reduced total selenium or total arsenic concentration.

The preceding discussion makes it clear that the determination of total selenium in such complex samples as the studied waters is complicated, and that not all interferences can be compensated for, leading to possibly "wrong" total selenium concentrations, which in turn would impact the selenium speciation mass balance. This is probably one of the main reasons of why this mass balance did not work well in samples with low total selenium and high concentrations of certain matrix elements. Besides the mentioned HG sample introduction, an elegant way to eliminate many of the discussed interferences would be isotope dilution, which involves spiking a known amount of a particular selenium isotope to the sample prior to analysis. This is, however, expensive, because pure selenium isotopes would need to be obtained, and was consequently not available and could not be developed during this project. Given the (eco) toxicological importance of measuring relatively low total selenium concentrations in complex aqueous samples, this is an area which should be explored in future research, so that a much improved and reliable method for total selenium determinations by ICP-MS becomes available.

All analytical issues discussed above hold true for arsenic as well, but contrary to selenium, arsenic is monoisotopic, and consequently does not offer the possibility of compensating for (or even recognizing) certain interferences by "switching" to another isotope, which suggests that the total arsenic data quality should be poorer than for total selenium (which of course cannot be proven directly). The suggested improvements like HG sample introduction would also remedy many of the raised problems, and even isotope dilution with a long-lived arsenic radionuclide could be used for internal standardization. However, similar to selenium, these aspects were not explored during this project, and the fact that the arsenic speciation mass balance did not work well in some samples can certainly be partially attributed to problems associated with the total arsenic determination.

Determination of Arsenic, Selenium, and Chromium Speciation

The determination of Cr(III) and Cr(VI) by AEC-ICP-MS worked quite well, as supported by the reasonable chromium speciation mass balance. The only issue that was addressed during this

project was the relatively high background caused by the presence of inorganic carbon in the used chromatographic eluant: this leads to the formation of $^{40}Ar^{12}C^{+}$, which interferes with the determination of the main chromium isotope ^{52}Cr, but this background was easily eliminated by using NH_3 as the reaction gas in the DRC.

For arsenic and selenium, the measurement of their speciation in the collected water samples was more complicated, and a number of significant interferences were encountered. These interferences are generally not related to the presence of spectral interferences, as discussed for the total arsenic and total selenium determinations above, because typically the interfering sample constituent is separated chromatographically in time from the analyte species. As an example, bromide in the samples will still produce a signal on mass 82, but this does not interfere with the measurement of Se(IV) or Se(VI), because the bromide signal either elutes before the Se(IV) peak, or–if the interfering peak is too large–Se(IV) at mass 77 can be used for quantification. Rather, besides the preservation/stability issues discussed above for the cryofrozen sample, the main problems encountered are caused by high salinity in some of the collected water samples, and by the presence of major trace elements that are incompatible with the chosen chromatographic conditions, so both are chromatographic issues occurring in the AEC, and not spectroscopic issues arising in the ICP-MS.

The salinity-based interference is caused by the fact that major anions, especially sulfate in the studied waters, are present in very high concentrations (up to 300 mmol/L), whereas the arsenic and selenium species are present in much lower concentrations (up to 9 µmol/L for selenium and 7 µmol/L for As), so the major anions are present in 30,000-fold excess. During the AEC analysis, the major anion competes with the trace element anions for binding sites on the chromatographic column, and if this competition becomes too strong, then the analytes are "flushed" out of the column without interacting properly with the stationary phase, which results in bad peak shapes that makes quantification inaccurate to impossible, and in the change of retention times, which makes identification uncertain or eliminates separation of different species altogether. The best way to eliminate this problem is by diluting the sample prior to analysis, but this approach is limited by the absolute concentration of the analytes in the same, so if the ratio of major anions to analytes is too large, the samples would have to be diluted to the point where the analytes fall below the detection limits to overcome the chromatographic problems.

This issue was encountered for a large number of the studied samples, and was addressed by modifying the AEC separation. Sulfate (instead of hydroxide) was used as the eluant anion, and this increases the tolerance of the separation for elevated sulfate concentrations in the sample (this approach is called "matrix matching"). However, even this remedy is limited by the absolute binding capacity of the column, so if the total amount of matrix anions injected exceeds this capacity, then proper separation of the analytes is no longer possible. Matrix matching yielded a significant improvement for the speciation mass balance of arsenic and selenium in many samples collected in 2004 and 2005, and for those samples where the mass balance still remained poor, there appeared to be a general correlation with the ratio of sample salinity to analyte concentration.

The second chromatographic issue was caused by high iron and especially manganese concentrations in some of the studied waters. Since the AEC separation is conducted under

alkaline conditions (even after modification) to prevent the loss of acid-labile arsenic and selenium species, major sample constituents that precipitate under strongly alkaline conditions may cause problems. Although many of the collected samples were alkaline to begin with, the separation conditions were even more alkaline; this pH change during analysis particularly affected those samples that were acidic or circumneutral in the field. Under such conditions, manganese (and iron) can precipitate in the form of (oxy)hydroxide minerals within the AEC, and these precipitates bind the species As(V) and Se(IV) very strongly, which could lead to artificially low results for these two species. This issue was addressed by raising the pH of the eluant by about one unit, and by adding some oxalate into the eluent, which keeps manganese in solution. As for the salinity issue, though, there are limits to this approach, and the problems could not be eliminated in all samples, which is probably the main reason for the very low speciation mass balances encountered in some samples.

As the constitution of real world samples is highly variable and unpredictable, the best way to resolve this problem is by using more sensitive detection principles, because then the problematic samples can be diluted even more. At this point, though, ICP-MS is the most sensitive detection approach, even if certain ICP-MS instruments not available during this project may possibly yield lower detection limits for the AEC-ICP-MS determination of arsenic and selenium species than the used ICP-DRC-MS (in the standard mode for arsenic and selenium speciation). Further increases in detection sensitivity for arsenic and selenium can be achieved by using high-efficiency sample introduction systems, such as HG or membrane desolvation, between the AEC separation and the ICP-MS detection. This, however, is complicated and more expensive for use on a routine basis, and the required equipment was either not available permanently at Trent, or was incompatible with the relatively high chromatographic flow rates (and would thus have necessitated some modifications), so these options were not incorporated into the used methods. It should be noted, though, that AEC-HG-ICP-DRC-MS has been used successfully to measure selenium speciation at ng/L-levels in sea water, so this approach could be used in future studies, because it works in principle for the species As(III)/As(V) and Se(IV)/Se(VI), while its suitability for any other arsenic or selenium species is untested, which constitutes another reason why this technique was not routinely used in this project.

EPRI | ELECTRIC POWER RESEARCH INSTITUTE

Speciation and Attenuation of Arsenic and Selenium at Coal Combustion By-Product Management Facilities

Volume 2: Arsenic Adsorption

Final Report
October 1, 2002 - September 30, 2005

DOE Award Number: DE-FC26-02NT41590

Principal Investigators:

L. Lee, Purdue University
I. Murarka, Ish Inc.

ARSENIC ADSORPTION ABSTRACT

This report contains results of the laboratory batch equilibrium studies for chemical attenuation of arsenic species by soils from three coal-fired power plant sites. Several soil samples were collected from three power plant sites to conduct the laboratory chemical attenuation studies. Adsorption isotherms and coefficients were developed for both arsenic(III) and arsenic(V) species. Physical and chemical characterization data for the soils were obtained so that correlations between soil properties and adsorption of arsenic species can be established to the extent possible. Linear, Freundlich, and Langmuir adsorption isotherms were fitted to the data as appropriate.

The effects of calcium and sulfate, the dominant ionic constituents in coal ash leachates, on the adsorption of the As(III) and As(V) by soils were measured. The effects of pH on arsenic species adsorption by soils were also measured. Sequential leaching studies were performed on coal ash samples collected from each of the three landfill sites. Kinetic leaching tests on ash samples were also performed.

Adsorption of arsenic species was generally non-linear with respect to concentration. For all three sites, adsorption of As(V) was significantly greater than As(III). Linear distribution coefficients calculated from adsorption isotherms at a concentration of 1 mg/L ranged from about 30 to 350 L/kg for As(V), and from about 5 to 50 L/kg for As(III). The impact of sulfate concentrations on adsorption were soil dependent and most pronounced for As(III). In general sulfate tends to decrease adsorption of arsenic species onto the soils. Adsorption of As(V) was generally enhanced by calcium in solution but As(III) adsorption was not much influenced by calcium.

Linear regression analysis of the adsorption coefficients and soil chemical and physical properties indicates that the best correlation was found with 15-second DC extractable iron. However, reasonably good correlations were also found for percent clay content and for DC-extractable Fe and Al in soils.

These chemical attenuation data for the arsenic species can be used to model arsenic migration in groundwater at the coal ash management sites for the coal fired power plant sites.

CONTENTS

LIST OF FIGURES

LIST OF TABLES

1
INTRODUCTION

Chemical attenuation of arsenic in subsurface soils is highly dependent on the arsenic species present in solution (leachate) and the characteristics of the soil. This project was designed to evaluate chemical attenuation of As(III) and As(V) at three coal-fired power plant sites. One site is located in the northeastern United States (NE), one site is located in the Southeast (SE), and one site is located in the Midwest (MW). These data can be used to model arsenic migration in groundwater at the sites for comparison to monitoring well data. This report presents the results of laboratory determinations of attenuation characteristics for soils collected from the three sites.

Objectives

The overall objectives of this research project were to:

- Collect soil samples from each of the three power plant sites and characterize them for selected physical and chemical properties,
- Conduct laboratory batch equilibrium experiments to develop adsorption isotherms and coefficients for both As(III) and As(V) species from multiple soil samples from each of the three sites,
- Collect coal ash samples from the three power plants and perform sequential batch leaching tests to characterize arsenic release from these ashes, and
- Carry out laboratory batch tests to assess the effects of ash leachate composition and pH on the chemical attenuation of both As(III) and As(V) species by the three site soils.

Literature Review

The widespread occurrence of arsenic in soils and groundwater from both natural and anthropogenic sources has spawned considerable public and regulatory interest pertaining to the environmental impact of arsenic in drinking water. The toxicity and mobility of arsenic species in the subsurface environment are dependent on its reduction-oxidation (redox) state. Under chemically oxidizing conditions, the As(V) species predominates and exists as oxyanions of arsenic acid ($H2AsO^{4-}$ between pH 2.2-7.0 and $HAsO_4^{2-}$ above pH 7). Under chemically reducing conditions, the As(III) species is dominant and exists as arsenious acid ($H_3AsO_3^{0}$) below a pH of 9.2. The As(III) species is considerably more toxic than As(V), and is usually reported to be more weakly bound to most mineral surfaces compared to As(V) (Goldberg 2002; Goldberg & Johnston 2000; Manning & Goldberg 1997).

A large body of research is currently available on the adsorption of arsenic on both pure mineral surfaces and soil particles (EPRI, 2000). Inorganic constituents of soils that have been recognized to adsorb significant amounts of arsenic include Fe and Al oxides/oxyhydroxides (hereafter referred to as Fe and Al oxides), alumino-silicates, and carbonates. Both As(V) and As(III) have strong affinities to adsorb onto Fe and Al oxides; however, the two species behave differently with regard to the influence of pH. In the pH range of 3 to 9, adsorption of As(V) onto both Fe and Al oxides is reported to be at the maximum and decreases with increasing pH (Goldberg 2002; Manning & Goldberg 1996; Xu et al.,1988; Pierce & Moore 1982; Anderson et al.,1976), while As(III) adsorption generally increases with increasing pH up to a maximum at pH 7 to 8 (Goldberg 2002; Manning & Goldberg 1997; Pierce & Moore 1982; Gupta & Chen 1978). Adsorption of arsenic species onto alumino-silicate clay minerals (kaolinite, illite, and montmorillonite) may also be appreciable, but to a far lesser degree than adsorption onto Fe and Al oxides. Arsenate [As(V)] adsorption onto kaolinite, illite, and montmorillonite is highest at low pH values, exhibiting an adsorption maxima in the pH 3 to 7 range, and decreases at higher pH (Goldberg 2002; Manning & Goldberg 1996; Goldberg & Glaubig 1988). Arsenite [As(III)] adsorption on each of these alumino-silicates minerals increases up to a pH of 9 (Goldberg 2002; Manning & Goldberg 1997). Under alkaline environments adsorption of arsenic onto carbonate minerals may also be substantial. Capacities for arsenic adsorption onto calcite fall between those reported for Fe and Al oxides and clay minerals, with both As(V) and As(III) adsorption increasing with increasing pH up to a maximum at around pH 10 (Goldberg & Glaubig 1988; Brannon & Patrick 1987).

Aside from pH, Eh, and soil mineral composition, the ionic composition of the interstitial water of soils also impacts arsenic adsorption. Anionic constituents such as phosphate and sulfate may directly compete with either arsenic species for available surface binding sites, or indirectly influence arsenic adsorption by altering the electrostatic charge at solid surfaces (Jain & Loeppert 2000). Adsorption of As(V) onto Fe oxides, gibbsite, and alumino-silicates is significantly reduced in the presence of phosphate (Jain & Loeppert 2000; Manning & Goldberg 1996a). However, the competitive effects of sulfate anions on As(V) adsorption are dependent on the sorbent. Adsorption of As(V) onto amorphous Fe oxides is only slightly affected by sulfate (Jain & Loeppert 2000; Wilkie & Hering 1996), while As(V) adsorption onto alumina is significantly decreased in the presence of sulfate, although to a much lesser extent than would be caused by phosphate anions (Xu et al.,1988). As(III) adsorption by Fe oxides is significantly decreased by both phosphate and sulfate with phosphate having a greater effect (Jain & Loeppert 2000; Wilkie & Hering 1996). Some types of sorption sites appear to have a higher selectivity for As(III) than either sulfate or phosphate (Jain & Loeppert 2000).

Calcium has been show to enhance the adsorption of both As(V) and As(III) by soils with As(III) generally being less enhanced than As(V) (Smith et al., 2002). Although the detailed mechanisms of this enhancement have not been well documented, the specific adsorption of cations onto soil surfaces likely plays a significant role in mediating the charge on the adsorbing surfaces. Specifically adsorbed cations can shift the charge potential in the plane of sorption to be more negative, thereby increasing anion sorption (Smith et al., 2002; Bowden et al.,1973 & 1977; Bolan et al.,1993). An alternative mechanism may be the formation of intra-molecular bridges between As(V) ions and negatively charged surface sites (e.g., organic matter and alumino-silicate surfaces) by the divalent cations.

Published literature also suggests a potentially significant microbial role in altering the redox state of arsenic such that the dominant redox state in the field may be contrary to predictions based on chemical parameters alone. Microbial populations do both reduce and oxidize arsenic depending on whether they are trying to detoxify arsenic or using it to shuttle electrons during metabolic activity.

One of the anthropogenic sources of arsenic to the environment is leachate derived from coal ash disposal facilities. During the combustion of coal in the utility boilers, arsenic contained in organic matter and sulfide compounds in coal is volatilized into combustion gases (Eary et al.,1990). Once these gases, and fly ash particles entrained in the gases, are vented from the combustion furnace they quickly cool down leading to the condensation of relatively soluble oxides or inorganic salts of arsenic onto the surface of fly ash particles (Eary et al.,1990; Theis et al.,1982; Theis & Wirth 1977).

The enrichment of arsenic on the surfaces of fly ash particles substantially increases its potential for leaching giving rise to elevated concentrations in leachates. EPRI (1987) reported ranges between < 0.1 and 0.51 mg/L in water soluble arsenic in hot-water extracts (1:20 mass-to-volume ratio at 105°C) of 38 fly ash samples from various source coals and combustion technologies. Jackson and Miller (1998) reported a similar range between < 0.001 and 1.65 mg/L As in (1:40 mass-to-volume ratio at room temperature) water extracts of 23 fly ash samples. Additionally, Jackson and Miller (1998) reported that As(V) was the primary redox species found in nearly all of the water extracts, with As(III) typically below the limits of detection. In contrast, varying amounts of As(III) were measured by Turner (1981) in aqueous extracts of 12 fly ash samples, with As(III) comprising between 2% and 66% of soluble arsenic.

Adsorption onto soil surfaces is a dominant chemical attenuation mechanism for arsenic in leachate released from unlined coal ash disposal facilities. In order to establish a theoretical framework to predict arsenic species attenuation by soil contacted by ash leachate, this study focused on the following objectives: (1) characterizing the adsorption of As(V) and As(III) onto power plant site soils having a wide range of physical and chemical properties; (2) establishing a range of partition coefficients that may be used in assessing the retardation of arsenic in ash leachate by soils; (3) quantifying the competitive effects of Ca and SO_4 on the adsorption of As(V) and As(III); (4) quantifying pH effects on arsenic species adsorption; and (5) if possible, developing a predictive tool for estimating arsenic species attenuation by soil using easily quantifiable soil and solution properties.

2
METHODS AND MATERIALS

Soil Sampling and Characterization

Soils samples were collected from several depths at each of the three sites by split spoon sampling equipment with a plastic insert. Two to three soil borings were advanced within about 200 feet of the downgradient edge of the ash fill using a hollow stem auger, and samples were collected at five to ten foot intervals. The samples were sealed in the field in two foot sections with end caps and then taped so that the plastic tubes endured the shipping without spilling out the samples. Several soil samples were collected from each of the soil borings and if appropriate were composited in the laboratory from consecutive depths. The soil samples were shipped to the laboratory in chilled coolers. Ash samples from the landfill site were collected in a similar manner. Soil samples were also collected underneath the ash landfill at the northeastern power plant site. The other two sites could not be samples underneath the ash landfill due to engineering considerations.

Upon arrival at the laboratory at Purdue University, soil and ash samples were transferred to plastic bins, and stored moist (or dry if moisture was not present in the samples) at 4°C. Soil pH and texture was used to screen samples received in order to select a subset of samples considered representative of the site for use in the adsorption studies. For each sample selected, a subsample (≈ 200 g) was air dried, sieved to particle diameter less than 2 mm, and thoroughly homogenized prior to chemical/physical characterization and use. Each processed soil sample was characterized for the following physical and chemical properties: particle size distribution by the hydrometer method (Grossman & Reinsch, 2002), pH of 1:1 (5 g soil: 5 mL H_2O) soil suspensions, pH of 1:1 (5 g soil:5 mL $CaCl_2$) soil suspensions, cation exchange capacity (Chapman, 1965), dithionite-citrate extractable iron and aluminum (Loeppert & Inskeep, 1996), acid ammonium oxalate extractable iron and aluminum (Loeppert & Inskeep, 1996), percent base saturation (by summation of 1M NH_4^- extractable basic cations), percent organic matter (Nelson & Sommers, 1996), Bray P1 extractable phosphorus (Bray and Kurtz 1945), X-ray diffraction analysis of clay minerals, and timed dithionite-citrate-bicarbonate (DCB) extractions of Fe and Al.

The dominant clay minerals in each of the soil samples were measured using an x-ray diffraction analysis method. Briefly, 15 g of soil was homogenized and sieved at 2 mm followed by carbonate removal (soil reacted with 50-mL 1 M ammonium acetate, pH = 5) and removal of organics and manganese oxides via soil digestion with 30-mL 30% H_2O_2 at 45°C. The soil was then dispersed by sonication, and the clay size fraction of particles fractionated by a centrifugation scheme intended to separate particles at 2 μm. The clay size fraction was then frozen using liquid nitrogen and freeze-dried for later analysis. For each soil, two slides were

prepared for x-ray diffraction. These slides consisted of samples which either had been K-saturated or had been Mg-saturated and glycerol solvated. X-ray diffraction patterns of the clay size fraction were obtained using CuKα radiation and a type F Siemens Diffractometer with omega drive. The diffractometer was equipped with a 1 degree divergence slit, 0.25° receiving slit, 0.4° scatter slit, and a graphite monochromator. Samples were scanned from 2 to 30° 2(θ) using a 0.02 degree increment and a 1 second count time. During the analysis the K-saturated samples were analyzed after being exposed to four separate temperature regimes (room temperature, 100°C, 300°C, and 550°C).

Timed dithionite-citrate-bicarbonate (DCB) extractions of soils were performed by accurately weighing 2 g of sodium dithionite into a 250-mL beaker containing 50-mL 0.3 M sodium citrate and 0.2 M sodium bicarbonate. A shaft-driven stirrer was placed into the solution and the stir rate was adjusted to 200 rpm. One gram of soil was then quickly added to the DCB solution. A small aliquot (~2 mL) of this suspension was then drawn from the beaker after 15 seconds using a 10 mL plastic syringe. The aliquot drawn from the beaker was quickly filtered by passing it through a 0.45 μm regenerated cellulose syringe filter. Filtered samples were analyzed for iron and aluminum using flame atomic adsorption spectrophotometry (FAAS).

Adsorption Isotherms on Site Soils

Adsorption isotherms were constructed independently for both As(V) and As(III) in an ionic matrix of 10-3 M $CaSO_4$ using a minimum of four As concentrations and up to eight concentrations plus zero As control. Applied solution concentrations generally ranged from 0.2 to 5 mg/L in the case of As(V), and 0.3 to 1.2 mg/L for As(III). Arsenic solutions were added to 50 mL polypropylene centrifuge tubes containing 0.5 g to 1 g (oven dried weight, o.d.w) of soil to obtain solid suspension densities of 20 g/L for As(V) and 50 g/L for As(III). Soil suspensions were then allowed to equilibrate at 22 ± 2°C on a rotary shaker (~45 RPM) for 48 h for As(V) and 16 h for As(III). Arsenic concentrations in solution were measured after equilibration (C_w, mg/L), and sorbed concentrations (C_s, mg/kg) were estimated by the difference in the As mass applied and the As mass remaining in solution after equilibration with soil.

Equilibration times were selected to achieve near equilibrium without having significant shifts in the redox state of the As remaining in solution; the redox state of sorbed As was assumed to be the same as what was measured in the initial solution. In the preliminary kinetic experiments, total As was determined by atomic adsorption/graphite furnace (GFAA), As(III) by AA/HVG, and As(V) by difference between total As and As(III) concentrations, which was confirmed with inductively coupled plasma-mass spectrometry (ICP-MS). Suspensions containing As(III) were equilibrated for a shorter period of time due to concerns that a significant amount of As(III) would oxidize to As(V) within a 48 hour equilibration period. Based on preliminary work (Figure 2-1), and previous studies by Pierce and Moore (1982), who found that 99% of adsorption on soils takes place within 9 hours, the equilibration time in each case was sufficient to attain near equilibrium conditions.

After equilibration, the pH of the soil suspensions was measured using an Accumet® AR25 pH meter in conjunction with an Accumet® double junction glass pH electrode. Ten milliliters of suspension was collected from each sample and filtered at 0.45 μm using a 10 mL plastic syringe

with a 0.45 µm regenerated cellulose luer-lock syringe filter. Filtered samples were preserved by adding 0.1 mL of concentrated HNO_3. Analysis of arsenic concentrations in the filtered samples was performed using GFAA.

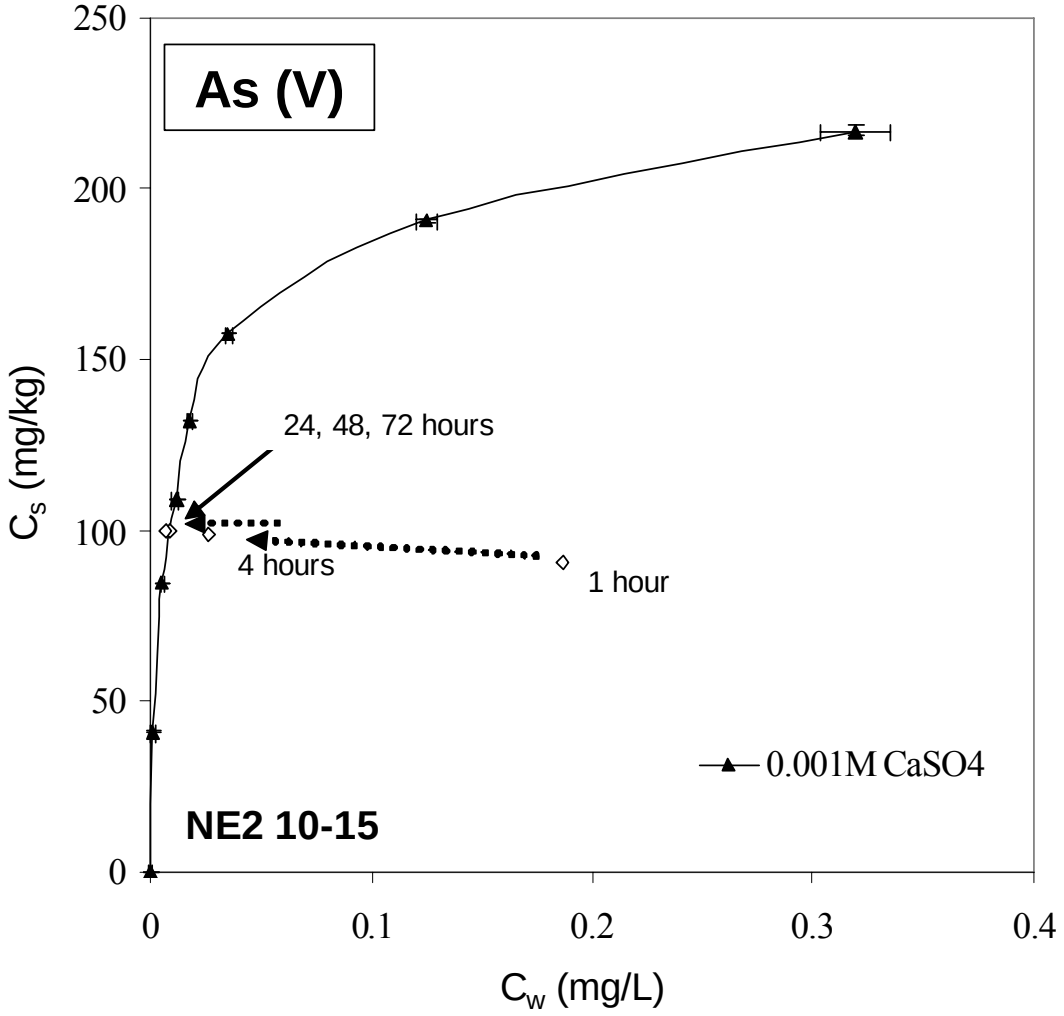

Figure 2-1
Sorption by a NE site soil sample from a single solution concentration of As(V) measured at several times, and a complete multi-concentration sorption isotherm measured after 48 hours. C_s=sorbed concentration; C_w=solution concentration.

Data Analysis

Arsenic isotherms were constructed by plotting sorbed (C_s, mg/kg) versus solution (C_w, mg/L) concentrations and fit using Statistical Analysis System (SAS) v. 8.2 to the three sorption models most commonly used to describe the sorption behavior of a chemical over a specified concentration range.

$$C_S = K_d\, C_w \qquad \textbf{Linear} \qquad (2\text{-}1)$$

$$C_s = K_f C_w^{\,N} \qquad \textbf{Freundlich} \qquad (2\text{-}2)$$

$$C_s = \frac{K_L C_{s,\max} C_w}{1 + K_L C_w} \qquad \textbf{Langmuir} \qquad (2\text{-}3)$$

where C_s (mg/kg) is the chemical concentration in the soil at equilibrium; C_w (mg/L) is the chemical concentration in the aqueous phase at equilibrium; K_d (L/kg) is the linear sorption coefficient; K_f is the Freundlich sorption coefficient, which has units of $mg^{1-N}\ L^N\ kg^{-1}$ or $mmol^{1-N}\ L^N\ kg^{-1}$ depending on whether you choose to use chemical mass or mole units, and the Freundlich N (unitless), which is a measure of isotherm nonlinearity in the Freundlich equation; K_L (L/mg or L/mmol) is Langmuir affinity coefficient; and C_s,max is the maximum monolayer adsorption capacity (mg/kg). Note that $C_{s,\,max}$ reflects the maximum sorption capacity suggesting that all sorption sites are filled assuming site-specific sorption. However, this assumption also does not account for any precipitation that may occur. The regression analysis performed provided best-fit estimates for the parameters of the models along with an estimate of the goodness-of-fit (R^2). Note that both the Freundlich and Langmuir models have sorption coefficients (K_f and K_L) that contain a concentration unit for the chemical; therefore, the magnitude of these values will be different if calculated on a mass scale (e.g., mg) versus a molar scale (e.g., mmol), unlike the linear sorption coefficient (K_d). Also note that for K_f values the conversion is not straightforward because C_w is raised to a power; the difference between mass-based K_f values and mole-based K_f values is, therefore, MW^{N-1} where MW stands for molecular weight (g/mol).

Both the Freundlich and Langmuir models are capable of characterizing the nonlinear sorption behavior of arsenic species. The Freundlich model reflects multi-mechanistic sorption and/or sorption sites that range in their sorption affinities. The Langmuir model was derived assuming that there is a maximum number of sites on the soil surface ($C_{s,\,max}$) to which a solute can adsorb. The Freundlich model collapses to the linear sorption model when N is exactly equal to one, and approaches the Langmuir model at small values of N. The $C_{s,\,max}$ estimated using Langmuir model fits to isotherms constructed from a limited concentration range can be in error; typically isotherms are not constructed using high enough solute concentrations to achieve the true $C_{s,\,max}$. Also, as higher solute concentrations are applied to the soil, the soil surface can be sufficiently changed such that other sorption mechanisms or precipitation chemistry become operational, thus a true $C_{s,\,max}$ may not actually be achieved.

The Freundlich model is often the best approach to predicting sorption as a function of concentration when sorption is substantially nonlinear over the concentration range of interest and the specific sorption mechanisms are not known. Problems arise using this approach when predictive transport models only allow for the input of a linear sorption coefficient (K_d). In the latter case, the model can estimate a concentration-specific K_d* value using the Freundlich isotherm model coefficients (K_f and N):

$$K_d = K_f C_w^{N-1} \quad (2\text{-}4)$$

Note that at C_w = 1 μg/mL using a mass-based K_f value, $K_d^* = K_f$ (likewise for C_w = 1 μmol/mL using a mole-based K_f). For isotherms with Freundlich N values less than one, K_d^* increases as C_w values decrease. Therefore, when an incoming solution (e.g., fly ash leachate) first contacts the soil given N <1, the operational K_d is the highest and becomes smaller (thus less attenuation) as the concentration in the pore-water becomes equal to the incoming solution (e.g., $C_w = C_i$). This nonlinear (N<1) behavior results in a solute breakthrough curve (C_w versus pore volumes past through the soil matrix), for example at a well, that exhibits a self sharpening front. Eventually after the incoming solution is void of the chemical, the chemical concentration profile will exhibit an extended tail.

Matrix Effects Studies

The effects of Ca and SO_4, the dominant ionic constituents of many coal ash leachates, on the adsorption of As(V) and As(III) were characterized on two soils (NE2 10-15 and NE1 25-30) having considerably different capacities to adsorb arsenic. Two types of experiments were conducted for each arsenic species on both soils. In the first set of experiments, adsorption of two different initial concentrations of either As(V) or As(III) was quantified as a function of solution concentrations of Ca or SO_4 for each As concentration. In the second set of experiments, adsorption isotherms of each arsenic species were produced in 10^{-3} M KCl, 10^{-3} M $CaCl_2$, 10^{-3} M K_2SO_4, and 10^{-3} M $CaSO_4$ at eight initial concentrations of As(V) or As(III).

Arsenic solutions for the adsorption envelope experiments were prepared by poising the ionic strength of solutions containing 0, 10^{-4}, $10^{-3.3}$, 10^{-3}, $10^{-2.3}$, and 10^{-2} M $CaCl_2$ or K_2SO_4 to an ionic strength of 0.03 M using 1M KCl. Small aliquots of 1,000 mg/L As(V) or As(III) (from $Na_2HAsO_4 \cdot 7H_2O$ or $NaAsO_2$) were then spiked into the appropriate solution matrix to obtain initial As concentrations of 1 mg/L and 0.75 mg/L, respectively. Arsenic solutions were then added to 50-mL polypropylene centrifuge tubes containing 0.5 grams o.d.w. (oven dried weight) soil in duplicate to obtain solid suspension densities of 10 g/L for As(V) and 25 g/L for As(III). Equilibration and analysis were as previously described for the determination of the multi-concentration isotherms. Arsenic speciation analysis of selected samples, using ion chromatography-inductively coupled plasma-mass spectroscopy (IC-ICP-MS), confirmed that conversion of As(III) to As(V) was insignificant during the 16 h equilibration time at all pH values observed in the experiments.

Arsenic solutions for adsorption isotherm experiments consisted of 10^{-3} M KCl, 10^{-3} M $CaCl_2$, 10^{-3} M K_2SO_4, and 10^{-3} M $CaSO_4$. No attempts were made at controlling the ionic strength of the equilibrating solutions; however, the effect of ionic strength on arsenic sorption is reported to be negligible for the range of ionic strengths used in the current study (10^{-3} – $10^{-2.4}$ M) (Goldberg and Johnston, 2001; Manning and Goldberg, 1997). Adsorption of each arsenic species was measured in duplicate at eight concentrations in the concentration range of 0 to 3 mg/L for As(V) and 0 to 1 mg/L for As(III). All other experimental protocols, including solid suspension

densities, equilibration times, and sampling regimes, were identical to those described for the fixed As concentration experiments.

pH Effect on Arsenic Adsorption

Similar to the matrix effect studies, the effects of pH on arsenic species adsorption were characterized for the same two soils using two types of experiments. In the first set of experiments, adsorption of fixed initial concentrations of either As(V) or As(III) in 10^{-3} M KCl was quantified as a function of solution pH yielding a profile referred to as an adsorption envelope or pH-edge. In the second group of experiments, As(V) and As(III) adsorption isotherms from 10^{-3} M KCl were produced at the native pH of the soil, and at pH values that were one pH unit above and below the native soil pH. The arsenic solution of either 1 mg/L As(V) or 0.5 mg/L As(III) was adjusted to a desired range of pH values (3 to 11) using 0.25 M KOH or HCl. Multi-concentration arsenic adsorption isotherms at the native soil pH ± 1 pH unit were constructed using six As concentrations in duplicate by varying the initial concentrations of both As(V) or As(III) from 0 to 1 mg/L As. All other experimental protocols, including solid suspension densities, equilibration times, and sampling regimes, were identical to those used in the adsorption envelope studies.

Fly Ash Leaching

Moisture Content

Fly ash samples were stored in an airtight container to ensure no evaporation took place after collection. Moisture contents were determined by weighing the moist ash into a pre-weighed container, placed in an oven at 105°C for 24 hours, cooled to room temperature in a desiccator, and re-weighing. Moisture content was estimated by the difference in moist and oven-dried weights.

Sequential Leaching

Sequential leaching studies were performed in triplicate for ash samples collected at 15-20 feet below ground surface (bgs) in cores NE3 and NE4. Approximately 20 g of ash and 68 g of reagent-grade water (Barnstead Nanopure System) were added to 80-ml Nalgene polycarbonate test tubes. All tubes were rotated end-over-end and allowed to equilibrate for 24 hours, followed by centrifugation at 2,700 RPM for 1 hour using the Jouan Laboratory Equipment Centrifuge, model CR422. Values of pH were measured and recorded. The supernatant was removed using a Becton Dickinson and Company 10-cc Luer Lok syringe, filtered using Alltech 0.45-µm cellulose filters, and split into two subsamples of which one was acidified with two drops of concentrated (70%) trace-metal grade nitric acid and the other with 2 drops of concentrated HCl. Acidified samples were stored in acid-washed Nalgene polyethylene or polypropylene bottles with polypropylene screw closures. Reagent-grade water was then added to the ash remaining in the tube to replace the solution removed, and the leaching procedure was repeated 10-15 times. Samples were analyzed using the Thermo Jarrell Ash ICP (model AtomScan16) in combination

with a CETAL Technologies Ultrasonic Nebulizer (model U5000AT+) or using the AA/GF furnace as previously described.

Kinetic Leaching

Kinetic leaching studies were performed in duplicate from the same ash samples. Approximately 12.5 g of ash and 43 g of reagent-grade water (Barnstead Nanopure System) were added to acid-washed 60-ml Nalgene polycarbonate test tubes. For each time increment, a set of duplicate tubes were destructively sampled. All tubes were rotated end-over-end and allowed to equilibrate for specified time increments that include: 2 h, 4 h, 8 h, 1 d, 2 d, 4 d, 8 d, 12 d, 20 d, and 30 d. Tubes were centrifuged at 2,000 RPM for 20 minutes using the Jouan Laboratory Equipment Centrifuge (Model CR422). Values of pH and subsequent arsenic concentrations were determined as previously described.

Attenuation by Soils of Arsenic in Leachate

Fly ash leachate obtained from a first sequential leaching of ash from the NE site was spiked with 150 ppb As(V) and 50 ppb As(III) and applied to soils at mass (g) to volume (mL) ratios of 1:100, 1:40, and 1:20. Samples were rotated end-over-end, followed by quantification of As(V) and As(III) in the solution phase of the soil suspensions. Spiked ash leachate was applied at different mass to volume ratio amounts in order to get multiple (C_s, C_w) points without changing the leachate matrix, for a better comparison with multi-concentration isotherms measured from the simulated matrix (0.001 M $CaSO_4$ in this case).

3
ARSENIC ADSORPTION ON SITE SOILS

NE Site

Soil Characterization Data

Selected soil properties for six soils representative of the NE site are shown in Table 3-1. NE site soils contained 13 to 29% clay composed predominantly of illite and mica with minor amounts of kaolinite. The soils contained less than 1% organic matter and their soil-water pH values ranged from 4.8 to 5.5. Selective Fe dissolution of the soils resulted in DC-extractable Fe (intended to estimate total reducible Fe oxides) levels ranging from approximately 6,000 to 32,000 mg/kg, and DC-extractable Al levels ranging from 270 to 1,300 mg/kg. Ranges in oxalate extractable Fe and Al were less variable, with Fe ranging from 320 to 5,465 mg/kg, and Al ranging from 240 to 513 mg/kg. Based on the assumption that the oxalate extraction primarily dissolves amorphous Fe and Al oxides, the differences between DC and oxalate extracts indicate that 5 to 91% of extractable Fe in the soils is amorphous, and 38 to 89% of extractable Al is amorphous. Fe extracted in 15 seconds with DCB ranged from 270 to 1,618 mg/kg, and was intended to estimate the most reactive portion of Fe oxides (i.e., Fe oxides exposed to solution and readily available for reaction).

Arsenic Adsorption on NE Site Soils

Adsorption data for As(V) and As(III) on the six soils representative of the NE sites were measured and fitted with Freundlich and Langmuir isotherm models. As(V) and As(III) isotherms are plotted in Figures 3-1 and 3-2, and modeling fits are summarized in Tables 3-2 and 3-3. Values of K_f (mg^{1-N} m^N kg^{-1}) ranged between 61 and 380 for As(V) sorption, and between 11 and 53 for As(III). Nonlinear sorption is evident for both As(V) (Freundlich N values 0.26 to 0.36 and As(III) (Freundlich N values 0.31 to 0.57). Sorption of As(V) is consistently much higher than that observed for As(III), with Freundlich K_f values being 5 to 9 times higher for As(V); similar trends are evident for the Langmuir $C_{s,max}$ values as well. To exemplify the overall arsenic sorption behavior by soils at the NE site, As(V) and As(III) isotherms for the lowest and highest sorption observed for the six soil samples were considered representative of the site, as well as the effect of nonlinearity on the concentration-specific K_d^* values that would be used to estimate site-specific transport, are shown in Figure 3-3.

Table 3-1
Selected properties of 6 soils representative of the NE site.

Soil	pH $*_{H2O}$	pH $*_{CaCl2}$	Sand %	Silt %	Clay %	CEC (cmol/kg)	DC* - Fe (mg/kg)	DC* - Al (mg/kg)	$Ox^{\dagger}$ - Fe (mg/kg)	$Ox^{\dagger}$ - Al (mg/kg)	DCB - Fe 15 sec (mg/kg)	Base Saturation %	Organic Matter %	Bray P1-PO_4 (ppm)	Dominant Clay Minerals
NE1 25-30	5.3	5.1	33	50	17	15.5	5,928	270	320	240	270	87	0.5	38	I, K, V
NE1 35-40	5.0	4.7	40	35	25	12.6	6,030	610	5,465	525	651	62	0.5	2	I, K, V
NE2 10-15	4.8	4.4	60	23	17	4.7	31,800	1,200	1,575	513	992	48	1	10	I, K
NE2 16-21	5.0	4.6	59	28	13	2.45	11,370	630	1,090	364	534	80	0.5	11	I, K
NE3 50-54	5.0	4.9	9	62	29	13.2	22,470	1,070	1,750	475	1,618	64	0.6	14	I, K
NE4 46-50	5.5	5.5	57	28	15	5.8	18,330	1,300	1,590	500	1,044	79	0.9	3	I, K

*dithionite carbonate extractable; † oxalate extractable; I = illite, K = kaolinite, V = vermiculite

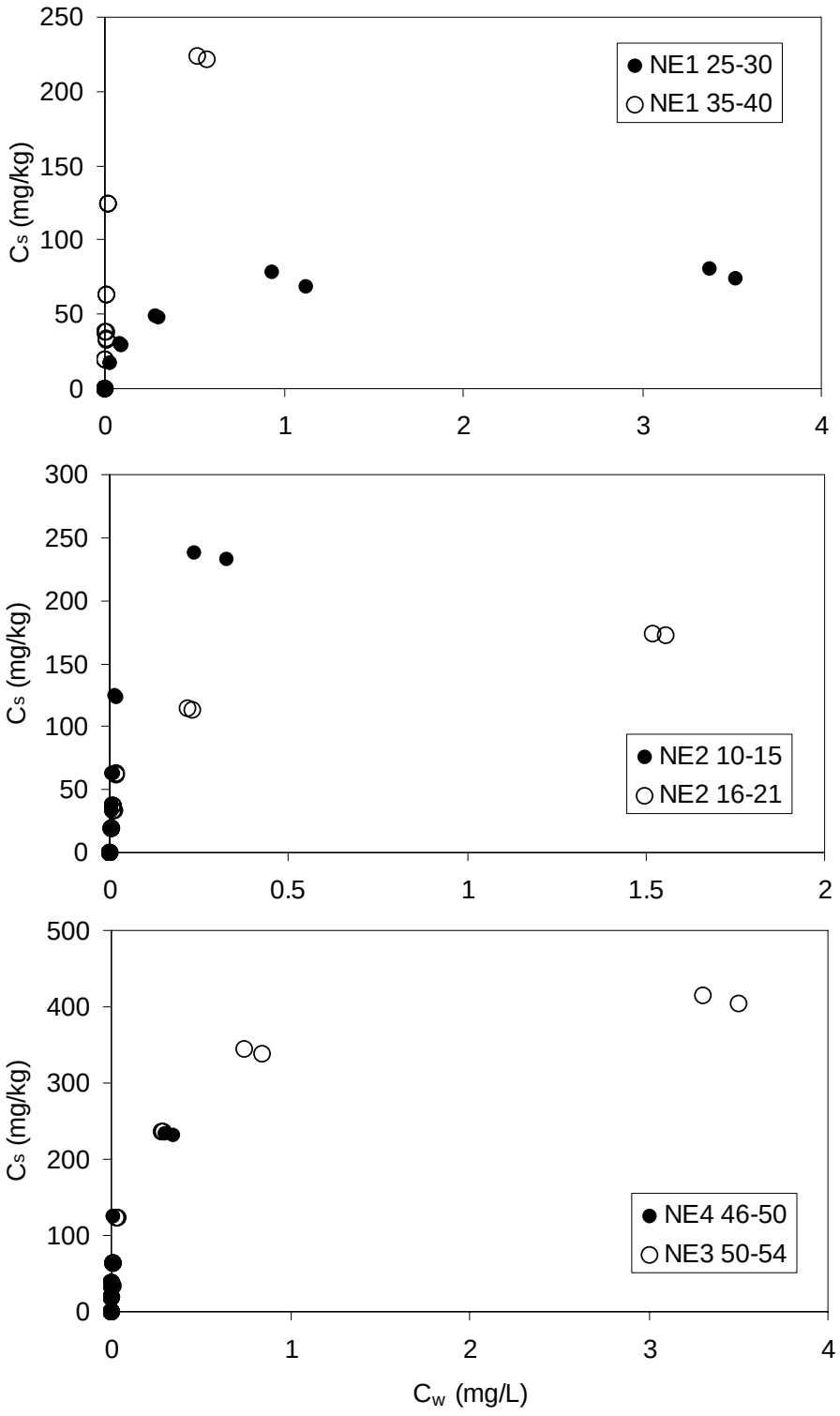

Figure 3-1
As(V) sorption isotherms for NE site soils.

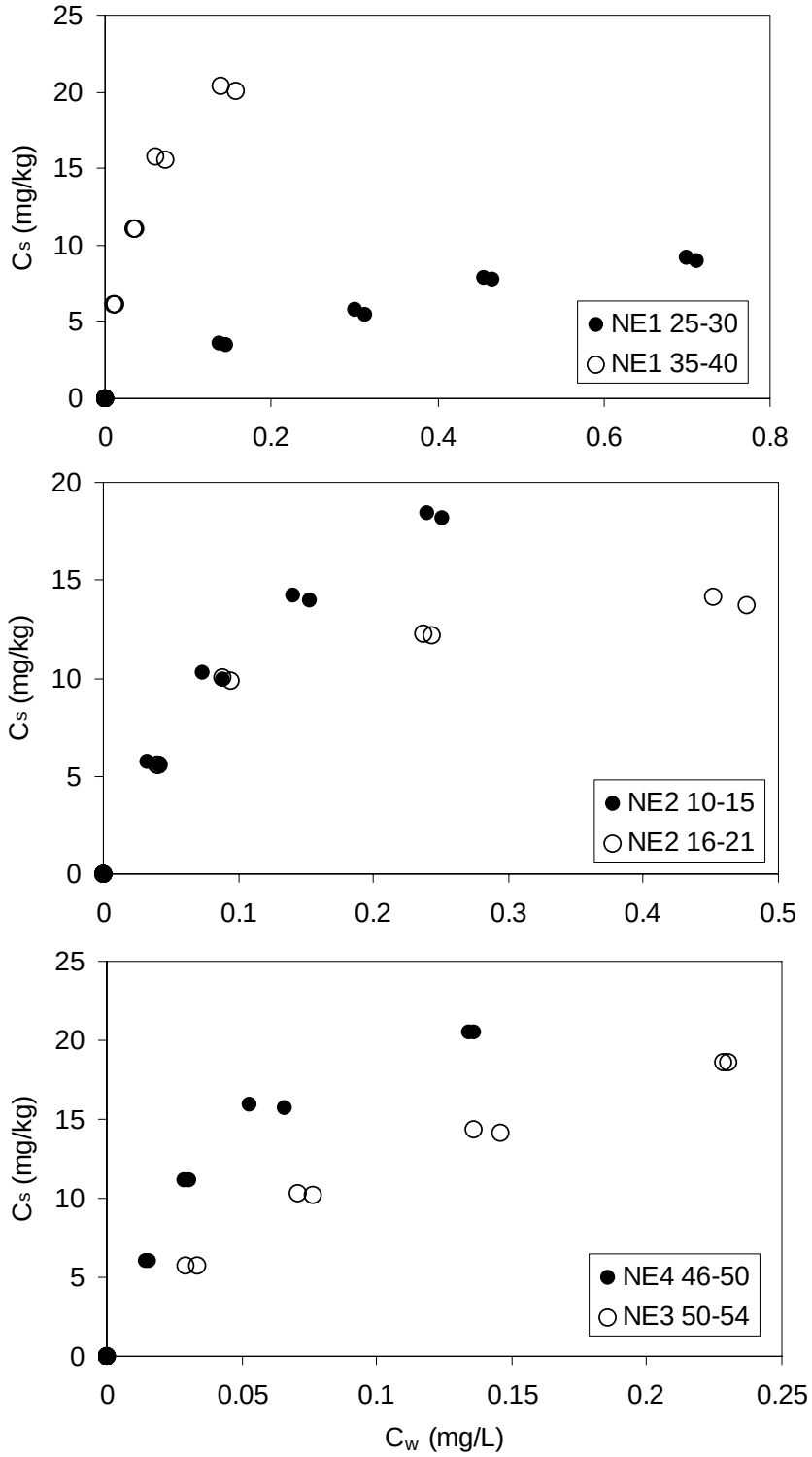

Figure 3-2
As(III) sorption isotherms for NE site soils.

Table 3-2
Isotherm fits for arsenate [As(V)] adsorption from 0.001 M $CaSO_4$ for NE site soils.

	Freundlich Parameters			Langmuir Parameters		
Soil	K_f	N	r^2	K_L	$C_{s,max}$	r^2
NE1 25-30	61.3	0.259	0.935	6.6	81.3	0.977
NE1 35-40	275.2	0.31	0.895	47.3	235.2	0.961
NE2 10-15	380.4	0.363	0.93	50	254.9	0.987
NE2 16-21	157.3	0.28	0.975	29	158.8	0.95
NE3 50-54	310.5	0.29	0.968	10.5	387.2	0.967
NE4 46-50	341.1	0.31	0.921	84.1	244.7	0.984

Table 3-3
Isotherm fits for arsenite [As(III)] adsorption from 0.001 M $CaSO_4$ for NE site soils.

	Freundlich Parameters			Langmuir Parameters		
Soil	K_f	N	r^2	K_L	$C_{s,max}$	r^2
NE1 25-30	11.4	0.57	0.973	2	15.7	0.982
NE1 35-40	45.7	0.41	0.971	25.5	25.3	0.979
NE2 10-15	41.4	0.57	0.981	6.3	28.9	0.984
NE2 16-21	18.27	0.31	0.91	15.5	15.8	0.977
NE3 50-54	42.8	0.56	0.993	7.3	29.3	0.99
NE4 46-50	53	0.46	0.948	21.8	27.6	0.986

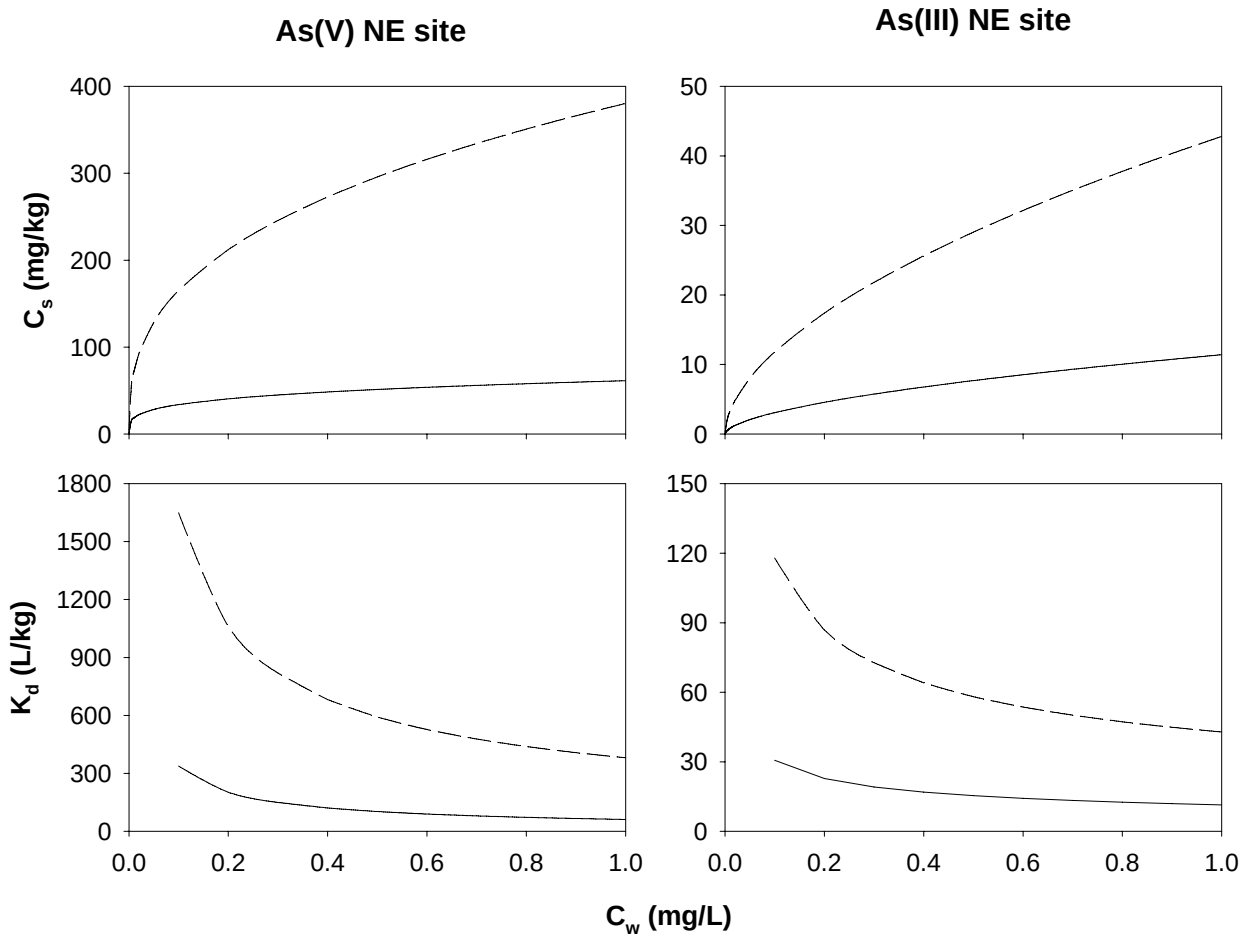

Figure 3-3
As(V) and As(III) sorption for NE site soils using NE1 25-30 soil (solid line) and NE2 10-15 soil (dashed line). Upper plots are isotherms; lower plots show concentration-specific K_d^*.

SE Site

Soil Characterization Data

Selected soil properties for six soils representative of the SE site are shown in Table 3-4. The SE site soils contained less than 5% clay, which was dominated by kaolinite and illite, with kaolinite being the dominant clay mineral in all soils except SE3 38.5 and SE2 23.5. Soils contained less than 1% organic matter and their soil-water pH values ranged from 5.6 to 6.4. Selective Fe dissolution of the soils resulted in DC-extractable Fe levels ranging from approximately 5,243 to 14,948 mg/kg, and DC-extractable Al levels ranging from 150 to 900 mg/kg. Ranges in oxalate extractable Fe and Al were less variable, with oxalate extractable Fe ranging from 245 to 757 mg/kg, and oxalate extractable Al ranging from 228 to 486 mg/kg. Based on the assumption

that the oxalate extraction primarily dissolves amorphous Fe and Al oxides, the differences between DC and oxalate extracts indicate that 4 to 8% of extractable Fe in the soils is amorphous, and that half to all of extractable Al is amorphous. Fe extracted in 15 seconds with DCB ranged from 56 to 330 mg/kg, and was intended to estimate the most reactive portion of Fe oxides (i.e., Fe oxides exposed to solution and readily available for reaction).

Arsenic Adsorption on SE Site Soils

Adsorption data for As(V) and As(III) on the six soils representative of the SE site were measured and fitted with Freundlich and Langmuir isotherm models. As(V) and As(III) isotherms are plotted in Figures 3-4 and 3-5, and modeling fits are summarized in Tables 3-5 and 3-6. Values of K_f ($mg^{1-N}\ L^N\ kg^{-1}$) ranged between 30 and 184 for As(V) sorption, and between 5 and 23 for As(III), which are lower than observed for NE site soils. Sorption was more nonlinear for SE site soils than NE site soils, with Freundlich N values as low as 0.13 and ranging to 0.28 for As(V) and 0.22 to 0.35 for As(III). Sorption of As(V) is again consistently much higher than that observed for As(III), with Freundlich K_f values being 4 to 14 times higher for As(V); similar trends are evident for the Langmuir $C_{s,max}$ values as well. To exemplify the overall arsenic sorption behavior at the SE site, As(V) and As(III) isotherms for the lowest and the highest sorption measured for the six soils considered representative of the site soils, as well as the effect of nonlinearity on the concentration-specific K_d^* values that would be used to estimate site-specific transport, are shown in Figure 3-6.

Table 3-4
Selected properties of 6 soils representative of the SE site.

Soil	pH $*_{H2O}$	pH $*_{CaCl2}$	Sand %	Silt %	Clay %	CEC (cmol/kg)	DC* - Fe (mg/kg)	DC* - Al (mg/kg)	Ox† - Fe (mg/kg)	Ox† - Al (mg/kg)	DCB - Fe 15 sec (mg/kg)	Base Saturation %	Organic Matter %	Bray P1- PO_4 (ppm)	Dominant Clay Minerals
SE1 48.5-50	5.7	5.4	62	33	5	4.3	7,105	450	576	486	150	72	0.6	8	K, I
SE1 60-62	6.0	5.8	56	39	5	4.8	14,948	900	757	423	330	75	0.7	8	K, I
SE2 23.5-25.5	6.1	6.1	66	31	3	4.1	8,399	182	413	305	56	71	0.3	31	K, I
SE2 33.5-35.5	6.4	6.2	60	35	5	2.7	5,243	280	245	228	60	100	0.2	19	K, I
SE3 5.5-7.5	5.6	5.4	66	29	5	3.1	6,209	280	226	395	84	62	0.4	4	K, I
SE3 38.5-40.5	6.2	6.1	62	35	3	4.1	6,647	150	500	243	73	71	0.4	32	K, I

* dithionite carbonate extractable; † oxalate extractable; I = illite, K = kaolinite

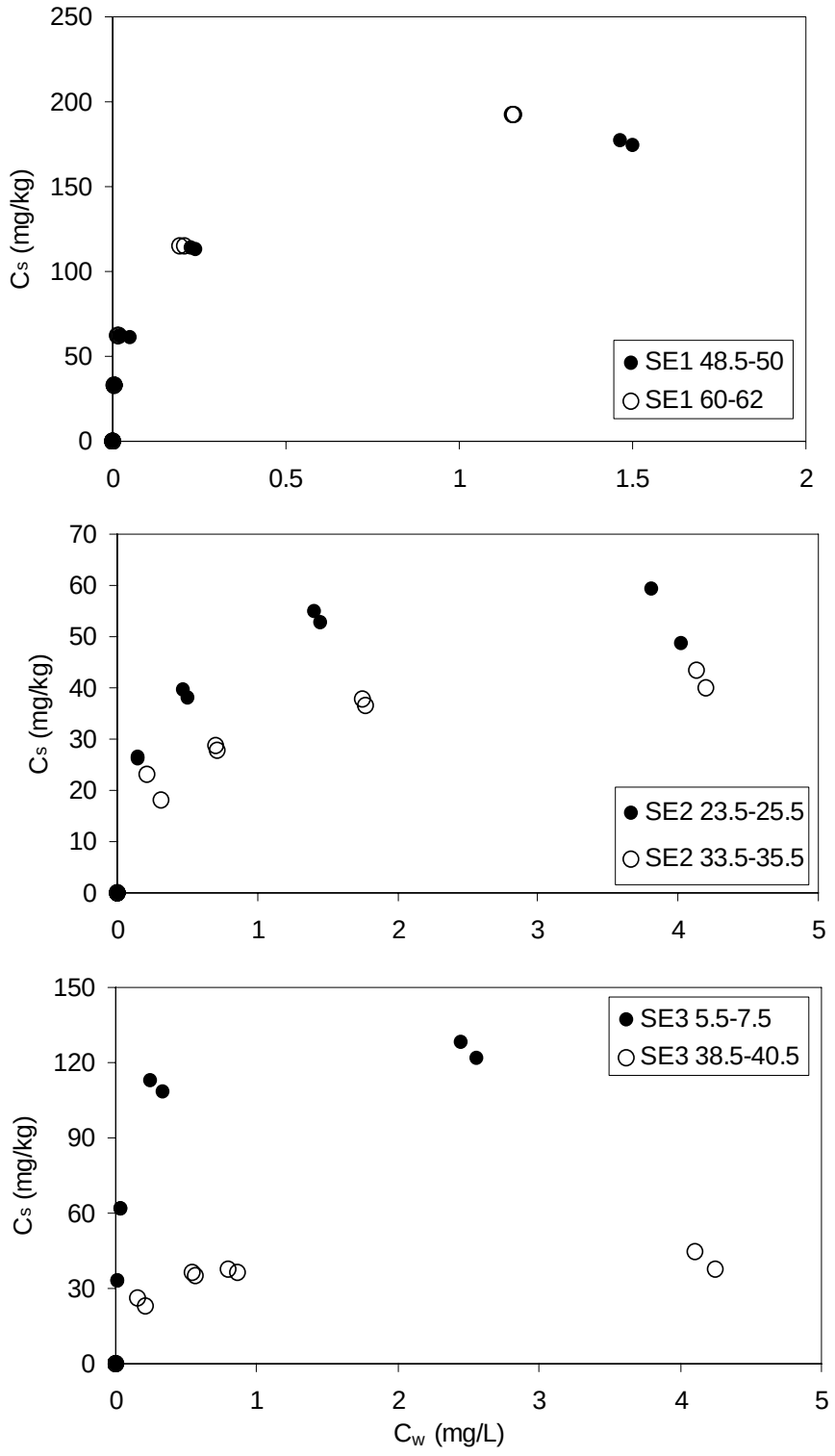

Figure 3-4
As(V) sorption isotherms for SE site soils.

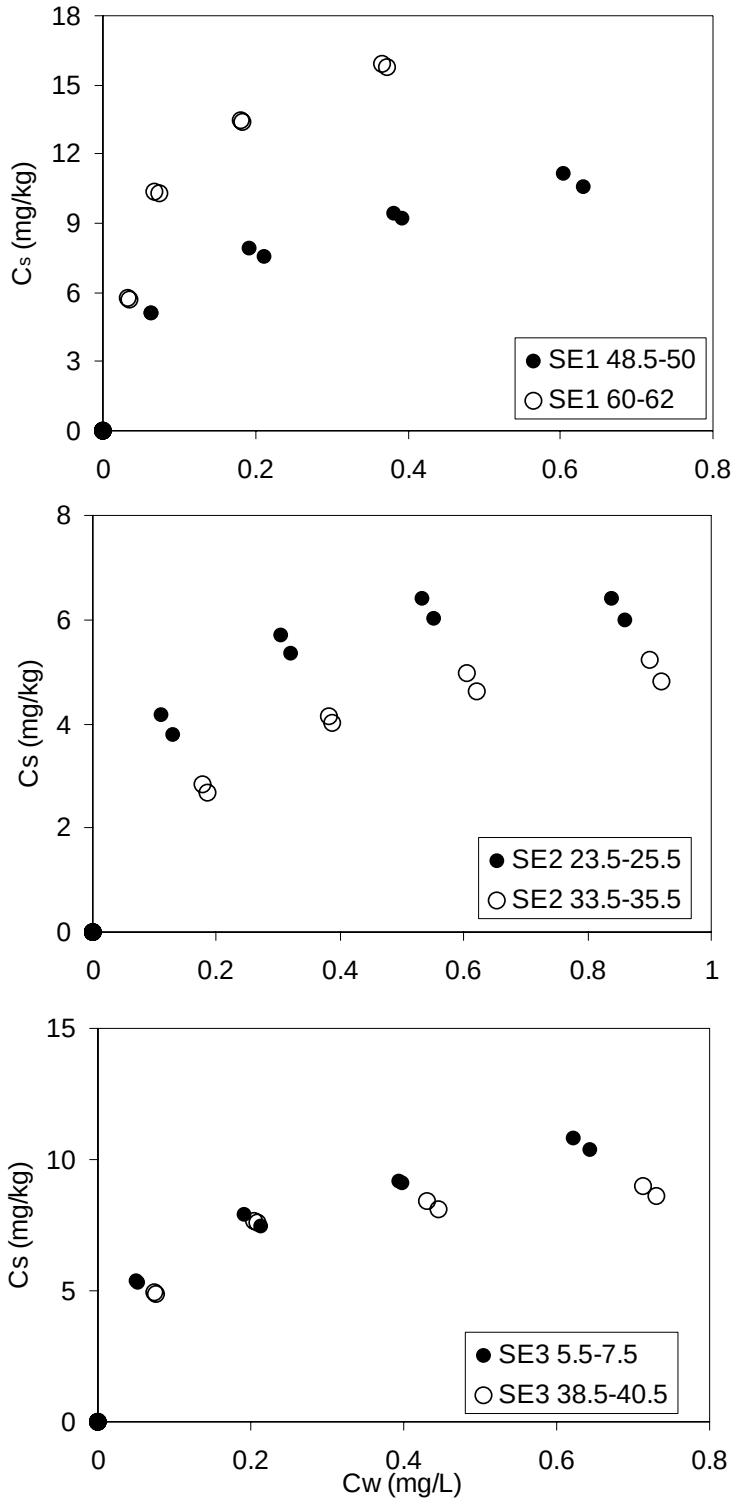

Figure 3-5
As(III) sorption isotherms for SE site soils.

Table 3-5
Isotherm fits for As(V) adsorption from 0.001 M $CaSO_4$ for SE site soils.

	Freundlich Parameters			Langmuir Parameters		
Soil	K_f	N	r^2	K_L	$C_{s,max}$	r^2
SE1 48.5-50	160.7	0.28	0.989	12.8	174.9	0.907
SE1 60-62	184.1	0.28	0.997	28.4	173.5	0.909
SE2 23.5-25.5	44.2	0.197	0.879	5.4	57.8	0.943
SE2 33.5-35.5	30.4	0.24	0.941	3	44.2	0.93
SE3 5.5-7.5	113.6	0.174	0.939	40.5	122.9	0.99
SE3 38.5-40.5	35.5	0.132	0.856	8	42.8	0.929

Table 3-6
Isotherm fits for As(III) adsorption from 0.001 M $CaSO_4$ for SE site soils.

	Freundlich Parameters			Langmuir Parameters		
Soil	K_f	N	r^2	K_L	$C_{s,max}$	r^2
SE1 48.5-50	12.7	0.32	0.99	10.3	12.1	0.972
SE1 60-62	23.2	0.35	0.975	15.1	18.6	0.994
SE2 23.5-25.5	6.8	0.22	0.837	11.5	7	0.91
SE2 33.5-35.5	5.4	0.35	0.91	4.4	6.4	0.958
SE3 5.5-7.5	11.9	0.272	0.997	15.9	10.9	0.983
SE3 38.5-40.5	9.8	0.22	0.878	14.9	9.7	0.973

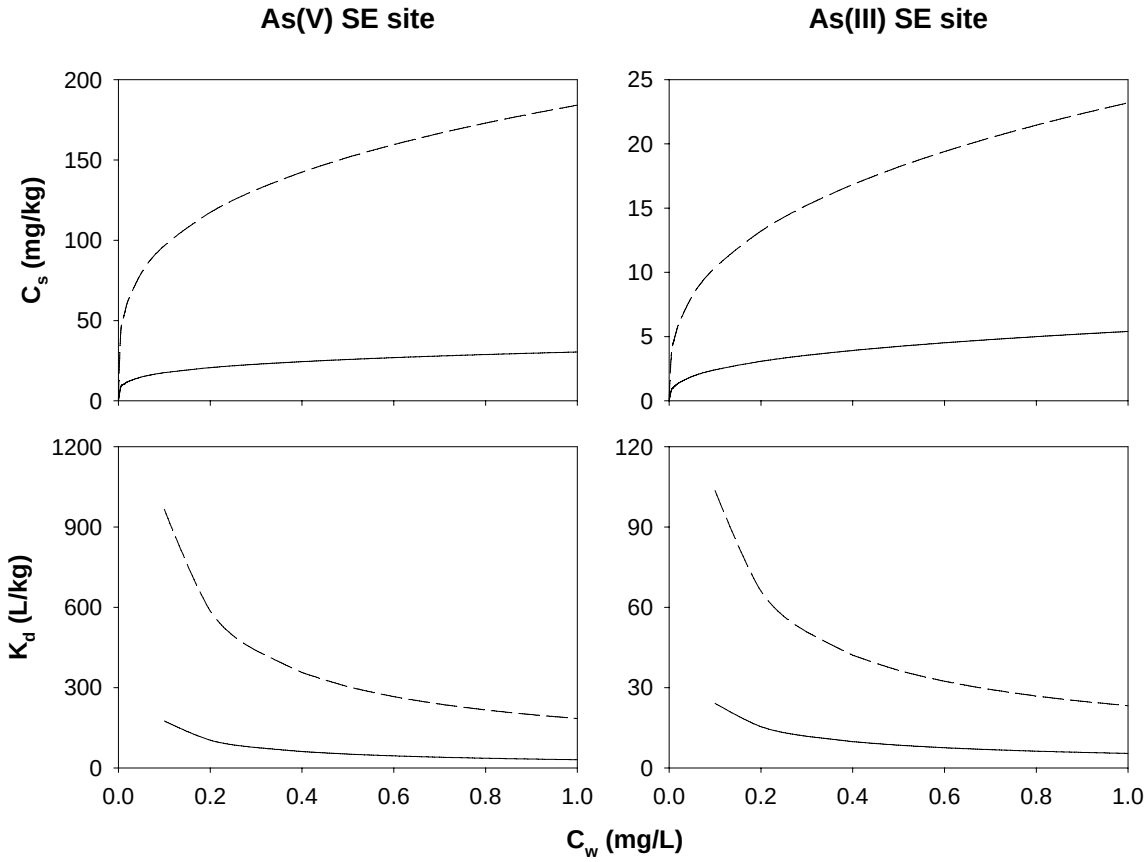

Figure 3-6
As(V) and As(III) sorption for SE site soils using SE2 33.5-35.5 soil (solid line) and SE3 60-75 soil (dashed line). Upper plots are isotherms; lower plots show concentration-specific K_d^*.

MW Site

Soil Characterization Data

Selected soil properties for six soils representative of the MW site are shown in Table 3-7. Most of the MW site soils contained less than 1% clay; therefore, clay type was not pursued. Soils contained less than 0.5% organic matter and their soil-water pH values ranged from 6.8 to 8.1. Selective Fe dissolution of the soils resulted in DC-extractable Fe levels ranging from 2,718 to 4,540 mg/kg, and DC-extractable Al levels ranging from 175 to 610 mg/kg. Ranges in oxalate extractable Fe and Al were less variable, with oxalate extractable Fe ranging from 217 to 570 mg/kg, and oxalate extractable Al ranging from 78 to 456 mg/kg. Based on the assumption that the oxalate extraction primarily dissolves amorphous Fe and Al oxides, the differences between DC and oxalate extracts indicate that 4 to 13% of extractable Fe in the soils is amorphous, and 39 to 100% of extractable Al is amorphous. Fe extracted in 15 seconds with

DCB ranged from 8 to 69 mg/kg, and was intended to estimate the most reactive portion of Fe oxides (i.e., Fe oxides exposed to solution and readily available for reaction).

Arsenic Adsorption on MW Site Soils

Adsorption data for As(V) and As(III) on the six soils representative of the MW site were measured and fitted with Freundlich and Langmuir isotherm models. As(V) and As(III) isotherms are plotted in Figures 3-7 and 3-8, and modeling fits are summarized in Tables 3-8 and 3-9. Values of K_f (mg^{1-N} m^N kg^{-1}) ranged between 28 and 48 for As(V) sorption, and between 5 and 17 for As(III), which are the lowest observed for the soils from the three sites. Although sorption was lowest on the MW site soils, sorption isotherms exhibited less nonlinearity, with Freundlich N values of 0.25 to 0.44 for As(V) and 0.57 to 0.83 for As(III). Sorption of As(V) is consistently higher than that observed for As(III), with both Freundlich K_f values being 2.5 to 7.4 times higher for As(V); similar trends are evident for the Langmuir $C_{s,max}$ values as well. Differences between As(III) and As(V) were less than observed for the soils at the two other sites. The overall arsenic sorption behavior at the SE site is exemplified in Figure 3-9, with As(V) and As(III) isotherms for the lowest and the highest sorption observed for the six site soils shown, as well as the effect of nonlinearity on the concentration-specific K_d^* values that would be used to estimate site-specific transport.

Table 3-7
Selected properties of 6 soils representative of the MW site.

Soil	pH*$_{H2O}$	pH*$_{CaCl2}$	Sand %	Silt %	Clay %	CEC (cmol/kg)	DC* - Fe (mg/kg)	DC* - Al (mg/kg)	Ox† - Fe (mg/kg)	Ox† - Al (mg/kg)	DCB - Fe 15 sec (mg/kg)	Base Saturation %	Organic Matter %	Bray P1-PO_4 (ppm)
MW1 17-19	8.1	7.3	93	4	3	3	4540	610	570	456	69	100	0.3	22
MW1 33-35	7.7	6.9	95	4	1	1.4	3781	198	145	78	15	100	0.3	5
MW2 17-19	7.5	6.2	95	4	1	1.4	3312	382	261	253	28	100	0.4	11
MW2 25-27	6.8	6.3	97	2	1	1.4	3143	175	217	95	12	97	0.4	4
MW3 17-19	7.7	6.8	95	4	1	1.7	2718	389	299	384	23	100	0.2	15
MW3 23-25	8.0	6.8	95	4	1	1.4	2964	105	241	105	8	100	0.5	4

* dithionite carbonate extractable; † oxalate extractable

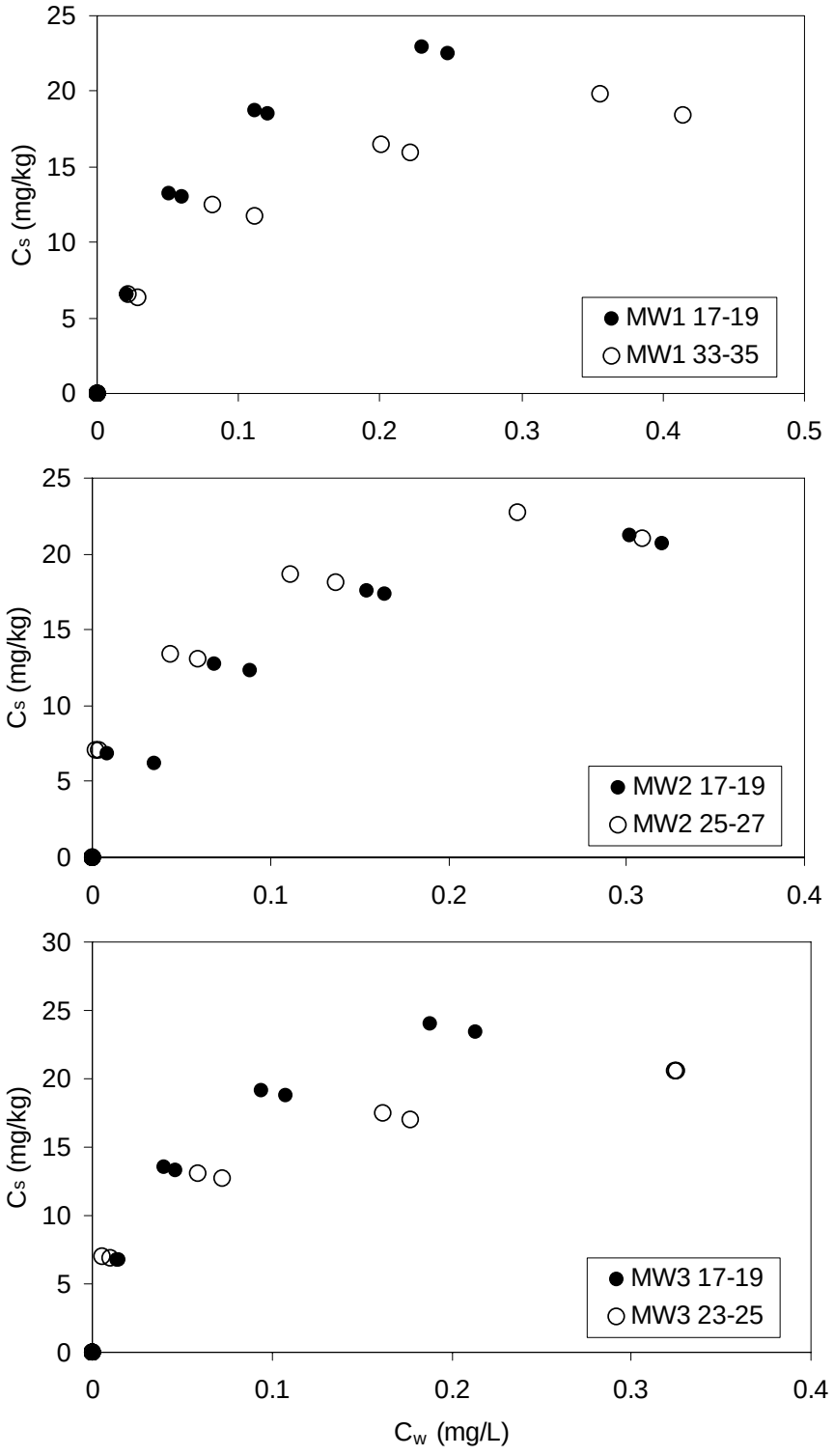

Figure 3-7
As(V) sorption isotherms on MW site soils.

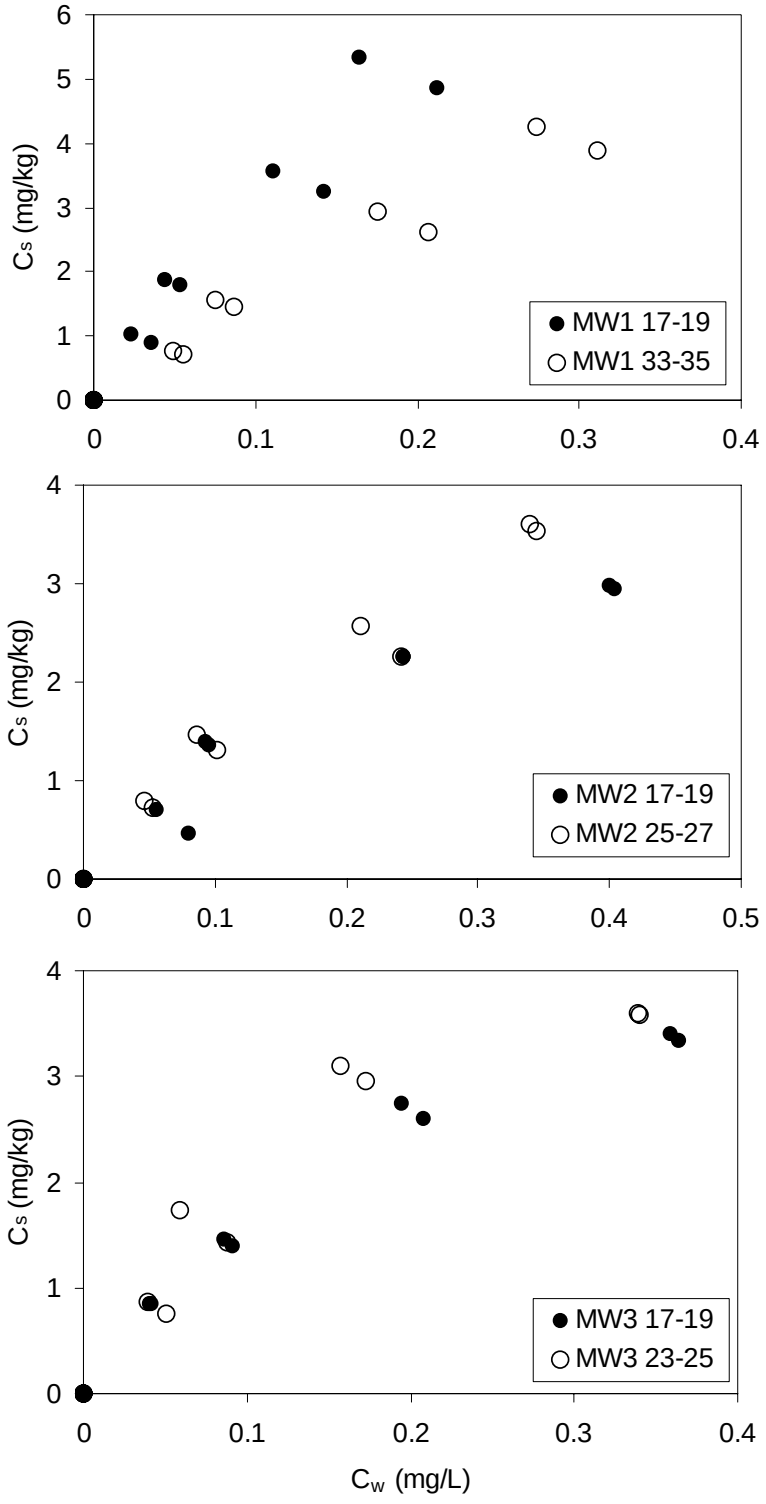

Figure 3-8
As(III) sorption isotherms on MW site soils.

Table 3-8
Isotherm fits for As(V) adsorption from 0.001 M $CaSO_4$ for MW site soils.

	Freundlich Parameters			Langmuir Parameters		
Soil	K_f	N	r^2	K_L	$C_{s,max}$	r^2
MW1 17-19	44	0.435	0.967	14.7	29.4	0.996
MW1 33-35	27.6	0.364	0.967	14.5	21.9	0.966
MW2 17-19	33.6	0.387	0.95	12.5	26.1	0.918
MW2 25-27	30.1	0.251	0.967	145.9	19.4	0.825
MW3 17-19	47.6	0.417	0.977	20.2	29.1	0.992
MW3 23-25	28.5	0.29	0.993	40.1	20.5	0.907

Table 3-9
Isotherm fits for As(III) adsorption from 0.001 M $CaSO_4$ for MW site soils.

	Freundlich Parameters			Langmuir Parameters		
Soil	K_f	N	r^2	K_L	$C_{s,max}$	r^2
MW1 17-19	16.9	0.747	0.91	3.4	12.3	0.917
MW1 33-35	11.1	0.832	0.949	1.3	14	0.952
MW2 17-19	5.6	0.68	0.938	2	6.8	0.944
MW2 25-27	7.9	0.765	0.972	1.8	8.7	0.966
MW3 17-19	6.4	0.599	0.98	4.1	5.7	0.992
MW3 23-25	7	0.566	0.895	5.2	5.8	0.928

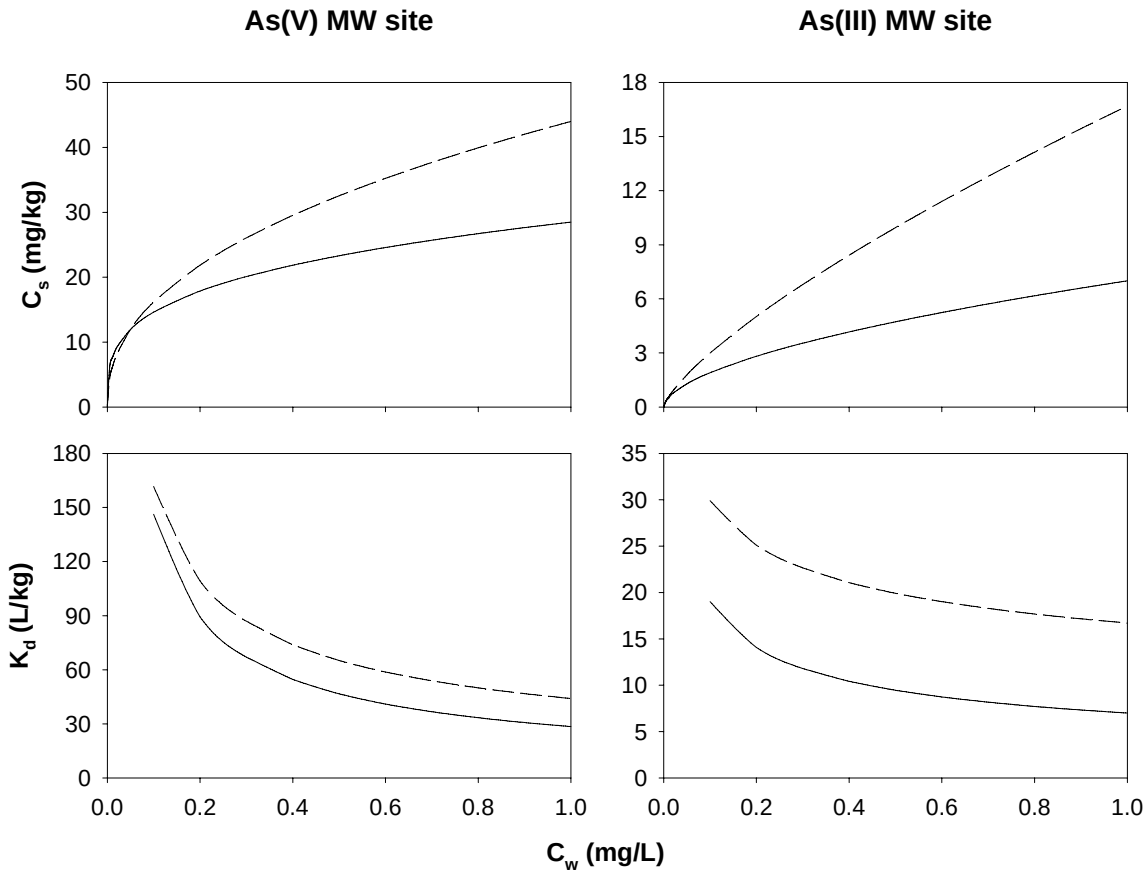

Figure 3-9
As(V) and As(III) sorption for MW site using MW3 23-25 soil (solid line) and MW1 17-19 soil (dashed line). Upper plots are isotherms; lower plots show concentration-specific K_d^*.

4
FACTORS AFFECTING ARSENIC SORPTION

Solution pH Effect on Arsenic Adsorption

Adsorption envelopes (upper graphs) and adsorption isotherms (lower graphs) produced for each arsenic species, at varying pH values, are shown in Figures 4-1 through 4-4 for two NE site soils. A significant influence of pH on both As(V) and As(III) adsorption is apparent, especially at the more alkaline pH values. However, the influence is small, within ±1 pH unit of the native soil pH for the NE site soils, which are acidic soils. One exception is As(III) sorption on soil sample NE1 25-30 (Figure 4-4b).

Features of the adsorption envelopes are similar to those reported for pure minerals. For example, As(III) adsorption onto soil sample NE1 25-30 displays an adsorption maxima at a pH greater than 8 (Figure 4-4b), corresponding to the adsorption behavior of As(III) onto aluminum hydroxides or alumino-silicates. For soil sample NE2 10-15, As(III) adsorption corresponded more closely to the reported adsorption behavior of As(III) onto iron oxides, with adsorption remaining relatively constant except at very high or very low pH values (Figure 4-3a). In contrast to As(III), the adsorption envelopes for As(V) for both NE site soils were similar, and corresponded to the behavior reported for arsenate adsorption on iron oxides/oxyhydroxides. As predicted from the pH envelopes and the native soil pH values, the effect of pH near the site-soil pH values on arsenic sorption was negligible except for As(III) sorption by soil sample NE1 25-30.

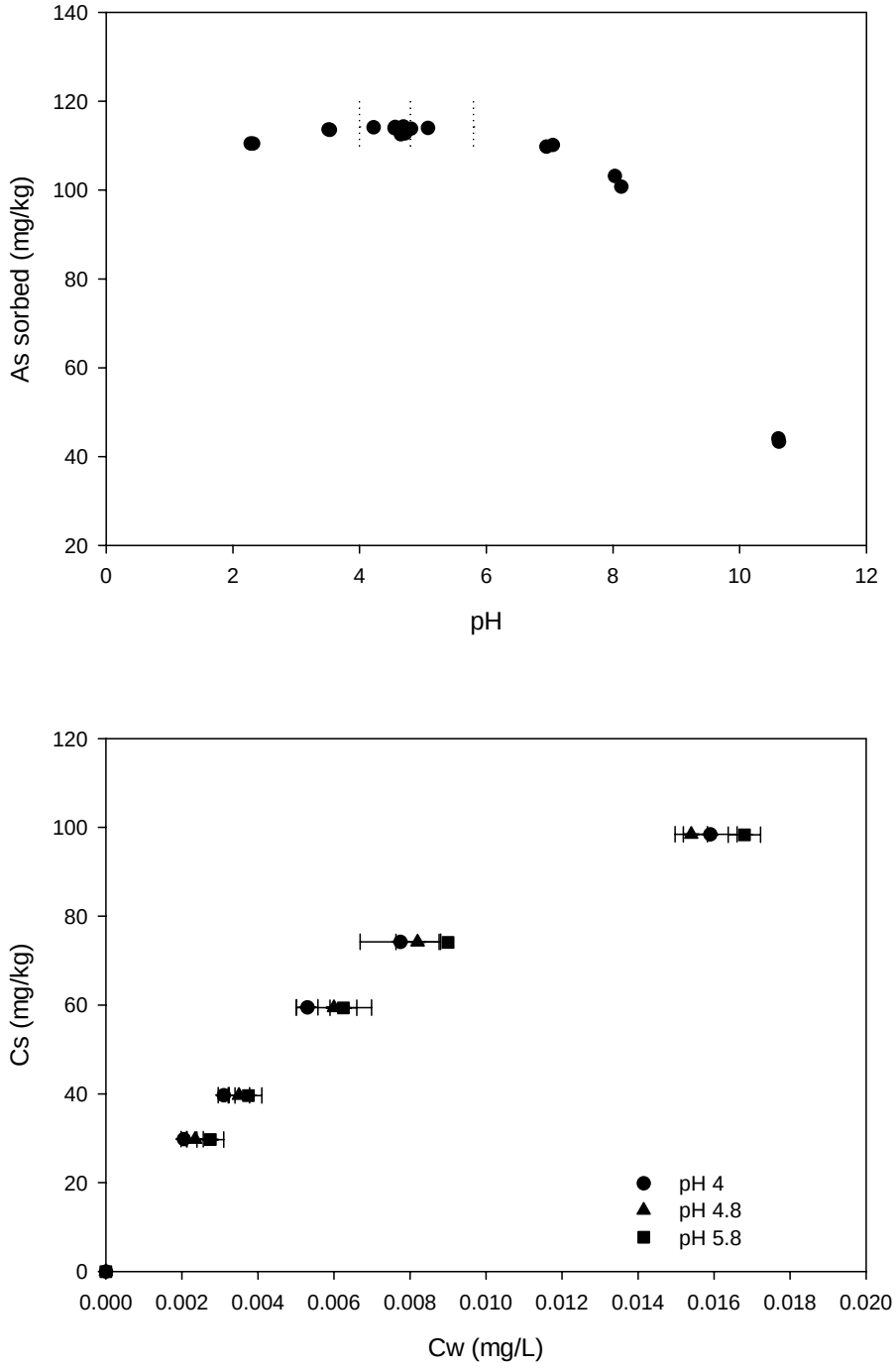

Figure 4-1
pH effects on As(V) adsorption on NE2 10-15: (a) Arsenate adsorption envelope at varying soil suspension pH values; (b) Arsenate adsorption isotherms at pH 4.0, 4.8, and 5.8.

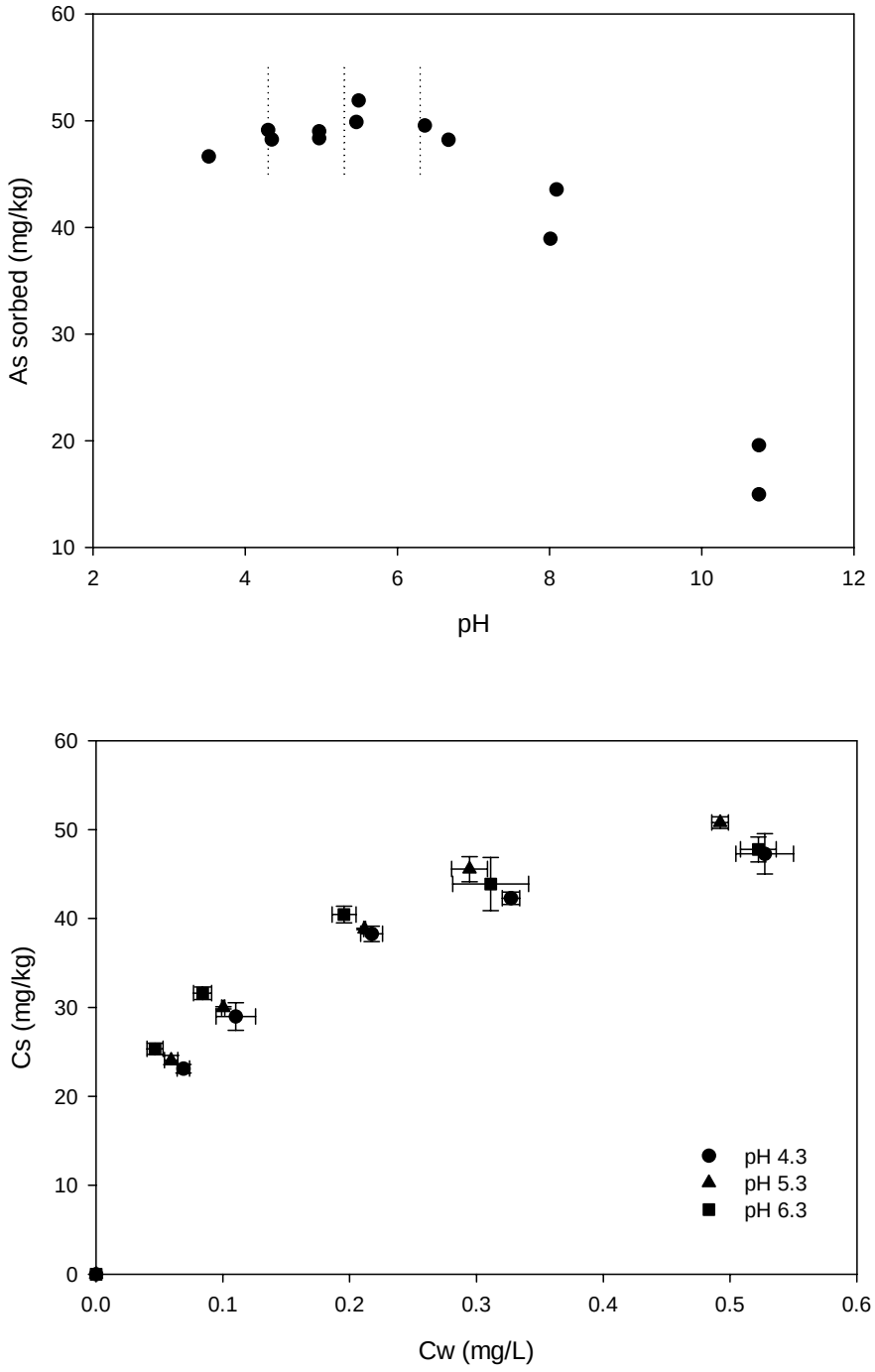

Figure 4-2
pH effects on As(V) adsorption on NE1 25-30: (a) Arsenate adsorption envelope at varying soil suspension pH values; (b) Arsenate adsorption isotherms at pH 4.3, 5.3, and 6.3.

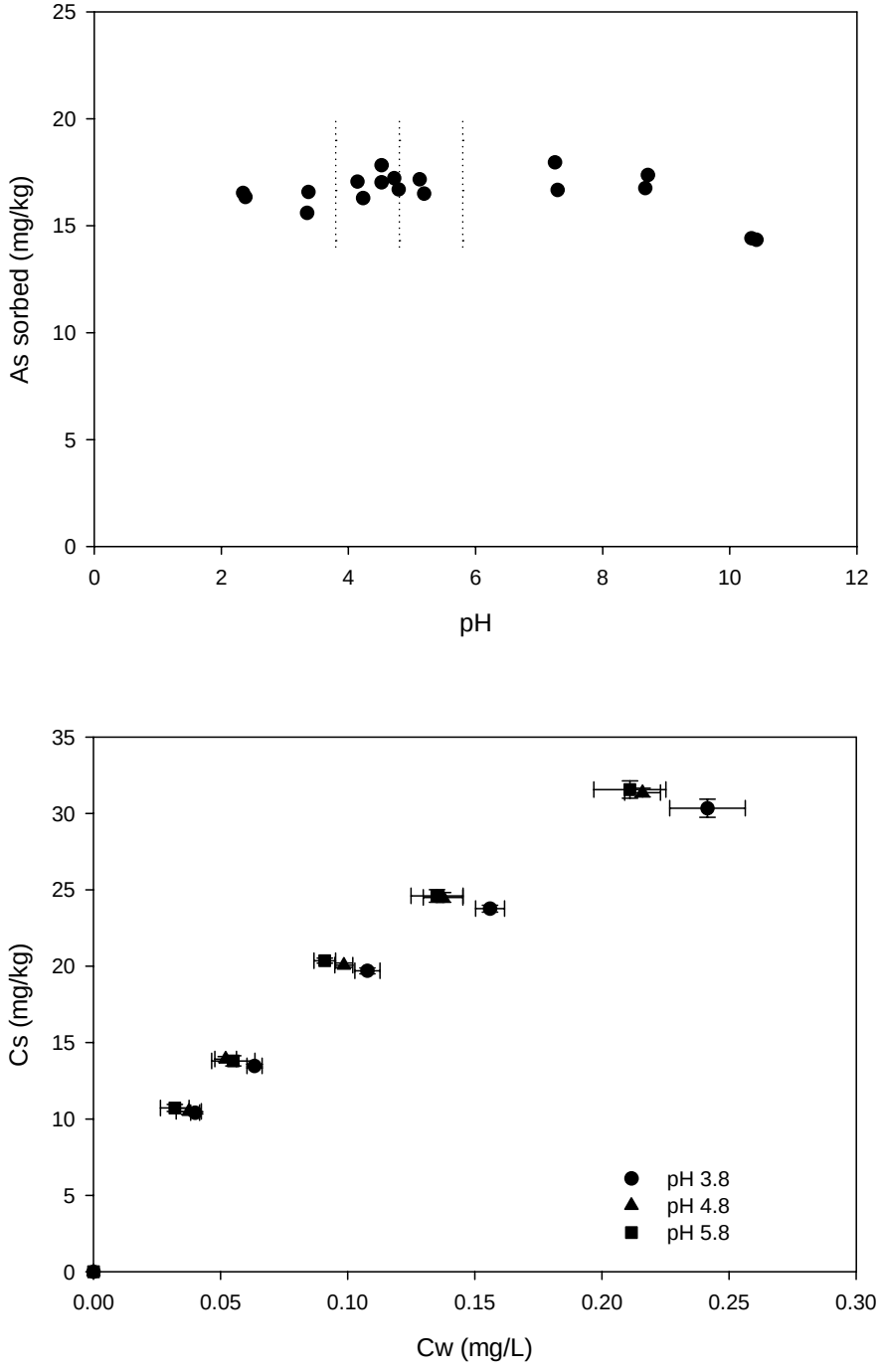

Figure 4-3
pH effects on As(III) adsorption on NE2 10-15: (a) Arsenite adsorption envelope at varying soil suspension pH values; (b) Arsenite adsorption isotherms at pH 3.8, 4.8, and 5.8.

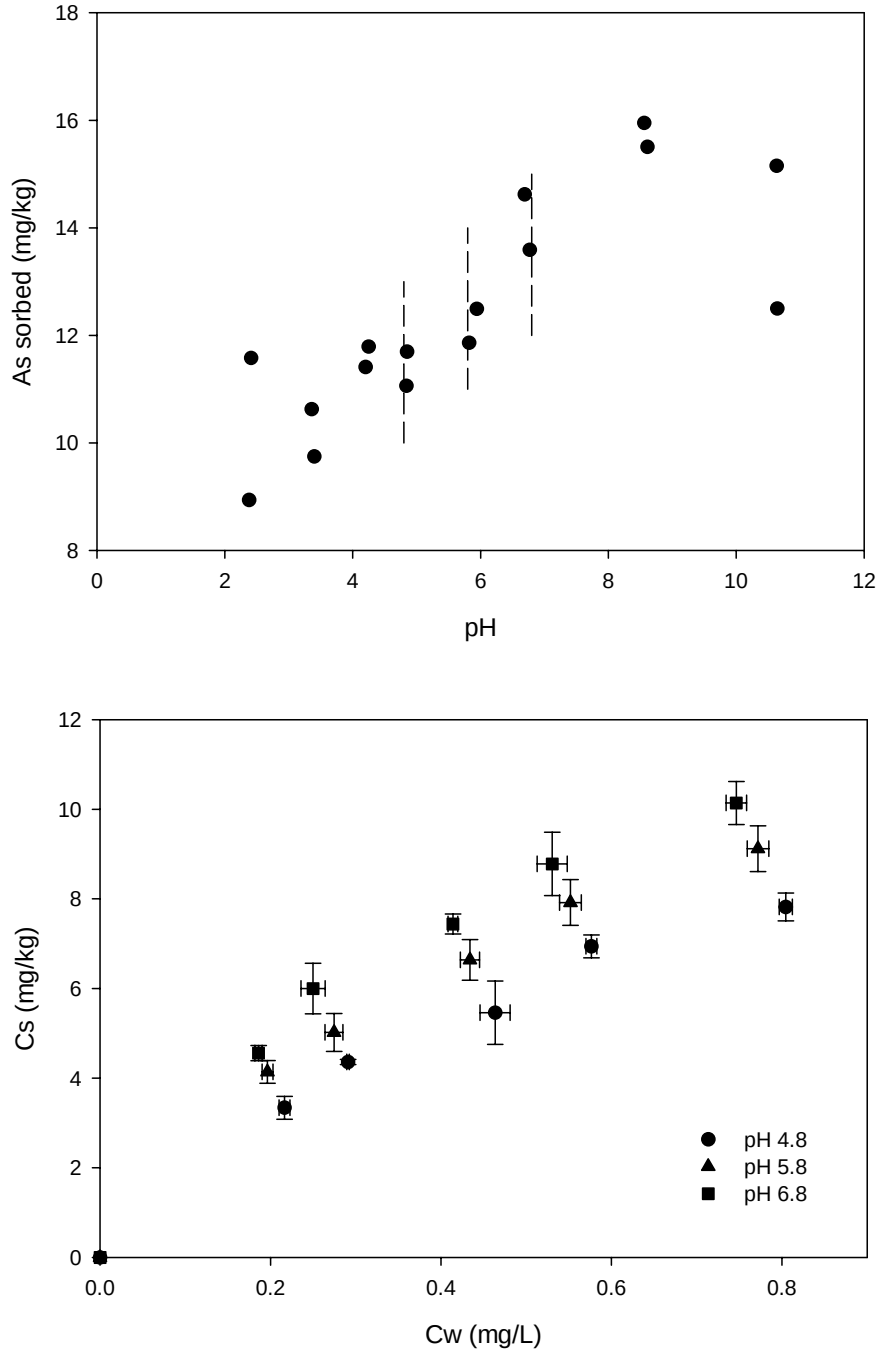

Figure 4-4
pH effects on As(III) adsorption on NE1 25-30: (a) Arsenite adsorption envelope at varying soil suspension pH values; (b) Arsenite adsorption isotherms at pH 4.8, 5.8, and 6.8.

Solution Matrix Effects on Arsenic Adsorption

The effect of sulfate and calcium on sorption of As(V) and As(III) on two NE site soils is depicted in Figures 4-5 through 4-8, with the upper graph (a) in each figure summarizing the effect of varied sulfate and calcium concentrations on arsenic absorption/adsorption from a fixed concentration of As (1 mg/L for As(V) and 0.75 mg/L for As(III)). The lower graph in each figure is the multi-concentration isotherms from 10^{-3} M KCl (I = 0.001 M), 10^{-3} M $CaCl_2$ (I=0.003 M), 10^{-3} M K_2SO_4 (I=0.003 M), and 10^{-3} M $CaSO_4$ (I=0.004 M).

Impact of sulfate concentration on adsorption was soil dependent and was most pronounced for As(III). For As(V) at a C_i = 1 mg/L, sorption decreased slightly (C_s = 108 to 105.2 mg/kg) with increasing sulfate concentrations from 0 to 10^{-2} M on soil sample NE2 10-15 (Figure 4-5a). The decrease was greater (52 to 39.5 mg/kg) on the NE1 25-30 soil (Figure 4-6a), which corresponds to decreases in As(V) sorption of 2.6% and 24%, respectively, for the two site soils. In Figures 4-5b and 4-6b, the single point data collected at the highest sulfate concentration is shown along with the multi-concentration isotherms. Note that the effect of sulfate on As(V) sorption appears to be greater at higher As(V) concentrations. This is most likely due to the fact that As(V) is preferentially sorbed over sulfate on the higher energy sites, but as only the lower energy sites remain (approaching an apparent plateau in isotherm, N<1 phenomenon), sulfate may compete more successfully for sorption sites. For As (III) at a C_i = 0.75 mg/L, increasing SO_4 concentrations from 0 to 10^{-2} M resulted in absorbed concentrations decreasing from 24.1 to 15.2 mg/kg for soil sample NE2 10-15 (Figure 4-7a) and from 10.1 to 5.6 mg/kg on soil sample NE1 25-30 (Figure 4-8a), corresponding to decreases in As(III) sorption of 37% and 45%, respectively.

Adsorption of As(V) was enhanced slightly in the presence of increasing concentrations of Ca (Figures 4-5 and 4-6), with the differences between the two soils being similar to what was observed with sulfate, whereas As(III) sorption was not influenced by changes in calcium concentrations (Figure 4-7 and 4-8). As the concentration of Ca was increased from 0 to 10^{-2} M the sorption of As(V) increased from 108 to 109.4 mg/kg on soil sample NE2 10-15 (Figure 6-5a) and 52 to 60 mg kg^{-1} on soil sample NE1 25-30 (Figure 4-6a), corresponding to increases in As(V) sorption of 1.3% and 15%, respectively. Similar increases in As(V) sorption in the presence of Ca have been reported in soils (Smith et al., 2002); however, little information is currently available concerning the specific mechanism of this enhanced sorption. Plausible explanations for this phenomenon include: (1) sorption of Ca^{2+} to negatively charged surface sites making the electrical potential at those sites less negative, thereby increasing the sorption of arsenate anions; and (2) the formation of intra-molecular bridges between arsenate ions and negatively charged surface sites (e.g., organic matter and alumino-silicate surfaces) by Ca^{2+} ions.

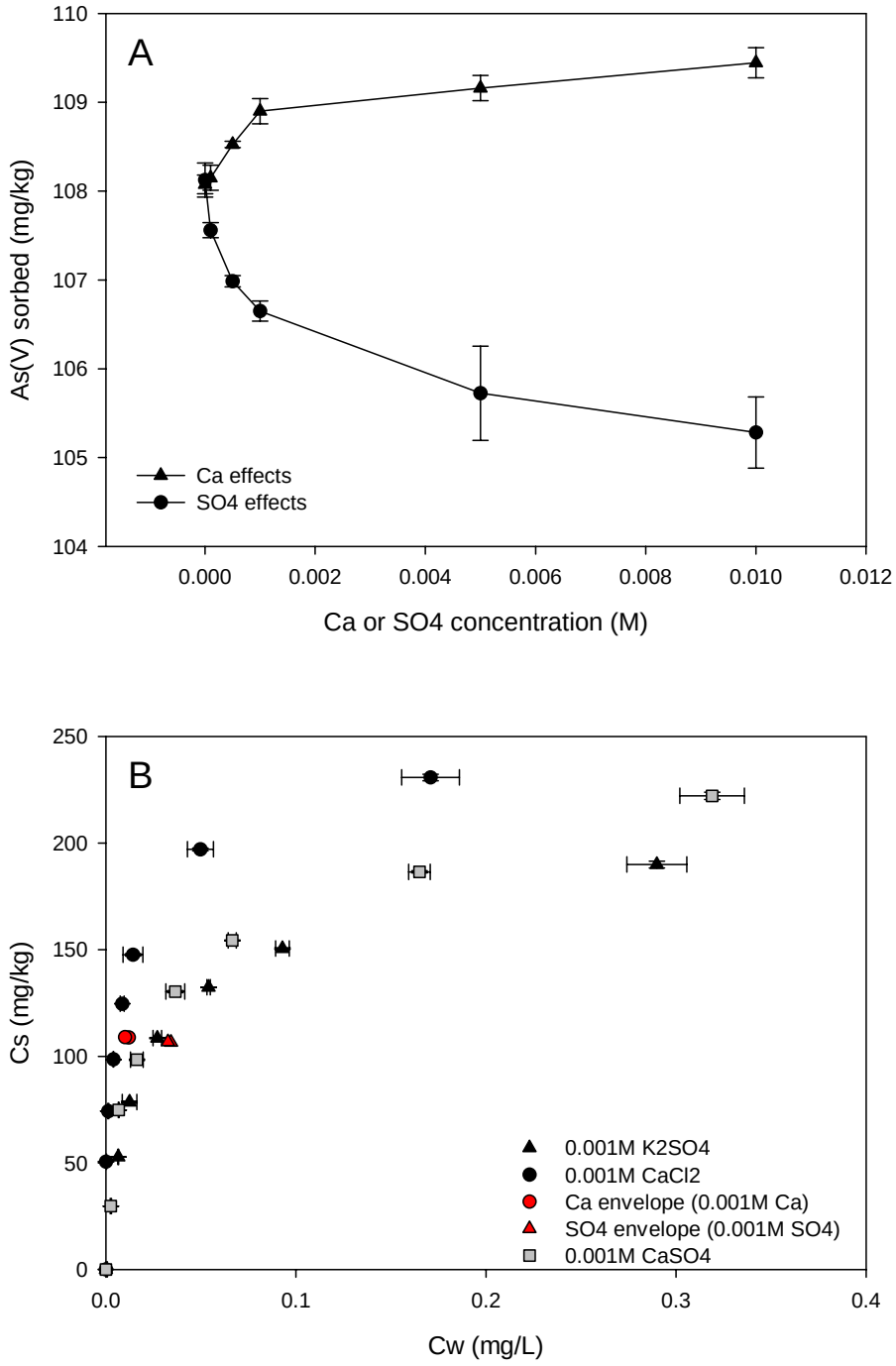

Figure 4-5
Ionic matrix effects on As(V) sorption onto NE2 10-15: (a) Arsenate adsorption envelopes in the presence of varying concentrations of Ca or SO_4 at a constant ionic strength of 0.03M; (b) Arsenate adsorption isotherms in 0.001M $CaCl_2$, 0.001M K_2SO_4, and 0.001M $CaSO_4$.

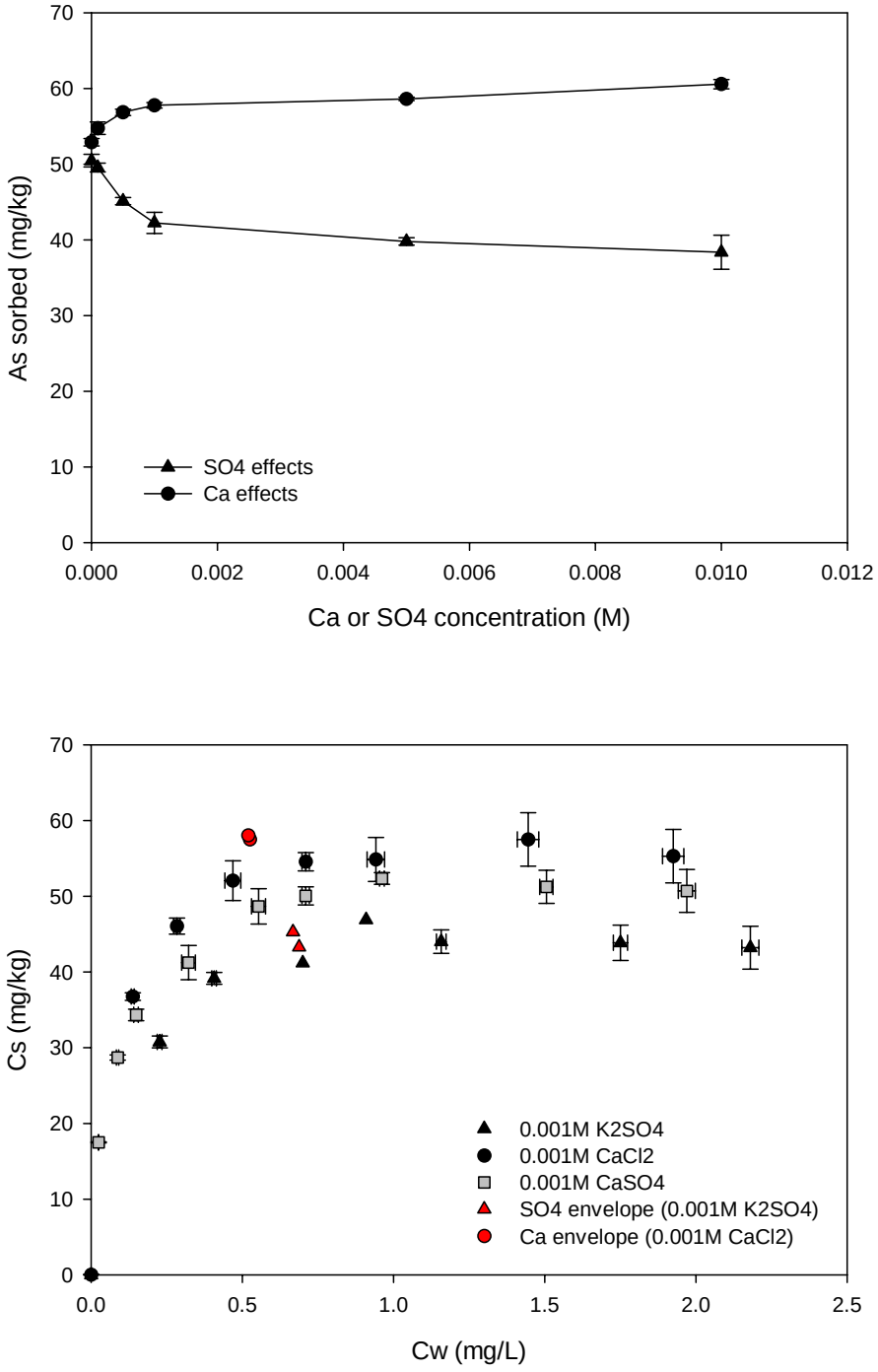

Figure 4-6
Ionic matrix effects on As(V) sorption onto NE1 25-30: (a) Arsenate adsorption envelopes in the presence of varying concentrations of Ca or SO_4 at a constant ionic strength of 0.03 M; (b) Arsenate adsorption isotherms in 0.001 M $CaCl_2$, 0.001 M K_2SO_4, and 0.001 M $CaSO_4$.

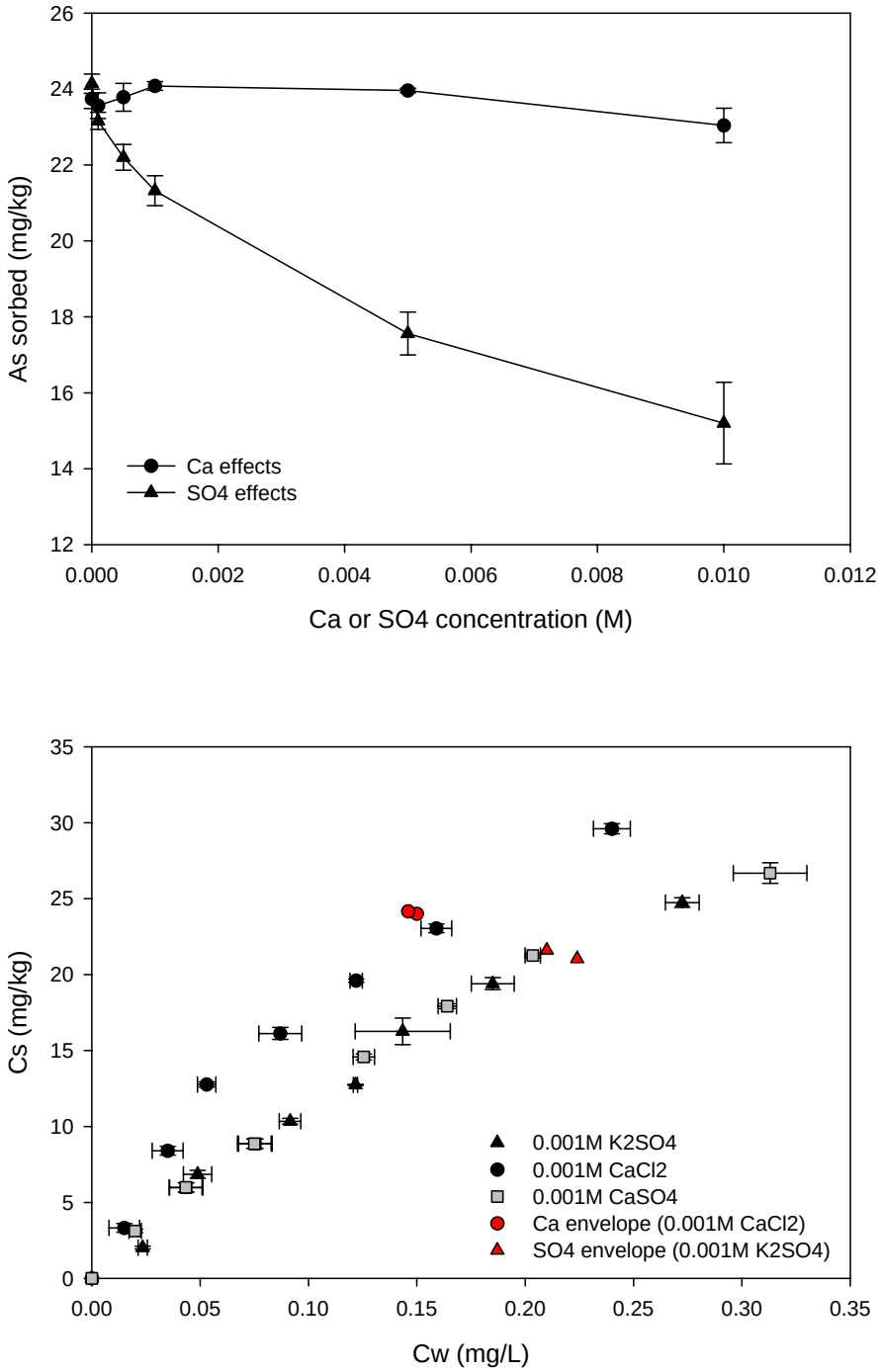

Figure 4-7
Ionic matrix effects on As(III) sorption onto NE2 10-15: (a) Arsenite adsorption envelopes in the presence of varying concentrations of Ca or SO_4 at a constant ionic strength of 0.03 M; (b) Arsenite adsorption isotherms in 0.001 M $CaCl_2$, 0.001 M K_2SO_4, and 0.001 M $CaSO_4$.

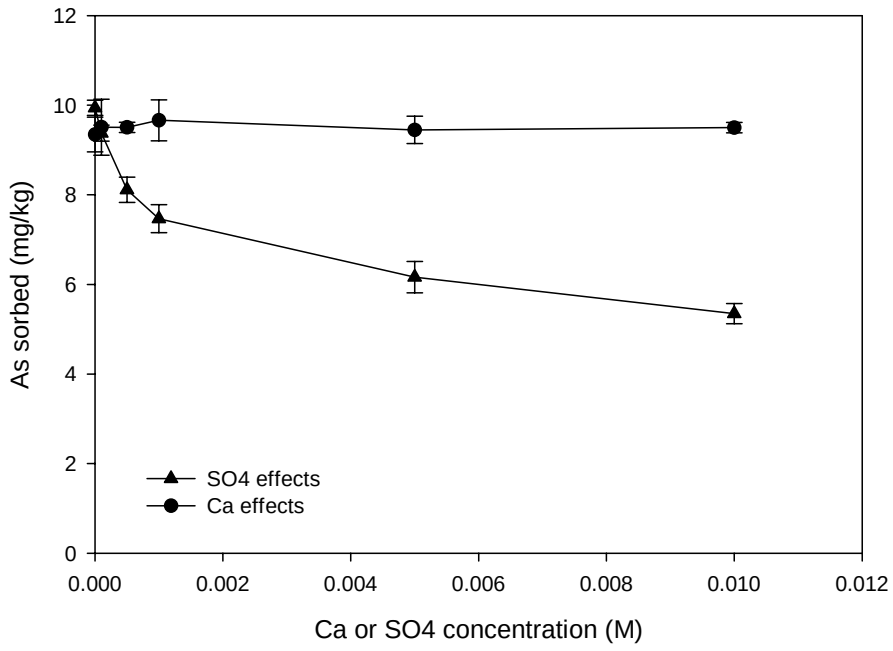

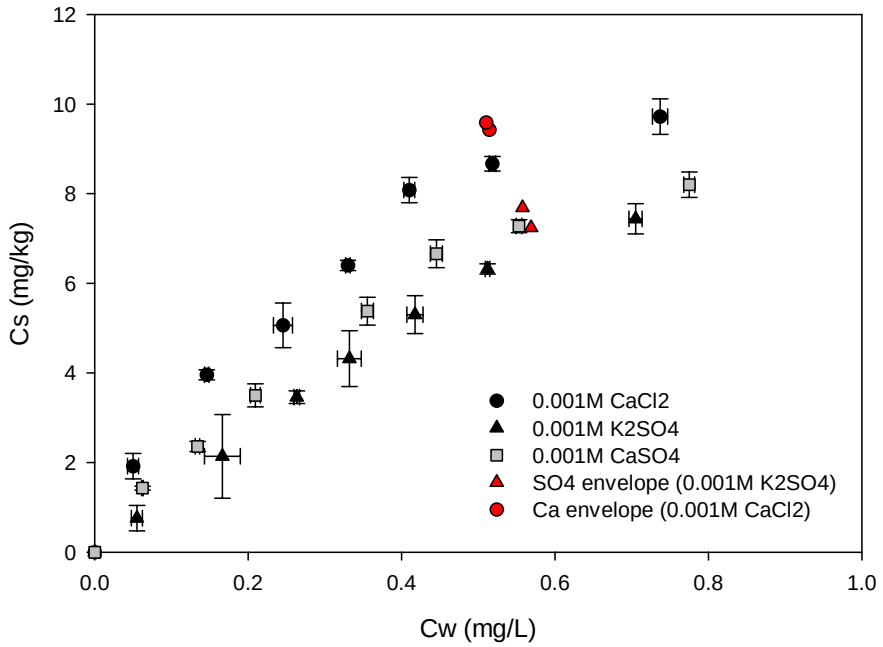

Figure 4-8
Ionic matrix effects on As(III) sorption onto NE1 25-30: (a) Arsenite adsorption envelopes in the presence of varying concentrations of Ca or SO_4 at a constant ionic strength of 0.03 M; (b) Arsenite adsorption isotherms in 0.001 M $CaCl_2$, 0.001 M K_2SO_4, and 0.001 M $CaSO_4$.

Sorption Data versus Soil Characteristics for All Sites

Based on previous studies, which have stressed the importance of Fe oxides in establishing adsorption capacities for As in soils (Manning and Goldberg 1997; Elkhatib et al.,1984), it was hypothesized that the Fe oxide content of the soils would be correlated to the adsorptive behavior of As. Linear regression analyses of both the Freundlich K_f and Langmuir model parameters with various soil parameters are summarized in Tables 4-1 and 4-2, respectively. The best correlations observed are with the 15-second DC extractable Fe and either Freundlich K_f values (0.726 and 0.730 for As(V) and As(III), respectively) or the Langmuir $C_{s,max}$ values (0.799 and 0.754 for As(V) and As(III), respectively), clearly exemplifying the role of easily reducible Fe sites in the adsorption of arsenic (Figure 4-9). Reasonable correlations also exist with DC extractable Fe and Al as well as % clay for As(V), and with DC extractable Al and clay for As(III), reflecting oxides in general, which reside in the clay size fraction. No reasonable correlations were obtained with the Langmuir K_L values (Table 4-3).

Table 4-1
Summary of linear regressions between various soil parameters and the mass-based Freundlich isotherm sorption coefficients.

Specie	Regression Parameter	pH_{H2O}	pH_{CaCl2}	% Clay	DC - Fe (mg/kg)	DC - Al (mg/kg)	Ox - Fe (mg/kg)	Ox - Al (mg/kg)	15-sec DCB-Fe (mg/kg)
As(III)	slope	-8.37	-11.27	1.446	0.001	0.031	0.009	0.068	0.029
	intercept	70.93	84.10	6.69	6.51	2.84	10.47	-3.63	9.02
	R2	0.368	0.375	0.658	0.453	0.552	0.533	0.381	0.730
As(V)	slope	-77.52	-107.2	10.85	0.01	0.24	0.06	0.53	0.22
	intercept	611.43	749.99	37.67	19.44	4.18	73.36	-47.30	53.10
	R2	0.528	0.568	0.619	0.599	0.561	0.391	0.391	0.726

Table 4-2
Summary of linear regressions between various soil parameters and the Langmuir model fits for $C_{s,\,max}$ (mg/kg).

Specie	Regression Parameter	pH_{H2O}	pH_{CaCl2}	% Clay	DC - Fe (mg/kg)	DC - Al (mg/kg)	Ox - Fe (mg/kg)	Ox - Al (mg/kg)	15-sec DCB-Fe (mg/kg)
As(III)	Slope	-4.965	-6.740	0.800	0.001	0.016	0.004	0.032	0.015
	Intercept	45.43	53.58	7.81	7.60	6.58	10.71	3.89	9.30
	R2	0.473	0.490	0.734	0.523	0.497	0.404	0.311	0.754
As(V)	Slope	-73.72	-98.18	10.56	0.01	0.19	0.05	0.44	0.21
	Intercept	577.70	687.57	30.04	29.00	19.94	72.32	-27.47	48.23
	R2	0.606	0.604	0.744	0.510	0.446	0.346	0.342	0.799

Table 4-3
Summary of linear regressions between various soil parameters and the Langmuir model fits for mass-based Langmuir K_L values.

Specie	Regression Parameter	pH^*_{H2O}	pH^*_{CaCl2}	% Clay	DC^* - Fe (mg/kg)	DC^* - Al (mg/kg)	$Ox^\dagger$ - Fe (mg/kg)	$Ox^\dagger$ - Al (mg/kg)	15-sec DCB-Fe (mg/kg)
As(III)	slope	-3.819	-4.401	0.361	0.0002	0.005	0.004	0.023	0.006
	intercept	33.39	35.11	6.57	7.95	7.00	6.12	1.85	7.67
	R2	0.312	0.233	0.166	0.033	0.059	0.379	0.185	0.114
As(V)	slope	-1.957	-3.516	0.038	0.000	0.008	0.004	-0.047	0.007
	intercept	44.07	52.26	31.55	29.76	28.06	28.02	47.28	29.58
	R2	0.0040	0.0073	0.0001	0.0027	0.0063	0.0228	0.0359	0.0080

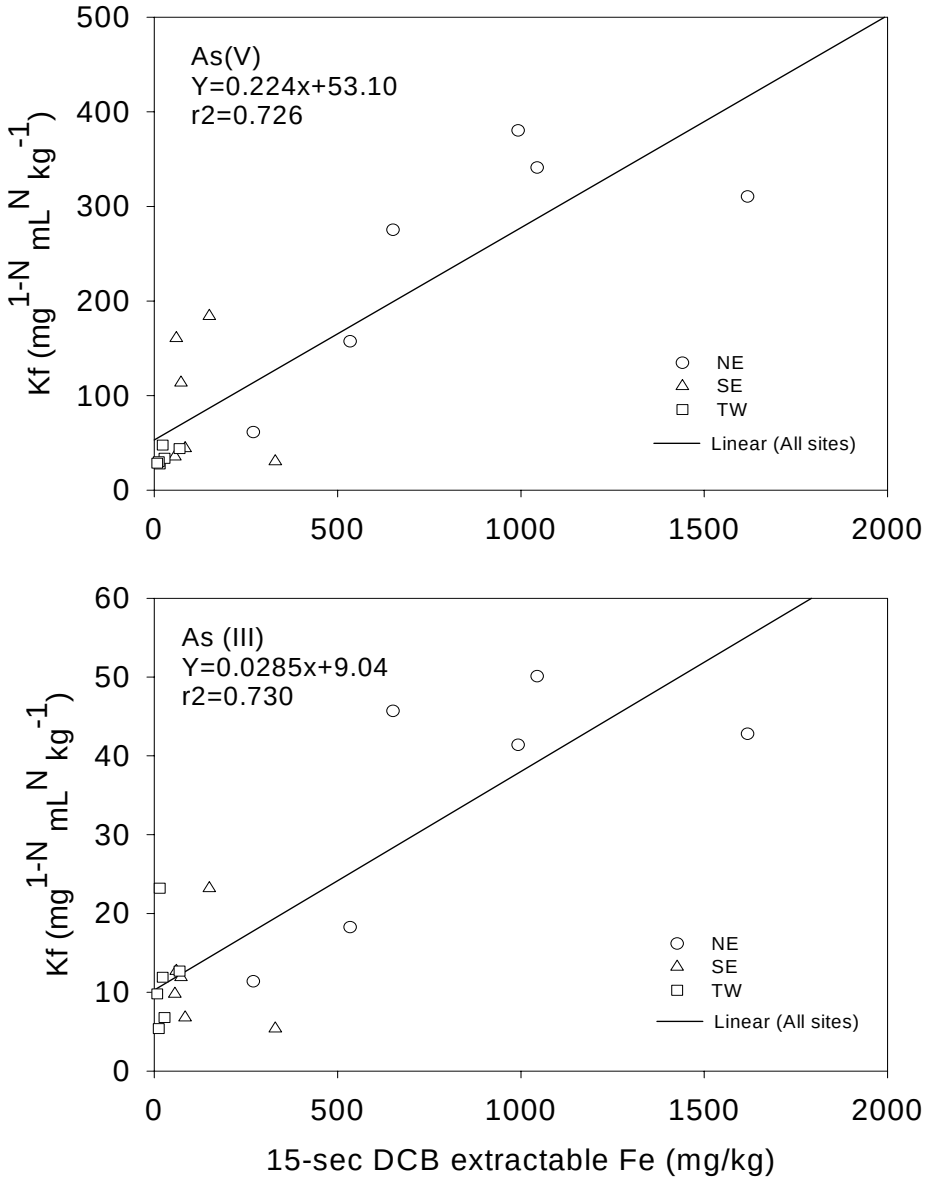

Figure 4-9
Correlation for As(V) (upper graph) and As(III) (lower graph) between Freundlich K_f values and easily reducible Fe assayed using a 15-second DCB extraction.

5
ATTENUATION OF ARSENIC IN ASH LEACHATE

Leaching and chemical adsorption experiments were performed using leachate generated from site ash samples and soil soils to evaluate the effect of the leachate matrix on arsenic adsorption. Two ash samples from each site were used in sequential and kinetic leaching studies. Ash samples were selected based on their location with respect to the water table. For each site, one ash was selected that resided predominantly above the water table (unsaturated) and one ash was selected that resided predominantly below the water table (saturated). In the case of the SE and MW sites, arsenic was below 10 ppb in the first few leachates of the sequential extractions and was verified to remain as such in a later sequential leaching; therefore, a detailed analysis of the sequential leaching of arsenic was not performed on those ashes. Only arsenic leaching and chemical attenuation data for the ash samples obtained from the NE site are presented in this report.

Sequential Leaching

Average pH values measured for sequential leachings of two NE site ash samples obtained from a depth of 15-20 ft bgs are summarized in Figure 5-1. Arsenic concentrations over the sequential leaching series are shown on Figure 5-2. For both ash samples, the pH increased by about 1 pH unit after the first few sequential leachings and then stabilized at about pH 6.4 to 6.6. As(V) concentrations increased more or less continuously to reach a plateau of about 65 – 80 ppb. As(III) concentrations started low and remained less than 10 ppb for the first 10 leachings before beginning to increase, but remained below 20 ppb for all 15 sequential leachings.

Leaching Kinetics

As(III) and As(V) leaching profiles over time for both NE ash samples are shown in Figure 5-3. In the leaching kinetic study, both As(III) and As(V) increased in concentration over the entire 30-day period. This gradual approach to equilibrium of As dissolution/desorption from ash, which is likely ash dependent, has two practical implications. First, often times laboratory leaching studies result in concentrations that are much lower than those measured in ash leachate wells, which is likely due to be the kinetic process observed in Figure 5-3. The contact time between pore water and the ash (residence time) in the field is usually much longer than the typical 24-h laboratory batch equilibration. Secondly, release concentrations of As from a given ash will not only be dependent on total available arsenic but also on the pore-water velocity at a given site. Therefore, if water travels much slower at one site versus another site, arsenic concentrations in the leachate wells are likely to be higher at that site as well. This kinetic process may also be why arsenic concentrations increase with sequential leaching number, because although the solution phase is being replaced with each leaching, the total time for

which the ash has been water-saturated increases with each leaching step. Therefore, this apparent mass-transfer limited process is also likely to include ash hydration kinetics (kinetics of the wetting process). Changes in pH over time in the kinetic studies were also similar to the sequential leaching studies as shown in Figure 5-1.

Leachate Arsenic Attenuation by NE Site Soils

Chemical attenuation by two NE site soil samples of arsenic species in the ash leachate is shown in Figure 5-4, along with the multi-concentration arsenic isotherms measured from 0.001 M $CaSO_4$. As(III) and As(V) present in the ash leachate were significantly attenuated by the acidic soils. The arsenic sorption was consistent with the isotherms developed using 0.001 M $CaSO_4$, presented in the previous section. Calcium and sulfate are dominant ions in ash leachate and the use of 0.001 M $CaSO_4$ appears to be a reasonably good simulated leachate matrix for conducting laboratory equilibrium adsorption tests.

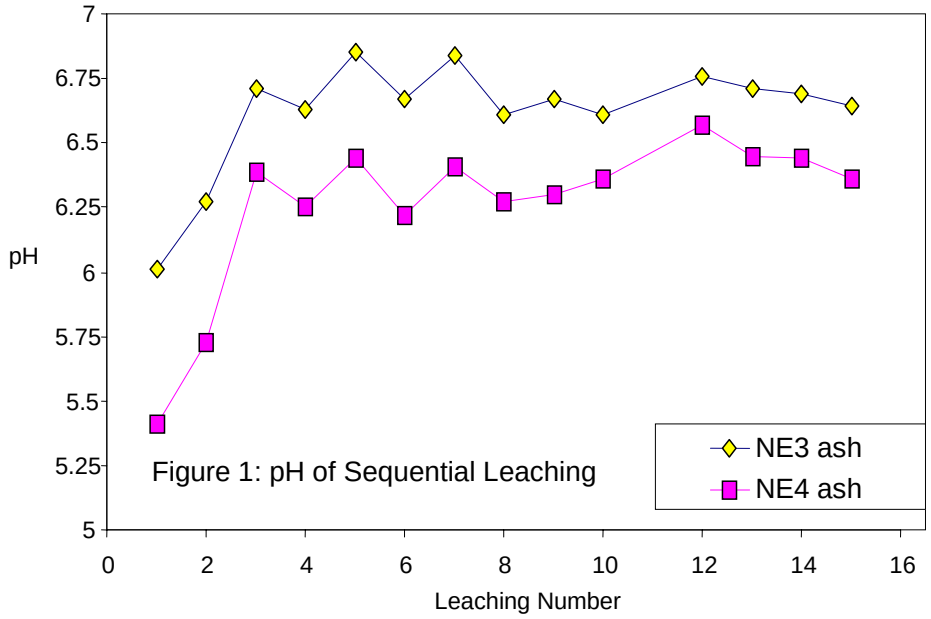

Figure 5-1
pH profile over sequential leaching series for ash samples collected from 15-20 ft depth in two cores at the NE site.

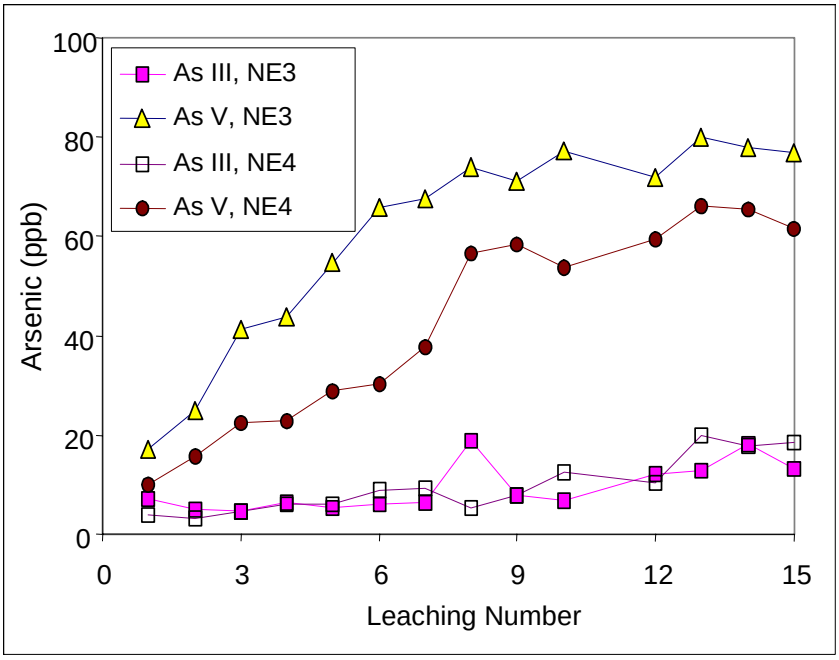

Figure 5-2
As(III) and As(V) profiles over sequential leaching series for ash samples collected from 15-20 ft depth in two cores at the NE site.

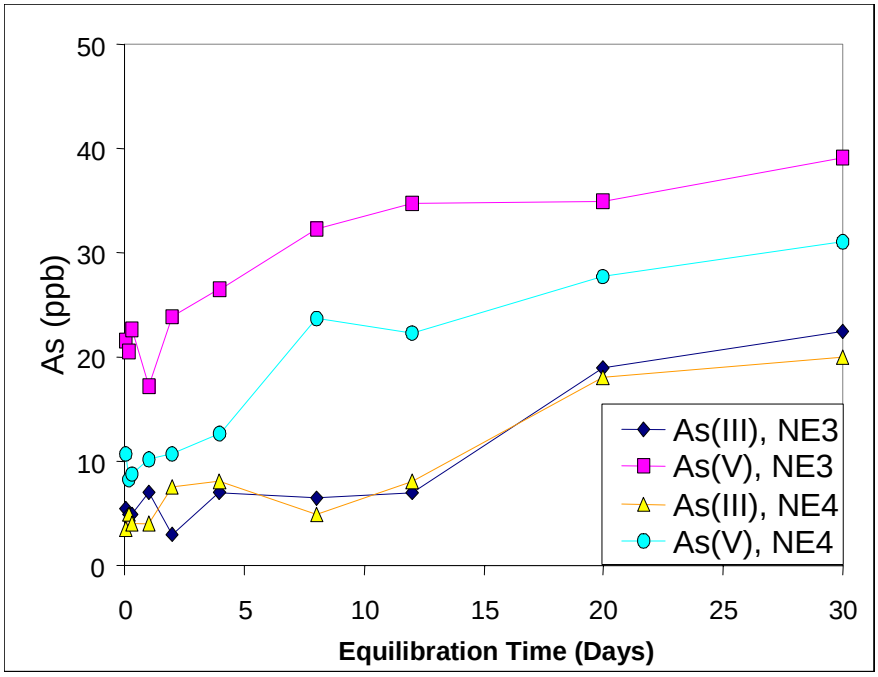

Figure 5-3
Batch leaching of As(III) and As(V) from NE ash samples versus time up to a maximum 30-day equilibration period.

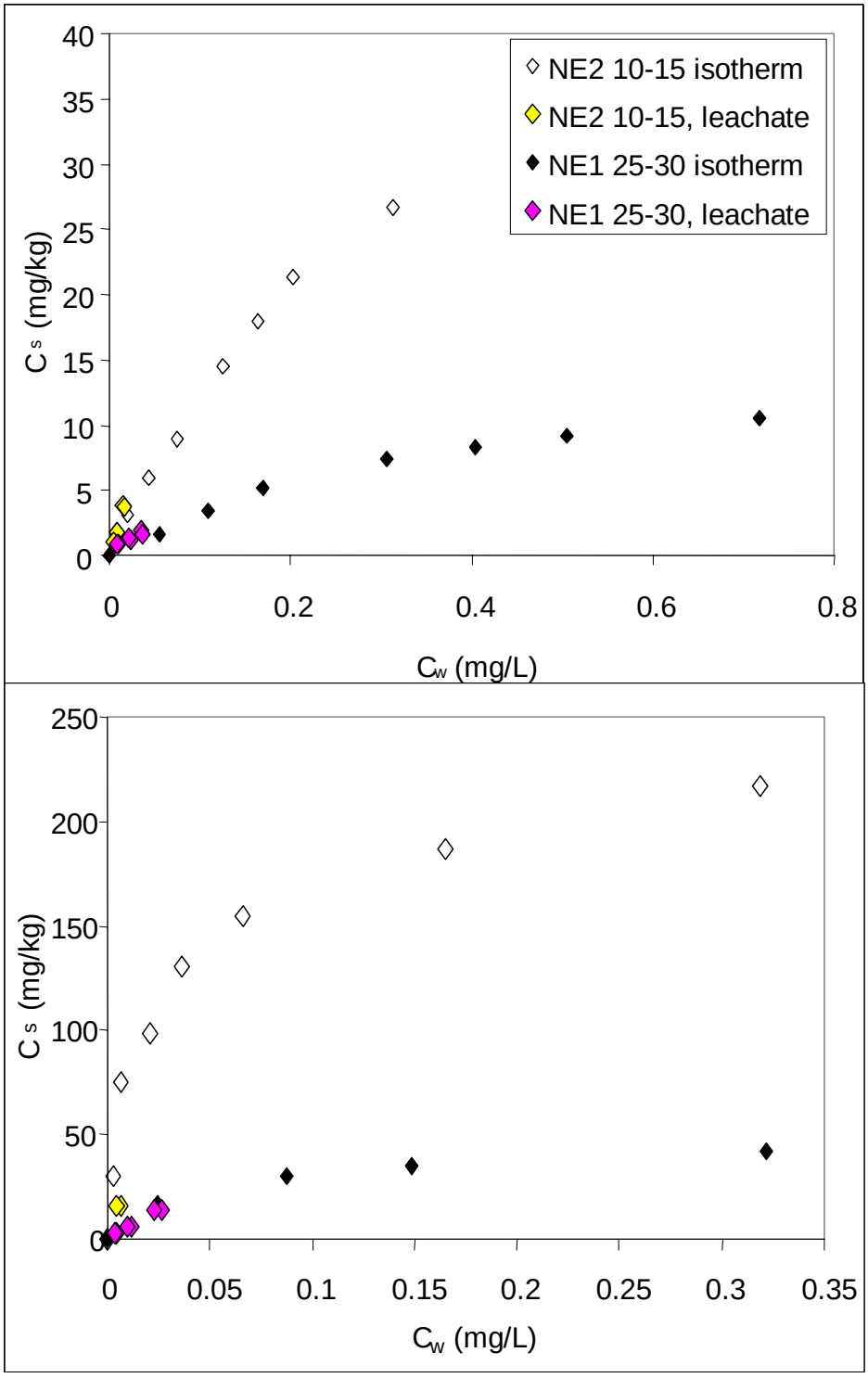

Figure 5-4
Attenuation of As(III) (upper plot) and As(V) (lower plot) present in ash leachate by two NE site soils, and multi-concentration arsenic isotherms measured from 0.001 M $CaSO_4$.

6
REFERENCES

Anderson, M.A., Furguson, J.F., and J. Gavis. 1976. Arsenate adsorption on amorphous aluminum hydroxide. J. Colloid Interface Sci. 54:391-399.

Bolan, N.S., Syers, J.K., and M.E. Sumner. 1993. Calcium-induced sulfate adsorption by soils. Soil Sci. Soc. Am. J. 57:691-696.

Bowden, J.W., Bolland, M.D.A., Posner, A.D., and J.P. Quirk. 1973. Generalised model for anion and cation adsorption at oxide surfaces. Nature 245:81-83.

Bowden, J.W., Posner, A.D., and J.P. Quirk. 1977. Ionic adsorption on variable charge mineral surfaces. Theoretical-charge development and titration curves. Aust. J. Soil Res. 15:121-136.

Brannon, J.M., and W.H. Patrick, Jr. 1987. Fixation, transformation, and mobilization of arsenic in sediments. Environ. Sci. Technol. 21:450-459.

Eary, L.E., Rai, D., Mattigod, S.V., and C.C. Ainsworth. 1990. Geochemical Factors Controlling the Mobilization of Inorganic Constituents from Fossil Fuel Combustion Residues: II Review of the Minor Elements. J. Environ. Qual. 19:202-214.

EPRI, 1987. Chemical Characterization of Fossil Fuel Wastes. EPRI, Palo Alto, CA, Report EA-5321.

EPRI, 2000. Environmental chemistry of arsenic: a literature review. EPRI, Palo Alto, CA, Report 1000585.

Goldberg, S., and R.A. Glaubig. 1988. Anion sorption on a calcareous, montmorillonitic soil – arsenic. Soil Sci. Soc. Am. J. 52:1297-1300.

Goldberg, S. 2002. Competitive adsorption of arsenate and arsenite on oxides and clay minerals. Soil Sci. Soc. Am. J., 66:413-421.

Goldberg, S., and C.T. Johnston. 2001. Mechanisms of arsenic adsorption on amorphous oxides evaluated using macroscopic measurements, Vibrational Spectroscopy, and Surface Complexation Modeling. J. Colloid Interface Sci., 234:204-216

Gupta, S.K., and K.Y. Chen. 1978. Arsenic removal by adsorption. J. Water Pollution Control Fed. 50:493-506.

Jackson, B.P., and W.P. Miller. 1998. Arsenic and selenium speciation in coal fly ash extracts by ion chromatography-inductively coupled plasma mass spectrometry. J. Anal. At. Spectrom. 13:1107-1112.

Jain, A. and R.H. Loeppert. 2000. Effect of competing anions on the adsorption of arsenate and arsenite by ferrihydrite. J. Environ. Qual. 29:1422-1430.

Manning, B.A., and S. Goldberg. 1996. Modeling competitive adsorption of arsenate with phosphate and molybdate on oxide minerals. Soil Sci. Soc. Am. J. 60:121-131.

Manning, B.A., and S. Goldberg. 1997. Arsenic(III) and arsenic(V) adsorption on three California soils. Soil Sci. 162:886-895.

Manning, B.A., and S. Goldberg. 1996. Modeling arsenate competitive adsorption on kaolinite, montmorillonite and illite. Clays Clay Miner. 44:609-623.

Pierce, M.L., and C.B. Moore. 1982. Adsorption of arsenite and arsenate on amorphous iron hydroxide. Water Res. 16:1247-1253.

Smith, E., Naidu, R., and A.M. Alston. 2002. Effect of phosphorus, sodium, and calcium on arsenic sorption. J. Environ. Qual. 31:557-563.

Theis, T.L. and J.L. Wirth. 1977. Sorptive behavior of trace metals on fly ash in aqueous systems. Environ. Sci. Technol. 11:1096-1100.

Theis, T.L., Halvorson, M., Levine, A., Stankunas, A., and D. Unites. 1982. Fly ash attenuation mechanisms. In Report and technical studies on the disposal and utilization of fossil-fuel combustion by-products. Vol. II. Submitted by the Utility Solid Waste Activities Group, the Edison Electric Institute, and the National Rural Electric Cooperative Association to the United States Environmental Protection Agency.

Theis, T.L., and J.L. Wirth. 1977. Sorptive behavior of trace metals on fly ash in aqueous systems. Environ. Sci. Technol. 11:1096-1100.

Turner, R.R., 1981. Oxidation state of arsenic in coal ash leachate. Environ. Sci. Technol. 15(9):1062-1066.

Wilkie, J.A., and J.G. Ghering. 1996. Adsorption of arsenic onto hydrous ferric oxide. Effects of adsorbate/adsorbent ratios and co-occurring solutes. Colloids Surf. A: Phys. Chem. Eng. Aspects 107:97-110.

Xu, H., Allard, B, and A. Grimvail. 1988. Influence of pH and organic substance on the adsorption of As(V) on geological materials. Water Air Soil Pollut. 40:293-305.

EPRI | ELECTRIC POWER RESEARCH INSTITUTE

Speciation and Attenuation of Arsenic and Selenium at Coal Combustion By-Product Management Facilities

Volume 3: Selenium Adsorption

Final Report
October 1, 2002 - September 30, 2005

DOE Award Number: DE-FC26-02NT41590

Principal Investigators:

L. Lee, Purdue University
I. Murarka, Ish Inc.

SELENIUM ADSORPTION ABSTRACT

This report contains results of the laboratory batch equilibrium studies for chemical attenuation of selenium species by soils from three coal-fired power plant sites. Several soil samples were collected from three power plant sites to conduct the laboratory chemical attenuation studies. Adsorption isotherms and coefficients were developed for both selenium (IV) and selenium (VI). Physical and chemical characterization data for the soils were obtained so that correlations between soil properties and adsorption of selenium species can be established to the extent possible. Linear and Freundlich adsorption isotherm models were fitted to the data as appropriate.

Adsorption of selenium species was generally non-linear with respect to concentration. For all three sites, adsorption of Se(IV) was significantly greater than Se(VI). Linearized concentration-specific distribution coefficients calculated from adsorption isotherms at an initial solution concentration of 1 mg/L ranged from 5 to about 500 L/kg for Se(IV), and from 2 to 18 L/kg for Se(VI) for the soils tested. The presence of sulfate decreases adsorption of selenium with effects being soil dependent but always greatest for Se(VI). The presence of calcium had a small effect on Se(IV) adsorption, but a negligible effect on Se(VI) adsorption.

Linear and a step-wise multiple linear regression analyses of the adsorption coefficients and soil chemical and physical properties indicate that 15-second DC extractable iron was the best single parameter correlation; however, reasonably good correlations for Se(VI) adsorption were also found with clay percentage. For both species, selenium adsorption was negatively correlated with soil isotherm pH. Combining pH with 15 sec-DCB-Fe content of the soils resulted in the best correlation for adsorption of both Se(IV) and Se(VI).

These chemical attenuation data for the selenium species can be used to model selenium migration in groundwater at the coal ash management sites for the coal fired power plant sites.

CONTENTS

LIST OF FIGURES

LIST OF TABLES

1
INTRODUCTION

Attenuation of selenium (Se) in the subsurface is highly dependent on the selenium species present and the characteristics of the soil. This project was designed to evaluate attenuation of selenite [Se(IV)] and selenate [Se(VI)] for soils at three coal-fired power plant sites from different geographical regions within the United States. One site is located in the northeastern United States (NE), one site is located in the Southeast (SE), and one site is located in the Midwest (MW). These data can be used to model selenium migration in groundwater at the sites and to compare to monitoring well data. This report presents the results of laboratory determinations of attenuation characteristics for soils collected at the three sites.

Objectives

The overall objectives of this research project were to:

- Collect soil samples from each of the three coal-fired power plant sites and characterize them for selected physical and chemical properties,
- Conduct laboratory batch equilibrium experiments to construct adsorption isotherms and estimate adsorption coefficients for Se(IV) and Se(VI) species with multiple soil samples from each of the three sites,
- Collect coal ash samples from the three power plants and perform sequential batch leaching tests to characterize Se(IV) and Se(VI) release from the ash samples, and
- Carry out laboratory batch adsorption tests with soils from the three sites to assess the effects of the ash leachate matrix on the attenuation of selenium species.

Literature Review

Although selenium is essential to humans and animal nutrition, it has been recognized to adversely impact aquatic ecosystems. Selenium in excess caused embryonic mortality and abnormalities of aquatic birds (Ohlendorf et al., 1986). Data in the late 1990s suggested that reproductive impairment in wildlife from Se pollution is more widespread than originally thought (Betts, 1998). Sources of selenium contamination associated with anthropogenic activities arise from application of agricultural pesticides, disposal of industrial wastes, and combustion of fuels. Selenium is naturally enriched in fossil fuels well above the level of abundance in the earth's curst of < 0.05 mg/kg (Bowen, 1979). Selenium is further concentrated in coal combustion by-products such as fly ash (e.g., 6.9 to 760 mg Se/kg ash) (Theis and Gardner, 1990). Approximately 45% of coal-derived fly ash is disposed of in landfills (USEPA, 1999; EPRI, 1997). Constituents present in ash landfills such as selenium may seep to adjacent

water bodies or groundwater, thus potentially impacting the aquatic ecosystem (Carlson and Adriano, 1993; Eary et al., 1990). Selenium concentrations of 10 to 540 μg/L were found in pore-water and leachate collected from typical ash disposal sites (Theis and Gardner, 1990 and references cited therein); and selenium concentrations of <1 to 1760 μg/L in a recent study of field leachate concentrations at 23 sites reported in a companion volume to this report (Ladwig et al., 2006).

Toxicity

Considerable controversy between biologists and industries was spawned and has continued since the issuance of the 1987 chronic criterion of 5 parts per billion (ppb, μg/L) by US EPA (Renner, 1998; Renner, 2005). Both Se species are bio-accumulated in tissues and thus chronic exposure to even lower concentration may result in developmental abnormalities in embryos for wildlife and disturbed reproduction cycles for domestic animals (Dhillon and Dhillon, 2003). On the other hand, selenium constitutes an active site of selenoproteins such as glutathione peroxidase (Himeno and Imura, 2002). Of the all US EPA priority and non-priority pollutants, selenium has the narrowest range of what is considered beneficial verses detrimental for biota. Selenium toxicity is also dependent on its oxidation status. Elemental Se and selenide is essentially insoluble in water (aqueous solubility too low to determine with current analytical techniques). Release of selenium to water from these insoluble forms of selenium can occur slowly through microbial metabolism to more soluble forms (Losi and Frankenberger, 1998; Dowdle and Oremland, 1998). For most aquatic and terrestrial wildlife, Se(IV) is known to be more toxic than Se(VI) when exposed at equal concentration level (US EPA, 2004). However, the specific mechanism of selenium toxicity still remains unclear.

Speciation in fly ash leachate

It is difficult to determine the redox speciation of selenium in ash leachate based only on the well-known pE-pH relationship due to ash heterogeneity, kinetic barriers to equilibrium, and biological processes. Several studies have been carried out to determine selenium speciation in fly ash and subsequent leaching from fly ash, which may vary with coal origin, the coal combustion process, the ash weathering process, and leaching methodology. In batch leaching studies, it was reported that 5% to 100% of total water extractable selenium could exist as Se(IV) (Jackson and Miller, 1998; van der Hoek et al., 1996). In field leachates, it was reported that Se(IV) was the predominant form, although the proportion of Se(VI) was high in leachates at landfills receiving ash from subbituminous or lignite coals (Ladwig et al., 2006).

Adsorption

The sorption behavior of Se is governed by various physical-chemical factors including oxidation-reduction potential (pE), mineralogical composition of the soil, soil pH, and the solution matrix. Selenium exists in four oxidation states in natural systems: selenate (Se(VI)), selenite [Se(IV)], elemental Se [Se(0)], and selenide [Se(-II)]. Under the prevailing pH-pE range in soils, selenium is most mobile in the Se(IV) and Se(VI) forms, while elemental Se(0) and Se(-II) are present as stable metal forms (Neal et al., 1987a). Se(VI) is present as SeO_4^{2-} over the entire pH range of soils, while the major Se(IV) species is $HSeO^{3-}$ (pK_a=2.68) at pH < 8.4 and

SeO_3^{2-} (pK_a=8.4) at pH > 8.4 (Séby et al., 1998). The interaction of the inorganic Se species (VI and IV) with model soil components has been extensively studied (Goldberg and Glaubig, 1988; Hansmann and Anderson, 1985; Neal et al., 1987a; Neal et al., 1987b; Rajan and Watkinson, 1976; Su and Suarez, 2000; Zhang and Sparks, 1990); these studies found that iron/aluminum (hydro) oxides and allophane appear to have the greatest affinity for Se. In alkaline calcareous soils, adsorption of Se(IV) by calcite is important (Goldberg and Glaubig, 1988). Of the phyllosilicate minerals, kaolinite with variable charge edge sites tends to adsorb selenium more than montmorillonite, which has a negative surface charge (Bar-Yosef and Meek, 1987; Goldberg and Glaubig, 1988). However at high Se concentrations where precipitation may be induced, removal of Se(IV) from aqueous solutions may be greater with montmorillonite due to its higher surface area (surface area; 700 to 800 cm^2/g) compared to kaolinite (surface area; 5 to 20 cm^2/g) (Frost and Griffin, 1977). The precipitation or co-precipitation of selenium-metal complexes such as ferric selenite $Fe_2(SeO_3)_3$ ($K_s = 2.0 \pm 1.7 \times 10^{-31}$) and basic ferric selenite $Fe(OH)_4SeO_3$ ($K_s = 10^{-61.7}$), which both have extremely low aqueous solubilities, can also be important in the environmental cycling of selenium (Manning and Burau, 1995).

Generally, Se(VI) has been shown to behave like sulfate anion (e.g., outer-sphere surface complex) with relatively low adsorption and high mobility (Goldberg and Glaubig, 1988; Neal and Sposito, 1989; Rajan and Watkinson, 1976). However, inner-sphere complexation on iron or aluminum oxides/hydroxides has also been concluded from spectroscopic data (Peak and Sparks, 2002; Manceau and Charlet, 1994; Wijnja and Schulthess, 2000). Negligible adsorption of Se(VI), was observed for several calcareous, montmorillonitic, alluvial soils, and purified humic acids (Neal and Sposito, 1989; Goldberg and Glaubig, 1988; Saeki and Matsumoto, 1994). However, Se(VI) sorption was reported significant on oxides, kaolinite, and oxide-enriched soils, especially in the acidic pH range (Balistrieri and Chao, 1987; Bar-Yosef and Meek, 1987; You et al., 2001; Su and Suarez, 2000). Se(IV) is considered to behave more analogous to phosphate anion (e.g., inner-sphere surface complex) and to adsorb more than Se(VI) (Hansmann and Anderson, 1985; Zhang and Sparks, 1990). Experimental evidence for specific Se(IV) adsorption on metal oxide surfaces includes a decrease in the soil's zero point of charge (ZPC) following selenite adsorption (Bowden et al., 1980; Rajan, 1979), reduced electrolytic mobility (Su and Suarez, 2000), and spectroscopically observed structural characteristics (Hayes et al., 1987).

Adsorption of both Se(IV) and Se(VI) by several sorbents including metal oxides, clay soils (kaolinite, montmorillonite), oxidic soils, and montmorillonitic soils is pH-dependent (Bar-Yosef and Meek, 1987; Bowden et al., 1980; Goh and Lim, 2004; Neal et al., 1987a; Saeki et al., 1995; Zhang and Sparks, 1990). The selenium adsorption generally decreases with increasing pH characteristic of anion adsorption on soil surfaces (Bowden et al., 1980; Hingston et al., 1972). With increasing pH, the soil surface becomes increasingly more negative while the anionic fraction of selenium increases, thus increasing repulsive forces. Se(VI) adsorption is more sensitive to pH than Se(IV) (Bar-Yosef and Meek, 1987) with the magnitude of the slope or the position of the inflection point in the pH envelope (adsorption versus pH) being soil-dependent.

Several studies have been conducted to quantify the relationship between selenium adsorption capacity and soil properties. For 66 New Zealand soils (John et al., 1976) and 58 Japanese soils (Nakamura et al., 2005), Se(IV) adsorption correlated best with oxalate-extractable Fe and to less

extent with Al. Limited information is available for correlating Se(VI) adsorption to specific soil properties. As previously stated, soil pH is known to influence selenium adsorption; however, differentiating the relative contributions of pH and oxide content to selenium adsorption in heterogeneous soil systems is currently lacking.

Selenium retention by soils is impacted by the ionic composition of the solution phase similar to what has been observed for other oxyanions. Se(VI) adsorption is more sensitive than Se(IV) to the presence of competing anions (Dhillon and Dhillon, 2002; Goh and Lim, 2004; Balistrieri and Chao, 1987; Monteil-Rivera et al., 2000; Saeki et al., 1995; You et al., 2001). For example, adsorption of 0.2 mM Se(VI) decreased approximately 50% in the presence of 0.01 M sulfate (Goh and Lim, 2004) whereas sulfate did not significantly impact Se(IV) adsorption (Balistrieri and Chao, 1987; You et al., 2001). Se(IV) also outcompeted phosphate for adsorption sites when present at equimolar concentrations; however, at a 2:1 phosphate:Se(IV) ratio in solution, Se(IV) adsorption by goethite was suppressed by 70% (Balistrieri and Chao, 1987). The sequence of inhibitory effect of competing inorganic anions for selenium adsorption generally follows; phosphate > citrate > oxalate > sulfate (Balistrieri and Chao, 1987; Saeki et al., 1995). Chloride competition for both Se(IV) and Se(VI) is minimal (Neal et al., 1987b).

Selenium adsorption has been shown to be enhanced by divalent cations, and has been attributed to i) surface precipitation with Fe^{2+} or Cu^{2+} (Benjamin, 1983; Manning and Burau 1995); and ii) decreased negative (or increased positive) surface potential caused by Ca^{2+} sorption (Neal et al., 1987b). In both cases, the impact of the divalent cations on selenium adsorption was greater at alkaline pH values where adsorption of the divalent cations (Cu^{2+} and Ca^{2+}) is more favorable.

Microbial reduction and oxidation of selenium

Microbial transformation of selenium includes both reduction and oxidation processes and appears to be similar to the biological cycling of sulfur (Losi and Frankenberger, Jr., 1997a). Mechanisms for microbial transformations include assimilatory reduction (used as a nutrient source), dissimilarity reduction (terminal electron acceptors in energy metabolism), and detoxification (e.g., biomethylation to volatile forms). The reductive microbial processes include reduction of Se(VI) to Se(IV) or further to elemental selenium, depending on microbial species and growth time (Lortie et al., 1992; Losi and Frankenberger, Jr., 1997b; Maiers et al., 1988). Both pH and redox potential can also affect the microbial transformation of selenium (Masscheleyn et al., 1990). From an environmental perspective, microbial reduction processes are favorable, because the reduced Se forms [e.g., Se(0) or Se(IV)] are less soluble and more easily adsorbed by soils than Se(VI) (the oxidized form). Less is known about microbial oxidation of selenium; however, it appears to be primarily a slow biotic process and the major mechanism by which solubilization of Se(0) occurs (Losi and Frankenberger, 1998). Dowdle and Oremland (1998) reported that 17% Se(0) was transformed into Se(IV) over a 25-day period in a soil slurry system with transformation rates being 3 to 4 orders-of-magnitude smaller than the rates of reduction of Se(IV) to Se(0). Similarly, only 2% to 13% of Se(0) spiked into soil at 100 mg/kg Se(0) was oxidized within a 125-day period in studies by Losi and Frankenberger (1998), and the amount of selenium oxidized appeared correlated with prior exposure of the soil to selenium.

Understanding adsorption behavior is critical for assessing the amount of selenium that may be released from ash disposal facilities and the ability for soils surrounding the facilities to attenuate transport towards near-by water bodies. Such information is critical in assessing the true risk potential of Se contamination from ash disposal facilities. In order to establish a theoretical framework for predicting selenium attenuation by soil, this study focused on the following objectives: (1) quantifying the adsorption of Se(VI) and Se(IV) onto soils from coal-fired power plant sites having a wide range of physical and chemical properties; (2) establishing a range of distribution coefficients that may be used in assessing selenium mobility in ash leachate; (3) characterizing the competitive effects of Ca and SO_4 on the adsorption of Se(VI) and Se(IV); and (4) characterizing pH effects on selenium adsorption by soils.

2
METHODS AND MATERIALS

Soil Sampling and Characterization

Soils samples were collected from several depths at each of the three sites by split spoon sampling equipment with a plastic insert. Two to three soil borings were advanced within about 200 feet of the downgradient edge of the ash fill using a hollow stem auger, and samples were collected at five to ten foot intervals. The samples were sealed in the field in two foot sections with end caps and then taped so that the plastic tubes endured the shipping without spilling out the samples. Several soil samples were collected from each of the soil borings and if appropriate were composited in the laboratory from consecutive depths. The soil samples were shipped to the laboratory in chilled coolers. Ash samples from the landfill site were collected in a similar manner. Soil samples were also collected underneath the ash landfill at the northeastern power plant site. The other two sites could not be samples underneath the ash landfill due to engineering considerations.

Soils samples were collected from several depths at each of the three sites by spilt spoon sampling equipment with a plastic insert. Two to three soil borings were advanced within about 200 ft of the downgradient edge of the ash fill using a hollow stem auger, and samples were collected at five to ten foot intervals. The two-foot sections were sealed with end caps for transport to the laboratory in chilled coolers. Ash samples from the landfill site were collected in a similar manner for the NE and SE sites. A sample of bulk ash was taken at the MW site.

Upon arrival at the laboratory at Purdue University, soil and ash samples were transferred to plastic bins, and stored moist at 4°C. A soil pH and texture screening of samples received was performed to select a subset of samples considered representative of the site for use in detailed studies. For the soil samples selected and all the ash samples, moisture content was determined gravimetrically by the loss of water after heating at 105 °C for 24 h and cooled in a desiccator. For each soil sample selected, a subsample (≈ 200 g) was air dried, sieved to particle diameter less than 2 mm, and thoroughly homogenized prior to characterization and use. Each processed soil sample was characterized for the following physical and chemical properties: particle size distribution by the hydrometer method (Gee and Bauder, 1996), pH of 1:1 (5 g soil: 5 mL H_2O) soil suspensions, organic carbon content by combustion (Nelson and Summers, 1996), cation exchange capacity (CEC) (Sumner and Miller, 1996), dithionite-citrate-bicarbonate (DCB) extractable iron and aluminum (Loeppert and Inskeep, 1996), acid ammonium oxalate extractable iron and aluminum (Loeppert and Inskeep, 1996), X-ray diffraction analysis of clay minerals, and timed DCB extractions of Fe and Al. Quick (15-sec) releasable DCB extraction of Fe was measured with method previously reported (EPRI, 2004). Characterization of the dominant clay mineralogy in each of the soil samples was performed by X-ray diffraction

analysis. Details with regard to X-ray slide preparation, mineral identification and characterization were also previously reported (EPRI, 2004).

Adsorption Isotherms on Site Soils

Adsorption isotherms were constructed independently for both Se(IV) and Se(VI) in an ionic matrix of 1 mM $CaSO_4$ using four to eight Se concentrations plus a zero Se concentration control. Applied solution concentrations generally ranged from 0.11 to 2.7 mg/L in the case of Se(IV), and 0.11 to 1.0 mg/L for Se(VI). Selenium solutions were added to 50-mL polypropylene centrifuge tubes containing 0.5 g to 1 g of soil resulting in soil to solution ratios of 20 g/L for Se(IV) and 50 g/L for Se(VI). Soil suspensions were then allowed to equilibrate at 22 ± 2 °C on a rotary shaker (≈ 45 rpm) for 16 h for Se(IV) and 48 h for Se(IV). Selenium concentrations in solution were measured after equilibration (C_w, mg/L), and sorbed concentrations (C_s, mg/kg) were estimated by the difference in the Se mass applied and the Se mass remaining in solution after equilibration with soil.

Equilibration times were selected to achieve near equilibrium without having significant shifts in the redox state of the Se remaining in solution; the redox state of adsorbed Se was assumed to be the same as what was measured in solution. Suspensions containing Se(IV) were equilibrated for a shorter period of time (≈16 h) due to concerns that a significant amount of Se(IV) would oxidize to Se(VI) within a 48-h equilibration period. Preliminary studies performed with NE1 25-30, NE2 10-15, and MW3 23 soils and applied solution concentrations of 1.5 μmol L^{-1}, 15 μmol L^{-1}, or 30 μmol L^{-1} at 50 g/L showed that within a 16-h equilibration period, less than 10% of the Se(IV) was oxidized. This subset of soils represented the highest and almost the lowest K_f values, high and low values of pH, extractable iron, extractable aluminum, organic matter, and clay content of the soils used in this study. Balistrieri and Chao (1987) found that the Se(IV) adsorption from aqueous solutions reaches apparent equilibrium in 2 h and without oxidizing to Se(VI) over an additional 22-h time period.

After equilibration, the pH of the soil suspensions was measured using a double junction glass pH electrode. A 10-mL aliquot of the suspension was collected from each sample and filtered using a 10-mL plastic syringe with a 0.45 μm regenerated cellulose luer-lock syringe filter. Filtered samples were preserved by adding 0.1 mL of concentrated $NiNO_3$ for total selenium or HCl for Se(IV). Analysis of selenium concentrations in the filtered samples was performed using an automated Shimadzu graphite furnace atomic absorption spectrometry (GFAA).

pH Effects

The effect of pH on Se(IV) and Se(VI) adsorption was characterized by measuring adsorption isotherms from pH adjusted 1 mM $CaSO_4$ solutions for selected soils from each site (NE1 25-30, SE1 48.5-50, and MW1 17-19 soils). Pre-determined amounts of diluted HCl or NaOH were added to 1 mM $CaSO_4$ solution to obtain pH values of equilibrated soil suspensions between 3 and 9. Duplicated initial concentrations of 0.52 mg/L for Se(IV) and 0.41 mg/L for Se(VI) were equilibrated with soils at a soil to solution ratio of 20 g/L and 50 g/L, respectively. Equilibration times, sample preparation, and selenium analysis were identical to those previously described.

Matrix Effects

The effect calcium (Ca^{2+}) and sulfate (SO_4^{2-}) concentrations on adsorption of Se(IV) and Se(VI) from a fixed concentration of 1.39 mg/L for Se(IV) and 0.53 mg/L for Se(VI) was investigated on NE1 25-30 soil. Ca^{2+} or SO_4^{2-} concentrations were 0, 0.1, 0.5, 1, 5, and 10 mM prepared with $CaCl_2$ and K_2SO_4 solutions at a constant ionic strength (I) of 0.03 by adding appropriate concentrations of KCl. For example, 0 mM Ca^{2+} (or SO_4^{2-}) solution was prepared by 30 mM KCl solution yielding an I = 0.03; 5 mM Ca^{2+} (or SO_4^{2-}) solution was prepared by 15 mM $CaCl_2$ (or K_2SO_4) mixed in 15 mM KCl yielding an I = 0.03; 10 mM Ca^{2+} (or SO_4^{2-}) solution was prepared by 10 mM $CaCl_2$ (or K_2SO_4) yielding an I = 0.03 without addition of a KCl solution. (Note $I = 0.5\Sigma\, c_i\, z_i^2$ were c_i is the molar concentration of the i^{th} ion and z is the charge of the i^{th} ion).

The competitive effects of Ca^{2+} and SO_4^{2-} were furthered investigated by measuring multi-concentration isotherms from 1 mM KCl (I = 0.001), 1 mM $CaCl_2$ (I=0.003), 1 mM K_2SO_4 (I=0.003), and 1 mM $CaSO_4$ (I=0.004)) for selected soils (NE1 25-30, NE2 10-15, SE1 48.5-50, and MW1 17-19). To minimize the effect of the pH shifts that occur with different ionic solutions, pre-determined amounts of diluted HCl or NaOH solution were added such that pH was relatively constant for the four electrolyte solutions. Ionic strength of the equilibrating solutions was not controlled; however, ionic strength effects on selenium adsorption are small (Neal et al., 1987b, Peak and Sparks, 2002).

Data Analysis

The amount of selenium adsorbed (C_s, mg/kg) was calculated by the difference in selenium masses present in the applied solution and aqueous phase (C_w, mg/L) after equilibration with the soil. Selenium isotherms were fit with the Freundlich adsorption model;

$$C_s = K_f\, C_w^{\,N} \qquad (2\text{-}1)$$

where K_f is the Freundlich adsorption coefficient ($mg^{1-N}\, L^N\, kg^{-1}$) and N (unitless) is a measure of isotherm linearity. Adsorption model parameter (K_f and N) optimization (nonlinear fits) and statistical regression analysis were performed using SAS/STAT program (SAS institute, 1989).

The Freundlich model is often the best approach to predicting adsorption as a function of concentration when adsorption is substantially nonlinear over the concentration range of interest and the specific adsorption mechanisms are not known. Problems arise using this approach when predictive transport models only allow for the input of a linear adsorption coefficient (K_d, $L\, kg^{-1} = C_s$ [mg/kg]/C_w [mg/L]). In the latter case, the model can estimate a linearized concentration-specific K_d^* value using the Freundlich isotherm model coefficients (K_f and N) as follows:

$$K_d^* = K_f\, C_w^{\,N-1} \qquad (2\text{-}2)$$

Note K_d* is equal to K_f when C_w = 1 mg/L.

Fly Ash Leaching

Sequential Leaching

Sequential leaching experiments were performed in triplicate for ash samples collected from each site to imitate the recurrent flushing of disposed fly ash with water flow through the disposal site. For NE site, two ash samples were collected from 15-20 feet below ground surface (bgs) in cores NE3 and NE4 (labeled NE3 15-20 and NE4 15-20, respectively). For the SE site, four cores were collected from depths of 5-7 feet, 7-9 feet, 23.5-25.5 feet, and 33.5-37.5 feet in cores SE1. Ash samples were combined to result in only 2 samples for leaching by mixing the samples collected at 5-7 feet with 7-9 feet for one representative sample labeled SE1 5-9, and samples 23.5-25.5 feet and 33.5-37.5 feet for a second representative sample labeled SE1 23.5-37.5. For the MW site, ash was obtained from a bulk ash depository awaiting landfill placement. Approximately 9 g of ash and 35 mL of reagent-grade water were added to 80-mL Nalgene polycarbonate tubes. Tubes were rotated end-over-end for 24 h, followed by centrifugation at 2,700 rpm for 1 h. Aqueous equilibrium pH was measured after equilibration followed by removal and filtration of the supernatant using a 20 mL luer-lock syringe with 0.45 μm cellulose filter. Filtered solutions were divided into two subsamples with one acidified with HNO_3/$NiNO_3$ for total selenium analysis and the other acidified with HCl for Se(IV) analysis. Reagent-grade water was then added to the ash remaining in the tube to replace the solution removed, and the sequential leaching procedure was repeated approximately 15-25 times. Total selenium concentration in supernatants were determined after oxidizing Se(IV) to Se(VI), and Se(IV) was measured by hydride vapor generation atomic absorption spectrometry (HVGAA). Se(VI) was estimated by subtracting Se(IV) concentrations from total selenium concentrations (Fio and Fujii, 1990).

Leaching Kinetics

A kinetic assay was performed on the same ash samples as used in the sequential leaching study to model the effect of varying residence times of water in ash disposal sites on the concentration of Se. Approximately 3 g of ash and 30 mL of reagent-grade water were added to acid-washed 80-mL Nalgene polycarbonate tubes. Tubes were rotated end-over-end. For each time increment, a set of triplicate bottles were removed, centrifuged at 2,700 rpm for 1 h, and the supernatant sampled and filtered for selenium analysis as previously described. Sampling times were as follows: 2 h, 4 h, 8 h, 1 d, 2 d, 4 d, 8 d, 12 d, 20 d, and 30 d. Supernatants were analyzed for total Se and Se(IV) as previously described.

Leachate Selenium Attenuation by Site Soils

An attenuation study was performed to assess the degree to which soils present at the site of disposal would attenuate Se present in the fly ash leachate compared to the 1 mM $CaSO_4$ solution which was considered to represent typical ash leachate and used in the standard

adsorption studies. Leachate of SE1 5-9, SE1 23.5-37.5, and MW ashes was tested for site soils. Because of similar Se adsorption behavior between SE1 48.5-50 and SE1 60-62 soils, two soils were mixed (shown as SE1 48.5 + SE1 60) for this experiment and suspended with SE ash leachate. Ash leachate generated by one 24-hour equilibration cycle (i.e., a first sequential leaching) was spiked with Se(IV) or Se(VI) at 0, 100, or 250 μg/L. One gram of soil and 10 mL spiked leachate were mixed in 15-mL Nalgene polycarbonate test tubes. The tubes were rotated end-over-end for 24 h, centrifuged at 4000 rpm for 20 min, and the supernatant sampled and filtered for selenium analysis as previously described. Se(IV) and Se(VI) were analyzed as previously described.

3
SELENIUM ADSORPTION ON SITE SOILS

NE Site

Soil Characterization Data

Selected soil properties for six soils representative of the NE site are shown in Table 3-1. NE site soils contained 13 to 29% clay composed predominantly of illite and mica with minor amounts of kaolinite. The soils contained less than 1% organic matter and their soil-water pH values ranged from 4.8 to 5.5. Selective Fe dissolution of the soils resulted in DCB-extractable Fe (intended to estimate total reducible Fe oxides) levels ranging from approximately 6,000 to 32,000 mg/kg, and DCB-extractable Al levels ranging from 270 to 1,300 mg/kg. Ranges in oxalate-extractable Fe and Al were less variable, with Fe ranging from 320 to 5,465 mg/kg, and Al ranging from 240 to 513 mg/kg. Based on the assumption that the oxalate extraction primarily dissolves amorphous Fe and Al oxides, the differences between DCB and oxalate extracts indicate that 5 to 91% of extractable Fe in the soils is amorphous, and 38 to 89% of extractable Al is amorphous. Fe extracted in 15 seconds with DCB ranged from 270 to 1,618 mg/kg, and was intended to estimate the most reactive portion of Fe oxides (i.e., Fe oxides exposed to solution and readily available for reaction). Of the 3 sites sampled in this study, the NE site has soils that are generally more acidic, have higher % clay, and have the higher upper range in DCB-extractable and oxalate-extractable Fe and Al than all other site soils.

Table 3-1
Selected properties of six soils representative of the NE site.

Soil	pH		Sand	Silt	Clay	CEC[a]	DCB[b]-Fe	DCB-Al	Ox[c]-Fe	Ox-Al	DCB-Fe 15 sec	Dominant Clay Minerals[d]
	H_2O	$CaCl_2$	----------%---------			cmol/kg	----------mg/kg----------					
NE1 25-30	5.3	5.1	33	50	17	15.5	5,928	270	320	240	270	I, K, V
NE1 35-40	5.0	4.7	40	35	25	12.6	6,030	610	5,465	525	651	I, K, V
NE2 10-15	4.8	4.4	60	23	17	4.7	31,800	1,200	1,575	513	992	I, K
NE2 16-21	5.0	4.6	59	28	13	2.45	11,370	630	1,090	364	534	I, K
NE3 50-54	5.0	4.9	9	62	29	13.2	22,470	1,070	1,750	475	1,618	I, K
NE4 46-50	5.5	5.5	57	28	15	5.8	18,330	1,300	1,590	500	1,044	I, K

[a] cation exchange capacity
[b] dithionite-citrate bicarbonate extractable
[c] oxalate extractable
[d] I = illite, K = kaolinite, V = vermiculite

Selenium Adsorption on NE Site Soils

Adsorption data for Se(IV) and Se(VI) on the six soils representative of the NE sites were measured and fit with the Freundlich isotherm model. Se(IV) and Se(VI) isotherms are plotted in Figures 3-1 and 3-2, and modeling fits are summarized in Table 3-2. K_f adsorption coefficients ($mg^{1-N}\ L^N\ kg^{-1}$) ranged between 40.4 and 107 for Se(IV), and between 6.69 and 13.3 for Se(VI). Nonlinearity was greater for Se(IV) with Freundlich N values ranging from 0.249 to 0.436 compared to Se(VI) with N values ranging from 0.859 to 0.982. Adsorption of Se(IV) is also consistently much higher than that observed for Se(VI) with Freundlich K_f values being 6 to 11 times higher those for Se(IV). To exemplify the overall selenium adsorption behavior observed for the six representative samples of the NE site, Se(IV) and Se(IV) isotherms for the lowest and highest adsorption profiles are shown in the upper graphs of Figure 3-3. Also shown in Figure 3-3 (lower graphs) is the concentration-specific K_d^* values as a function of concentration that could be used to estimate site-specific transport at a given ash leachate concentration. Note that the more nonlinear the sorption isotherms, the larger the range in the concentration-specific K_d^* values (e.g., compare the more nonlinear Se(IV) profiles with the Se(VI) profiles).

Table 3-2
Freundlich isotherm fits for selenite [Se(IV)] and selenate [Se(VI)] adsorption from 1 mM CaSO4 for NE site soils.

Soil	Se(IV)				Se(VI)			
	pH[a]	K_f[b]	N	r^2	pH	K_f	N	r^2
NE1 25-30	5.24	40.4 (1.6)[c]	0.436 (0.037)[c]	0.970	5.34	6.69 (1.37)	0.952 (0.107)	0.965
NE1 35-40	5.52	71.0 (2.6)	0.331 (0.028)	0.951	5.62	10.8 (1.0)	0.904 (0.054)	0.987
NE2 10-15	4.78	107 (4)	0.312 (0.024)	0.959	4.68	10.1 (1.3)	0.982 (0.070)	0.986
NE2 16-21	4.85	75.0 (2.7)	0.339 (0.028)	0.952	4.89	6.77 (0.92)	0.871 (0.071)	0.977
NE3 50-54	4.95	83.2 (3.1)	0.249 (0.020)	0.956	4.88	13.3 (1.4)	0.859 (0.063)	0.981
NE4 46-50	5.51	101 (3.1)	0.400 (0.025)	0.977	5.47	11.5 (2.5)	0.946 (0.122)	0.950

[a] average aqueous pH values in which isotherm was measured
[b] $K_f = mg^{(1-N)}\ L^N\ kg^{-1}$
[c] numbers in parentheses are standard errors

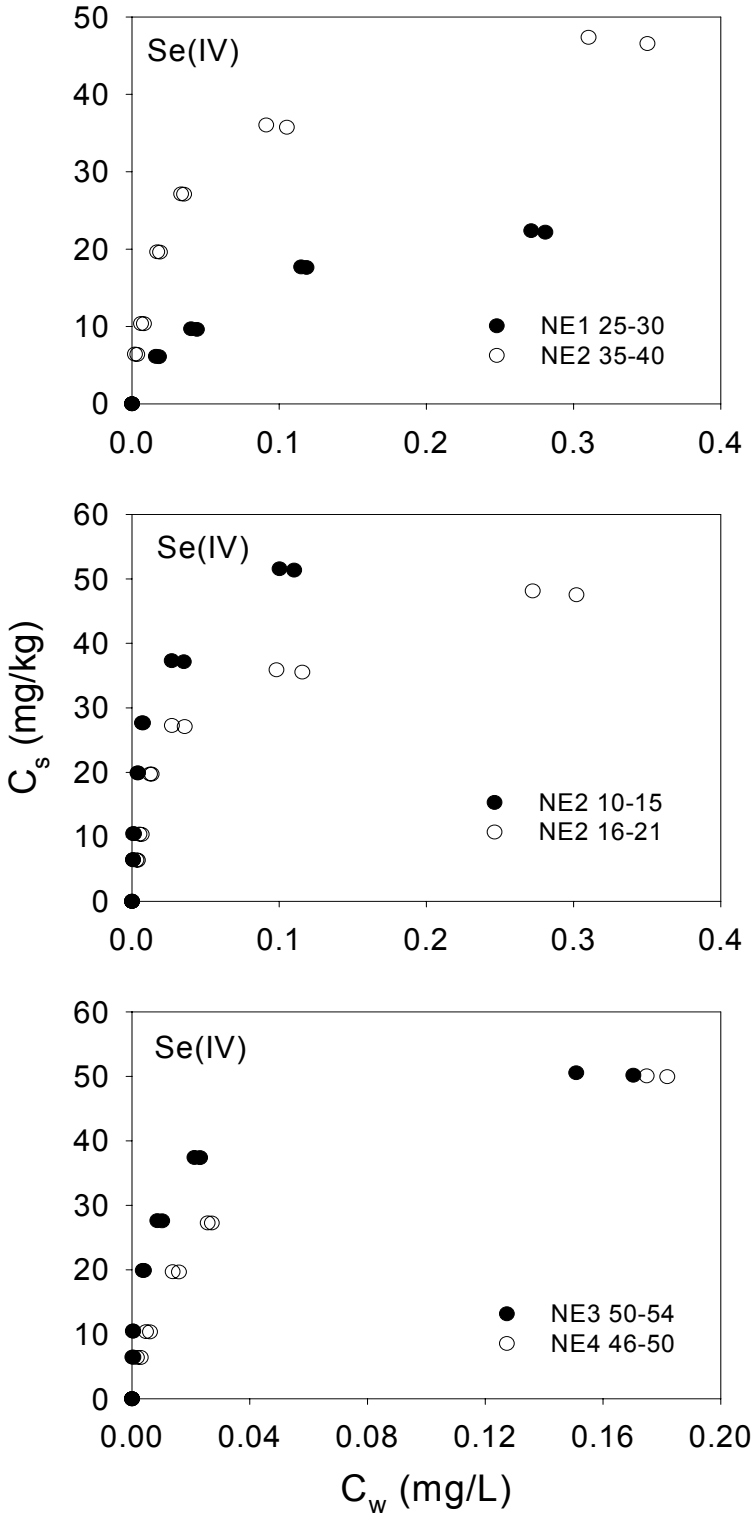

Figure 3-1
Se(IV) adsorption isotherms for NE site soils.

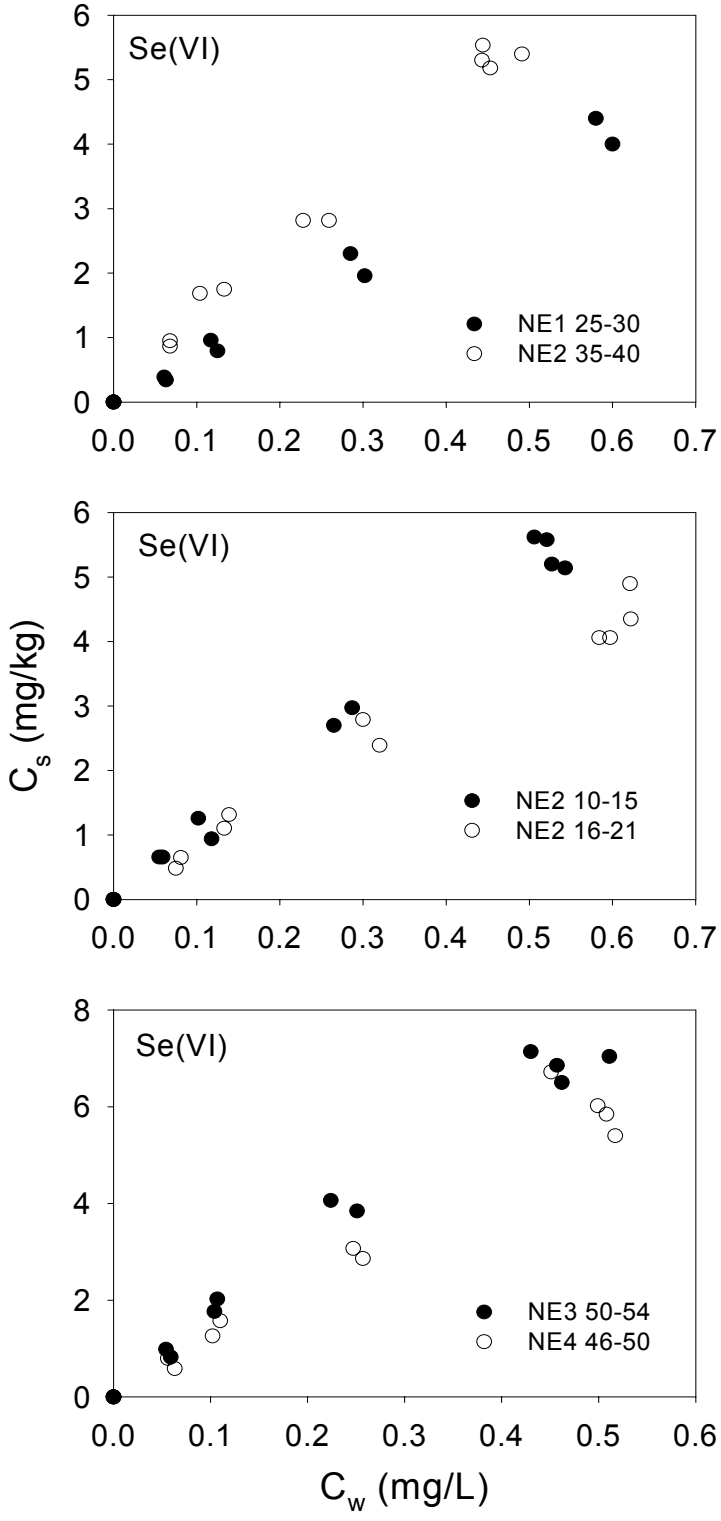

Figure 3-2
Se(VI) adsorption isotherms for NE site soils.

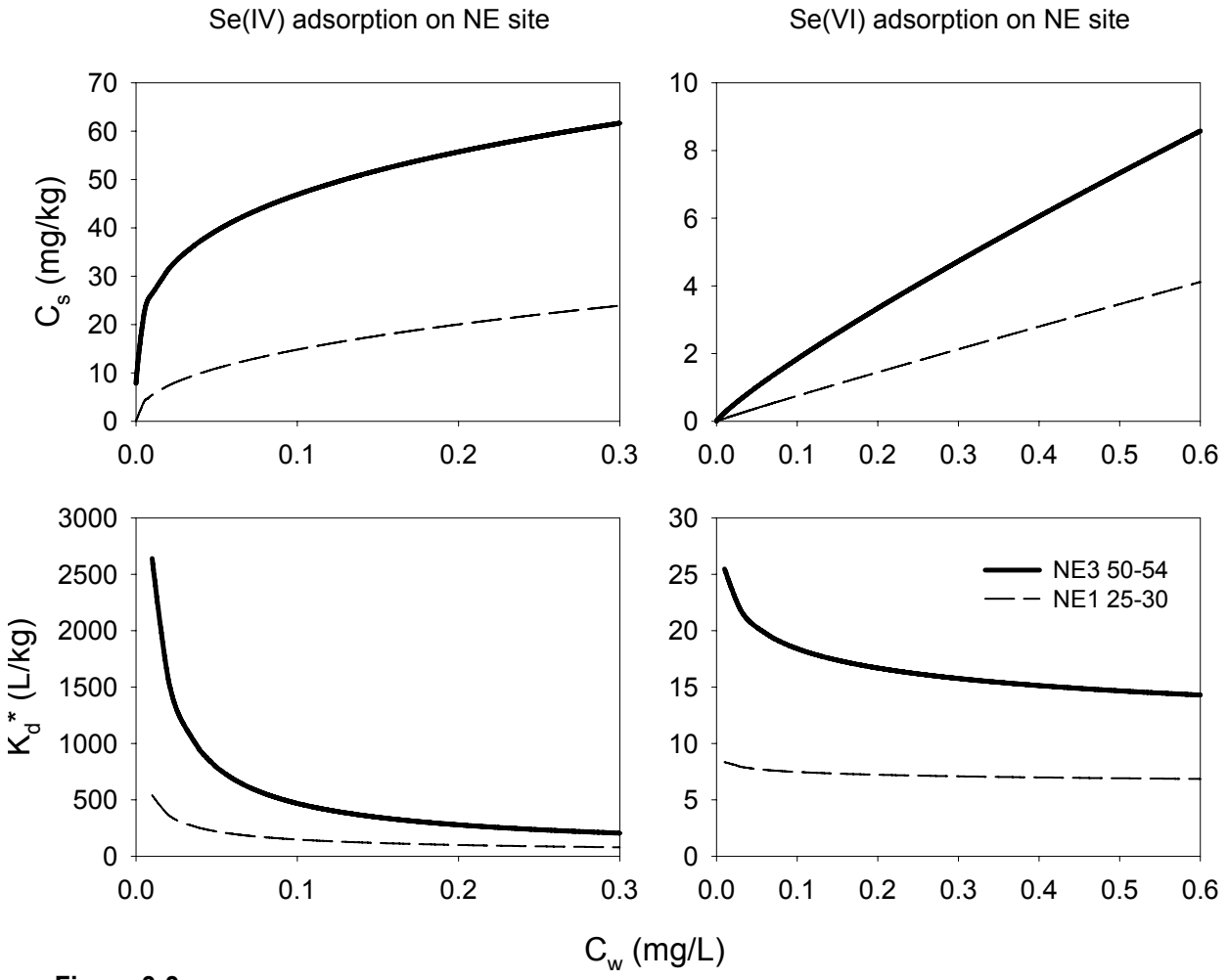

Figure 3-3
Se(IV) and Se(VI) adsorption profiles (upper graphs) for NE site soils using NE3 50-54 soil (solid line) and NE1 25-30 soil (dashed line); and effect of nonlinearity and Se concentration on concentration-specific Kd* values (lower graphs)

SE Site

Soil Characterization Data

Selected soil properties for six soils representative of the SE site are shown in Table 3-3. The SE site soils contained <5% clay, which was dominated by kaolinite and illite, with kaolinite being the dominant clay mineral in all soils except SE3 38.5 and SE2 23.5. Soils contained less than 1% organic matter and their soil-water pH values ranged from 5.6 to 6.4. Selective Fe dissolution of the soils resulted in DCB-extractable Fe levels ranging from approximately 5,243 to 14,948 mg/kg, and DCB-extractable Al levels ranging from 150 to 900 mg/kg. Ranges in oxalate-extractable Fe and Al were less variable, with oxalate extractable Fe ranging from 245 to

757 mg/kg, and oxalate extractable Al ranging from 228 to 486 mg/kg. Based on the assumption that the oxalate extraction primarily dissolves amorphous Fe and Al oxides, the differences between DCB and oxalate extracts indicate that 4 to 8% of extractable Fe in the soils is amorphous, and that half to all of extractable Al is amorphous. Fe extracted in 15 seconds with DCB ranged from 56 to 330 mg/kg, and was intended to estimate the most reactive portion of Fe oxides (i.e., Fe oxides exposed to solution and readily available for reaction). Of the 3 sites sampled in this study, the SE site soils represent the middle range for pH, % clay, and DCB-extractable and oxalate-extractable Fe and Al range.

Selenium Adsorption on SE Site Soils

Adsorption data for Se(IV) and Se(VI) on the six soils representative of the SE site were measured and fit with Freundlich and Langmuir isotherm models. Se(IV) and Se(VI) isotherms are plotted in Figures 3-4 and 3-5, and modeling fits are summarized in Table 3-4. K_f adsorption coefficients ($mg^{1-N}\ L^{N}\ kg^{-1}$) ranged between 25.0 and 84.2 for Se(IV) adsorption, and between 3.91 and 9.27 for Se(VI), which are lower than observed for NE site soils. Similar to the NE site soils, Se(IV) was more adsorbed and isotherms more nonlinear than Se(VI), but overall adsorption nonlinearity was less for SE site soils with Freundlich N values of 0.332 to 0.570 for Se(IV) and 0.935 to 1.03 for Se(VI). Freundlich K_f values for Se(IV) are 5.4 to 11 times higher than observed for Se(VI). To exemplify the overall selenium adsorption behavior at the SE site, Se(IV) and Se(VI) isotherms for the lowest and highest adsorption observed for the six soils considered representative of the site are shown in Figure 3-6, as well as the effect of nonlinearity on the concentration-specific K_d^* values that would be used to estimate site-specific transport. Note that the lowest sorption was observed for Se(VI) with an N values of 1.032, which is not statistically different than unity; however, this slightly greater than unity N value resulted in a slight decline in concentration-specific K_d^* values with decreasing C_w values, which is the opposite of what is observed when N<1. Nevertheless, there is essentially a negligible effect of concentration on the K_d^* value for this soil, because sorption is nearly linear.

Table 3-3
Selected properties of six soils representative of the SE site.

Soil	pH		Sand	Silt	Clay	CEC[a]	DCB[b]-Fe	DCB-Al	Ox[c]-Fe	Ox-Al	DCB-Fe 15 sec	Dominant Clay Minerals[d]
	H_2O	$CaCl_2$	----------%---------			cmol/kg	----------mg/kg----------					
SE1 48.5-50	5.7	5.4	62	33	5	4.3	7,105	450	576	486	150	K, I
SE1 60-62	6.0	5.8	56	39	5	4.8	14,948	900	757	423	330	K, I
SE2 23.5-25.5	6.1	6.1	66	31	3	4.1	8,399	182	413	305	56	K, I
SE2 33.5-35.5	6.4	6.2	60	35	5	2.7	5,243	280	245	228	60	K, I
SE3 5.5-7.5	5.6	5.4	66	29	5	3.1	6,209	280	226	395	84	K, I
SE3 38.5-40.5	6.2	6.1	62	35	3	4.1	6,647	150	500	243	73	K, I

[a] cation exchange capacity
[b] dithionite-citrate bicarbonate extractable
[c] oxalate extractable
[d] K = kaolinite, I = illite

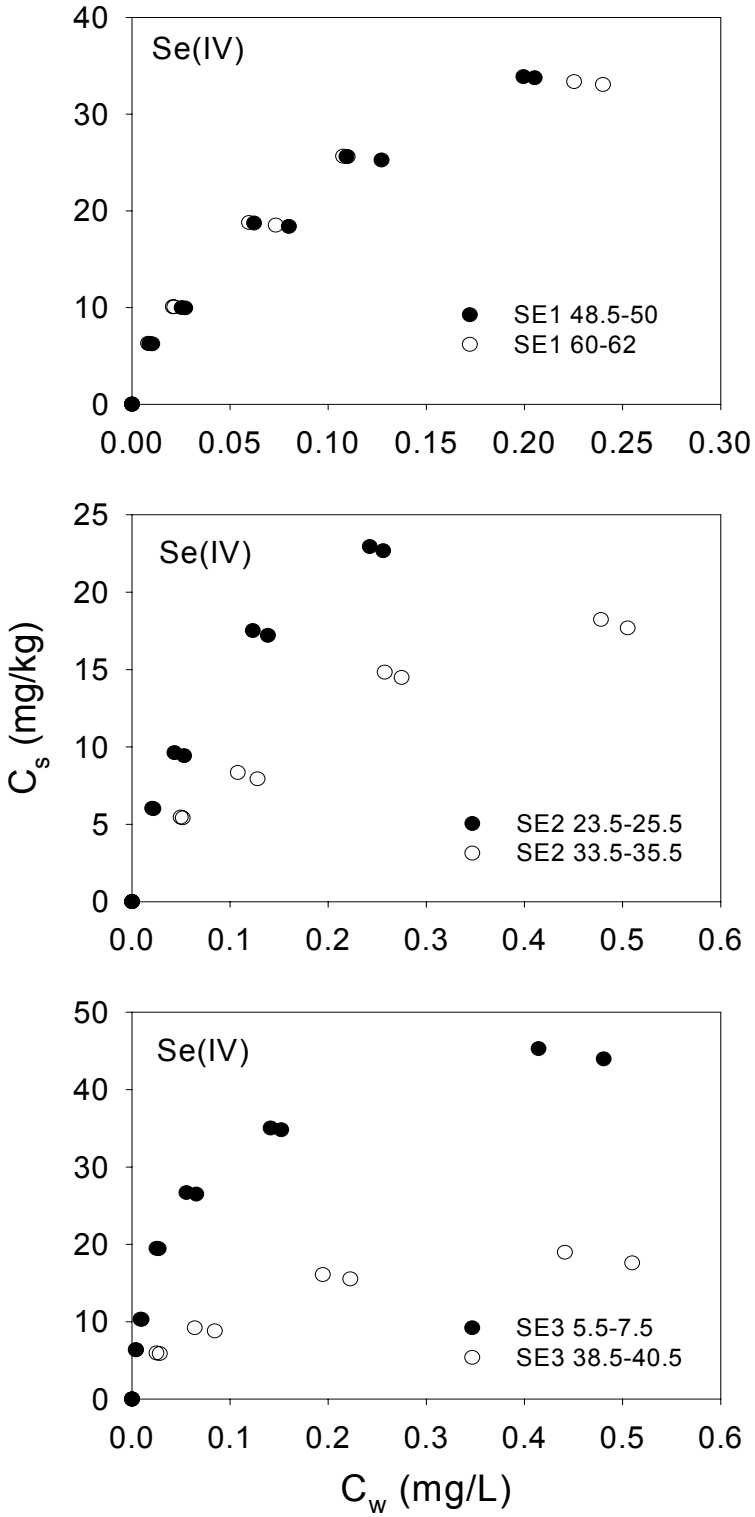

Figure 3-4
Se(IV) adsorption isotherms for SE site soils.

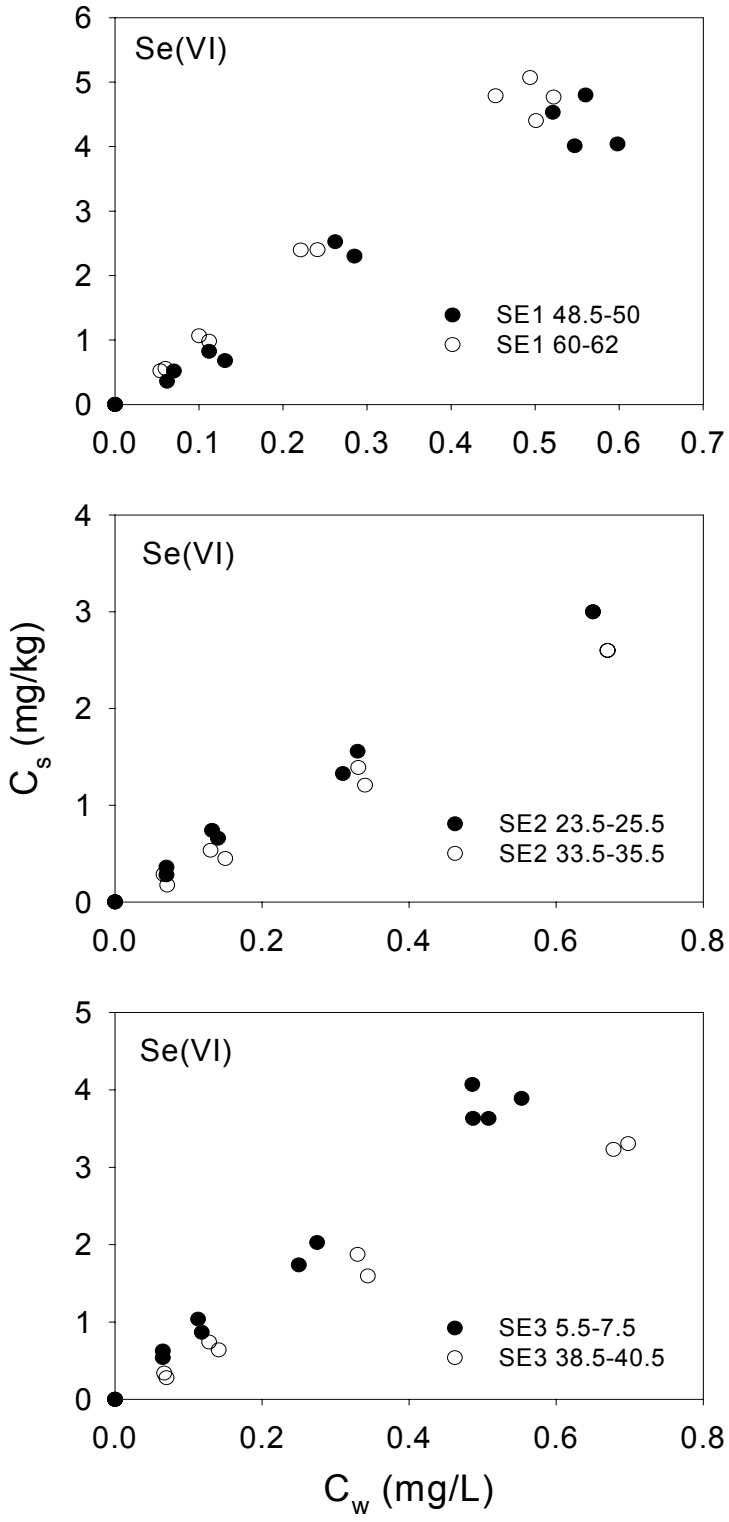

Figure 3-5
Se(VI) adsorption isotherms for SE site soils.

Table 3-4
Freundlich isotherm fits for selenite [Se(IV)] and selenate [Se(VI)] adsorption from 1mM CaSO4 for SE site soils.

Soil	Se(IV)				Se(VI)			
	pH[a]	K_f[b]	N	r^2	pH	K_f	N	r^2
SE1 48.5-50	4.67	84.2 (1.7)[c]	0.570 (0.026)[c]	0.991	4.47	7.67 (1.7)	0.968 (0.118)	0.958
SE1 60-62	4.89	68.7 (1.6)	0.480 (0.026)	0.985	4.70	9.27 (1.2)	0.945 (0.071)	0.982
SE2 23.5-25.5	5.34	48.0 (1.3)	0.524 (0.029)	0.988	5.20	4.52 (0.32)	0.977 (0.036)	0.996
SE2 33.5-35.5	5.42	26.7 (1.8)	0.522 (0.045)	0.969	5.53	3.91 (0.55)	1.032 (0.069)	0.988
SE3 5.5-7.5	4.51	61.0 (2.2)	0.332 (0.025)	0.961	4.56	7.18 (0.89)	0.952 (0.070)	0.982
SE3 38.5-40.5	5.84	25.0 (1.7)	0.368 (0.047)	0.933	5.62	4.64 (0.64)	0.935 (0.067)	0.985

[a] average aqueous pH values in which isotherm was measured
[b] $K_f = mg^{(1-N)} L^N kg^{-1}$
[c] numbers in parentheses are standard errors

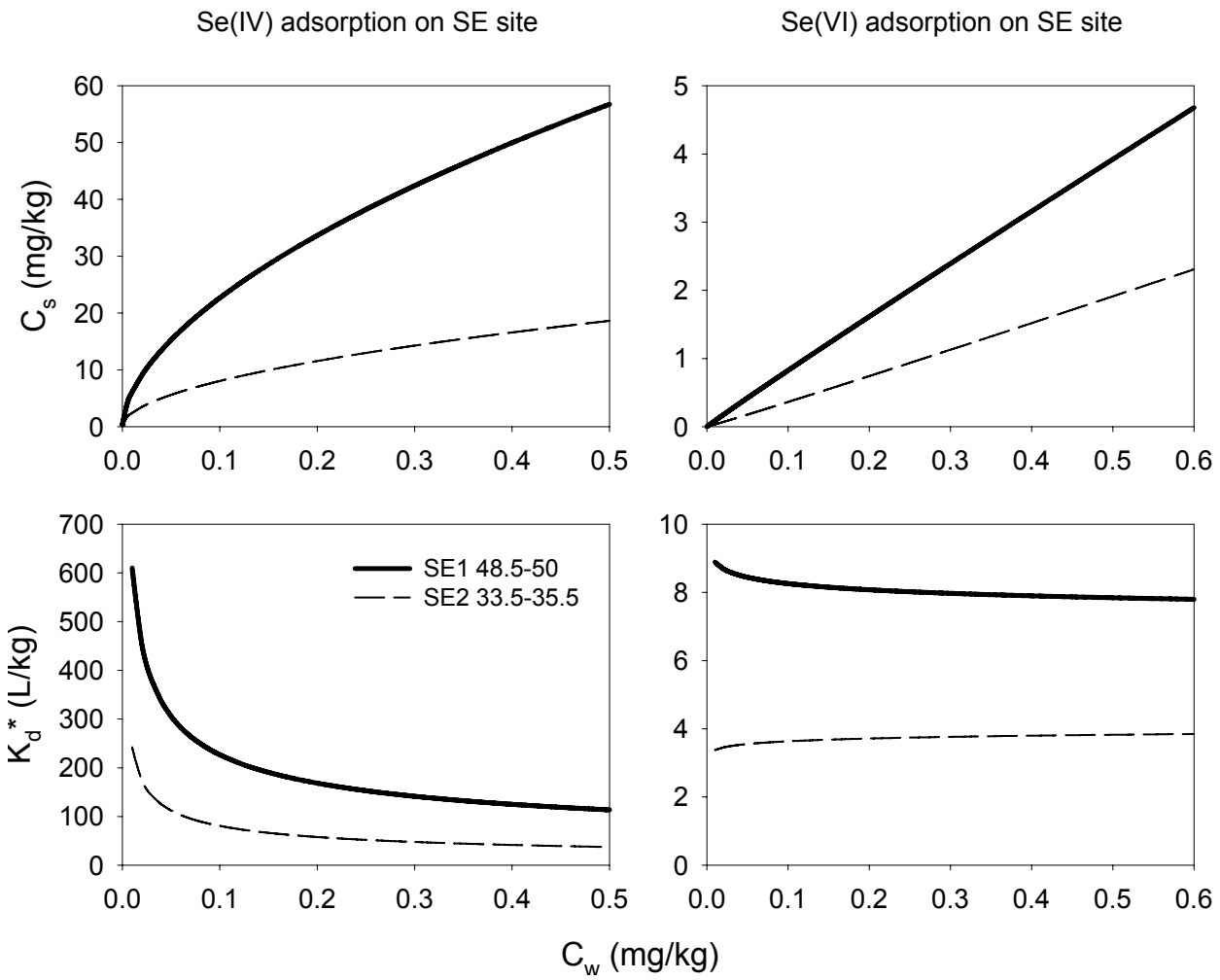

Figure 3-6
Se(IV) and Se(VI) adsorption profiles (upper graphs) for SE site soils using SE1 48.5-50 soil (solid line) and SE2 33.5-35.5 soil (dashed line); and effect of nonlinearity and Se concentration on concentration-specific Kd* values (lower graphs).

MW Site

Soil Characterization Data

Selected soil physical-chemical properties for six soil samples representative of the MW site are shown in Table 3-5. The MW soils are predominately sands (93 to 97% sand) with <1% clay; therefore, clay type analysis was not pursued. Soils contained less than 0.5% organic matter and their soil-water pH values ranged from 6.8 to 8.1. Selective Fe dissolution of the soils resulted in DCB-extractable Fe levels ranging from 2,718 to 4,540 mg/kg, and DCB-extractable Al levels ranging from 175 to 610 mg/kg. Ranges in oxalate extractable Fe and Al were less variable, with oxalate-extractable Fe ranging from 217 to 570 mg/kg, and oxalate-extractable Al ranging from 78 to 456 mg/kg. Based on the assumption that the oxalate extraction primarily dissolves amorphous Fe and Al oxides, the differences between DCB and oxalate extracts indicate that 4 to 13% of extractable Fe in the soils is amorphous, and 39 to 100% of extractable Al is amorphous. Fe extracted in 15 seconds with DCB ranged from 8 to 69 mg/kg, and was intended to estimate the most reactive portion of Fe oxides (i.e., Fe oxides exposed to solution and readily available for reaction). Of the 3 sites sampled in this study, the MW site soils have the highest sand content by far, the higher soil pH range (neutral to alkaline pH values), and the lowest levels of DCB-extractable Fe relative to all other site soils.

Selenium Adsorption on MW Site Soils

Adsorption data for Se(IV) and Se(VI) on the six soil samples representative of the MW site were measured and fit with Freundlich isotherm model. Se(IV) and Se(VI) isotherms are plotted in Figures 3-7 and 3-8, and modeling fits are summarized in Tables 3-6. K_f adsorption coefficients ($mg^{1-N} L^N kg^{-1}$) ranged between 8.16 and 15.8 for Se(IV), and between 1.96 and 3.12 for Se(VI), which are the lowest observed for any of the three sites. Adsorption was lowest on the MW site soil samples, but adsorption isotherms exhibited less nonlinearity, with Freundlich N values of 0.489 to 0.750 for Se(IV) and 0.772 to 0.989 for Se(VI). Similar to the NE and SE sites, adsorption of Se(IV) is consistently higher on these soils than that observed for Se(VI) with Freundlich K_f values being 2.5 to 7.4 times higher than for Se(VI), although differences between Se(IV) and Se(VI) were much less than observed for soil samples from the other two other sites. The overall selenium adsorption behavior at the MW site is exemplified in Figure 3-9, with Se(IV) and Se(VI) isotherms for the lowest and highest adsorption observed for the six soils shown as well as the effect of nonlinearity on the concentration-specific K_d^* values that would be used to estimate site-specific transport.

Table 3-5
Selected properties of six soils representative of the MW site.

Soil	pH		Sand	Silt	Clay	CEC[a]	DCB[b]-Fe	DCB-Al	Ox[c]-Fe	Ox-Al	DCB-Fe 15 sec
	H_2O	$CaCl_2$	----------%---------			cmol/kg	----------mg/kg----------				
MW1 17-19	8.1	7.3	93	4	3	3	4540	610	570	456	69
MW1 33-35	7.7	6.9	95	4	1	1.4	3781	198	145	78	15
MW2 17-19	7.5	6.2	95	4	1	1.4	3312	382	261	253	28
MW2 25-27	6.8	6.3	97	2	1	1.4	3143	175	217	95	12
MW3 17-19	7.7	6.8	95	4	1	1.7	2718	389	299	384	23
MW3 23-25	8.0	6.8	95	4	1	1.4	2964	105	241	105	8

[a] cation exchange capacity
[b] dithionite-citrate bicarbonate extractable
[c] oxalate extractable

Table 3-6
Freundlich isotherm fits for selenite [Se(IV)] and selenate [Se(VI)] adsorption from 1mM CaSO4 for MW site soils.

Soil	Se(IV)				Se(VI)			
	pH[a]	K_f[b]	N	r^2	pH	K_f	N	r^2
MW1 17-19	7.63	15.8 (0.8)[c]	0.646 (0.030)[c]	0.992	7.35	2.51 (0.37)	0.772 (0.041)	0.987
MW1 33-35	7.06	14.5 (1.5)	0.750 (0.062)	0.977	6.74	1.96 (0.31)	0.877 (0.055)	0.983
MW2 17-19	6.45	7.93 (0.87)	0.489 (0.062)	0.939	6.38	2.18 (0.43)	0.918 (0.076)	0.971
MW2 25-27	6.57	8.16 (0.6)	0.468 (0.040)	0.971	6.53	2.91 (0.33)	0.989 (0.053)	0.988
MW3 17-19	6.98	10.8 (1.4)	0.655 (0.074)	0.953	6.89	3.12 (0.75)	0.787 (0.070)	0.963
MW3 23-25	6.84	11.3 (1.0)	0.506 (0.054)	0.953	6.78	2.06 (0.39)	0.828 (0.059)	0.977

[a] average aqueous pH values in which isotherm was measured
[b] $K_f = mg^{(1-N)} L^N kg^{-1}$
[c] numbers in parentheses are standard error

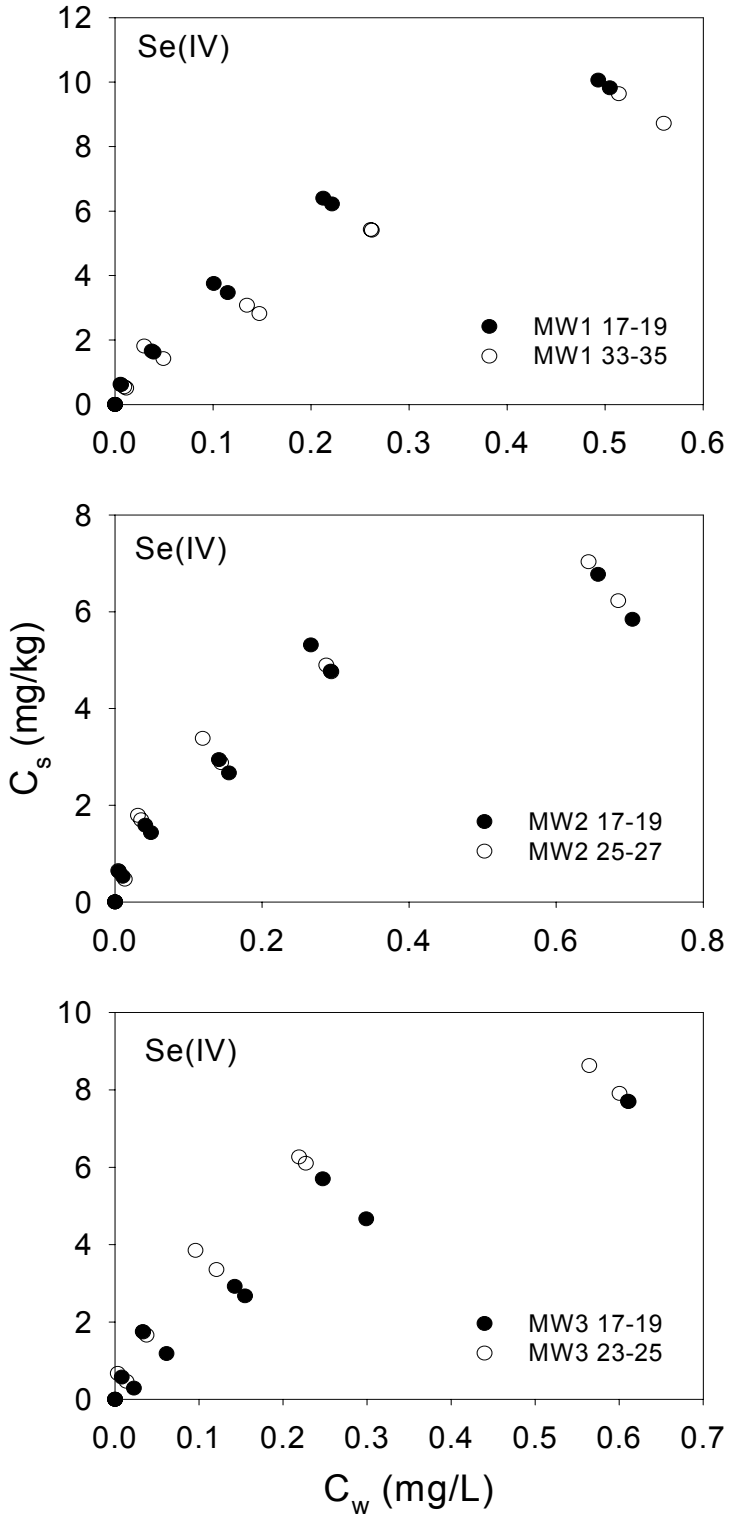

Figure 3-7
Se(IV) adsorption isotherms on MW site soils.

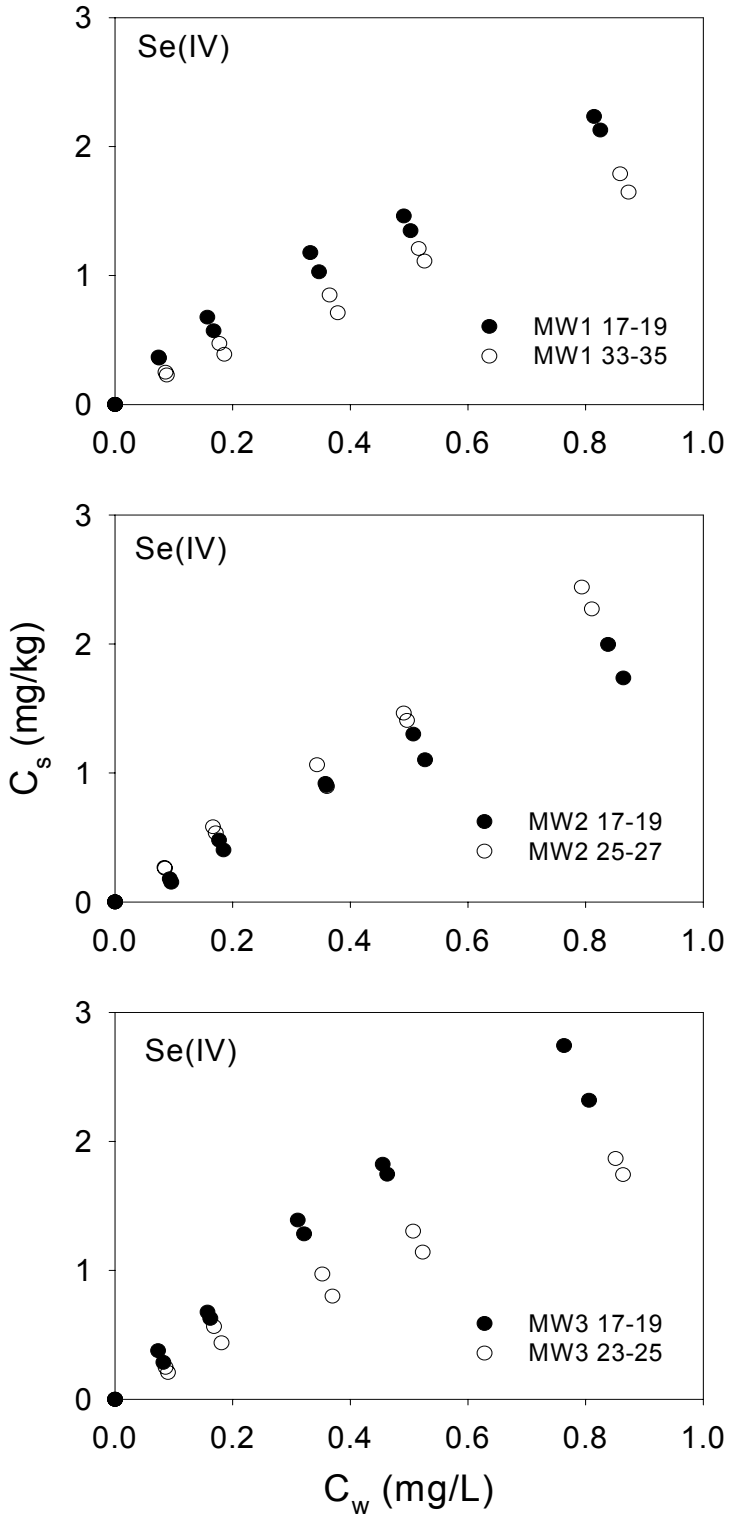

Figure 3-8
Se(VI) adsorption isotherms on MW site soils.

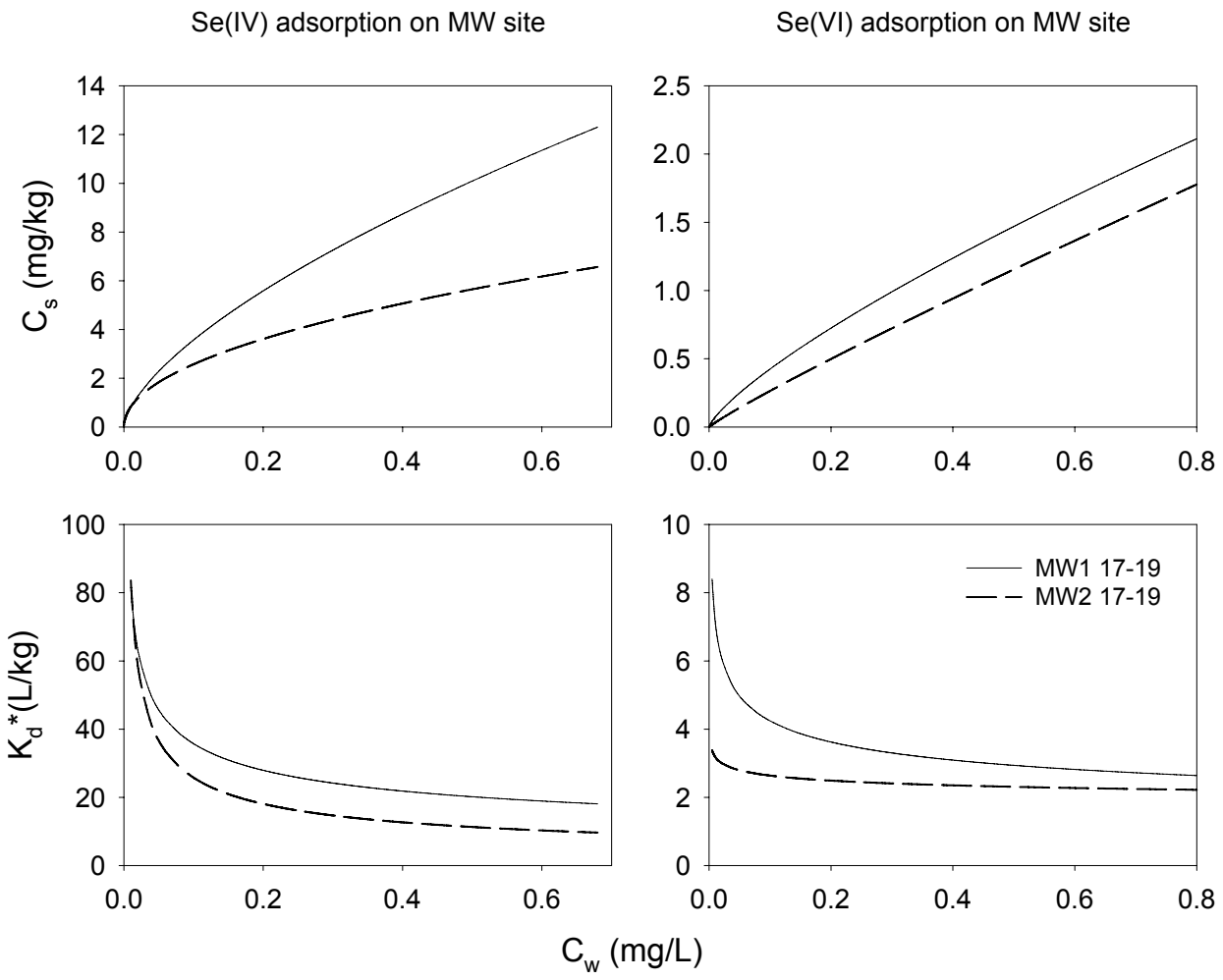

Figure 3-9
Se(IV) and Se(VI) adsorption profiles (upper graphs) for MW site using MW1 17-19 soil (solid line) and MW2 17-19 soil (dashed line; and effect of nonlinearity and Se concentration on concentration-specific Kd* values (lower graphs).

4
FACTORS AFFECTING SELENIUM ADSORPTION

Effects of Solution pH on Selenium Adsorption

The adsorption of selenium was expressed quantitatively as the percentage of selenium adsorbed (removed from the initial solution) relative to the applied concentration. Adsorption envelopes produced for each selenium species as a function of pH are shown in Figures 4-1, 4-2, and 4-3 for one soil sample from each site (NE1 25-30, SE1 48.5-50, and MW1 17-19). The initial concentration of spiked selenium of 0.52 mg/L for Se(IV) and 0.41 mg/L for Se(VI) is approximately mid range of the concentrations used in the multi-concentration isotherm measurements from 1 mM $CaSO_4$ system. Two arrows shown in each figure indicate the range of equilibrium pH values observed when soils were mixed with water, 1 mM $CaCl_2$, and 1 mM $CaSO_4$ solutions (no pH adjustments).

It is evident that selenium adsorption of selenium species is strongly dependent on pH with the greatest adsorption occurring in the acidic pH range. For Se(IV), the apparent adsorption maxima varies with soil type with NE1 25-30, SE1 48.5-50, and MW1 17-19 exhibiting apparent maxima or adsorption plateaus at pH < 4.5, pH < 5.5, and pH < 7, respectively. Adsorption of Se(VI) is pH-dependent over the entire pH range studied (approximately 3 to 9) with sorption consistently decreasing with increasing pH. The increase in adsorption with decreasing pH of the soil is characteristic of anion adsorption. Similar pH-dependent Se(IV) adsorption was reported for oxides, pure clay minerals, and natural soils (Balistrieri and Chao, 1987; Hingston et al., 1972; Neal et al., 1987a). Increased protonation of soil surface functional groups ($\equiv OH_2^+$) with decreasing pH is expected to increase the anion exchange capacity, and therefore, increase the amount of anions sorbed on the soil particles. Frequent observations that Se(IV) adsorption maxima (μmol/g) greater than expected from surface positive charge of sorbent suggests that Se(IV) can replace the uncharged OH_2 surface groups (ligand exchange) (Rajan, 1979).

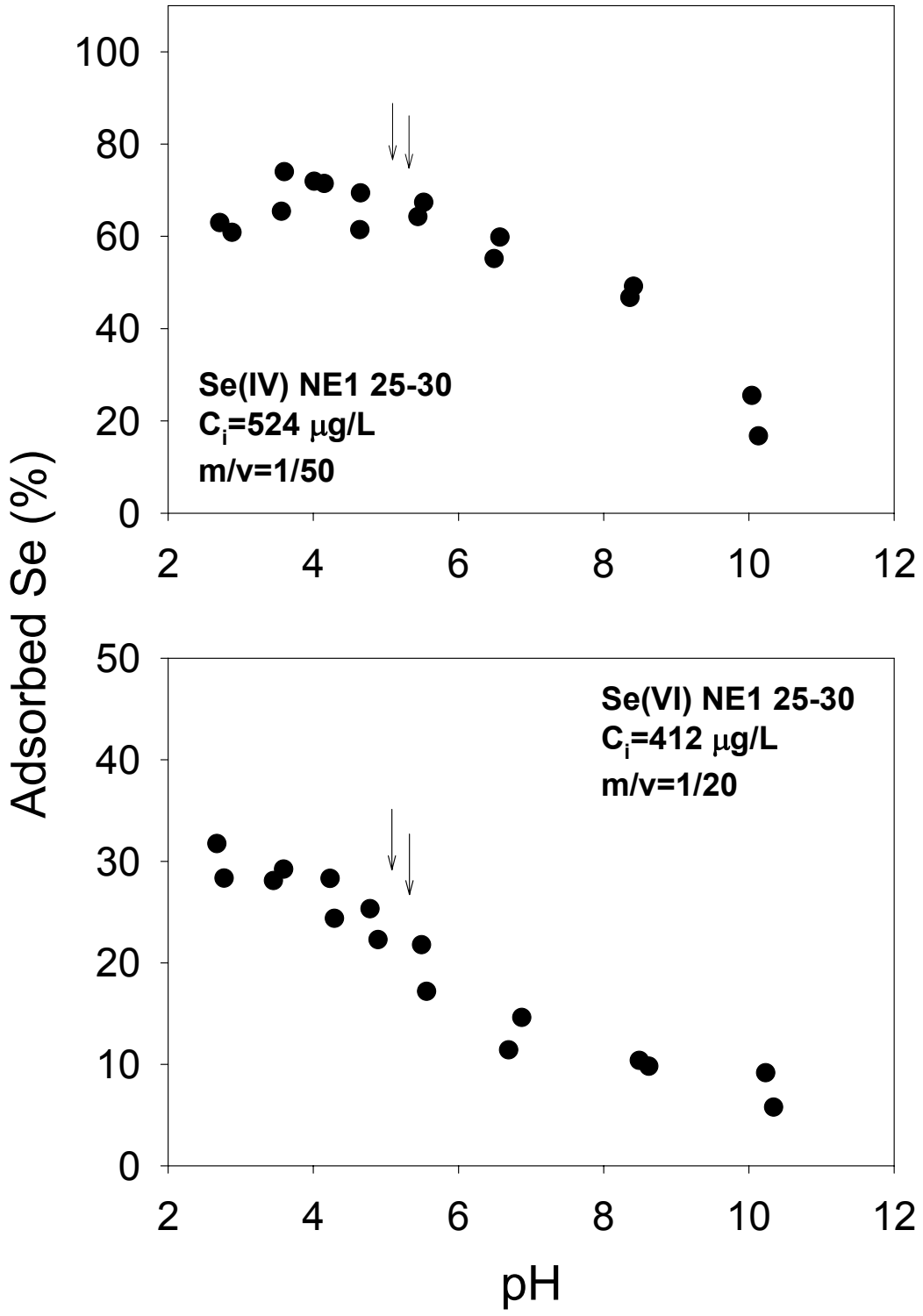

Figure 4-1
pH effects on Se adsorption on NE1 25-30 soil (C_i is the applied Se concentration).

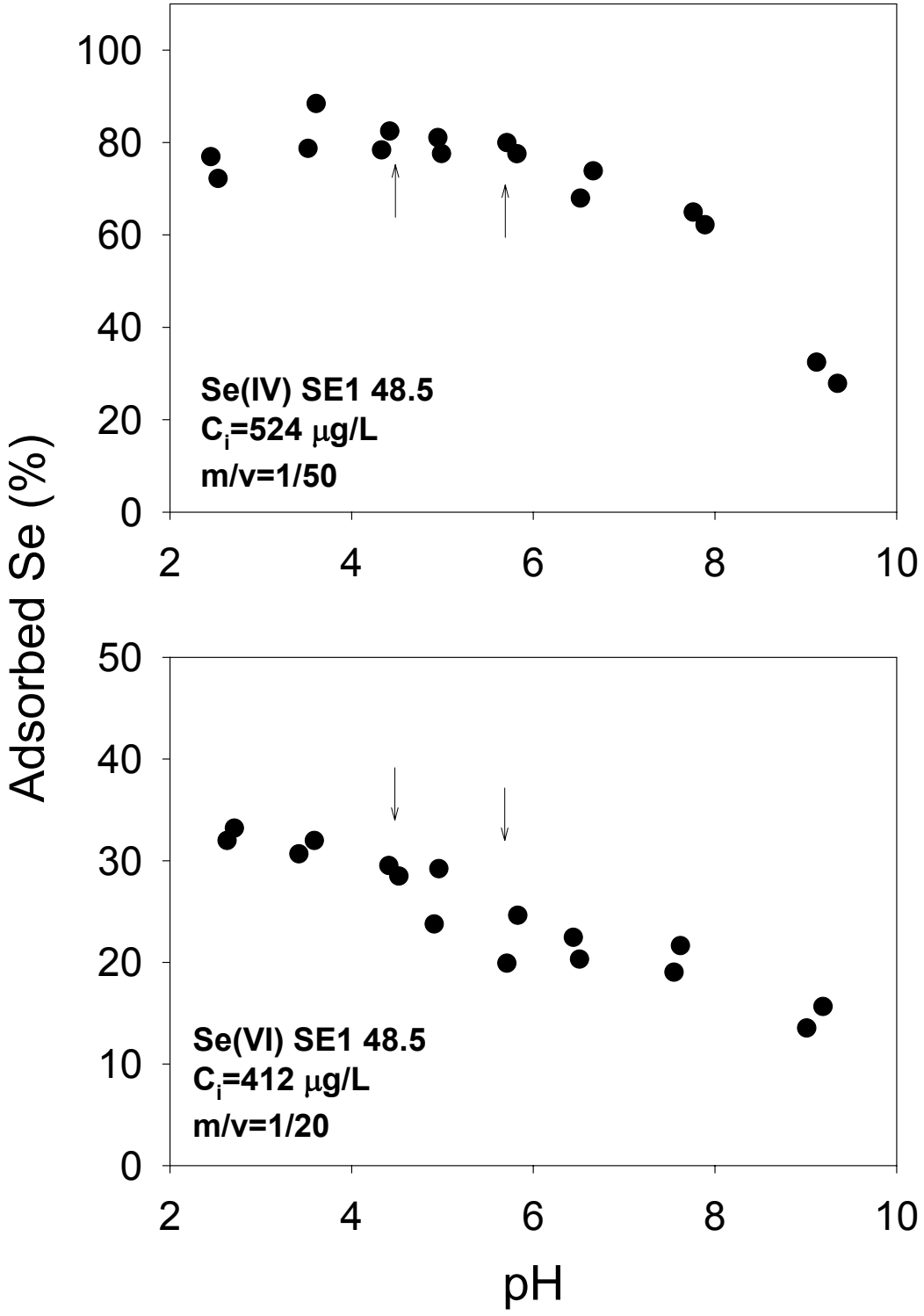

Figure 4-2
pH effects on Se adsorption on SE1 48.5 soil (Ci is the applied Se concentration).

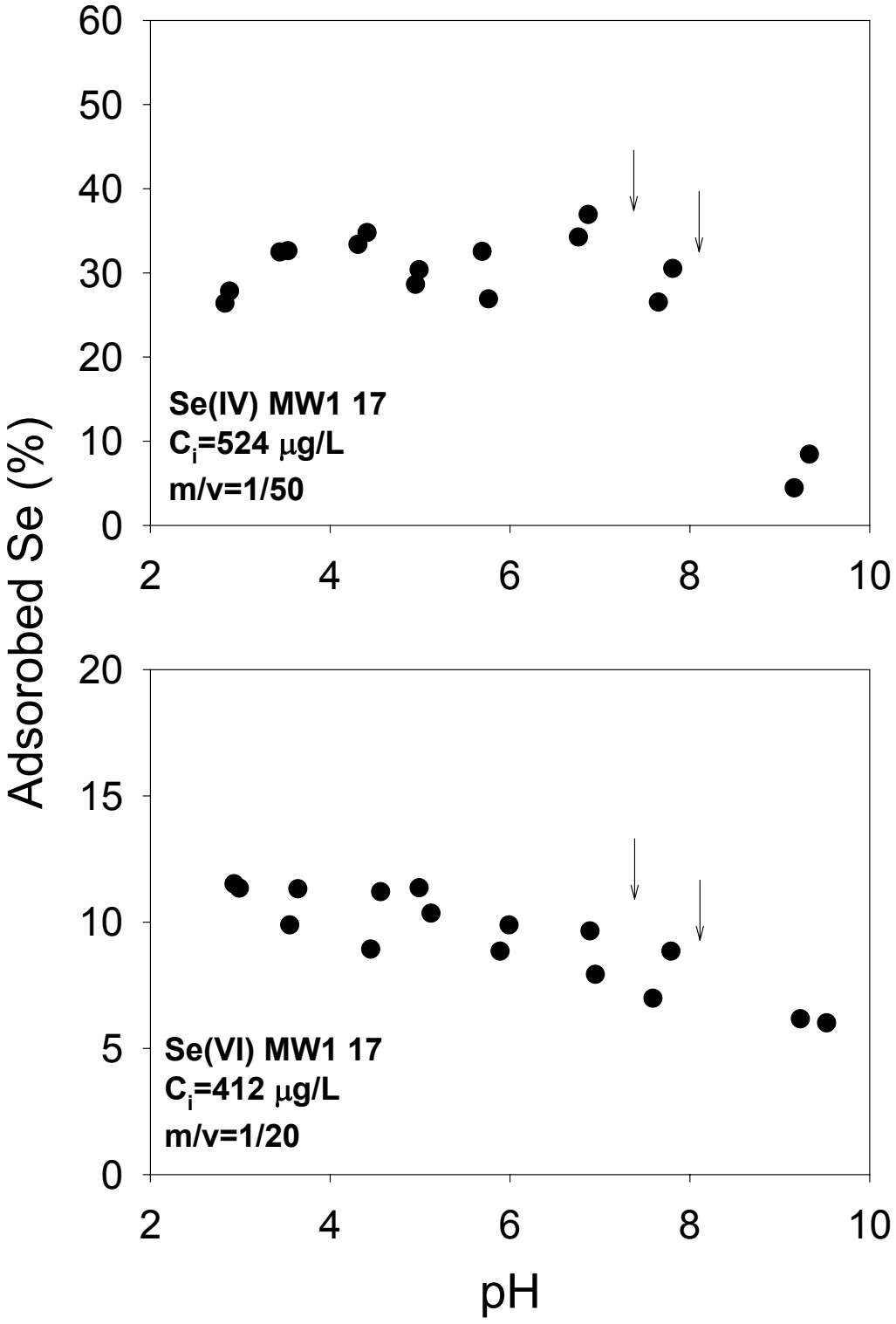

Figure 4-3
pH effects on Se adsorption on MW1 17-19 (Ci is the applied Se concentration).

Soil solution pH may change as the ash leachate plume moves through soils down gradient of an ash landfill, thus affecting selenium mobility. The potential changes in soil solution pH will depend on the natural soil pH, the buffer capacity of the soil, the pH and buffer capacity of the ash leachate, and residence time. For the NE soils, the range in soil pH in water and 1 mM $CaCl_2$ is between 4.4 and 5.5, and the ash pH associated with that site ranged between 5.5 and 6.2 (Chapter 5). Therefore, assuming the pH envelope for NE1 25-30 is representative of the NE site, substantial changes in mobility of Se(VI) only may be expected as a worse case scenario, which assumes that the buffer capacity of the ash is much greater than the soil buffer capacity. Given that the NE soils contain about 1% carbon, significant % clay, and high extractable Fe and Al, the soil is likely to have a reasonable capacity to buffer pH changes. For the SE soils, the range in soil pH in water and 1 mM $CaCl_2$ is between 5.4 and 6.4, and the ash associated with that site has a pH ≈ 6 (Chapter 5). Assuming the pH envelope for SE1 48.5 is representative of the SE site, soil solution pH and therefore selenium adsorption is unlikely to change much over time. For the MW soils, the range in soil pH in water and 1 mM $CaCl_2$ is between 6.2 and 8.1; however, the ash associated with this site yields a leachate with a much higher pH of 11 to 12 (Chapter 5). Soils at this MW site are also very sandy (93 to 97% sand), thus have little buffer capacity or adsorption capacity. Therefore, enhanced mobility of both Se(IV) and Se(VI) is likely as ash leachate plume passes through the soil.

Effects of Solution Matrix on Selenium Adsorption

The effect of calcium (Ca^{2+}) and sulfate (SO_4^{2-}) in solution on adsorption of Se(IV) and Se(VI) on NE1 25-30 soils is shown in Figure 4-4 from a fixed concentration of 1.39 mg/L for Se(IV) and 0.53 mg/L for Se(VI)). The impact of increased sulfate concentration on both Se(IV) and Se(VI) adsorption is much greater than impact of calcium over the range of concentrations (0 to 10 mM). From sulfate free to 10 mM SO_4^{2-} solutions, Se(IV) adsorption decreased from 43.8 mg/kg to 27.9 mg/kg, and Se(VI) adsorption decreased from 7.22 mg/kg to 1.49 mg/kg for Se(VI), which corresponds to a 36% and 79% decrease, respectively. The greater decrease in Se(VI) adsorption relative to Se(IV) is in agreement with the hypothesis that Se(VI) forms outer-sphere complexes similar to sulfate, whereas Se(IV) tends to form inner-sphere complexes more like phosphate (Neal et al., 1987b). Increases in adsorption with increasing calcium concentrations up to 10 mM were small and similar for both selenium species with a 17.4% and 17.9% increase in sorption for Se(IV) and Se(VI), respectively. Similar increases in selenium adsorption in the presence of Ca have been reported for several soils (Neal et al., 1987b); however, little information is currently available concerning the specific mechanism of this enhanced adsorption. Plausible explanations for this phenomenon include: (1) sorption of Ca^{2+} to negatively charged surface sites making the electrical potential at those sites less negative, thereby increasing the adsorption of selenium anions; (2) intramolecular bridging of Ca^{2+} between an oxyanion and negatively charged surface site; and (3) co-precipitation. The latter is unlikely given the relatively low concentration of selenium in solution used in this study.

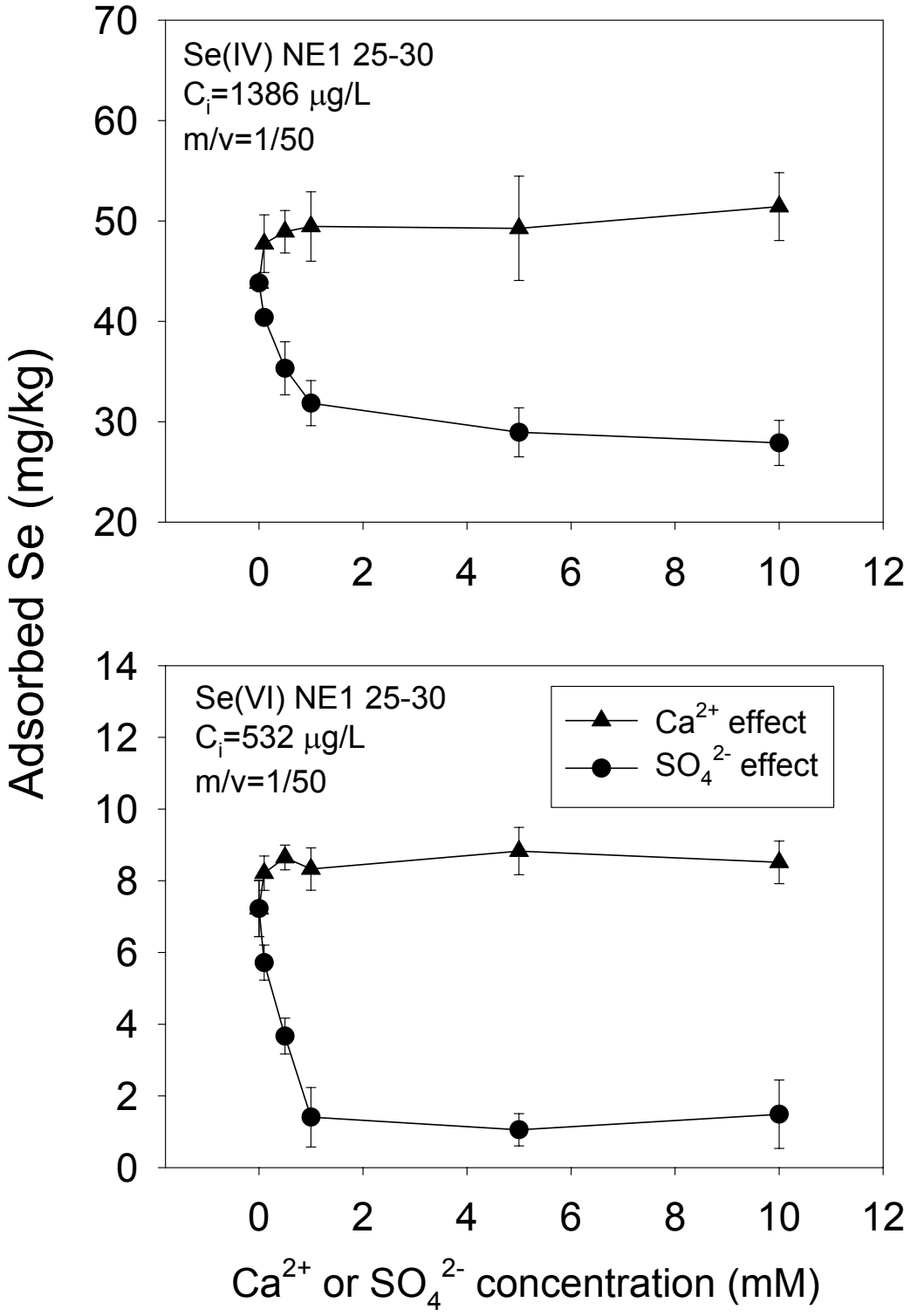

Figure 4-4
Impact of concentration of Ca2+ and SO42- on Se adsorption on NE1 25-30 (Ci is the applied Se concentration).

In Figures 4-5 and 4-6, the multi-concentration isotherms measured from 1 mM KCl, 1 mM $CaCl_2$, 1 mM K_2SO_4, and 1 mM $CaSO_4$ are shown for Se(IV) and Se(VI), respectively. For Se(VI), only SO_4^{2-} appears to affect sorption significantly, thus sorption is similar and suppressed in $CaSO_4$ and K_2SO_4 and higher but similar in $CaCl_2$ and KCl (Figure 4-6). Se(IV) sorption is also reduced by SO_4^{2-}; but in addition, Ca^{2+}enhanced sorption resulting in the following trends for all three soils investigated: 1 m*M* $CaCl_2$ > 1 m*M* $CaSO_4$ > 1 m*M* KCl > 1 m*M* K_2SO_4 (Figure 4-6).. This phenomena supports the conclusion derived from Figure 4-4 with the one exception that the effects of sulfate on Se(IV) adsorption is much greater than calcium, yet adsorption of Se(IV) from 1 mM $CaSO_4$ is greater or similar to 1 mM $CaCl_2$. Se(IV) adsorption from 1 mM K_2SO_4 is less than 1 mM KCl, but the difference is less than expected. Also in all cases, increases in Se(IV) adsorption from 1 mM $CaSO_4$ and 1 mM $CaCl_2$ relative to 1 mM KCl are much greater. The less than expected differences between Se(IV) adsorption from1 mM K_2SO_4 and 1 mM KCl, and the larger than expected differences between Se(IV) adsorption in 1mM $CaSO_4$ and 1 mM $CaCl_2$ relative to 1 mM KCl may partially be due to the differences in solution ionic strength. Ionic strength increased as follows: 1 mM KCl (I = 0.001) < 1 mM K_2SO_4 = 1 mM $CaCl_2$ (I = 0.003) < 1 mM $CaSO_4$ (I=0.004). Ionic strength was not controlled in the multi-concentration isotherms experiment, because the differences in ionic strength (0.001 to 0.004) were hypothesized to be small based on existing literature (Neal et al., 1987b; Peak and Sparks, 2002). However, based on Se(IV) adsorption from 1 mM K_2SO_4 and 1 mM $CaCl_2$ at a constant and where Ca^{2+} and SO_4^{2-} coexist in equal concentrations, Ca^{2+} has the greater impact on Se(IV).

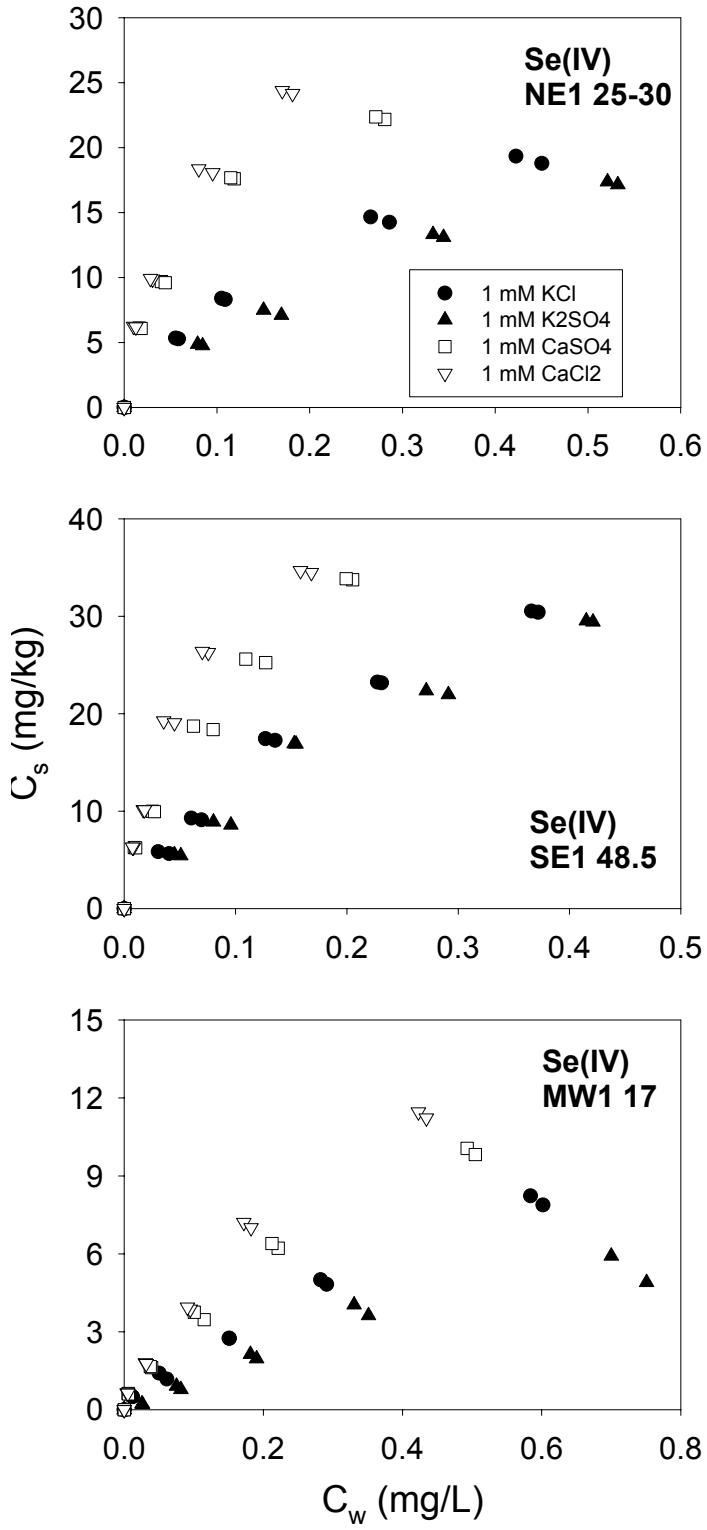

Figure 4-5
Ionic matrix effects on Se(IV) adsorption on NE1 25-30, SE1 48.5-50, and MW1 17-19 soils.

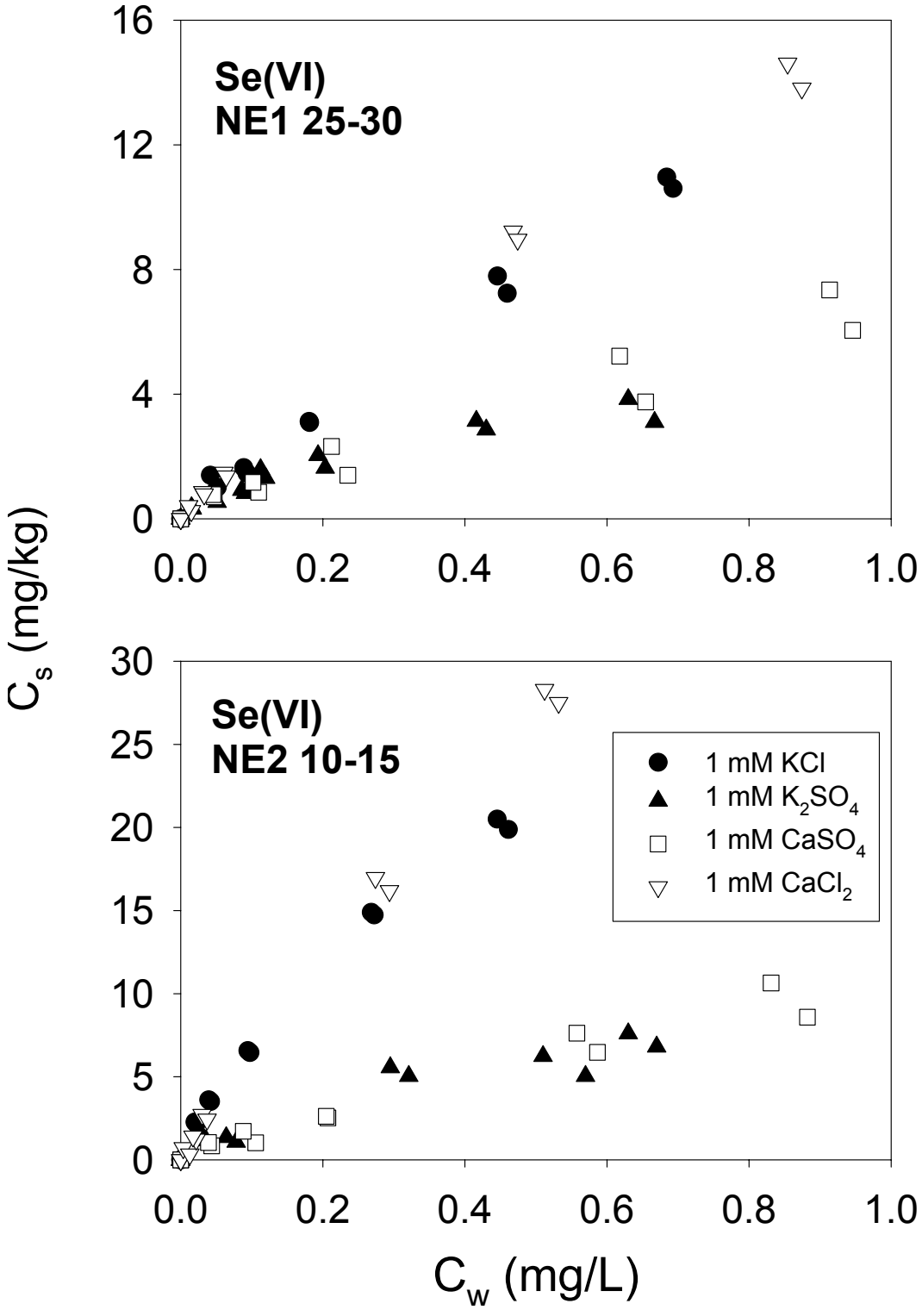

Figure 4-6
Ionic matrix effects on Se(VI) adsorption on NE1 25-30 and NE2 10-15 soils.

Adsorption Data versus Soil Characteristics for All Sites

Evaluating the main soil factors involved in adsorption mechanism of selenium in soil and quantifying correlations between sorption and key soil properties can be useful in making approximate a priori predictions of selenium mobility at a site. Towards this goal, simple and multiple linear regression analyses were performed between Se(IV) and Se(VI) adsorption and several soil properties. For both the simple and the multiple linear regression analyses, similar results were obtained using either K_f adsorption coefficients or concentration-specific K_d* values estimated using equation 2-2 with different concentrations. The results of the simple linear regression analysis for both Se(IV) and Se(VI) using the K_f adsorption coefficients and K_d* values calculated at C_w = 100 μg/L are shown in Tables 4-1 and 4-2, respectively.

From the simple linear regression analysis, soil clay and oxide contents were found to show the best positive correlations. For the oxide data, the best correlation was found with easily reducible Fe for both Se(IV) and Se(VI) (shown as15-sec DCB-Fe in Tables 4-1 and 4-2) as exemplified in Figure 4-7. For both species, selenium adsorption was negatively correlated with soil isotherm pH, supporting the general trend of decreasing adsorption with increasing pH shown in Figures 4-1 through 4-3. Based on the simple linear regression analysis, pH, clay content, and 15-sec DCB-Fe appear to be the most important soil properties affecting selenium adsorption from a constant solution matrix (1 mM $CaSO_4$).

A summary of the stepwise multiple linear regression analyses using K_d* values for both Se(IV) and Se(VI) calculated at C_w = 100 μg/L (Table 4-3) shows that correlations are improved when clay and oxide contents were combined with pH. The best prediction for selenium adsorption in this study was made using 15 sec-DCB-Fe content in combination with isotherm pH with r^2 being 0.884 and 0.818, for Se(IV) and Se(VI), respectively. Combining pH and clay content also gave good predictions for Se(IV) and Se(VI) adsorption with r^2 = 0.802 and 0.836, respectively. Note that the fraction of oxides will be present in the clay fraction (< 2 μm); however, not all clays are oxides; therefore, the relatively high correlation coefficients for clay is a little surprising. Both pH and clay content are easily measured on any soil sample making this particular correlation appealing for predicting adsorption characteristics of selenium species by a soil. Note that correlations using simultaneously both clay and oxides parameters also appear good, but since the oxides are within the clay fraction, this in part, gives weight to the same parameter twice.

Table 4-1
Summary of simple linear regressions between various soil parameters and the mass-based Freundlich isotherm adsorption coefficients (Kf, mg1-N LN kg-1) estimated in 1 mM CaSO4.

Specie	Regression Parameter	pH[a]	Clay	DC - Fe	DC - Al	Ox - Fe	Ox - Al	15-sec DCB-Fe
			%	mg/kg				
Se(IV)	slope	-28.40	2.68	0.003	0.057	0.013	0.139	0.053
	intercept	210	25.4	19.9	18.9	36.4	1.90	30.0
	R^2	0.635	0.479	0.499	0.385	0.212	0.339	0.514
Se(VI)	slope	-2.76	0.351	0.0003	0.006	0.002	0.016	0.007
	intercept	22.0	3.25	3.39	3.14	4.58	1.06	4.00
	R^2	0.530	0.727	0.439	0.377	0.368	0.373	0.685

[a] equilibrium pH values of adsorption isotherm

Table 4-2
Summary of simple linear regressions between various soil parameters and the concentration-specific selenium adsorption coefficients (Kd*,L/kg; Cw=100 µg/L) estimated in 1 mM CaSO4.

Specie	Regression Parameter	pH[a]	Clay	DC - Fe	DC - Al	Ox - Fe	Ox - Al	15-sec DCB-Fe
			%	mg/kg				
Se(IV)	slope	-129	15.2	0.017	0.302	0.072	0.684	0.303
	intercept	931	65.7	38.8	39.3	127.4	-34.0	90.9
	R^2	0.556	0.652	0.641	0.460	0.295	0.350	0.712
Se(VI)	slope	-3.019	0.448	0.0003	0.007	0.002	0.019	0.008
	intercept	24.4	3.66	4.26	3.76	5.37	1.15	4.62
	R^2	0.382	0.786	0.372	0.360	0.398	0.370	0.740

[a] equilibrium pH values of adsorption isotherm

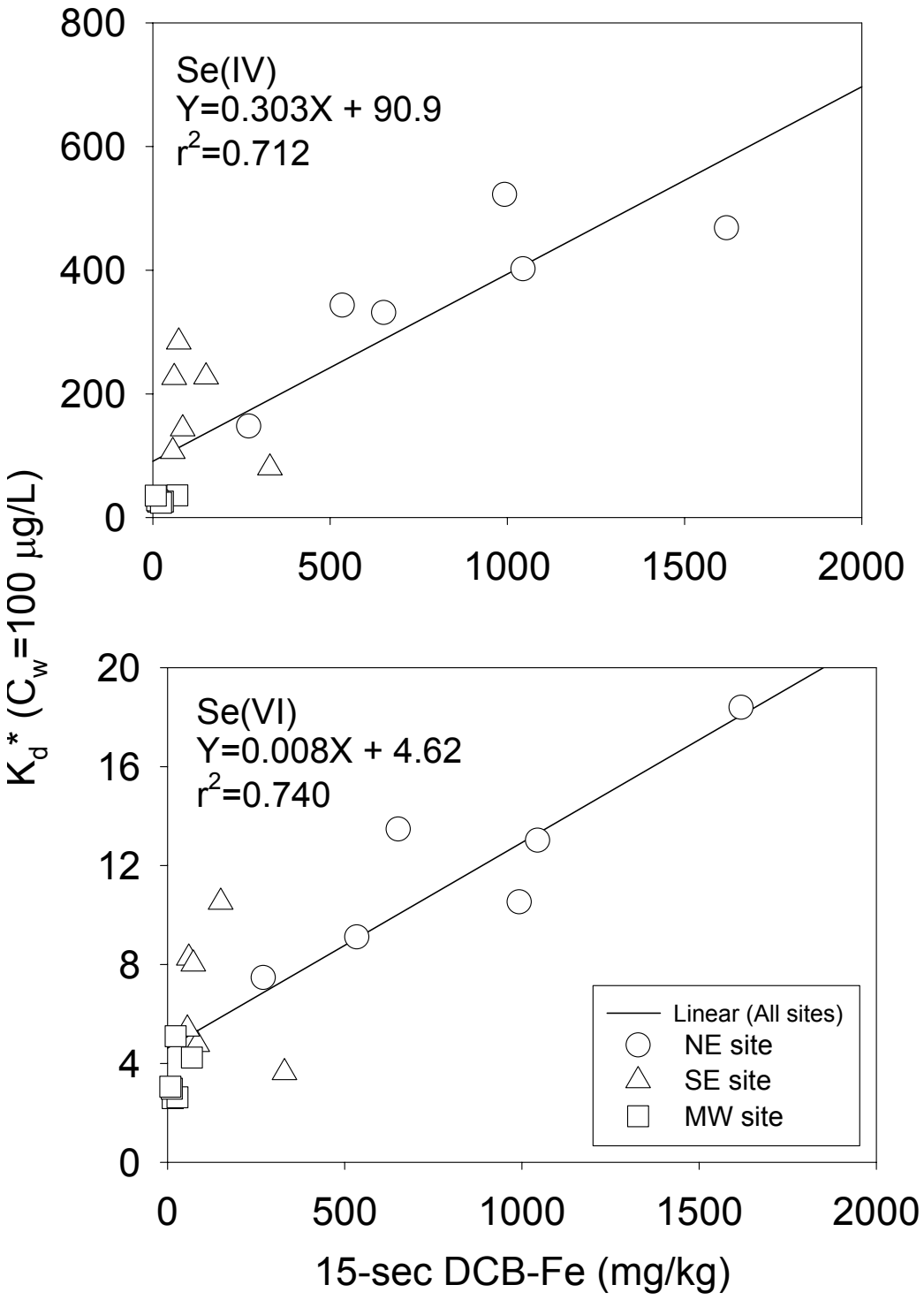

Figure 4-7
Linear correlation for Se(IV) and Se(IV) between concentration specific Kd* values and easily reducible Fe assayed using a 15-second DCB extraction method.

Table 4-3
Summary of multiple linear regression analyses between various soil parameters and the concentration-specific selenium adsorption coefficients (Kd*,L/kg; Cw=100 µg/L)

											r^2
Se(IV)	-78.0	pH	+	10.8	Clay	+	548				0.802
	-79.0	pH	+	0.012	DCB-Fe	+	536				0.796
	-104	pH	+	0.227	DCB-Al	+	674				0.794
	-113	pH	+	0.052	Ox-Fe	+	794				0.700
	-106	pH	+	0.432	Ox-Al	+	656				0.678
	-80.0	pH	+	0.229	15sec-Fe	+	573				0.884
	5.35	clay	+	0.213	15sec-Fe	+	76.4				0.730
	0.02	DCB-Fe	-	0.030	DCB-Al	+	42.8				0.643
	0.05	Ox-Fe	+	0.511	Ox-Al	-	19.7				0.456
	-88.7	pH	+	0.007	DCB-Fe	+	0.117	DCB-Al	+	581	0.811
	-101	pH	+	0.040	Ox-Fe	+	0.300	Ox-Al	+	635	0.751
	9.80	clay	+	0.013	DCB-Fe	-	0.082	DCB-Al	+	29.9	0.807
	14.6	clay	+	0.018	Ox-Fe	+	0.301	Ox-Al	-	12.7	0.707
Se(VI)	-1.24	pH	+	0.387	Clay	+	11.2				0.836
	-2.03	pH	+	0.0002	DCB-Fe	+	16.8				0.499
	-2.40	pH	+	0.006	DCB-Al	+	18.1				0.584
	-2.53	pH	+	0.002	Ox-Fe	+	20.0				0.656
	-2.24	pH	+	0.014	Ox-Al	+	15.5				0.552
	-1.50	pH	+	0.007	15sec-Fe	+	13.5				0.818
	0.29	clay	+	0.003	15sec-Fe	+	3.84				0.814
	0.0002	DCB-Fe	+	0.003	DCB-Al	+	3.80				0.392
	0.002	Ox-Fe	+	0.013	Ox-Al	+	1.64				0.542
	-2.81	pH	-	0.0002	DCB-Fe	+	0.008	DCB-Al	+	20.5	0.598
	-2.15	pH	+	0.002	Ox-Fe	+	0.008	Ox-Al	+	15.4	0.709
	0.41	clay	+	0.00001	DCB-Fe	+	0.001	DCB-Al	+	3.25	0.795
	0.42	clay	-	0.0002	Ox-Fe	+	0.007	Ox-Al	+	1.84	0.824

5
ATTENUATION OF SELENIUM IN ASH LEACHATE

Leaching and adsorption experiments were performed using leachate generated from site ash samples to evaluate the effect of the leachate matrix on selenium adsorption. One or two ash samples from each site were used in sequential and kinetic leaching studies. Ash samples were selected based on their location with respect to the water table. For each site, if appropriate, one ash was selected that resided predominantly above the water table (unsaturated) and one ash was selected that resided predominantly below the water table (saturated).

Sequential Leaching

Average pH values measured for sequential leaching of ash samples obtained from each site are summarized in Figure 5-1 (upper figure). In all but the high pH of MW ash, pH values were lowest in the first leaching and then stabilized at slightly higher pH values for subsequent leachings, with NE 4 15-20 exhibiting the largest increase in pH of one unit from the first to third sequential leaching. All ashes stabilized at pH values between 6 and 6.4 except the MW ash, which had a pH of about 11.7 in the first leaching and 11.3 by the 15th sequential leaching.

Selenium concentrations over the sequential leaching series are shown on Figure 5-2. In all cases Se(VI) is the primary form of selenium in sequential leaching. Total selenium was less than 50 μg/L in all ashes except NE3 15-20, in which Se(IV) approaches 20 μg/L for several leachings. For the NE and MW ash, selenium concentrations in the first leachate were 0 to <20 μg/L (ash dependent) followed by increasing concentration up to approximately the 5th leaching and then remained at this concentration of 35 to 50 μg/L (ash dependent) for the remaining 10 leachings. The 2 ashes from the SE site behaved distinctly different from each other as well as the other ashes. SE1 5-9 had the highest concentration in the first leachate (≈ 32 μg/L) and then decreased rapidly to approximately 5 μg/L by the 6th leaching and remained at that concentration for the next 10 leachings. The other SE ash (SE1 23.5-37.5) had constant and relatively high concentrations (≈ 32 μg/L) through the first 6 leachings and then increased to a plateau concentration of just over 50 μg/L for the remaining leachings. The difference in leaching patterns implies possible differences in the mineral form of Se as well as the location of Se in the ash particles (on the ash surface versus within the internal volume of the ash). The sequential leaching pattern for SE1 23.5-27.5 is indicative of a change in the solubility control as various inorganic constituents are leached. The complex or precipitate that has the lowest solubility product for a given pH-redox condition will limit the Se concentrations that can exist in solution. As the lower solubility limit precipitate is washed away, another complex or precipitate of higher solubility will become the new limiting factor. Whereas, the sequential leaching pattern of SE1 5-9 is indicative of an easily removed fraction of Se, perhaps surface associated followed by mass transfer constrained release from within the ash particle. Changes in

pH and redox state can also contribute to concentration changes with sequential leachings; however, after the first leaching, pH was relatively constant with leaching.

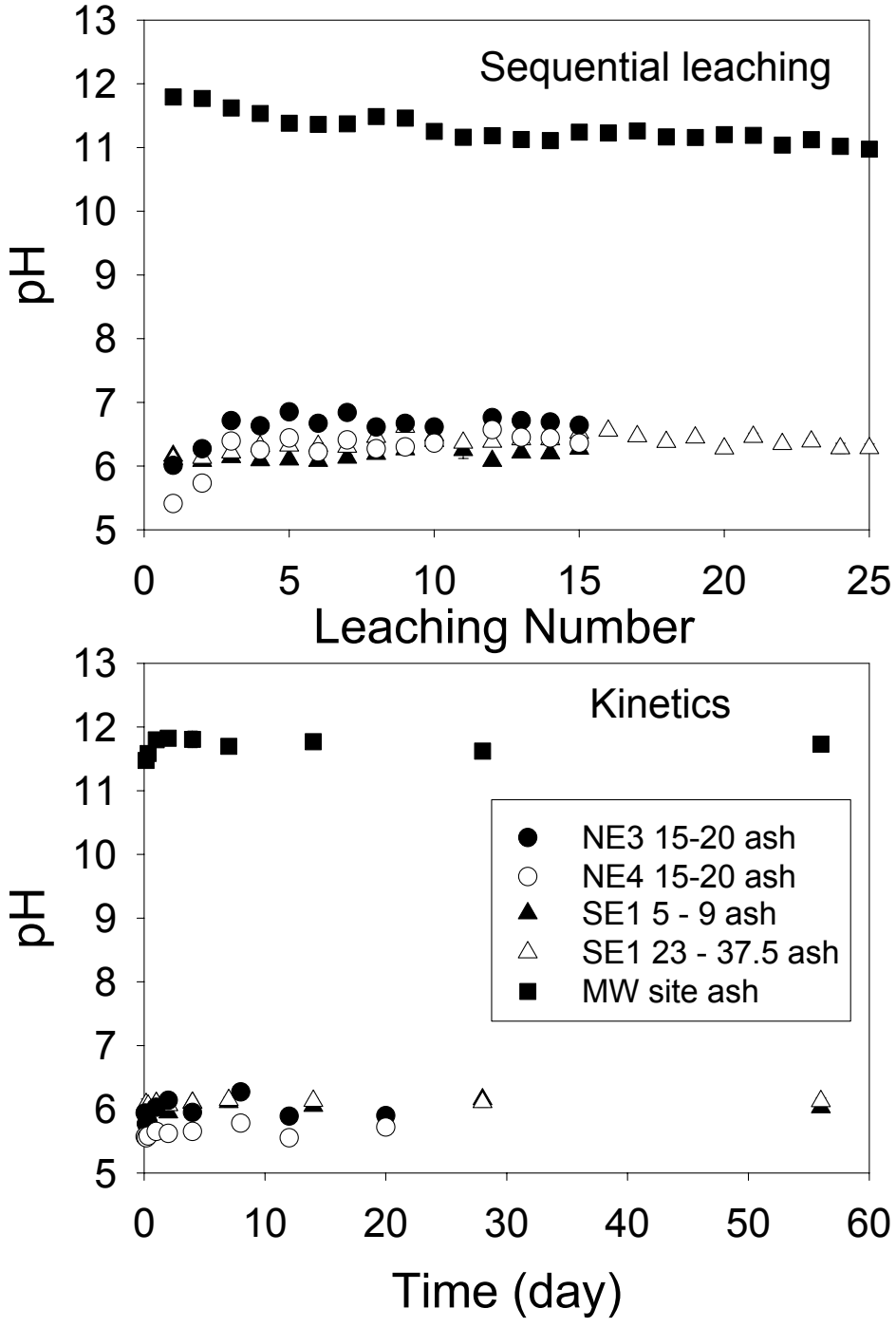

Figure 5-1
pH profile over sequential and kinetic leaching series for ash samples collected from SE site and NW site

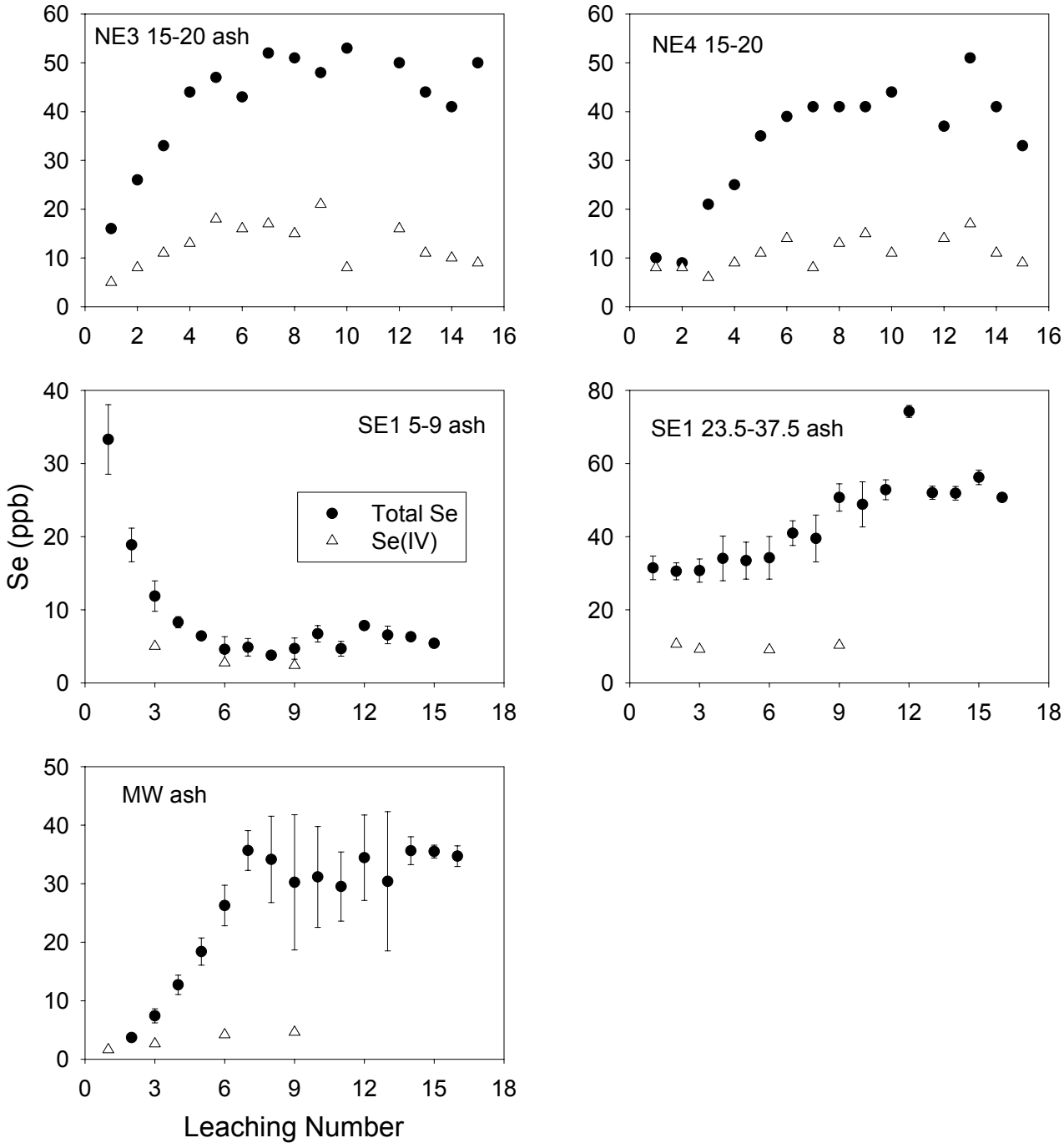

Figure 5-2
Total selenium (IV+VI) and Se(IV) profiles over sequential leaching series for ash samples collected from NE, SE, and MW sites. Total Se are the average values of triplicate and the standard deviations are shown as error bars.

Leaching Kinetics

Average pH values measured for leaching kinetics of ash samples obtained from each site are summarized in Figure 5-1 (lower figure). Total selenium and Se(IV) leaching profiles over time for ash samples are shown in Figure 5-3. The average pH values and selenium concentrations were similar to what was observed in the sequential leaching study with one exception. SE1 23.5-37.5 only reached 35 μg/L over the 2 month period whereas 50 μg/L was observed in the sequential leaching. However, Se concentrations in the first 6 leachings are around 32 μg/L (Figure 5-2), which is comparable to the upper concentration reached within the 60 day time frame in the kinetics study (Figure 5-3) before a change in the solubility control occurred. Therefore, even in the absence of mass transfer constraints, maximum observed concentrations in a kinetic study, where no leachate replacement occurs, may likely not compare well to what is observed in the field. For all ashes, Se concentrations appear to increase over the time frame of the study with the initial rate of increase being orders of magnitude greater than at later times with the exception of MW ash. For the latter, Se concentrations continued to rise at what appears to be a steady rate of increase for the entire 2 months. Although laboratory leaching studies can be insightful, several factors including residence time and release kinetics, ash mass to solution volume ratio, total pore volumes passed, and microbial activity will contribute to differences of the maximum concentrations observed in a laboratory study compared to a field scenario.

Leachate Selenium Attenuation by Onsite Soils

Attenuation of selenium by the SE and MW soils from ash leachate collected at those sites is shown for Se(IV) in Figure 5-4 and for Se(VI) in Figure 5-5 along with the multi-concentration selenium isotherms measured from 1 mM $CaSO_4$. Se(IV) and Se(VI) present in the ash leachate were significantly attenuated through adsorption by the site soils in a manner consistent with the isotherms developed using 1 mM $CaSO_4$. Therefore, the use of 1 mM CaSO4 for selenium adsorption matrix appear to be a reasonably good simulated leachate matrix for conducting laboratory equilibrium adsorption test.

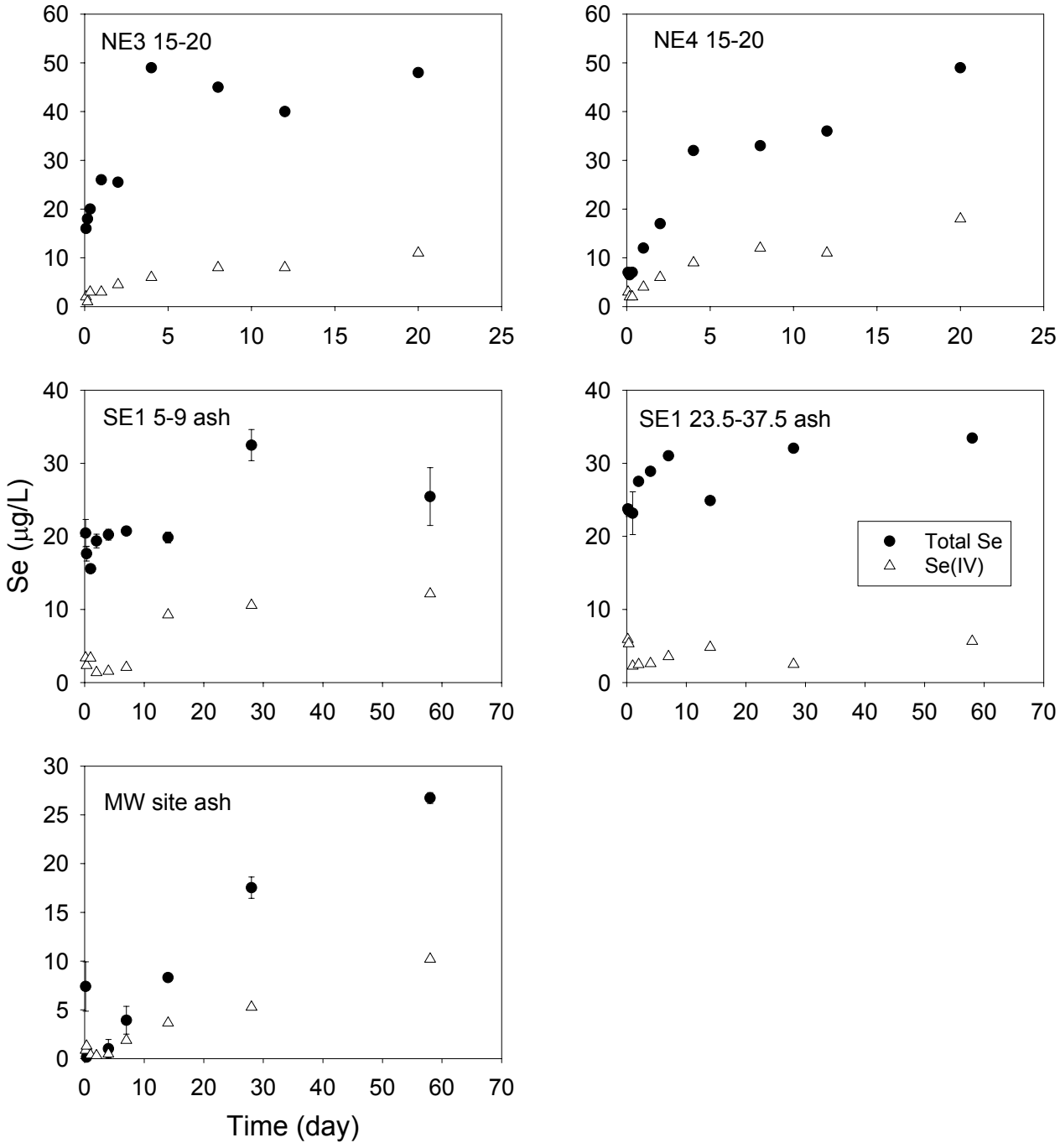

Figure 5-3
Batch kinetic leaching of total selenium (IV+VI) and Se(IV) from SE and MW ash samples. Total Se are the average values of duplicate and the data ranges are shown as error bars.

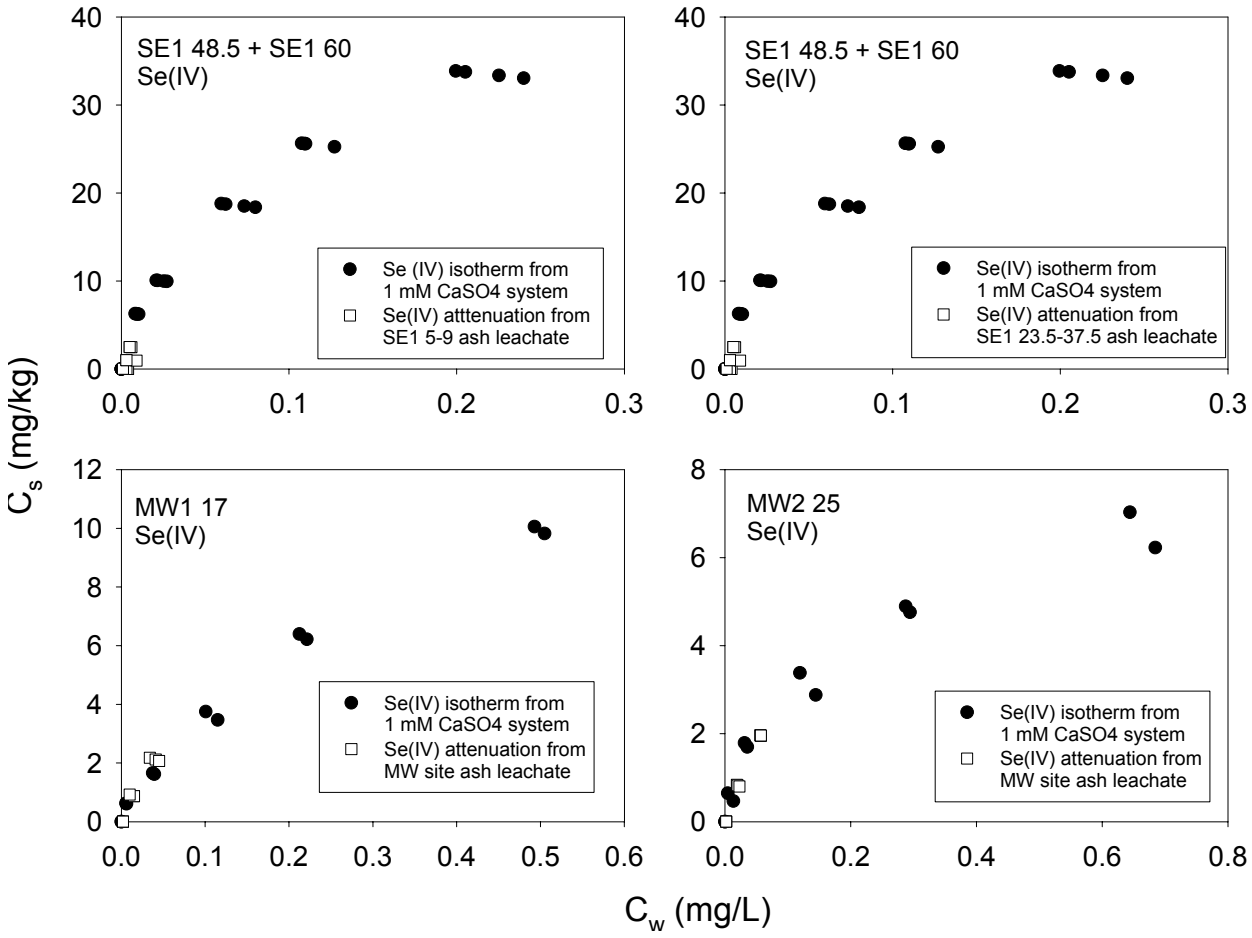

Figure 5-4
Attenuation of Se(IV) by soil adsorption present in ash leachate by SE and MW site soils, along with multi-concentration Se(IV) isotherms measured from 1 mM CaSO4.

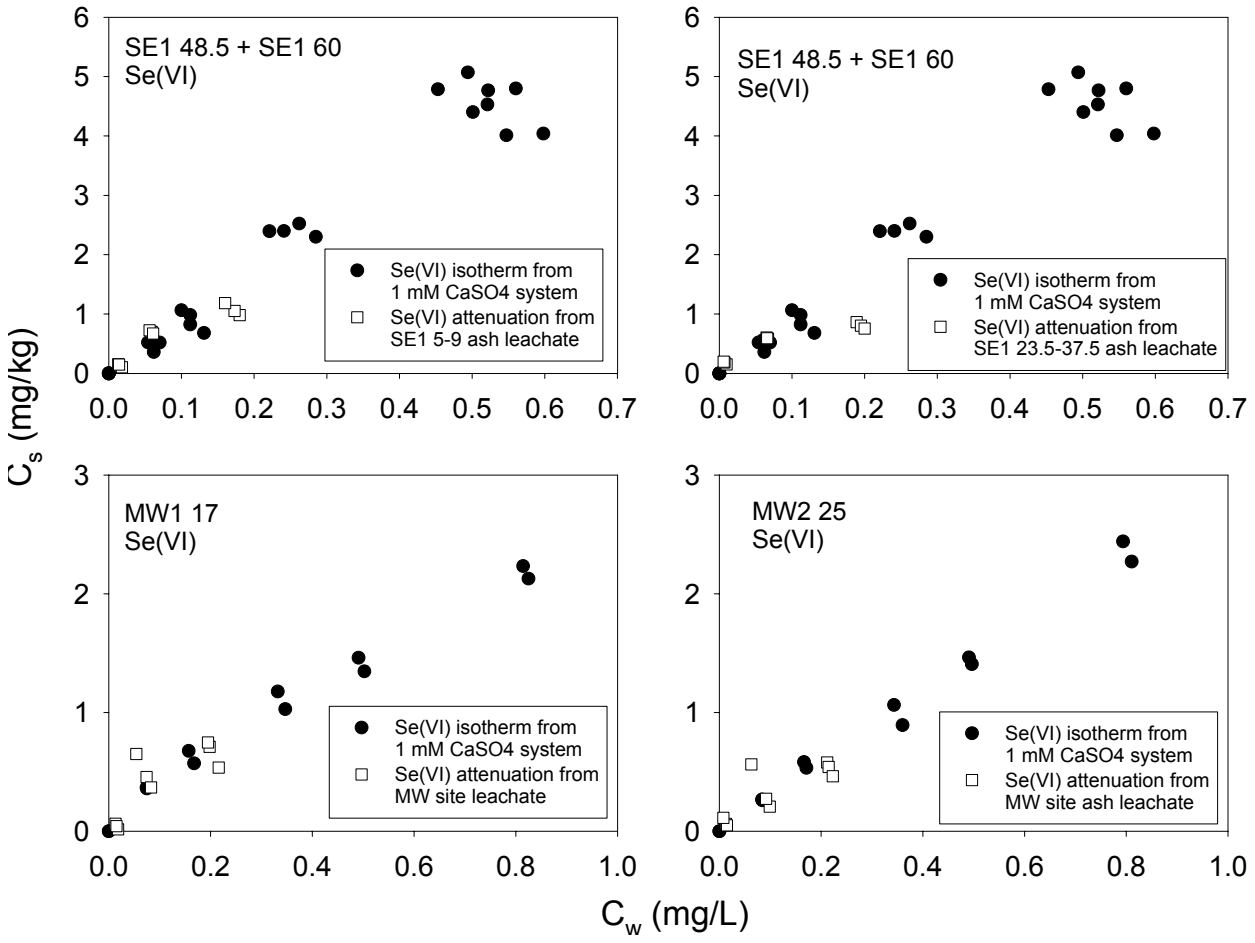

Figure 5-5
Attenuation of Se(VI) by soil adsorption present in ash leachate by SE and MW site soils, along with multi-concentration Se(VI) isotherms measured from 1 mM CaSO4.

6
REFERENCES

Bar-Yosef, B. and D. Meek. 1987. Selenium sorption by kaolinite and montmorillonite. Soil Sci. 144:11-19

Balistrieri, L. S. and T. T. Chao. 1987. Selenium adsorption by goethite. Soil Sci. Am. Soc. J. 51:1145-1151.

Benjamin, M. M. 1983. Adsorption and surface precipitation of metals on amorphous iron oxyhyroxide. Environ. Sci. Technol. 17:686-692.

Betts, K. S. 1998. EPA decision to revise selenium standard stirs debate. Environ. Sci. Technol., 32:350A-351A.

Bowen, H. J. M. 1979. Environmental chemistry of the elements. Academic Press, London.

Bowden, J. W., S. Nagarajah, N. J. Barrow, A. M. Posner, and J. P. Quirk. 1980. Describing the adsorption of phosphate, citrate, and selenite on a variable-charge mineral surface. Aust. J. Soil Res. 18:49-60.

Carlson, C. L. and D. C. Adriano. 1993. Environmental impacts of coal combustion residues. J. Environ. Qual. 22:227-247.

Dhillon, S. K. and K. S. Dhillon, K. S. 2002. Selenium adsorption in soils influenced by different anions. J. Plant Nutr. Soil Sci. 163:577-582.

Dhillon, S. K. and K. S. Dhillon, K. S. 2003. Distribution and management of seleniferous soils. p. 119-184. In D. L. Sparks (ed.) Advances in agronomy, volume 79. Academic Press, New York, NY.

Dowdle, P. R. and R. S. Oremland. 1998. Microbial oxidation of elemental selenium in soil slurries and bacterial cultures. Environ. Sci. Technol. 32:3749-3755.

Eary, L. E., D. Rai, S. V. Mattigod, and C. C. Ainsworth. 1990. Goechemical factors controlling the mobilization of inorganic constituents from fossil fuel combustion residues: II. Review of the minor elements. J. Environ. Qual. 19:202-204.

EPRI. 1997. Coal Combustion By-Products and Low-Volume Wastes Comanagement Survey, EPRI, Palo Alto, CA: 2004. 1005505.

EPRI. 2004. Chemical attenuation coefficients for arsenic species using soil samples collected from selected power plant sites: Laboratory studies, EPRI, Palo Alto, CA, and U.S. Department of Energy: 2004. 1005505.

Fio, J. L. and R. Fujii. 1990. Selenium speciation methods and application to soil saturation extracts from San Joaquin Valley, California. Soil Sci. Soc. Am. J. 54:363-369.

Frost, R. R. and R. A. Griffin. 1977. Effect of pH on adsorption of arsenic and selenium from landfill leachate by clay minerals. Soil Sci. Am. Soc. J. 41:53-57.

Gee, G. W. and J. W. Bauder. 1996. Particle-size analysis. p. 384-411. *In* A. Klute (ed.), Method of soil analysis: Physical and mineralogical methods. Part I. 2nd Ed., Agronomy Monograph No. 9. Amer. Soc. Agron., Madison, WI.

Goh, K-H. and T-T. Lim. 2004. Geochemistry of inorganic arsenic and selenium in a tropical soil: effect of reaction time, pH, and competitive anions on arsenic and selenium adsorption. Chemosphere. 55:849-859.

Goldberg, S. and R. A. Glaubig. 1988. Anion sorption on a calcareous, montmorillonitic soil-selenium. Soil Sci. Soc. Am. J. 52:954-958.

Hansmann, D. D. and M. A. Anderson. 1985. Using electrophoresis in modeling sulfate, selenite, and phosphate adsorption onto goethite. Environ. Sci. Technol. 19:544-551.

Hayes, K. F., A. L. Roe, G. E. Brown. Jr., K. O. Hogson, J. O. Leckie, and G. A. Parks. 1987. In situ X-ray absorption study of surface complexes: Selenium oxyanions on α-FeOOH. Science. 238:783-786.

Himeno, S. and N. Imura. 2002. Selenium in nutrition and toxicology. p. 587-629. In B. Sarkar (ed.), Heavy metals in the environment. Marcel Dekker, Inc., New York, NY.

Hingston, F. J., A. M. Posner, J. P. Quirk. 1972. Anion adsorption by goethite and gibbsite. I. The role of the in determining adsorption envelops. J. Soil Sci. 23:177-192.

Jackson, B. P. and W. P. Miller. 1998. Arsenic and selenium speciation in coal fly ash extracts by ion chromatography-inductively coupled plasma mass spectrometry. J. Anal. At. Spectrom. 13:1107-1112.

John, M. K., W. M. H. Saunders, and J. W. Watkinson. 1976. Selenium adsorption by New Zealand soils: 1. Relative adsorption of selenite by representative soils and the relationship to soil properties. N. Z. J. Agric. Res. 19:143-151.

Ladwig, K., B. Hensel, and D. Wallschlager. 2006. Speciation and Attenuation of Arsenic and Selenium at Coal Combustion By-Product Management Facilities: Volume 1: Field Leachate. DOE Project DE-FC26-02NT41590.

Loeppert, R. H. and W. P. Inskeep. 1996. Iron. p. 639-664. *In* D. L. Sparks et al. (ed.), Method of soil analysis: Chemical methods, Part III. Agronomy Monograph No. 5. Amer. Soc. Agron., Madison, WI.

Lortie, L., W. D. Gould, S. Rajan, R. G. L. McCready, and K.-J. Cheng. 1992. Reduction of selenate to elemental selenium by a *Pseudomona stutzeri* isolate. Appl. Environ. Microbiol. 58:4042-4044.

Losi, M. E. and W. T. Frankenberger, Jr. 1997a. Bioremediation of selenium in soil and water. Soil Science, 162:692-702.

Losi, M. E. and W. T. Frankenberger, Jr. 1997b. Reduction of selenium oxyanions by *Enterbacter cloacae* strain SLD1a-1: Reduction of selenate to selenite. Environ. Toxicol. Chem. 16:1851-1858.

Losi, M. E. and W. T. Frankenberger, Jr. 1998. Micribial oxidation and solubilization of precipitated elemental selenium in soil. J. Environ. Qual. 27:836-843.

Maiers, D. T., P. L. Wichlacz, D. L. Thompson, and D. F. Bruhn. 1988. Selenate reduction by bacteria from a selenium-rich environment. Appl. Environ. Microbiol. 54:2591-2593.

Manceau, A., and L. Charlet. 1994. The mechanism of selenate adsorption on goethite and hydrous ferric oxide. J. Colloid Interface Sci. 168:87–93.

Manning, B. A. and R. G. Burau. 1995. Selenium immobilization in evaporation pond sediments by in situ precipitation of ferric oxyhydroxide. Environ. Sci. Technol. 29: 2639-2646.

Masscheleyn, P. H., R. Delaune, and W. H. Patrick, Jr. 1990. Transformations of selenium as affected by sediment oxidation-reduction potential and pH. Environ. Sci. Technol. 1:91-96.

Monteil-Rivera, F., M. Fedoroff, J. Jeanjean, L. Minel, M. G. Barthes, and J. Dumonceau. 2000. Sorption of selenite (SeO_3^{2-}) on hydroxyapatite: an exchange process. J. Colloid Interface Sci. 221:291-300.

Nakamara, Y., K. Tagami, and S. Uchida. 2005. Distribution coefficient of selenium in Japanese agricultural soils. Chemosphere. 58:1347-1354.

Neal, R. H., G. Sposito, K. M. Holtzclaw, and S. J. Traina. 1987a. Selenite adsorption on alluvial soils: I. Soil composition and pH effects. Soil Sci. Soc. Am. J. 51:1161-1165.

Neal, R. H., G. Sposito, K. M. Holtzclaw, and S. J. Traina. 1987b. Selenite adsorption on alluvial soils: II. Solution composition effects. Soil Sci. Soc. Am. J. 51:1165-1169.

Neal, R. H. and G. Sposito. 1989. Selenate sorption on alluvial soils. Soil Sci. Soc. Am. J. 53:70-74.

Nelson, D. W. and L. E., Sommers. 1996. Total carbon, organic carbon, and organic matter. p. 961-1010. *In* D. L. Sparks et al. (ed.), Method of soil analysis: Chemical methods, Part III. Agronomy Monograph No. 5. Amer. Soc. Agron., Madison, WI.

Ohlendrof, H. M., D. J. Hoffman, M. K. Saiki, and T. W. Aldrich. 1986. Embryonic mortality and abnormalities of aquatic birds; Apparent impacts of selenium from irrigation drainwater. Sci. Total Environ. 52:48-63.

Peak, D. and D. L. Sparks. 2002. Mechanisms of selenite adsorption on iron oxides and hydroxides. Environ. Sci. Technol. 36:1460-1466.

Rajan, S. S. S. and J. H. Watkinson. 1976. Adsorption of selenite and phosphate on an allophane clay. 40:51-54.

Rajan, S. S. S. 1979. Adsorption of selenite, phosphate, and sulfate on hydrous alumina. J. Soil Sci. 30:709-718.

Renner, R. 1998. EPA decision to receive selenium standard stirs debate, Environ. Sci. Technol. 39:350A.

Renner, R. 2005. Proposed selenium standard under attack, Environ. Sci. Technol. 39:125A-126A.

Saeki, K. and S. Matsumoto, 1994. Selenite adsorption by a variety of oxides. Commun. Soil Sci. Plant Anal.25:2147-2158.

Saeki, K., S. Matsumoto, and R. Tatsukawa. 1995. Selenium adsorption by manganese oxides. Soil Sci. 160:265-272.

SAS Institute. 1989. SAS/STAT user's guide. Version 6. 4th ed. SAS Inst., Cary, NC.

Séby, F., M. Potin-Gauntier, E. Giffaut, and O.F.X. Donard. 1998. Assessing speciation and the bigoeochemical processes affecting the mobility of selenium from a geological repository of radioactive wastes to the biosphere. Analusis, 26:193-198.

Su, C. and D. L. Suarez. 2000. Selenate and selenite sorption on iron oxides: An infrared and electrophoretic study. Soil Sci. Soc. Am. J. 64:101-111.

Sumner, M. E. and W. P., Miller. 1996. Cation exchange capacity and exchange coefficients. p. 1201-1229. *In* D. L. Sparks et al. (ed.), Method of soil analysis: Chemical methods, Part III. Agronomy Monograph No. 5. Amer. Soc. Agron., Madison, WI.

Theis, T. L. and K. H. Gardner. 1990. Environmental assessment of ash disposal. Crit. Rev. Environ. Contr. 20:21-42.

U. S. Environmental Protection Agency. 2004. Draft aquatic life water quality criteria for selenium-2004. USEPA Rep. 822-D-04-001. USEPA, Washington, DC.

U. S. Environmental Protection Agency. 1999. Wastes from the combustion of fossil fuels. USEPA Rep. 530-R-99-010. USEPA, Washington, DC.

van der Hoek, E. E., J. T. van Elteren, and R. N. J. Comans. 1996. Determination of As, Sb, and Se speciation in fly-ash leachates. Intern. J. Environ. Anal. Chem. 63:67-79.

Wijnja, H., and C.P. Schulthess. 2000. Vibrational spectroscopy study of selenate and sulfate adsorption mechanisms on Fe and Al hydr(oxide) surfaces. J. Colloid Interface Sci. 229:286–297

You, Y., G. F. Vance, and H. Zhao. 2001 Selenium adsorption on Mg-Al and Zn-Al layered double hydroxides. Appl. Clay Sci. 20:13-25.

Zhang, P. C. and D. L. Sparks. 1990. Kinetics of selenate and selenite adsorption/desorption at the goethite/water interface. Environ. Sci. Technol. 24:1848-1856.